O^{18}/O^{16} AND D/H RATIOS OF SOILS, WEATHERING ZONES AND CLAY DEPOSITS

Thesis by

James Robert Lawrence

In Partial Fulfillment of the Requirements

For the Degree of

Doctor of Philosophy

California Institute of Technology

Pasadena, California

1970

(Submitted May 21, 1970)

ACKNOWLEDGEMENTS

I wish to thank Dr. Hugh P Taylor, Jr. for guidance and encouragement throughout the course of this research.

I am indebted to Dr. S. Epstein for meaningful discussions and for the use of his laboratories and mass spectrometer facilities.

I am grateful for valuable discussions I have had with Drs. L.T.Silver, H. Tourtelot, A.C. Waters, R.P. Sharp, A.L. Albee, H. A. Lowenstam, S.M. Savin, and S.M.F. Sheppard.

Large sample suites were generously provided by Drs. L.T. Silver, H. Tourtelot, J.W. Hosterman, R.P. Sharp, H.P. Taylor, Jr., M. Bass and M. Stephens.

A large suite of samples was collected with the generous help of A. C. Waters.

Other samples were generously contributed by Drs. R.E. Folinsbee, J.A.S. Adams, I.L. Tailleur, M.T. Huntling, R.E. Cameron, and W.G. Melson.

Assistance with the construction and/or maintenance of the apparatus was received from Messrs. E.V. Nenow, C. Bauman, A. Chodos, P. Yanagisawa and Mmes. E. Bingham and L. Ray.

A differential thermal analyzer used in the research was donated by F. Bailey.

I would like to express my thanks to Mmes. R. Talovich and J. Billerbeck for their help in the preparation of the thesis.

I would like to express my thanks to my wife, Mary Ann, for her encouragement and assistance during this study.

During part of this research the writer was supported by a National Science Foundation Summer Fellowship. This research was supported by grants from the National Science Foundation Grant No. GA-12945 and Project Agreement #7 under Atomic Energy Commission Contract No. AT(04-3)-767.

ABSTRACT

D/H and O^{18}/O^{16} ratios have been determined for a large variety of bulk samples and mineral separates from : Quaternary soils and clay-rich weathering zones; Tertiary, Cretaceous and Pennsylvanian kaolinite deposits; a number of montmorillonite occurrences (from bentonites, fossil soils, alteration of pillow lavas, etc.) ; Precambrian, Paleozoic and Cretaceous shales; and Pleistocene glacial lake clays. Most samples are from the western and southern United States, but analyses have also been obtained from Hawaii and other parts of North America.

Laboratory experiments indicate that kaolinites do not suffer any significant amount of hydrogen isotopic exchange at room temperature when in contact with D enriched waters. This also applied in general to montmorillonites, but in many instances partial hydrogen isotopic exchange occurs with interlayer water during the normal heating and outgassing that precedes extraction of OH water. The hydroxyl of halloysite, however, does undergo marked hydrogen isotopic exchange with its interlayer water in a few hours or days at room temperature, largely negating the usefulness of this mineral in isotopic studies.

The D/H and O^{18}/O^{16} ratios of clay minerals and hydroxides in Quaternary soils and weathering zones throughout the United States show a systematic correlation with the isotopic values of present-day meteoric waters. The δD and δO^{18}, respectively, of these weathering products range as follows: Hawaii: -27 to -65 and +24 to +15; Southern United States: -55 to -75 and +22 to +17; coastal California: -55 to -80 and +23 to +16; Sierra Nevada, California: -75 to -95 and +19 to +14; Colorado: -95 to -110 and +16 to +8; Montana and Idaho: -105 to -165 and +12 to 0. The δD values of the clay

minerals are generally 0 to 40‰ lighter than local meteoric waters and the δO^{18} values are generally 22 to 28‰ heavier than local meteoric waters. The isotopic values of the clay minerals plot in the vicinity of Savin and Epstein's (1970a) kaolinite line. The δD and δO^{18} values of the hydroxides (e.g., gibbsite) are generally 10 to 20‰ lighter and 15 to 20‰ heavier, respectively, than local meteoric waters. The isotopic values of the hydroxides plot in the vicinity of the line $\delta D = 7.7\ \delta O^{18} - 155$.

A kaolinite soil profile from Georgia and a montmorillonite profile from California, both formed on granitic rock types, were studied in detail. Other detailed sampling was done on a halloysite profile formed on basalt, on three poorly-developed profiles on Cretaceous shales, and a poorly-developed profile on a Precambrian shale. These studies indicate that igneous and sedimentary parent rock minerals do not undergo appreciable oxygen or hydrogen isotopic exchange with meteoric waters in the weathering environment. However, the clay minerals and hydroxides produced by the alteration of the parent rock are formed essentially in isotopic equilibrium with the local meteoric waters.

The D/H and O^{18}/O^{16} ratios of most Pre-Quaternary kaolinites, bentonites, and shales are significantly higher than those of clay-rich Quaternary soils in the same geographic areas. The D/H ratios of Lower Paleozoic and Precambrian shales from eastern United States to Montana and British Columbia show no correlation with the D/H ratios of present-day meteoric waters. The D/H ratios of glacial lake clays, which were exposed to glacial melt waters highly depleted in deuterium are identical to the D/H ratios of Lower Paleozoic shales of the eastern United States from which they were largely derived. All these data suggest that the isotopic ratios of the Pre-Quaternary clay minerals are largely

preserved.

Because the isotopic values of ancient clay minerals seem to be commonly preserved, the D/H ratios of ancient kaolinites formed by weathering processes can be used to estimate the D/H ratios of ancient meteoric waters. Using the δD values of the Tertiary kaolinites and a $\alpha^{hy}_{kaolinite-H_2O} = 0.970$ a tentative contour map of the δD values of "mid-Tertiary" meteoric waters has been drawn. The distribution of the δD values of Tertiary meteoric waters are similar to the present-day distribution except that the contrast in δD values between coastal and high inland regions in the Tertiary was less extreme than the present contrast. The interpretation is that the distribution of land and the meteorological patterns in the Tertiary were somewhat similar to today but that the climate was generally warmer. Also it is possible that many present-day topographic barriers were absent or less important in the Tertiary. This is in agreement with climatic data suggested by paleobotanical evidence.

The wide range of D/H and O^{18}/O^{16} ratios determined for relatively pure ($>$ 80%) kaolinites formed by the weathering process confirms that the kaolinite line derived by Savin and Epstein (1970a) is essentially correct. However, the D/H and O^{18}/O^{16} ratios of montmorillonites formed as weathering products or in sedimentary environments display a much greater scatter than kaolinites, presumably as a result of (1) the greater range of chemical compositions of montmorillonites compared to kaolinites, (2) the greater range of the temperatures of formation of montmorillonites, and (3) the possibility that the D/H ratios determined for montmorillonite OH are contaminated during heating and outgassing procedures. Hence, the montmorillonite line derived by Savin and Epstein (1970a) apparently does not apply to most montmorillonites in nature.

TABLE OF CONTENTS

PART	SECTION	TITLE	PAGE
I		INTRODUCTION	1
	1.1	Object of the research	1
	1.2	Previous work	2
		Natural waters	2
		Clay minerals	4
		Soils	6
	1.3	Isotopic equilibrium	7
		Theoretical	7
		Experimental	8
	1.4	Isotopic exchange in clay minerals	9
II		EXPERIMENTAL PROCEDURES	18
	2.1	Sample collection	18
	2.2	Mineral identification	19
	2.3	Mineral separations	20
	2.4	Isotopic analysis	21
		Definition of terms	21
		Oxygen isotopic analyses	22
		Hydrogen isotopic analyses	24
III		EXPERIMENTAL EVALUATION OF D/H AND O^{18}/O^{16} ANALYSES OF CLAY MINERALS	31
	3.1	Hydrogen isotopic exchange experiments	31
		General statement	31
		Procedures	31
		Discussion of procedure 2	40
		Discussion of procedure 1	40
		Discussion of procedures 3 and 4	45
		Discussion of procedure 5	46
	3.2	Systematic treatment of samples equilibrated with atmospheric vapor	46
	3.3	Summary	54

PART	SECTION	TITLE	PAGE
IV		ISOTOPIC, MINERALOGICAL AND CHEMICAL DATA	57
V		DETAILED ISOTOPIC STUDIES OF WEATHERING PROFILES	81
	5.1	General statement	81
	5.2	Elberton, Georgia kaolinite profile	81
		Parent rock minerals	84
		C-zone	91
		A- and B-zones	100
	5.3	Big Sur, California montmorillonite profile	102
		Parent minerals	112
		Weathered horizons	112
	5.4	Spokane County, Washington halloysite profile	120
	5.5	Pierre shale profiles	127
	5.6	Missoula, Montana profile	134
VI		ISOTOPIC SURVEY OF QUATERNARY SOILS FROM THE UNITED STATES	139
VII		ANCIENT KAOLINITE AND ILLITE DEPOSITS	163
VIII		MONTMORILLONITES	185
IX		SHALES AND GLACIAL LAKE CLAYS	203
X		SUMMARY AND CONCLUSIONS	215
	10.1	Mineral-H_2O fractionation factors for kaolinite, montmorillonite and gibbsite	215
	10.2	Preservation of the hydrogen and oxygen isotopic compositions of clay minerals	221
	10.3	Isotopic evidence for climatic conditions during the Tertiary	225
	10.4	Isotopic criteria for distinguishing clay minerals of different origins	228
BIBLIOGRAPHY			231
APPENDIX I : SAMPLE LOCATIONS AND DESCRIPTIONS			237

PART SECTION TITLE PAGE

APPENDIX II : X-RAY DIFFRACTION PATTERNS OF SELECTED SAMPLES FROM THE ELBERTON, GEORGIA AND BIG SUR, CALIFORNIA WEATHERING PROFILES..... 256

APPENDIX III: OXYGEN ISOTOPIC REPRODUCIBILITY OF THE KAOLINITE AND ROSE QUARTZ STANDARDS.. 260

I. INTRODUCTION

1.1 Object of the research

If a weathering zone is considered to be a dynamic system approaching chemical and isotopic equilibrium with its environment, the O^{18}/O^{16} and D/H ratios of weathering products will be determined by: (1) the isotopic composition of the coexisting waters; (2) the isotopic composition of the parent rock; (3) the relative amounts of water and parent rock; (4) the isotopic fractionations between water and the minerals formed during weathering; and (5) the temperature.

Because the weathering process commonly involves very large quantities of meteoric water, the ratio of water to altered parent rock is generally high. Under such conditions the isotopic composition of the parent rock has virtually no effect on the isotopic composition of the weathering products. Weathering at the Earth's surface generally takes place within a relatively narrow temperature range of 0° to 30° C, and equilibrium isotopic fractionation factors are dependent only on the temperature. Therefore, the D/H and O^{18}/O^{16} ratios of a given weathering product will also be confined within narrow limits, if the isotopic composition of the local meteoric water is essentially constant.

Isotopic compositions of meteoric waters are known to vary systematically with climate, generally becoming progressively depleted in the heavy isotopes in the colder climatic regions. If ancient weathering products have preserved their D/H and O^{18}/O^{16} values, they contain a record of ancient meteoric-water isotopic compositions. This line of reasoning is the basis for the present study.

The first objective of this study was to determine if the isotopic compositions of recent weathering products reflect the systematic variations of isotopic

composition observed in present-day meteoric waters. An outgrowth of such a study would be the more accurate determination of equilibrium fractionation factors for D/H and O^{18}/O^{16} between water and the various minerals formed during the weathering process.

Secondly, the isotopic compositions of both parent minerals and weathering products were to be studied in detail on selected weathering profiles. This is to ascertain if the weathering products are in isotopic equilibrium with local meteoric waters, and whether the parent-rock minerals change isotopically as a function of the intensity of weathering.

Thirdly, the isotopic compositions of ancient weathering products and other clay mineral deposits were to be studied to determine if the hydrogen and/or oxygen isotopic compositions of such clay minerals are preserved through geologic time. Such studies would also allow us to better understand isotopic exchange phenomena between clay minerals and water at low temperatures.

Finally, if sufficient knowledge of isotopic preservation and exchange phenomena are obtained, distinctions might be made between weathering-product clays and clays formed by other processes. It might also be possible to calculate the isotopic compositions of waters that coexisted with ancient clay minerals, and this in turn could allow us to infer something about ancient climates and rainfall patterns.

1.2 Previous work

Natural waters: Variations of the O^{18}/O^{16} ratio in the Earth's atmosphere, hydrosphere and lithosphere are reviewed in a broad context in Epstein (1959), Epstein and Taylor (1967) and Garlick (1969). References to more specific

studies are given in the above publications. Variations of the D/H ratio on Earth are much less well understood, although much is known concerning the D/H variations in natural waters.

Epstein and Mayeda (1953) studied the O^{18}/O^{16} ratios of both ocean waters and fresh waters. A correlation was observed between the O^{18}/O^{16} content and the salinity of ocean waters. They attributed the abnormally high O^{18}/O^{16} ratios of certain ocean waters to the evaporation of H_2O vapor having an O^{18}/O^{16} ratio 7 per mil lower than the liquid water (this is the equilibrium fractionation at Earth surface temperatures). O^{18}/O^{16} ratios of ocean waters less than that of mean ocean water were attributed to addition of very light polar melt waters with δO^{18} of about $-20‰$. Thus it became apparent that there were large isotopic variations in natural waters. Friedman (1953) found that natural evaporation and condensation fractionated hydrogen isotopes in a manner similar to that previously demonstrated for oxygen isotopes. He observed that the ratio of these two fractionations was equal to the ratio of $(pH_2O/pHDO)$ to (pH_2O^{16}/pH_2O^{18}), where p is the vapor pressure.

Epstein (1956) observed systematic variations of O^{18}/O^{16} in rainfall as a function of elevation of the land surface. He also observed that summer rains were higher in O^{18}/O^{16} than winter snows in those same localities. Craig (1961a) analyzed about 400 meteoric water samples from a great variety of localities and found that the δD and δO^{18} values of these samples fit a very precise relationship, namely $\delta D = 8\delta O^{18} + 10$.

Clayton et al. (1966) analyzed δD and δO^{18} contents and dissolved solids from 95 oil-field brines from the Illinois, Michigan and Alberta basins and the Gulf Coast. Interbasin variations of δD were much greater than intrabasin variations. δO^{18} variations were large within a given basin, and showed a strong

correlation with salinity. It was concluded that these brines were derived predominantly from local meteoric waters that had acquired large salt concentrations by percolation through the rocks. The deuterium contents of these waters were not greatly altered, but their O^{18}/O^{16} ratios were changed through oxygen exchange with the adjoining sedimentary rocks, particularly limestones.

Clay minerals: Savin (1967) undertook the first detailed study of oxygen and hydrogen isotopic variations in sedimentary minerals, emphasizing the clay minerals. One of the biggest problems in analyzing certain minerals for oxygen and hydrogen isotopes is to obtain completely dry samples, because absorbed water is a contaminant. Because clay minerals are fine grained and some contain interlayer water, Savin (1967) conducted numerous experiments to determine how to treat clays in order to avert this problem. He found that those clay minerals lacking interlayer or zeolitic water could be treated by standard methods used for other minerals. However, clay minerals with interlayer water required more thorough treatment before the hydroxyl hydrogen or the oxygen could be extracted. This treatment involved (1) drying in a H_2O-free atmosphere at room temperature before extracting the oxygen, and (2) outgassing in vacuum at 200°C before extracting the hydrogen. Savin (1967) concluded that these procedures reduced interlayer-water contamination to negligible amounts. Contamination is a more serious problem for D/H analyses than for O^{18}/O^{16} analyses because interlayer water constitutes a significant proportion of the total hydrogen in the mineral.

Savin and Epstein (1970a) determined the isotopic compositions of several pure sedimentary minerals and estimated mineral-water fractionation factors at low temperatures. They observed a hydrogen and oxygen isotopic correlation between these minerals and meteoric waters. Table 1-1 lists their estimated

TABLE 1-1

Estimated Mineral-Water Fractionation Factors
at 25°C (after Savin, 1967)

Mineral	Fractionation Factors $\alpha^{ox}_{min-H_2O}$ *	$\alpha^{hy}_{min-H_2O}$ †	Derived $\delta D - \delta O^{18}$ Relationship #
Quartz	1.034		
Alkali feldspar	1.034		
Phillipsite	1.034		
Montmorillonite	1.0273	0.938	$\delta D = 7.3\ \delta O^{18} - 260$
Kaolinite	1.0265	0.970	$\delta D = 7.6\ \delta O^{18} - 220$
Glauconite	1.0263	0.926	$\delta D = 7.2\ \delta O^{18} - 250$
Manganese Nodule	1.015	0.923	

* $\alpha^{ox}_{min-H_2O} = \dfrac{O^{18}/O^{16}\ (mineral)}{O^{18}/O^{16}\ (H_2O)}$ † $\alpha^{hy}_{min-H_2O} = \dfrac{D/H\ (mineral)}{D/H\ (H_2O)}$

Savin (1967) Appendix I

fractionation factors for several minerals at 25°C . Application of these fractionation factors to the kaolinite-H_2O and montmorillonite-H_2O systems results in a linear relationship for δD and δO^{18} in these minerals, assuming that they form in equilibrium with a large reservoir of meteoric water. Analyzed natural kaolinites were observed to fit the derived "kaolinite line" very closely, but the analogous line for montmorillonite is much less well defined.

Savin and Epstein (1970b) found that detrital ocean sediments isotopically reflect their continental origins, whereas authigenic ocean sediments reflect equilibration with ocean water at low temperatures. Detrital ocean sediments as old as 250,000 years showed no sign of isotopic reequilibration with ocean water.

Sheppard et al. (1969) determined the δO^{18} and δD content of kaolinite, dickite, halloysite and montmorillonite from 19 different hydrothermal mineral deposits, using the same analytical techniques utilized by Savin (1967). They were able to distinguish between supergene and hypogene kaolinites, and they also observed a geographic correlation between the isotopic compositions of the clay minerals and present-day meteoric waters. It was concluded that these clays had largely preserved their original O^{18}/O^{16} and D/H ratios.

Soils: Taylor and Epstein (1964) determined the δO^{18} contents of 13 soils formed on a variety of parent rocks, observing a range in δO^{18} of 10.0—15.9‰ . A soil profile formed on a granite from Elberton, Georgia showed a variation from 8.5‰ for the fresh rock, to 13.5‰ for the most clay-rich zone. The A-zone was observed to have a δO^{18} of +10.1‰ . This was interpreted to be due to larger amounts of residual parent-rock quartz in the A-zone, as a result of differential removal of the O^{18}-rich clay minerals. In addition, they noted that soils appear

to have δO^{18} values about 20‰ higher than the coexisting ground waters. They postulated that δO^{18} values of soils from high elevations or latitudes would have low δO^{18} values, whereas soils from tropical islands such as Hawaii would have high δO^{18} values.

Rex et al. (1969) studied the O^{18}/O^{16} composition of quartz in soils of the Hawaiian Islands and in Pacific pelagic sediments. The uniform and characteristic O^{18}/O^{16} values, unlike either low temperature silica or Hawaiian hydrothermal quartz, indicated an aeolian origin. An aeolian origin was also indicated by the size range and the shard-like morphology of the quartz. These results emphasized the importance of the aeolian contribution to certain soils and sediments on the Earth's surface.

1.3 Isotopic equilibrium

Theoretical: Isotopic exchange reactions may be written in the general form:

$$bB_1 + cC_2 \rightleftharpoons bB_2 + cC_2$$

where B and C are two molecules having an element as a common constituent and the subscripts 1 and 2 refer to the light and heavy isotope, respectively. The standard free energy of such a reaction can be written:

$$\Delta F^\circ = -RT \ln \left[a_{B_1}^b \cdot a_{C_2}^c \Big/ a_{B_2}^b \cdot a_{C_2}^c \right]$$

$$= -RT \ln K$$

where a = the activity of a particular molecule and K equals the equilibrium constant. Because ΔF° for an isotopic exchange reaction is very near zero, equilibrium constants are ordinarily very close to unity. The experimentally determined quantity, the fractionation factor α, is related to the equilibrium constant K as follows:

$\alpha = K^{1/n}$ where n is the number of equivalent exchangeable atoms in the reaction. The equilibrium constant is related to the partition functions of the molecules (Q) as follows:

$$K = \left(\frac{Q_{A_2}}{Q_{A_1}}\right)^{a} \Big/ \left(\frac{Q_{B_2}}{Q_{B_1}}\right)^{b}$$

Urey (1947) developed the detailed theory relating partition functions to observable vibrational frequencies for isotope exchange reactions. He was able to estimate equilibrium constants for a large number of isotopic exchange reactions involving gases and ions in solution. McCrea (1950), employing additional approximations, was able to estimate the equilibrium constant for O^{18}/O^{16} distribution in the calcite-water system. Bottinga (1968) made additional calculations of fractionation factors for the distribution of both O^{18}/O^{16} and C^{13}/C^{12} in the system calcite-carbon dioxide-water. O'Neil et al. (1969), using a modification of McCrea's method, calculated equilibrium fractionation factors for O^{18}/O^{16} distribution between other alkaline-earth carbonates and water. Oxygen and carbon isotopic distributions in reactions involving solid carbonates and aqueous solutions have in certain cases been successfully treated theoretically. However, oxygen isotope exchange reactions involving silicate minerals cannot be successfully calculated at present, and hydrogen isotopic distributions have only been treated theoretically in perfect gas reactions.

Experimental: The approximated partition function formulas of Urey (1947) predict that:

(1) At low temperature, ln K is proportional to $1/T$.

(2) At high temperature, ln K is proportional to $1/T^2$.

(3) At very high temperatures, ln K approaches 0.

Several oxygen isotope equilibrium constants between minerals and H_2O have been investigated experimentally as a function of temperature. The fractionation factors for the pairs calcite-H_2O, quartz-H_2O, feldspar-H_2O and muscovite-H_2O as a function of $1/T^2$ are illustrated graphically in Figure 1-1. Linear extrapolations are made to lower temperatures, even though it is doubtful that this is a completely valid procedure.

Savin (1967) made estimates of fractionation factors for O^{18} distribution at low temperatures for the pairs montmorillonite-H_2O and kaolinite-H_2O using the approximation methods of Taylor and Epstein (1962b). The montmorillonite-H_2O fractionation factor, plotted as a function of $1/T^2$, is illustrated graphically in Figure 1-1. Sheppard et al. (1969) estimated fractionation factors for O^{18} and deuterium distribution at various temperatures for the pairs kaolinite-H_2O, montmorillonite-H_2O, muscovite-H_2O and biotite-H_2O. Theoretical calculations, experimental data and data on natural samples were used to make the approximations. The estimated hydrogen isotope fractionation factors for the pairs kaolinite-H_2O and montmorillonite-H_2O, plotted as a function of $1/T$, are illustrated in Figure 1-2.

1.4 Isotopic exchange in clay minerals

Savin (1967) calculated the amount of low temperature O^{18} exchange in sedimentary minerals that might conceivably occur by solid-state diffusion. His estimates included a range of particle sizes and a range of diffusion coefficients. Diffusion was rejected as a significant mechanism of isotopic exchange, except perhaps for particles $< 10\mu$ in diameter.

Many workers have undertaken experiments attempting to exchange the hydroxyl of clays with D_2O, HTO or H_2O^{18}. For the sake of the following

Figure 1-1. Oxygen isotopic fractionation factors for various mineral-water pairs, plotted as a function of $1/T^2$. Experimentally determined values for the pairs quartz-H_2O (Clayton et al., 1967), feldspar-H_2O (O'Neil and Taylor, 1967), muscovite-H_2O (O'Neil and Taylor, 1969) and calcite-H_2O (O'Neil et al., 1969) are extrapolated to low temperatures. The oxygen isotopic fractionation factor for the pair montmorillonite-H_2O was approximated by Savin (1967) for low temperatures. The oxygen isotopic fractionation factor for the pair kaolinite-H_2O was approximated by Taylor (unpublished data) for low temperatures.

Figure 1-2. Estimated hydrogen isotopic fractionation factors of kaolinite-H_2O and montmorillonite-H_2O, plotted as a function of $1/T$. The estimates are based on theoretical calculations, experimental data and data on natural samples, Savin, 1967; Sheppard et al., 1969, p. 764). Both curves are tentative, and in view of the chemical variations in natural montmorillonites, the montmorillonite-H_2O curve in particular must be considered only an approximation.

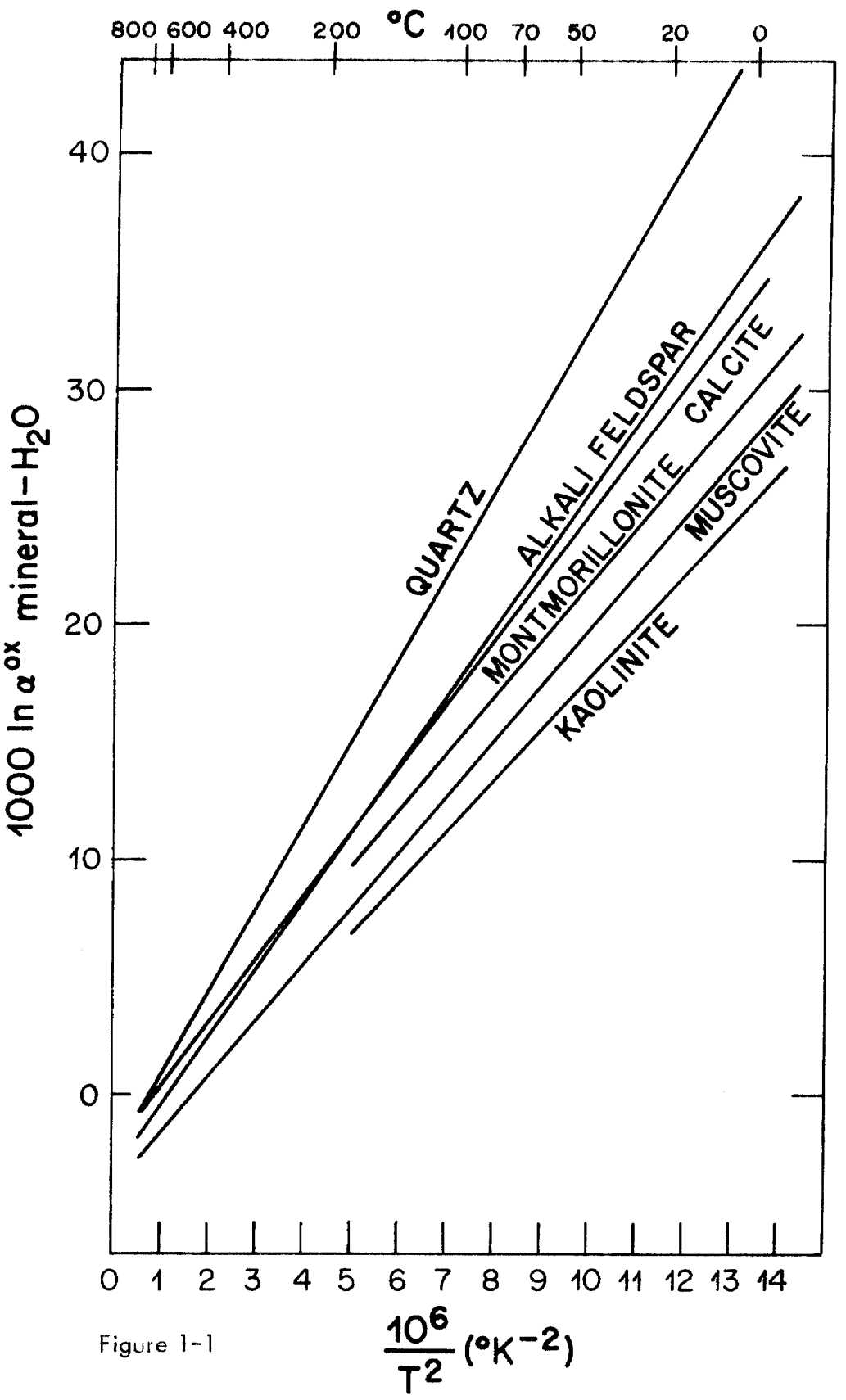
800 600 400 200 °C 100 70 50 20 0
40
30
20
10
0
1000 ln α ox mineral-H2O
QUARTZ
ALKALI FELDSPAR
MONTMORILLONITE
CALCITE
MUSCOVITE
KAOLINITE
0 1 2 3 4 5 6 7 8 9 10 11 12 13 14
10^6/T^2 (°K^-2)

Figure 1-1

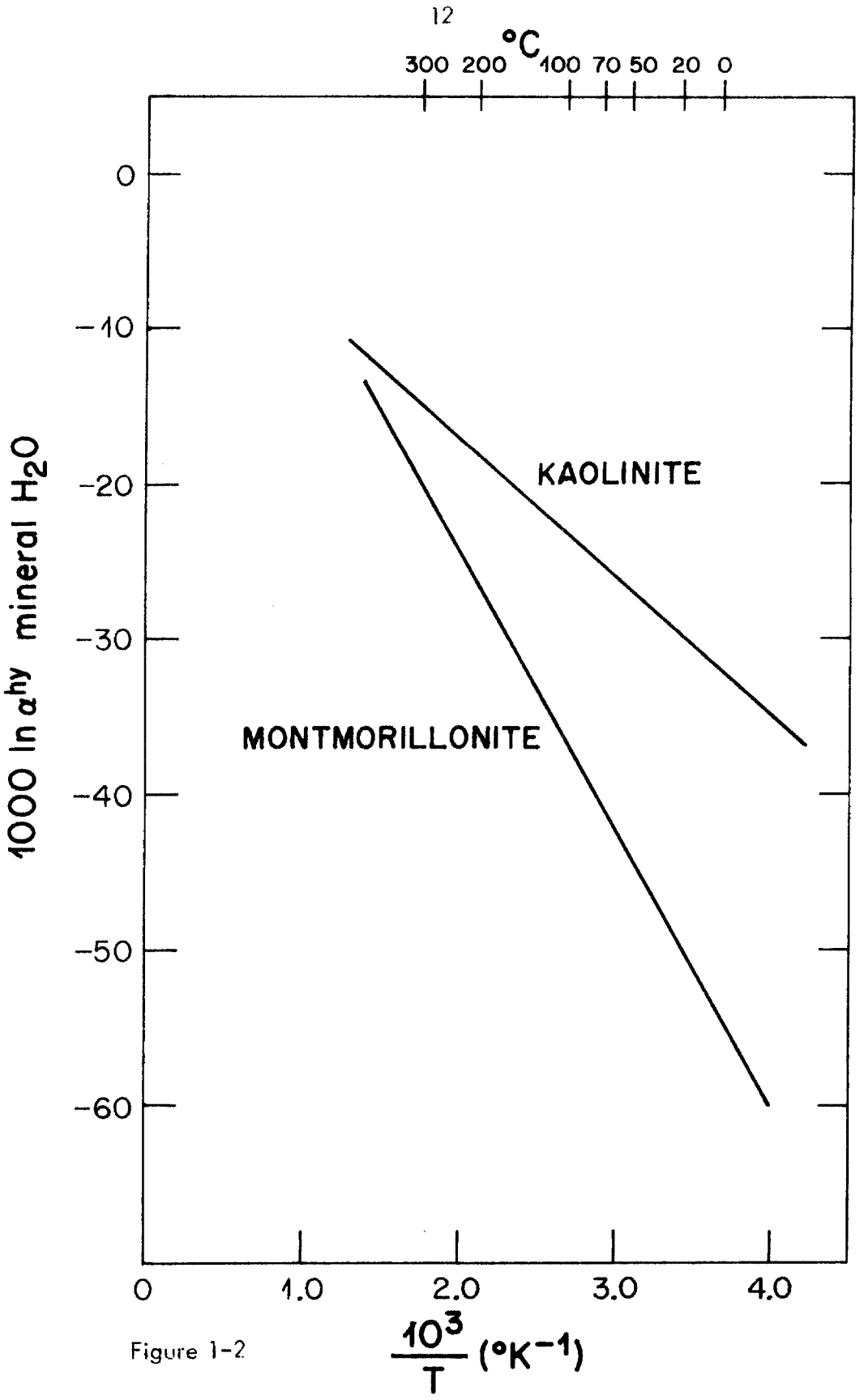
°C
300 200 100 70 50 20 0
0
-10
-20
-30
-40
-50
-60
1000 ln α^{hy} mineral H_2O
KAOLINITE
MONTMORILLONITE
0
1.0
2.0
3.0
4.0
$\frac{10^3}{T}$ (°K^{-1})

Figure 1-2

discussion, the terminology described in Figure 1-3 will be used to specify OH groups in the kaolinite structure. McAuliffe et al. (1947) first investigated the problem using liquid density measurements and concluded that during exchange with D_2O at room temperature, over periods of a few days to a month, all the surface OH ("A" and "B" sites, Figure 1-3) of kaolinite was replaced by OD. This amounts to only about 2-4% of the hydrogen in the mineral.

Roy and Roy (1956, 1957) tried to exchange D_2O with kaolinite, dickite and montmorillonite at room temperature. After drying the clays either at 110°C or 315°C they observed less than 2% exchange for D_2O exposures of 4 days to 4 weeks. Apparently only the "outer hydroxyls", sites "A" and "B", suffered significant exchange. However, with exposure to D_2O at higher temperatures (190°C or 370°C), all three clays displayed considerable exchange, 10 - 50%. Kaolinite exhibited 10% exchange at 190°C when exposed to D_2O for 3 to 4 weeks, while at 370°C it displayed 50% exchange. Hydroxyl sites "C" and "D", and probably "E", must have experienced exchange.

Romo (1956), using infrared methods, found that kaolinite underwent more than 50% exchange with D_2O in a matter of hours at 300°C and 10,000 p.s.i.

Ledoux and White (1964a), using potassium acetate on hydrazine to expand the kaolinite structure, were able to extensively deuterate kaolinite by exposure to D_2O at room temperature, followed by drying at 110°C. Shifts in infrared OH-stretch bands led them to conclude that all the sites, including "C", "D" and "E", underwent exchange. In a follow-up study (1964b) they extended this work and concluded that site "C" exchanged 60 to 67% and sites "D" and "E" exchanged about 22% when expanded with hydrazine, treated with D_2O for 30 minutes at room temperature, and dried at 110°C.

Figure 1-3. Projection of the structure of kaolinite on (100) plane, showing the stacking of successive layers in a microcrystal (modified after Ledoux and White, 1964b). The terminology used to specify the OH groups in the kaolinite structure is as follows: "Outer hydroxyls" refer to structural OH groups at the surface of the microcrystals, including both hydroxyls at the broken edges "A" and hydroxyls of the octahedral sheet found at the upper surface denoted by "B". OH groups located at the surface of the octahedral sheets opposite the tetrahedral oxygens of the adjacent kaolinite layer, and having their OH dipole normal or nearly normal to the (001) plane, are designated by "C". The OH groups at 4.37Å that have their dipoles directed toward an empty octahedral site are designated by "D". The OH groups in the plane common to octahedral and tetrahedral sheets are designated by "E".

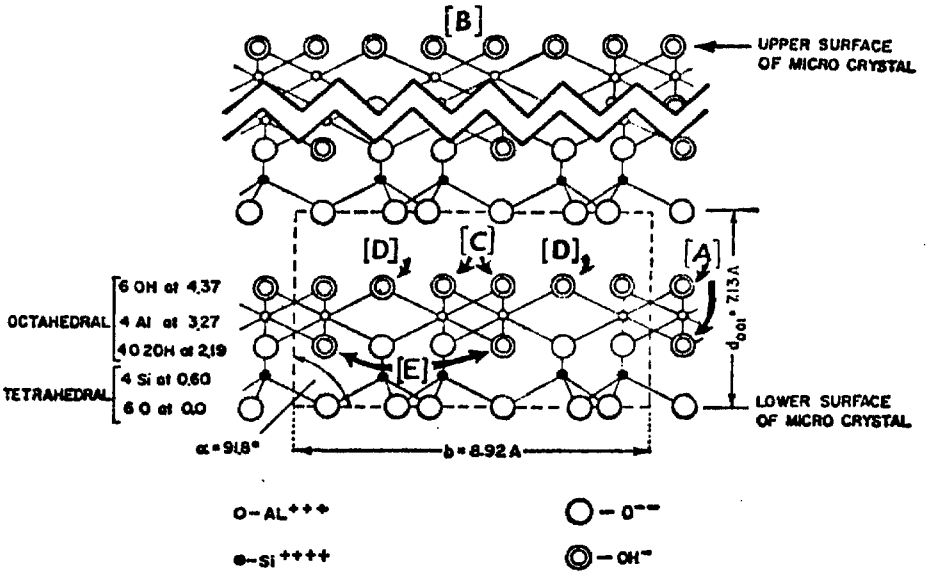
[B]
UPPER SURFACE
OF MICRO CRYSTAL
[D]
[C]
[D]
[A]
[E]
6 OH at 4.37
4 Al at 3.27
4 O 2OH at 2.19
OCTAHEDRAL
4 Si at 0.60
6 O at 0.0
TETRAHEDRAL
d_{001} = 7.13 A
LOWER SURFACE
OF MICRO CRYSTAL
α = 91.8°
b = 8.92 A
O – AL+++
O – O--
● – Si++++
◎ – OH-

Figure 1-3

The relative amount of exchange in site "D" versus "E" is not known, but it is clear that all the inner sites experience significant exchange when the lattice is expanded and intimate exposure to D_2O occurs. A halloysite (American Petroleum Institute No. 12b from Bedford, Indiana) treated by Ledoux and White (1964b) suffered even greater exchange under similar treatment.

An artificially expanded muscovite, when treated in the above manner for 15 hours, showed very little shift in infrared frequencies. Ledoux and White (1946b) concluded that the hydroxyls of muscovite, which are "E"-like sites between layers of silica tetrahedra, are very difficult to exchange at room temperature. The same conclusion might apply as well to montmorillonite, as this mineral can be considered to be analogous to an "expanded muscovite".

Halevi (1964) performed exchange experiments with kaolinite using HTO and H_2O^{18}. The kaolinite, after drying at 110°C, was exposed to HTO and H_2O^{18} by shaking at room temperature for 24 hours, and it then was dried at 350°C. The exchange was less than 0.5%, with roughly equivalent tritium and O^{18} exchange.

Sheppard and Taylor (1970) conducted hydrogen and oxygen isotopic exchange experiments between kaolinite and water at 200° to 300°C and near-neutral pH. Noticeable hydrogen isotope exchange occurred at these temperatures, and hydrogen exchanged much more rapidly than oxygen.

In summary, laboratory experiments demonstrate that very little hydrogen isotope exchange takes place between kaolinite and water at 20° to 110°C. Only the surface hydroxyls of kaolinite are exchanged at room temperature. On the basis of a few isolated experiments we may tentatively infer that this also holds true for illite and montmorillonite. Halloysite, however, which contains interlayer water in direct contact with "C" and "D" sites, is apparently much more

susceptible to hydrogen isotope exchange. In montmorillonite the interlayer water is a few angstroms distant from "E" type hydroxyl sites; it is therefore reasonable that montmorillonite would be somewhat more susceptible to exchange than either kaolinite or illite, but less susceptible than halloysite. At high temperatures, rates of hydrogen isotope exchange are expected to be significant for all clay minerals.

If hydrogen isotope exchange takes place between water and the hydroxyl of a clay mineral, it is likely that oxygen exchange also occurs, though perhaps to a lesser degree. In any event, most of the oxygen in clay minerals is in non-hydroxyl sites. As these oxygens are bonded directly to silicons, they are probably much more difficult to exchange, and it is expected that the bulk oxygen in clay minerals will be less susceptible to exchange than the bulk hydrogen.

II. EXPERIMENTAL PROCEDURES

2.1 Sample collection

Recent weathering products and soils were collected primarily from roadcuts where residual parent-rock features and textures were observable. The clay-rich portions of soil zones, usually the B or C zones, were collected. Sampling was also done along joints or fractures where it was possible to demonstrate that the alteration had been produced by downward percolations of surface waters. In a few cases, clay-rich portions of spheroidally weathered boulders were sampled.

Prior to collection all loose debris was removed from a portion of the roadcut surface. Then 0.5 to 5 kgm of sample was collected from a single site at each locality. In the case of detailed studies of soil profiles, several 0.5 - 5 kgm samples were collected at various sites in the roadcuts. Samples were immediately placed in clean cardboard cartons for storage. Most of the samples were dry or only slightly damp at the time of collection. Because it was not considered to be of importance, no care was taken to maintain the moisture content of the sample at its original level. By the time the samples were removed from the cartons for study, they were all essentially "dry".

Sampling of ancient clay deposits was primarily carried out on outcrops and from open-pit mines. Precautions were taken to insure that samples were fresh and in place. Sampling of the ancient clays was done only on deposits for which detailed geologic descriptions are available in the literature. Several samples were provided by other geologists. A few samples were obtained from the California Institute of Technology rock and mineral collections.

In conjunction with the collection of soils and clay deposits, samples of unweathered parent rock were collected wherever possible. Also several water samples from springs or small streams were collected. Detailed descriptions of all sample localities, in some cases including sketches or photographs of roadcuts, are presented in Appendix I or Chapter V.

2.2 Mineral identification

Mineral identification techniques included X-ray diffraction, differential thermal analysis, visual inspection using a binocular microscope and standard petrographic methods. X-ray diffraction techniques were the most useful for qualitative and quantitative determinations.

All X-ray diffraction studies were conducted using a Phillips X-ray diffractometer, using Ni-filtered Cu-radiation with a chart speed of 1° 2θ per minute, a 1° divergence slit, a 0.006" receiving slit and a 1° scatter slit. Almost all the samples were packed into a standard geometry for X-ray analysis. Clay-rich samples were settled in water onto glass slides in order to enhance basal reflections. Glycolation was used to identify expandable clays. Occasionally, heat treatments described by Warshaw and Roy (1961) were used.

Semiquantitative determinations of mineral abundances were made by visual comparisons of the X-ray charts, using a set of artificially-prepared standards, a fixed packing geometry, and a silicon-metal disk to monitor the received signal. The standard powders were prepared by mixing corundum powder with different proportions of each of the following minerals: quartz, plagioclase, muscovite, kaolinite and montmorillonite. All samples and clay standards were ground to a fine powder. A few illustrative X-ray charts are shown in Appendix II.

In order to determine the variations in intensity of X-ray peaks caused by lack of uniformity in packing procedure and nonuniform grain sizes, some samples were run twice. No significant variations were observed.

Because the intensity of the Cu radiation and/or certain electronic effects were not constant, the signal received by the recorder was monitored by placing a silicon disk in the sample position before each set of samples done on a given day. On a few days the signal intensity was checked several times. In general, hourly variations were insignificant compared with day to day variations.

Differential thermal analysis was a very useful qualitative method when used in conjunction with the X-ray diffraction technique. It confirmed X-ray determinations, allowed the identification of amorphous clays and permitted an estimation of mineral crystallinity not always revealed by X-ray. A few illustrative D.T.A. charts are shown in Appendix II.

A differential thermal analyzer with a Honeywell temperature controller and multipoint recorder was used to analyze six 1-gram samples over a 30° to 1100°C temperature range. The rate of change of temperature was fixed at 500°C per hour.

For two of the weathering profiles studied (the Elberton, Georgia profile and the Big Sur, California profile) petrographic thin sections were made and described. For a few of the samples total iron contents were determined by X-ray fluorescence using mixtures of hematite and corundum powder as standards.

2.3 Mineral separations

Clay minerals were separated from bulk samples using two methods, either handpicking or settling techniques in water solutions. Neither technique

was wholly successful in obtaining pure clay separates, but typically 50-100% concentration was possible. The amounts of weathering products and residual parent minerals in the analyzed samples are indicated in Table 4-1.

The settling techniques were undertaken as follows. 100g of sample were placed in a 800ml beaker with 300ml of Calgon solution at a concentration of 60 g/l . The mixture was stirred for 30 minutes using a motor-driven paddle (100 - 200 r.p.m.). The resulting suspension was then allowed to stand for three minutes. The top 5 cm of the liquid suspension was then poured off. Stoke's law indicated the decanted liquid contained particles less than 20μ in diameter. This suspension was centrifuged four times, washing each time with distilled water.

Handpicking was done on samples where the clay was concentrated along mineral grain boundaries, where the feldspars were differentially altered or where some portion of the specimen was more highly weathered.

The most careful separations were made on samples from profiles studied in detail. In these profiles quartz was concentrated by dissolving all coexisting minerals in HF (aqueous). Ilmenite, hornblende and biotite were separated magnetically with a Frantz separator and then cleaned ultrasonically in a 10% Calgon solution.

2.4 Isotopic analysis

Definition of terms: the δ-notation used to report O^{18}/O^{16} and D/H ratios in this study is defined below.

$$\delta O^{18} = \left[\frac{\left(\frac{O^{18}}{O^{16}}\right)_{sample} - \left(\frac{O^{18}}{O^{16}}\right)_{standard}}{\left(\frac{O^{18}}{O^{16}}\right)_{standard}} \right] \times 1000$$

$$\delta D = \left[\frac{\left(\frac{D}{H}\right)_{sample} - \left(\frac{D}{H}\right)_{standard}}{\left(\frac{D}{H}\right)_{standard}} \right] \times 1000$$

Fractionation factors between two compounds or phases are defined as follows.

$$\alpha^{ox}_{A-B} = \frac{\left(\frac{O^{18}}{O^{16}}\right)_A}{\left(\frac{O^{18}}{O^{16}}\right)_B} \quad ; \quad \alpha^{hy}_{A-B} = \frac{\left(\frac{D}{H}\right)_A}{\left(\frac{D}{H}\right)_B}$$

Oxygen isotopic analyses: The methods of determination of O^{18}/O^{16} ratios used in this study are discussed by earlier workers. Clayton and Mayeda (1963) and Garlick (1964) describe the method of oxygen extraction using bromine pentafluoride. Taylor and Epstein (1962a) discuss the method of oxygen conversion to carbon dioxide. The method of carbon dioxide extraction from carbonates is described by McCrea (1950).

Carbon dioxide samples were analyzed on a mass spectrometer of the type described by Nier (1947) with modifications by McKinney et al. (1950). Because the ratio $\frac{46}{44+45}$ actually measured by the mass spectrometer does not

exactly equal O^{18}/O^{16}, corrections for C^{13} and O^{17} described by Craig (1957) were made. The mass spectrometer background and leakage correction was variable. The correction used was determined by measuring the background each day an isotopic analysis was done. All oxygen isotopic values are reported relative to standard mean ocean water (SMOW) as defined by Craig (1961b). The analytical errors are estimated to be ± 0.1 - 0.2‰ for clay mineral separates and ± 0.3 - 0.4‰ for bulk soil samples.

Two mineralogically pure working standards were used: a kaolinite from Langley, South Carolina originally analyzed by Savin (1967) and a quartz from the Rose Quartz Pegmatite. Their O^{18} isotopic compositions on the SMOW scale are:

kaolinite	+21.70
Rose Quartz	+ 8.42

Using these values, the multiplicative $(1 + R_2/1000)$ and additive (R_2) corrections involved in changing from the mass spectrometer standard to the SMOW standard are given by:

$$\left[1 + \frac{R_2}{1000}\right] \delta^{*}_{ws\text{-}ms} + R_2 = \delta_{ws\text{-}SMOW}$$

where

$$\delta^{*}_{ws\text{-}ms} = \left[\frac{\left(\frac{O^{18}}{O^{16}}\right)_{\text{working standard}} - \left(\frac{O^{18}}{O^{16}}\right)_{\text{mass spectrometer standard}}}{\left(\frac{O^{18}}{O^{16}}\right)_{\text{mass spectrometer standard}}}\right] \times 1000$$

* δ value corrected for O^{17}, background and leakage.

and

$$\delta_{ws\text{-}SMOW} = \left[\frac{\left(\frac{O^{18}}{O^{16}}\right)_{\text{working standard}} - \left(\frac{O^{18}}{O^{16}}\right)_{SMOW}}{\left(\frac{O^{18}}{O^{16}}\right)_{SMOW}} \right] \times 1000$$

These multiplicative and additive corrections were variable due to changes in isotopic compositions of the mass spectrometer standard. Table 2-3 lists the correction values and the formulas used to correct raw δ values to SMOW.

Hydrogen isotopic analyses: The apparatus and methods used to extract hydrogen from clay minerals are described by Savin (1967). The only important modification made in the apparatus was that the CuO was heated to 650°C in a furnace independent of the sample furnace.

The hydrogen isotopic composition of each analyzed sample was contaminated to small extent by the previous sample, due to at least two independent "memory" effects, one involving the CuO furnace and one involving the U furnace. The "memory" effect caused by the uranium furnace was found to be less than 1% (Savin, 1967).

The first order "memory" effect caused by all effects (CuO, uranium and others) was measured and found to be about 4% for 400 to 600 micromole samples. Tables 2-1 and 2-2 illustrate that two independent methods of measuring the combined effects give about the same result. The first order and second order corrections (see Table 2-1) for the total "memory" effect were applied to all data presented in Chapter III because of the stongly contrasting D/H ratios of the samples analyzed. A first order correction was applied to all other data where a greater

TABLE 2-1

The Determination of the "Memory" Effect
of the Hydrogen Extraction Apparatus,
Using D-rich Samples

Sample No.	Experiment No.	Furnace No.	δD SMOW	Percent Memory Effect* 1st order	2nd order	Sample Size μm
12B-JH-61	3-a	2	+324	3.3		640
Standard kaolinite#		2	- 40			550
12B-JH-61		2	+384			590
Standard kaolinite	3-b	2	- 34	4.1		570
Standard kaolinite		2	- 47		1.4	670
Mon-Cal-1-6	3-d	1	+ 56	3.3		170
Standard kaolinite		1	- 49			540
12B-JH-61		2	+544			745
Standard kaolinite	5-a	2	- 27	4.2		715
Standard kaolinite		2	- 45		1.4	575
Mon-Cal-1-6		1	+596			440
Standard kaolinite	5-b	1	- 30	3.4		720
Standard kaolinite		1	- 45		1.2	650
		Average =		3.7%	1.3%	600μm

* Calculations done using deuterium concentrations in ppm.

\# Standard kaolinite $\delta D = -52.5$

TABLE 2-2

The Determination of the "Memory" Effect of the Hydrogen Extraction Apparatus Under Normal Operational Conditions

Sample Group #1	δD‰ sample	δD‰ s.k.	Sample Size*	Sample Group #2	δD‰ sample	δD‰ s.k.	Sample Size*
Cle-Ida-1	-104.7		340	Iny-Cal-5	-67.9		325
s.k.		-54.0	455	s.k.		-52.9	390
Cle-Ida-1	-108.3		360	Coco-Ariz-5	-58.6		
s.k.		-54.8	570	s.k.		-52.3	
L.a.C.-Mon-1	-107.6		340	Coco-Ariz-6	-67.9		
s.k.		-54.7	460	s.k.		-52.8	
Average =	-106.7	-54.5		Average =	-64.8	-52.7	

$$\text{Memory Effect} = \frac{54.5 - 52.7}{106.7 - 64.8} = 4.3\%$$

s.k. = standard kaolinite sample

* in micromoles

TABLE 2-3

Corrections Applied to Oxygen Isotopic Values

Description	Symbol	Correction
O^{17} correction	Q_1	1.001
C^{13} correction (carbonates only)	R_1	0.20 to 0.26
Mass spectrometer background and valve leakage	Q_2	1.020 to 1.050
Change of standard	R_2	+25.0 to +25.3

$$\delta_{x\text{-SMOW}} = Q_1 Q_2 (\delta_{x\text{-ms}}) + R_1 + R_2 + \frac{Q_1 Q_2 (\delta_{x\text{-ms}}) R_2}{1000}$$

where

$$\delta_{x\text{-SMOW}} = \left[\frac{\left(\frac{O^{18}}{O^{16}}\right)_{\text{sample}} - \left(\frac{O^{18}}{O^{16}}\right)_{\text{SMOW}}}{\left(\frac{O^{18}}{O^{16}}\right)_{\text{SMOW}}} \right] \times 1000$$

and

$$\delta_{x\text{-ms}} = \left[\frac{\left(\frac{O^{18}}{O^{16}}\right)_{\text{sample}} - \left(\frac{O^{18}}{O^{16}}\right)_{\text{mass spectrometer standard}}}{\left(\frac{O^{18}}{O^{16}}\right)_{\text{mass spectrometer standard}}} \right] \times 1000$$

than 25‰ difference existed between two samples extracted sequentially. If successive samples differed by less than 25‰, the correction is less than 1‰, whereas the analytical error is ± 2‰ for pure clay samples and ± 4-5‰ for bulk soil samples.

Hydrogen gas samples were analyzed on a Nier-McKinney null type mass spectrometer with a side arm for mass 2. The mass 2 beam consists of H_2^+. The mass 3 consists of HD^+ and H_3^+. A correction for H_3^+ described by Kirshenbaum (1951) and Friedman (1953) was applied to the $(DH + H_3)/H_2$ ratio to convert it to a D/H ratio. A leakage and background correction of 1.01 was used.

All hydrogen isotopic analyses are reported relative to standard mean ocean water (SMOW) as defined by Craig (1961b). All samples were analyzed with respect to a standard reference gas prepared from a standard water.

Multiplicative and additive corrections were used to change the δ-values to the SMOW scale (see Table 2-4).

A National Bureau of Standards water, NBS III, was defined by Craig (1961b) to have a $\delta D = -47.6‰$ relative to SMOW. Using this value the multiplicative and additive corrections involved in changing standards were determined as follows:

$$S_2 \delta^*_{NBS-ms} - T_1 = \delta_{NBS-SMOW}$$

where

$$\delta^*_{NBS-ms} = \left[\frac{\left(\frac{D}{H}\right)_{NBS\ III} - \left(\frac{D}{H}\right)_{\text{mass spectrometer standard}}}{\left(\frac{D}{H}\right)_{\text{mass spectrometer standard}}} \right] \times 1000$$

* δ value corrected for background and leakage.

$$\delta_{NBS-SMOW} = \left[\frac{\left(\frac{D}{H}\right)_{NBS\,III} - \left(\frac{D}{H}\right)_{SMOW}}{\left(\frac{D}{H}\right)_{SMOW}} \right] \times 1000$$

S_2 = multiplicative correction

T_1 = additive correction

Table 2-4 lists the correction values and the formula used to correct δ-values to SMOW.

TABLE 2-4

Corrections Applied to Hydrogen Isotopic Values

Description	Symbol	Correction
Mass spectrometer background and leakage	S_1	1.01
Change of standard		
Multiplicative	S_2	0.931
Additive	T_1	68.75

$$\delta_{x\text{-SMOW}} = S_1 S_2 (\delta_{x\text{-ms}}) - T_1$$

where

$$\delta_{x\text{-SMOW}} = \left[\frac{\left(\frac{D}{H}\right)_{sample} - \left(\frac{D}{H}\right)_{SMOW}}{\left(\frac{D}{H}\right)_{SMOW}} \right] \times 1000$$

and

$$\delta_{x\text{-ms}} = \left[\frac{\left(\frac{D}{H}\right)_{sample} - \left(\frac{D}{H}\right)_{mass\ spectrometer\ standard}}{\left(\frac{D}{H}\right)_{mass\ spectrometer\ standard}} \right] \times 1000$$

III. EXPERIMENTAL EVALUATION OF D/H AND O^{18}/O^{16} ANALYSES OF CLAY MINERALS

3.1 Hydrogen isotopic exchange experiments

General statement: In order to prove the validity of the isotopic techniques utilized to analyze various clay minerals, it was decided to amplify and extend the types of exchange experiments originally undertaken by Savin (1967). The experiments described below demonstrate that at room temperature hydrogen isotope exchange occurs between the interlayer water and some of the hydroxyl of halloysites.

Other experiments show that hydrogen isotope exchange takes place between the interlayer water and hydroxyl of montmorillonites during the normal preliminary heating and outgassing at 130°to 200°C (the method utilized by Savin and Epstein, 1970a, and Sheppard et al., 1969, for analysis of montmorillonites).

These exchange phenomena prevent accurate determinations of the δD of hydroxyl in halloysite, and they add to the difficulties involved in obtaining sound isotopic data on montmorillonites. However, none of these difficulties apply to kaolinites and dickites (or to illites), as it will be shown that only those clay minerals that contain interlayer water provide serious analytical problems.

Procedures: Two halloysites, two montmorillonites, one kaolinite and a bulk-soil sample containing kaolinite, hydrobiotite, quartz and feldspar were exposed at room temperature to waters of different δD contents for a variety of times. The samples used are described in Table 3-1. Each of the samples were dried in a variety of ways and dehydrated in stepwise fashion at different temperatures. The methods of treatment for each sample and all experimental results are

TABLE 3-1

Description of the Samples Used in Hydrogen Isotope Exchange Experiments

Sample No.	Location	Description	Origin	Age
12B-JH-61	Spokane Co., Washington	Moderately - well crystallized halloysite	Weathering Product	Miocene
Ind-H-12 *	Bedford, Indiana	Well crystallized halloysite	Underclay	Pennsylvanian
Mon-Cal-1-6	Big Sur, Monterey Co., California	Poorly crystallized montmorillonite	Weathering Product	Quaternary
Wy-H-26 *	Clay Spur, Wyoming	Well crystallized montmorillonite	Bentonite	Upper Cretaceous
Aik-S.C.-N11-11 *	Langley, Aiken Co., South Carolina	Well crystallized kaolinite	Weathering Product	Upper Cretaceous
G-E-Eg #15-6	Elbert Co., Georgia	Soil on Elberton Granite	Weathering Products	Quaternary

* Analyzed previously by Savin (1967).

listed in Tables 3-2 and 3-3. Samples on which temperature cuts were made are illustrated graphically in Figures 3-1 and 3-2.

One set of experimental procedures was as follows (procedure 1, Table 3-2). Approximately 0.5 to 1.0 g of sample was placed in 4 ml of water of a known isotopic composition, and sealed in a test tube for 48 hours. The wet sample was then placed into a capsule of aluminum foil and put in a dry box for 24 hours. Next the aluminum foil was folded several times to completely enclose the sample, and this was placed into a dessicator while still in the dry box. The aluminum foil capsule was then quickly transferred out of the dessicator to a nickel container and placed in a furnace under an atmosphere of dry air (the air had been passed through a liquid N_2 trap). The sample was outgassed for five minutes, after which the extraction was started. The evolved gases were split into fractions at various temperature intervals for periods ranging from 6 to 24 hours.

A similar set of experiments (procedure 3, Table 3-2) was identical to procedure 1 except that, prior to placement in the dry box, the samples were not immersed in water in the laboratory (i.e., no attempt was made to exchange the interlayer water).

In another set of experiments (procedure 3, Table 3-3) less care was taken to prevent contamination with atmospheric vapor. The samples were placed in D-rich waters for 2 to 10 days. They were then quickly transferred into the dry box. After 1 to 6 days, they were removed from the dry box, weighed, and placed in the vacuum line. During these operations the samples were exposed to the laboratory atmosphere for a total of 15 to 30 minutes. They were then heated and outgassed at 130° to 200°C for a few hours. After outgassing, the furnace temperature was raised to 700° to 900°C and the H_2O was collected for isotope

TABLE 3-2

HYDROGEN ISOTOPIC EXCHANGE EXPERIMENTS, PROCEDURES 1 AND 2

Sample No.	Experiment No.	Method of Treatment: δD of Water	Exposure Time[a]	Dry box Time[a]	Temperature Fractions: 30° to 200°C Time[a]	30° to 200°C δD	30° to 300°C Time[a]	30° to 300°C δD	200° to 400°C Time[a]	200° to 400°C δD	400° to 600°C Time[a]	400° to 600°C δD	200° to 900°C Time[a]	200° to 900°C δD	300° to 700°C Time[a]	300° to 700°C δD	400° to 900°C Time[a]	400° to 900°C δD	600° to 900°C Time[a]	600° to 900°C δD	δ_3[e]	δ_4[e]	X_1[f]	X_2[g]	δ_2[e]	δ_1[e]	P[e]
		Procedure 1																									
12B-JH-61	1-a	+1690	48	24	7	+ 92			10	+401							22	+383[d]			+345	+383	.11	.89	- 72	+3140	31
"	1-b	+1690	48	24			26	382							17	+380											
"	1-c	+1690	68	24	72	+785[c]			6	+552							37	+476[d]			+541	+517	.09	.91	- 72	+6732	41
"	1-d	- 70	49	24	6	- 19			9	- 43	14	- 45							24	- 18							
"	1-e	- 407	48	31	3.5	b							24	-106													
Ind-H-12	1-f	+1690	51	24	6	+111			10	+283							24	+223[d]			+258	+271	.08	.92	- 40	+3688	17
Mon-Cal-1-6	1-g	+1690	48	24	10	+1105			11	+619							22	+482[d]			+806	+569	.44	.56	- 45	+1900	
Wy-H-26	1-h	+1690	46	30	6	+516			11	+269	6	+108							16	+137	+222	+143	.20	.80	-100	+1515	
		Procedure 2																									
12B-JH-61	2-a	No Treatment		24	6	- 68			10	- 71	11	- 78							24	- 78		- 72					
Mon-Cal-1-6	2-b	No Treatment		24	6	- 20			10	- 42	8	- 45							28	- 36		- 43					

[a] Time given in hours

[b] Outgassed to the High Vacuum

[c] Three temperature fractions combined (30° to 50°C, 50° to 100°C and 100° to 200°C)

[d] Two temperature fractions combined (400° to 600°C and 600° to 900°C)

[e] δ_1, δ_2, δ_3, δ_4 and P are defined in Figure 3-1

[f] mole fraction of the total H_2 in the 30° to 200°C cut

[g] mole fraction of the total H_2 in the 200° to 900°C cut

TABLE 3-3

Hydrogen Isotopic Exchange Experiments, Procedures 3, 4 and 5

Sample No.	Experiment No.	Heavy Water Treatment δD	Heavy Water Treatment Time of Exposure	Drying Procedure	Vacuum Outgassing Temp. (°C)	Vacuum Outgassing Time (hrs.)	Collection Procedure Temp. (°C)	Collection Procedure Time (hrs.)	δD
				Procedure 3					
12B-JH-61	3-a	+1690	72 hrs.	D.B. 24 hrs. A.E. 15-30 min.	30 200	3 4	900	10	+338
"	3-b	+1690	50 hrs.	D.B. 5 days A.E. 15-30 min.	200	6	900	11	+400
"	3-c	+1690	10 days	D.B. 23 hrs. A.E. 15-30 min.	200	6	900	11	+512
Mon-Cal-1-6	3-d	+1690	72 hrs.	D.B. 24 hrs. A.E. 15-30 min.	30 130	3 4	700	14	+ 60
"	3-e	+1690	50 hrs.	D.B. 5 days A.E. 15-30 min.	130	6	700	11	- 23
"	3-f	+1690	10 days	D.B. 6 days A.E. 15-30 min.	130	4	700	12	+ 6
Aik-S.C.-N11-11	3-g	+1690	48 hrs.	D.B. 31 hrs. A.E. 15-30 min.	200	3	900	12	- 55
G-E-Eg #15-6	3-h	+1690	27 days	D.B. 23 hrs. A.E. 15-30 min.	130	6	700	11	+ 35

TABLE 3-3 (continued)

Sample No.	Experiment No.	Heavy Water Treatment δD	Time of Exposure	Drying Procedure	Vacuum Outgassing Temp. (°C)	Time (hrs.)	Collection Procedure Temp. (°C)	Time (hrs.)	δD
				Procedure 4					
12B-JH-61	4-a	+1690	10 days	D.B. 23 hrs. A.E. 5 days	200	4	900	12	-364
Mon-Cal-1-6	4-b	+1690	71 hrs.	D.B. 24 hrs. A.E. 13 days	130	8	700	16	- 5
12B-JH-61	4-c	+1690	42 hrs.	D.A. 15 days	200	8	900	16	- 50
				Procedure 5					
12B-JH-61	5-a	+1690	42 hrs.	A.E. 90 min. S.W.	200	6	900	15	-566
Mon-Cal-1-6	5-b	+1690	42 hrs.	A.E. 90 min. S.W.	130	6	700	14	-620

D.B. - Time in dry box
A.E. - Lab Atmosphere Exposure
D.A. - Dried in Lab Atmosphere
S.W. - Still Wet

Figure 3-1. Quantities and hydrogen isotopic compositions of various temperature fractions, for H_2O extraction from halloysites by procedures 1 and 2. The heights of the bars indicate the percent of the total hydrogen in a given temperature fraction. The δD values for each cut (temperature fraction) are indicated. δ_1 = δD in the original interlayer water; δ_2 = δD in the original hydroxyl of the clay mineral; δ_3 = δD of the total sample, a weighted average of all the temperature fractions; δ_4 = observed δD of the 200° to 900°C temperature fraction assumed to be entirely from the OH sites; and P = percent of exchangeable OH sites in the clay mineral.

Figure 3-2. Quantities and hydrogen isotopic compositions of various temperature fractions, for H_2O extracted from montmorillonites by procedures 1 and 2. The heights of the bars indicate the percent of the total hydrogen in a given temperature fraction. The δD values for each cut (temperature fraction) are indicated. δ_1, δ_2, δ_3 and δ_4 are as defined in Figure 3-1.

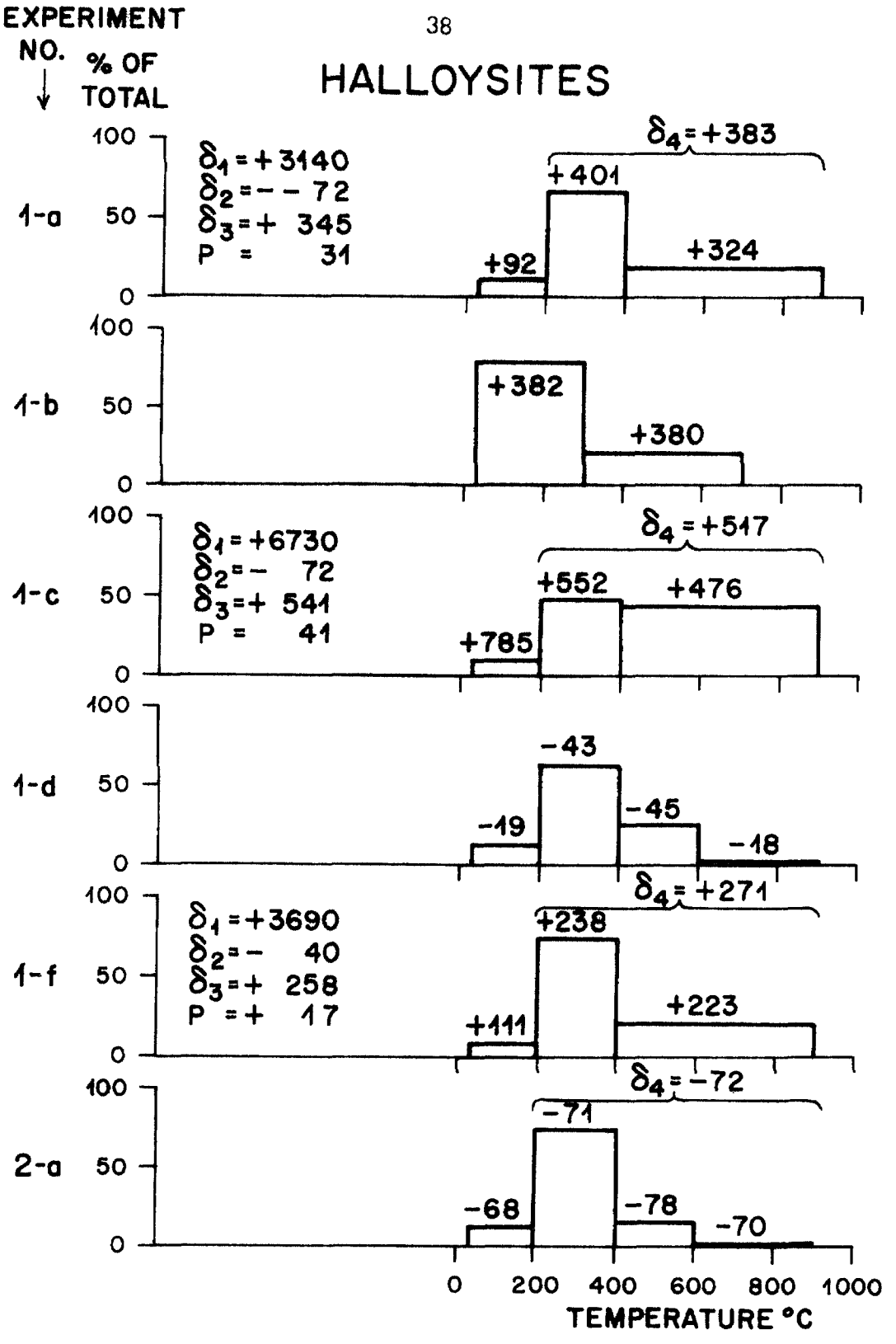
EXPERIMENT NO.
% OF TOTAL
HALLOYSITES
1-a
δ1 = +3140
δ2 = - - 72
δ3 = + 345
P = 31
δ4 = +383
+401
+92
+324
1-b
+382
+380
1-c
δ1 = +6730
δ2 = - 72
δ3 = + 541
P = 41
δ4 = +517
+552
+476
+785
1-d
-43
-45
-19
-18
1-f
δ1 = +3690
δ2 = - 40
δ3 = + 258
P = + 17
δ4 = +271
+238
+223
+111
2-a
δ4 = -72
-71
-68
-78
-70
100
50
0
0 200 400 600 800 1000
TEMPERATURE °C

Figure 3-1

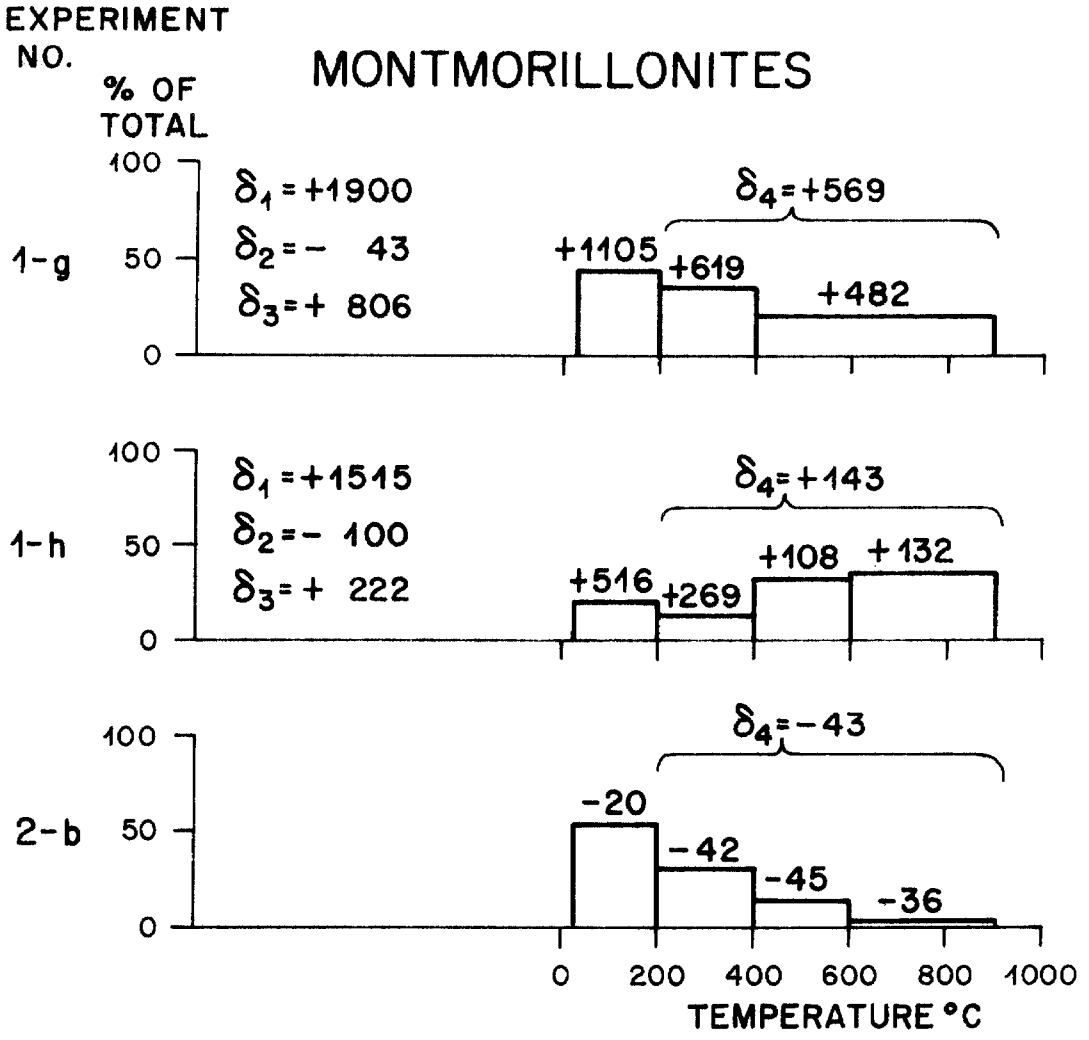
EXPERIMENT NO.
MONTMORILLONITES
% OF TOTAL
100
50
0
1-g
δ1 = +1900
δ2 = − 43
δ3 = + 806
δ4 = +569
+1105
+619
+482
1-h
δ1 = +1515
δ2 = − 100
δ3 = + 222
δ4 = +143
+516
+269
+108
+132
2-b
δ4 = −43
−20
−42
−45
−36
0
200
400
600
800
1000
TEMPERATURE °C

Figure 3-2

measurement.

Procedure 4 (Table 3-3) was similar to procedure 3 except that the samples were exposed to the laboratory atmosphere for 5 to 15 days either after dry-box exposure (experiments 4-a and 4-b) or without using the dry box at all (experiment 4-c).

In procedure 5 (Table 3-3) the samples were placed in D-rich waters for 42 hours, and while still wet with D-rich water, were placed in the vacuum line. They were outgassed at 130° to 200°C, after which the remaining H_2O (residual interlayer water plus hydroxyl water) was collected at 700° to 900°C.

Discussion of procedure 2: The data for experiment numbers 2-a and 2-b are illustrated graphically in Figures 3-1 and 3-2. Inasmuch as these experiments involved untreated clay samples, the data are useful in connection with the interpretation of experiments on samples treated with low- and high-D waters. Note that the δD values of the three fractions of H_2O collected above 200°C are very uniform (± 4 or 5 per mil) for each sample. Even though the 600°to 900°C fraction represents less than 5% of the total sample, its δD is almost identical to that of the H_2O evolved at lower temperatures. Savin (1967) observed similar relationships for two montmorillonites and a kaolinite.

Discussion of procedure 1: The isotopic composition of the interlayer water of montmorillonite has been shown to equilibrate with that of atmospheric H_2O vapor in a matter of days (Savin, 1967). The interlayer water of the montmorillonites in the present experiments (and presumably the halloysites as well) are therefore almost certainly exchanged after immersion in water for 48 hours. However, it must be remembered that drying the samples in the dry box could result in some enrichment in δD of the interlayer water (perhaps as much as 60‰,

see section 3.2). Also, exposure to the atmosphere for even a few minutes could result in partial rehydration of the interlayer water site, with a resulting change in δD of the interlayer water.

Inspection of the δD values of the various temperature fractions in experiments 1-a, 1-c, 1-f, 1-g, and 1-h (see Figures 3-1 and 3-2) points out that hydrogen isotopic exchange between the D-rich interlayer water and the hydroxyl has taken place either at room temperature or during outgassing at 30°to 200°C. If no hydrogen isotopic exchange had taken place, the 30° to 200°C temperature fraction (i.e., interlayer water) should have a δD of approximately $+1690‰$, and the 200°to 900°C fraction should have a δD of $-40‰$ to $-100‰$.

In order to determine whether the hydrogen isotopic exchange took place at room temperature or whether it took place during outgassing at 30° to 200°C, it is instructive to consider a simple model involving the following assumptions: (1) no exchange between interlayer water and hydroxyl occurred at room temperature; (2) the 30° to 200°C cut gives the total amount of interlayer water in the sample, but this interlayer water is assumed to have exchanged with the hydroxyl of the clay minerals during outgassing; and (3) the cuts above 200°C give the total amount of original hydroxyl, but this had previously undergone exchange with interlayer water during the 30° to 200°C outgassing.

Material balance calculations of the following type were made in the above experiments. For a given clay mineral, assuming the above model:

$$X_1\rho_1 + X_2\rho_2 = \rho_3$$

where

X_1 = mole fraction of hydrogen in the interlayer water (the 30° to 200°C cut)

X_2 = mole fraction of hydrogen in the hydroxyl (the 200° to 900°C cut)

ρ_1 = ppm deuterium in the original interlayer water

ρ_2 = ppm deuterium in the original hydroxyl of the clay mineral

ρ_3 = ppm deuterium of the total sample, a weighted average of the measured D/H ratios of all the temperature fractions

$\rho = 157\left(1+\frac{\delta D}{1000}\right)$, where the concentration of D in SMOW is assumed to be equal to 157 ppm (Craig, 1961b).

The original δ value of the interlayer water, δ_1, can be calculated on the basis of the model described above, because we measure the δ-value of the total sample, δ_3, and we know from previous analyses the approximate δ-value of the OH in the original sample, δ_2.

For experiments 1-g and 1-h the material-balance calculations yield δD values of +1900 and +1515‰ for the original interlayer water, a value similar to that of the δD of the water used in the actual experiments (+1690‰). This suggests that the original assumptions of the model are essentially valid for these two experiments. Note that both samples are montmorillonites.

For experiments 1-a, 1-c and 1-f, in which halloysite samples were used, the calculations yield abnormally high δD values for the interlayer water, +3140, +6730 and +3690 respectively. This undoubtedly represents a failure of assumption (1) indicating that significant hydrogen isotope exchange between interlayer water and hydroxyl has taken place at room temperatures. Hence, halloysites differ markedly in their isotopic behavior from the montmorillonites. This conclusion is in agreement with the work of Ledoux and White (1964b) who found that "C" sites

(see Figure 1-1) in expanded kaolinites and halloysites exchange very readily at low temperatures. It is essentially impossible for a failure of assumptions (2) and (3) to account for such anomalously high δ D values as those calculated above.

For experiments 1-a, 1-c and 1-f, another set of material-balance calculations can be made based upon a second model in which we assume that all exchange between interlayer water and OH occurs at room temperature and that it is complete for certain OH sites (e.g. the "C" sites) and nonexistent for all other OH sites in the clay mineral. For simplicity we also make the approximation that the equilibrium fractionations between external water, interlayer water, and OH are zero. The material balance equation utilized was:

$$(1-P)\rho_2 + P(423) = \rho_4$$

where 423 is assumed to be the original ppm of D in the interlayer water. Also,

ρ_2 = ppm deuterium of the original hydroxyl prior to treatment,

ρ_4 = observed ppm of deuterium of the 200° to 900°C temperature fraction, assumed to be entirely from the OH sites, and

P = percent of exchangeable OH sites in the clay mineral.

Utilizing the above model, calculations were made to determine P for halloysite. The percentages, 31, 41 and 17%, respectively for experiments 1-a, 1-c and 1-g would suggest 50-80% exchange of "C" sites (50% of the total hydroxyl, Figure 1-1) in good agreement with the interpretations of Ledoux and White (1964b). This model therefore indicates that the isotopic experiments can be explained by partial exchange at room temperature between the most easily exchanged OH sites and interlayer water.

For the cut taken at 30° to 200°C, experiment 1-c displays a much higher δD value than is observed in either experiment 1-a or 1-f. The reason for this anomaly is unknown, but it conceivably could be the result of rehydration of the halloysite in the latter experiments during the brief time (60 seconds) the halloysites were exposed to the atmosphere. The halloysite of 1-c apparently did not rehydrate as much as in 1-a or 1-f, if at all.

During outgassing at 30° to 200°C some exchange between the new δD of the interlayer waters and hydroxyl of the halloysites in 1-a and 1-f must have occurred, meaning that the δD of the 30° to 200°C cut of 1-a and 1-f must have been even lower before outgassing, and the δD of the 30° to 200°C cut of 1-c must have been higher. Therefore the values of P calculated above are minimum percentages for room-temperature exchange in 1-a and 1-f but represent a maximum value for 1-c.

The dehydration experiment 1-b (see Figure 3-2) was carried out in only two steps. Apparently, virtually complete homogenization of interlayer water and hydroxyl δD contents was achieved at temperatures below 300°C. The fraction at 30° to 300°C undoubtedly represents interlayer water and some hydroxyl, and it is presumed that the 300° to 700°C fraction represents only the remaining hydroxyl.

Experiment 1-e (data shown only in Table 3-2) illustrated that low-D water has apparently exchanged with halloysite hydroxyl at room temperature, as the measured 200° to 900°C fraction is about 30‰ lower in δD than the original OH in the mineral (see experiment 2-a).

In experiment 1-d, a halloysite was exposed to ordinary tap water. Figure 3-1 illustrates that the δD values of all fractions in experiment 1-d were heavier than the untreated sample of experiment 2-a. The δD value of the adsorbed

water in halloysite 1-d was undoubtedly raised by evaporation, as the sample was still very wet when it was placed in the dry box. The hydroxyl of the halloysite apparently exchanged with the adsorbed water as it evaporated, thereby producing the high δD values.

Discussion of procedures 3 and 4: The δD values of the 200° to 900°C cut from montmorillonites subjected to procedure 3 (Table 3-3) were abnormally low compared to the δD values of those from experiments 1-g and 1-h (see Figure 3-2). This also applies to the montmorillonites of experiment 4-b. These effects probably result from rehydration of the montmorillonites with water vapor from the atmosphere, as the samples in procedure 3 were all exposed for at least 15 - 30 minutes. The 1690‰ interlayer water was thus diluted by atmospheric H_2O having a δD of approximately -70‰. This new interlayer water then exchanged with the montmorillonite hydroxyl during subsequent heating and outgassing.

The δD values of the 200° to 900°C cut from halloysites subjected to procedure 3 were heavy and very similar to δD values of those of the higher temperature fractions of experiments 1-a, 1-c and 1-f (see Figure 3-1). Apparently the heavy δD values of the hydroxyl, which had resulted from exchange with heavy water for 2 to 10 days at room temperature, were not subject to much exchange with atmospheric H_2O in the short 15 - 30 minute period of exposure to the atmosphere.

A kaolinite subjected to procedure 3, experiment 3-g, apparently did not undergo any room temperature exchange between heavy water and hydroxyl; the δD value was identical to that obtained in the "normal" manner (see Table 4-3).

In bulk soil experiment 3-h exchange probably occurred between the hydroxyl and interlayer water of the hydrobiotite during outgassing at 130°C, or some heavy interlayer water still remained after outgassing at 130°C. It is highly

unlikely that the coexisting kaolinite underwent any significant exchange (see previous paragraph).

The halloysite in experiment 4-a, after heavy water treatment, probably contained hydroxyl with a δD similar to that in the 200° to 900°C cut of experiment 3-c (+512). Sample 4-a, however, was exposed to the atmosphere for 5 days; this probably allowed its hydroxyl to slowly approach isotopic equilibrium with atmospheric H_2O, yielding the lower δD value (+364‰).

The halloysite of experiment 4-c, after isotopic exchange with D-rich water, was dried for 15 days in air. Apparently the hydroxyl, after initially exchanging with the heavy water, reequilibrated with atmospheric H_2O-vapor and returned to an almost "normal" value (it approaches the value obtained in experiment 2-a).

Discussion of procedure 5: The greatest degree of contamination of the 200° to 900°C cut by D-rich waters is observed in procedure 5, for both montmorillonite and halloysite. This is undoubtedly the result of exchange between the water in the wet samples and mineral hydroxyl at low temperature in the case of halloysite, and at outgassing temperatures in the case of both the halloysites and the montmorillonite.

3.2 Systematic treatment of samples equilibrated with atmospheric H_2O vapor

Several montmorillonite samples of a variety of origins were subjected to a precise sequence of treatments. The object of these experiments was to determine the nature and the degree of hydrogen isotope exchange taking place between the interlayer water and the hydroxyl during heating and outgassing.

The method of treatment was as follows. 200 to 500g of sample were placed in an open Petri dish. Air from the normal laboratory atmosphere was circulated over the sample for 7 to 9 days. The sample was then placed in a nickel capsule in a high vacuum line and outgassed for exactly 20 minutes. The sample was sealed off and the furnace was turned up to 200°C for 12.0 ± 0.3 hours. The water driven off was collected in a liquid nitrogen trap and its δD value was determined in the usual manner. The temperature of the furnace was then increased to 900°C for 6 to 12 hours and the H_2O driven off from the sample was collected and isotopically analyzed. All the results are given in Table 3-4.

The interlayer waters that remained after 20 minutes of outgassing at room temperature, representing only 10 to 30% of the original interlayer water, exhibit a range of δD values from -79 to +4 . Presumably, prior to outgassing, all the interlayer waters had similar δD values of about -50‰ (i.e., typical water in equilibrium with Pasadena H_2O vapor).

Two effects are responsible for the change in δD from this initial value of -50‰. First, evaporation during the 20 minute outgassing period undoubtedly increases the δD of the residual interlayer water. However, no correlation is observed between the δD of the 30° to 200°C cut and the ratio of interlayer water to total H_2O in the sample. Secondly, in the light of the results in section 3.2, we know that the interlayer water can exchange with the hydroxyl of the mineral during the 30° to 200°C outgassing. Assuming a montmorillonite hydroxyl-water fractionation of about 15 to 20‰ at 150° to 200°C (see Figure 1-2), such exchange would in most cases tend to lower the deuterium content of the interlayer water, because the δD of the hydroxyl is generally more than 15 to 20‰ lower than that of the interlayer water.

TABLE 3-4

Isotopic Data on Montmorillonites Equilibrated with Atmospheric Water Vapor and Subjected to Systematic Analysis

Sample No.	Description	D.T.A. Peaks	Interlayer Water 30° to 200°C: H_2 yield μm/mg	Interlayer Water 30° to 200°C: mole fraction of total H_2 (X_1)[b]	Interlayer Water 30° to 200°C: δD (δ_a)[b]	Hydroxyl Water 200° to 900°C: H_2 yield μm/mg	Hydroxyl Water 200° to 900°C: mole fraction of total H_2 (X_2)[b]	Hydroxyl Water 200° to 900°C: δD (δ_b)[b]	δO^{18} calculated[a]	δD calculated (δ_d)[b]
L.a.C.-Mon-2	Holocene Soil	S150 W800	0.68	.38	-33	1.09	.62	- 96	+11.9	-122
Park-Wyo-1	Holocene Soil	M150 W660	0.58	.24	-24	1.86	.76	-114	+10.5	-125
Mon-Cal-1-6	Holocene Soil	M120 W830	1.52	.46	-37	1.81	.54	- 51	+19.2	- 91
Was-Ore-6	Miocene Fossil Soil	S140 W830	2.17	.52	-27	2.02	.48	- 88	+10.7	-128
Wy-H-26	Bentonite	S150 S710 M880	0.47	.16	+ 4	2.42	.84	-115	+17.6	-116
Cal-H-24	Bentonite	S180 M680 M840	2.96	.54	-36	2.54	.46	- 50	+19.0	-104

TABLE 3-4 (continued)

Sample No.	Description	D.T.A.[c] Peaks	Interlayer Water 30° to 200°C: H_2 yield μm/mg	Interlayer Water 30° to 200°C: mole fraction of total H_2 (X_1)[b]	Interlayer Water 30° to 200°C: δD (δ_a)[b]	Hydroxyl Water 200° to 900°C: H_2 yield μm/mg	Hydroxyl Water 200° to 900°C: mole fraction of total H_2 (X_2)[b]	Hydroxyl Water 200° to 900°C: δD (o_b)[b]	δO^{18}[a] calculated	δD calculated (δ_d)[b]
Wes-Wyo-1	Bentonite	S120 M700	0.31	.11	-26	2.62	.89	-120	+18.9	-124
TW-1-50-F-M	Oceanic Dredge Haul	S120 W800	2.11	.52	- 4	1.98	.48	- 64	+26.1	- 79
Carr II	Oceanic Dredge Haul	S120 W800	1.37	.42	-79	1.92	.58	-102	+25.8	-167

[a] see Table 4-1

[b] for definitions of δ_a, δ_b, δ_d, X_2, X_1 see text

[c] for definitions of D.T.A. peak symbols, see footnotes and abbreviations, Table 4-1

The data in Table 3-4 suggest that the residual interlayer water remaining after the 20 minute outgassing at 25°C is generally enriched in δD by evaporation, by at least 20 to 60 per mil. Therefore during later exchange in the temperature interval 30°to 200°C, the hydroxyl of the montmorillonite would be enriched in deuterium. If this condition prevails, the actual OH of a montmorillonite sample would be considerably lower in δD than the measured δD value. It is therefore instructive to examine the data in Table 3-4 in more detail.

All of the samples shown in Table 3-4 and Figure 3-3, with the exception of Was-Ore-6, are montmorillonites of a low temperature origin. The three Quaternary soils and the three bentonites probably were formed at about 15° to 25°C. The two oceanic montmorillonites probably formed at about 0°to 5°C (i.e., Holocene ocean bottom temperatures). Was-Ore-6, a fossil soil, probably formed at Earth-surface temperatures, but it was later buried by a lava flow and probably reequilibrated with H_2O at a higher temperature.

If the hydrogen and oxygen isotopic compositions of the montmorillonites, excluding interlayer water, represent preserved equilibrium values, the samples must have equilibrated with meteoric waters, ocean waters, or mixtures of the two. For a given temperature, δD and δO^{18} values should therefore plot on a line roughly parallel to the meteoric water line. Savin's (1967) montmorillonite line for 15° to 25°C is shown in Figure 3-3.

The lengths of the bars in Figure 3-3 represent the percent of the total hydrogen present in interlayer water (i.e., the 30° to 200°C fraction) after room-temperature outgassing for 20 minutes. Ignoring the fossil soil and the oceanic montmorillonites because they do not represent samples equilibrated at 15° to 25°C, a systematic pattern of displacement above Savin's (1967) montmorillonite line is observed. Those montmorillonites that contain a larger proportion of interlayer

Figure 3-3. A $\delta D - \delta O^{18}$ plot for montmorillonites equilibrated with atmospheric water vapor. The samples were subjected to a systematic extraction procedure (see text). For reference, the kaolinite line and montmorillonite line of Savin and Epstein (1970a) are shown. The relative amounts of interlayer water to hydroxyl, are indicated by the bar lengths. δD values of the hydroxyl, corrected for maximum plausible interlayer-water contamination, are shown by X's .

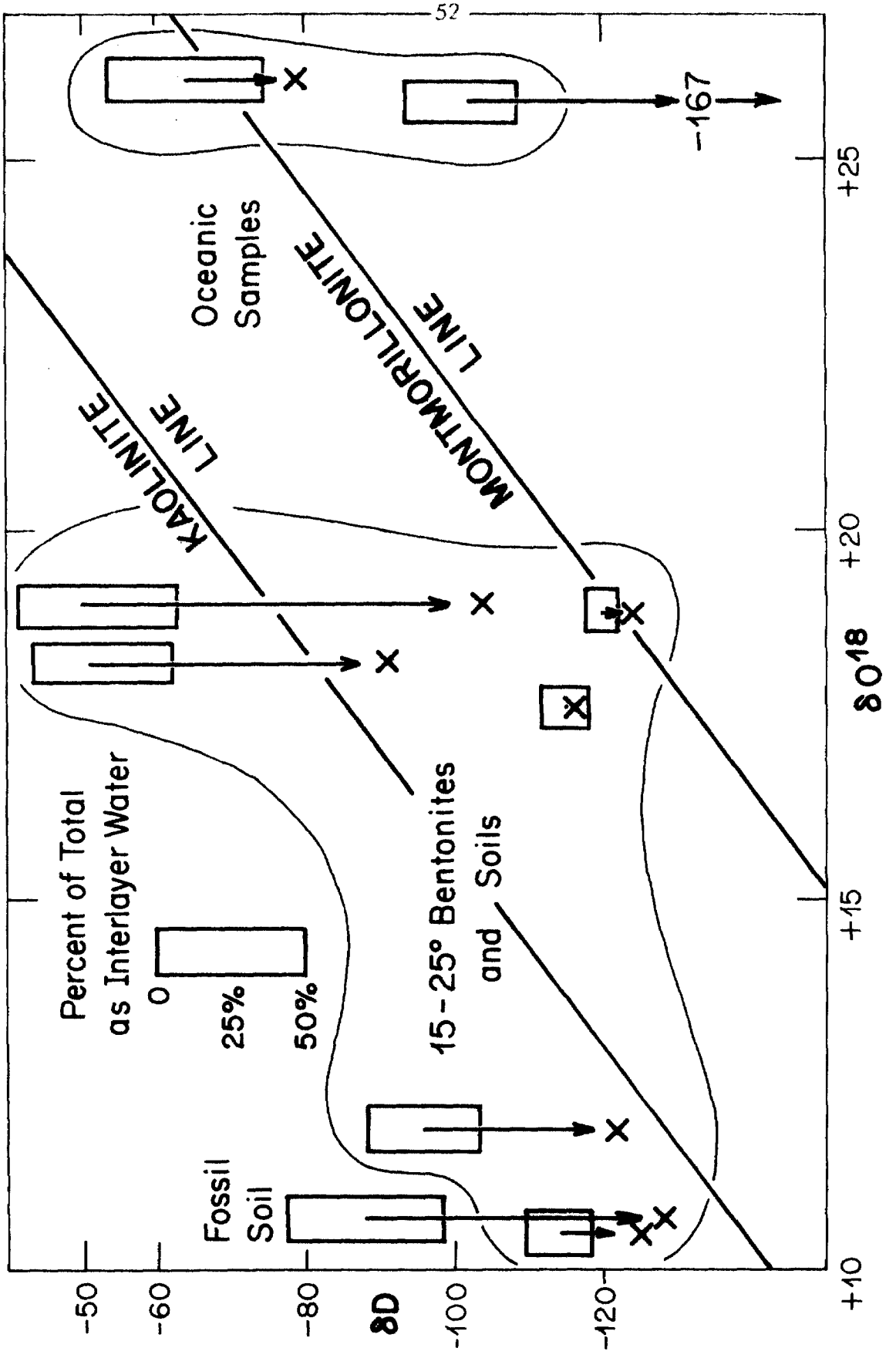
Oceanic Samples
MONTMORILLONITE LINE
KAOLINITE LINE
Percent of Total as Interlayer Water
0
25%
50%
15-25° Bentonites and Soils
Fossil Soil
-167
δD
δO18
-50
-60
-80
-100
-120
+10
+15
+20
+25

Figure 3-3

water to hydroxyl display greater divergence from the montmorillonite line. This suggests, if Savin's montmorillonite line is valid, and if the assumption concerning preservation is correct, that contamination of hydroxyl hydrogen by isotopic exchange with interlayer water is directly related to the proportion of interlayer water in the mineral at the time of heating and outgassing.

In order to estimate the maximum plausible δD correction of the montmorillonite hydroxyl, approximate material balance calculations of the following type were made on each montmorillonite.

$$X_1 \delta_a + X_2 \delta_b = X_1 \delta_c + X_2 \delta_d$$

X_1 = mole fraction of hydrogen in the 30° to 200°C temperature fraction

X_2 = mole fraction of hydrogen in the 200° to 900°C temperature fraction

δ_a = measured δD of the 30° to 200°C temperature fraction

δ_b = measured δD of the 200° to 900°C temperature fraction

δ_c = 10, maximum reasonable δD of the interlayer water prior to 30° to 200°C outgassing. $\delta_c = +10$ is slightly higher than the heaviest 30° to 200°C cut observed (sample no. Wy-H-26)

δ_d = calculated δD of the hydroxyl prior to 30° to 200°C outgassing (i.e., the points labeled by X's in Fig. 3-3)

For most montmorillonites, $X_1 = 0.6$ to 0.9 under normal atmospheric conditions. A change in X_1 from 0.8 to 0.5 represents about 75% evaporation. A change in X_1 from 0.8 to 0.1 represents more than 95% evaporation. Sample Wy-H - 26 thus must have undergone about 90% evaporation during the 20 minute outgassing period; this resulted in a $\delta = +4$. It therefore seems highly unlikely that δ_c could be much greater than +10‰ for any of these montmorillonites.

The values calculated by the above method are listed in Table 3-4 and illustrated in Figure 3-3. Although these corrections place the sample isotopic compositions nearer to Savin's (1967) montmorillonite line, some of the samples plot in the vicinity of the kaolinite line or intermediate to the two lines. This perhaps raises a question whether or not it is valid to assume that all montmorillonites formed at 15° to 25°C in the presence of meteoric H_2O should in fact plot on a single "line". For example, variations in chemical composition, particularly changes in Al/Si or Fe content, could result in variations in isotopic behavior. Possible reasons for the observed large scatter in the D/H and O^{18}/O^{16} values of montmorillonites are discussed subsequently in section 5.3, Chapter VIII, and Chapter X.

Until further work is undertaken to understand more thoroughly the nature and the degree of exchange between hydroxyl and interlayer water during heating and outgassing, it is suggested that hydrogen isotope analyses of montmorillonites be done systematically in two steps. After a fixed time period of cold outgassing, preferably several hours, the water given off below 200°C should be collected and its δD value measured. Following this, the "hydroxyl" water may be collected and its δD value measured. The maximum plausible contamination of the δD of the hydroxyl can then be calculated by material balance.

Oxygen isotopic compositions of montmorillonites are much less affected by the types of problems outlined above because the amount of oxygen contamination from interlayer water after dry box exposure for 24 hours is very small (see Savin, 1967, p. 65-67).

3.3 Summary

The hydrogen isotopic compositions of halloysites (a Type I clay, see

Table 3-5) are of limited use in geologic studies because of exchange between some of the hydroxyl and the coexisting interlayer water in a matter of hours or days at room temperature. This results primarily from the fact that in halloysites the interlayer water is in direct contact with 75% of the hydroxyls. However, inasmuch as most of the oxygen in halloysite is bonded to silicon, and because the oxygen of silicates does not exchange readily at room temperature, the oxygen isotopic composition of halloysites may be useful in geologic studies.

The hydrogen isotopic composition of the hydroxyl of montmorillonites (as well as other Type II clays, see Table 3-5) may be of use in geologic studies because the hydroxyl of montmorillonites apparently does not undergo rapid isotopic exchange at room temperature. However, at normal outgassing temperatures of 125° to 200°C, hydrogen isotope exchange between interlayer water and hydroxyl takes place, the extent of exchange depending in part on the relative proportions of interlayer water and hydroxyl. Limitations can be placed on the amount of hydrogen isotopic contamination of the hydroxyl, if systematic collection of both the interlayer water and the hydroxyl H_2O are undertaken. As noted above for halloysites, the oxygen isotopic values of Si-O bonded oxygen in montmorillonites will suffer little or no contamination from interlayer water. In addition all the OH sites of montmorillonites are partially protected from exchange with interlayer water by a sheet of silica tetrahedra.

Kaolinites and probably illites (as well as other Type III minerals, see Table 3-5) do not display any of the problems exhibited by either halloysite or montmorillonite and therefore their hydrogen and oxygen isotopic compositions will undoubtedly be very useful in geologica studies. As will be seen in later chapters on natural samples, kaolinites display a more systematic variation of D/H and O^{18}/O^{16} isotopic values than do montmorillonites or halloysites.

TABLE 3-5

Classification of Clay Minerals and Hydroxides on the Basis of Potential Ease of D/H Contamination of Their Hydroxyl Hydrogen

Layered Silicates with Interlayer Water in Direct Contact with Hydroxyl	Layered Silicates with Hydroxyl Protected from Interlayer Water by a Silica Tetrahedron Sheet	Sheet Structured Minerals with Little or No Interlayer Water
Type I	Type II	Type III
Halloysites	Montmorillonites (Smectites)	Kaolinites
	Vermiculite	Dickite
	Hydrobiotite	Nacrite
	Hydromuscovite	Illites
		Chlorite
		Serpentine
		Brucite
		Gibbsite

IV. ISOTOPIC, MINERALOGICAL AND CHEMICAL DATA

All the isotopic data* obtained in the present study are listed in Table 4-1 along with semiquantitative estimates (using X-ray diffraction techniques) of mineral quantities, some differential thermal analyses,⊗ hydrogen yields for samples on which hydrogen isotopic analyses were done, and some determinations of Fe_2O_3 contents (done by X-ray fluorescence). In many instances the δO^{18} values of the clay mineral or hydroxide end members in bulk samples were calculated by material balance.# Footnotes and abbreviations essential to a thorough understanding of the data in the table are given at the end of the table.

All the isotope data are also graphically illustrated in Figures 4-1 and 4-2 arranged according to mineralogy, geographic location, and age.

The location of the sample sites, descriptions of sample sites, and in some cases pertinent literature references are given in Appendix I.

* All the measured δD and δO^{18} values involved either one (no error given) or two (an average deviation from the mean given) separate sample extractions.

\# The material balance calculations were made on a 2 component basis: (1) residual parent rock or contaminant and (2) weathering product. the δO^{18} values of the parent rocks or contaminants used included: (1) directly measured δO^{18} values (one analysis for each sample locality); (2) assumed δO^{18} values, average values for a particular rock type (i.e., +8.5 for granitic rocks, +6.5 for basaltic rocks, Taylor, 1968); (3) in the case of the Hawaiian basalts a measured $\delta O^{18} = +6.4$ (Taylor, 1968); and (4) in the case of the ancient kaolinites and the montmorillonite +7.5 for residual basaltic-andesitic parent material, +10 for residual igneous quartz, and +13 for quartz in sedimentary kaolinites.

⊗ The differential thermal analyses were useful in confirming qualitative identifications by X-ray diffraction, in a few instances indicated the degree of crystallinity of a particular clay mineral, and in other instances revealed the presence of X-ray amorphous clay minerals or hydroxides.

Another thesis that you can run through the spudy scanner. I don't need it back. Thanks

5/2013

Geology & Planetary Sciences Library 170-25
201 North Mudd
Caltech
Pasadena, California 91125

Sample								H_2 yield μm/mg	wt. % Fe_2O_3	δD	δO^{18}
G-E											+ 8.5
											+10.0 ±0.1
											+ 3.8 ±0.1
											+ 7.1 ±0.1
G-								0.19		-83	+ 8.5 ±0.1
											+ 4.1 ±0.1
G-								0.73		-59	+ 9.6 ±0.1
											+ 9.9
											+ 8.3
											+ 5.7
											+ 5.8
											+ 5.5
G-E-Eg#15-3	w.r.	35	25	10	30			2.21		-61	+12.7
"	Q	100									+ 9.9
"	B[e]	5		70	25						+ 9.2
"	B[f]										+ 6.2
"	B[g]										+ 5.1 ± 0.1
G-E-Eg#15-4	w.r.	40	20	5	35			2.76		-62	+13.9 ±0.4
G-E-Eg#15-5	w.r.	40	15	5	40			3.01		-61	+14.2 ±0.1
G-E-Eg#15-6	w.r.	40	15	5	40		M550	3.18		-70	+13.8 ±0.2
"	Q	100									+ 9.9
"	Hyb										+10.6
"	K	15			85			6.45		-60	+19.4
G-E-Eg#20-1	w.r.	30	10	5	25	30[h]					+12.5
"	400P	15	T	T	30	40[i]		8.61		-49	+15.5
"	Q	100									+10.1
G-E-Eg#20-2	w.r.	40	40	5	T	T T					+10.1
"	400P	20	15	5	15	35[i] 10				-53	+12.4
"	Q	100									+10.0
"	B			90		T T					+ 5.5
"	B[k]			100							+ 4.3
"	B[l]			100							+ 3.9
G-E-Eg#20-3	w.r.[m]	40	20	5	T						+10.5
"	400P[m]	15	10	5	10						+12.4
"	Q	100									+10.1

Profile on a Quartz Diorite Gneiss
Big Sur, California

Sample No.	Desc.	Percent of Sample Q	F	M	Mo	K	Hal	G	Chl	Hbl	Ilm	D.T.A. peaks	H_2 yield µm/mg	wt. % Fe_2O_3	δD	δO^{18}
Mon-Cal-1-12	w.r.	30	40						10[n]	20						+10.5
"	Q	100														+12.5 ±0.1
"	F		100													+11.6
"	Hbl				5				30[n]	65						+ 6.9
Mon-Cal-1-11	w.r.	15	30		55								1.06		-48	
"	clay (h.p.)	5	15		80								1.72	3.8	-44	+19.2
Mon-Cal-1-10	w.r.	10	20		70								1.19		-54	
Mon-Cal-1-9	w.r.	20	40		25					15[n]						+13.2
"	Hbl[r]				75					25[n]						+10.9
"	F[o]															+13.1
"	Q															+12.0
Mon-Cal-1-8	w.r.	10	25		65								1.15		-53	+15.4
"	clay[p] (h.p.)	7	18		75							M120 W830	1.72	4.5	-44	+18.3
"	clay[q] (h.p.)	7	20		73								1.41	8.4	-65	+17.0
Mon-Cal-1-7	w.r.	10	25		65								1.30		-59	+14.5
"	Hbl[r]															+11.5
"	F															+10.9
Mon-Cal-1-6	clay[p] (h.p.)	15	10		75								1.47		-44	
"	clay[q] (h.p.)	15	10		75								1.23		-47	
Mon-Cal-1-4	clay[p] (h.p.)	7	18		75							M120 W830	1.62	4.2	-41 ±2	+19.8
"	clay[q] (h.p.)	7	18		75							M120 W830	1.53	6.6	-51 ±3	+16.4
"	R.F.	20	65		15											+12.6
Mon-Cal-1-3	clay[s] (h.p.)	15	10		75								1.76	4.8	-47	+19.2
Mon-Cal-1-2	w.r.	10	15		75											+17.1
"	clay (h.p.)	10	15		75								1.45	5.4	-55	+19.0
"	R.F.	35	65													+11.1
"	Q															+12.0
"	F[t]															+15.3
Mon-Cal-1-1	w.r.	12	23		35								1.87		-60	+13.8
"	R.F.	10	45		45											+12.9
"	F[t]															+12.1
"	Q															+13.1 ±0.4

Profile on the Columbia River Basalt
Spokane County, Washington

Sample No.	Desc.	Percent of Sample Q	F	M	Mo	K	Hal	G	Chl	Hbl	Ilm	D.T.A. peaks	H_2 yield μm/mg	wt. % Fe_2O_3	δD	δO^{18}
12K-JH-61	w.r.		50							35 U	15					+ 7.0
12J-JH-61	w.r.		45		10		10			20 U	15		1.53		-102	+ 8.8
12I-JH-61	w.r.		40		15					20 U	15	W120 W550	2.06		-101	+ 9.2
12H-JH-61	w.r.		5				80				15		5.29		- 70	+13.3
"	Hal						100									+14.4
12G-JH-61	w.r.		5				80				15		5.61		- 75	+13.3
12F-JH-61	w.r.		5				80				15	S120 S550	5.62		- 83	+13.8 ±0.2
"	Hal						100									+14.1
"	Ilm						5				95					+ 3.8
12E-JH-61	w.r.		5				80				15		5.36		- 78	+13.7 ±0.2
12D-JH-61	w.r.						85				15		6.22		-100 ±1	+12.7 ±0.5
"	Hal						100									+14.3
"	Ilm						5				95					+ 4.1
12C-JH-61	w.r.						85				15		6.13		- 71	+13.7 ±0.4
12B-JH-61	w.r.						85				15	S120 S550	5.99		- 77 ±1	+14.0
"	Hal						100						7.01		- 75	+15.1
"	Ilm						5				95					+ 2.9
12A-JH-61	w.r.	✓	✓	✓					✓	✓			3.19		- 84	+13.8

Profiles on the Pierre Shale or Equivalents
N.W. United States

C871	w.r. V				See Table 5-5								2.95		-108 ±1	+14.6 ±0.4
C872	w.r.				" " "								2.35		-105 ±4	+14.6 ±0.2
C873	w.r.				" " "								2.46		-108 ±2	+15.6 ± 0.4
C874	w.r.				" " "								2.46		-109 ±3	+15.7 ±0.6

Profile on Verendrye Member, Pierre Shale
Stanley County, South Dakota

C885	w.r. V				See Table 5-5								1.91		- 85	+19.7
C884	w.r.				" " "								1.92		- 86	+19.4
C881	w.r.				" " "								1.88		- 86	+20.0
C882	w.r.				" " "								2.02		- 88	+20.5
C883	w.r.				" " "								2.30		- 77	+19.4

Profile on a Pierre Shale Equivalent
Jefferson County, Colorado

Jef-Col-1-1	w.r.	35	10		40					15 W			1.64		- 89 ±2	+15.3
Jef-Col-1-2	w.r.	35	10		40					15 W			1.47		- 92 ±2	+14.9
Jef-Col-1-3 X	w.r.	15			20								2.15		-144 ±5	+10.6

SURVEY OF QUATERNARY WEATHERED ZONES

Sample No.	Desc.	Percent of Sample Q	F	M	Mo	K	O_a	O_b	D.T.A. peaks	H_2 yield um/mg	wt. % Fe_2O_3	δD	δO^{18} bulk	wt. % $O_{x_{clay}}$	δO^{18} p.r.	δO^{18} clay calculated
Coco-Ariz-2	clay (h.p.)				70		30		S150 M550	3.45		-66 ± 4				
Coco-Ariz-3	w.r.		50					50[p]		1.21		-75 ± 1	+ 9.1	53 ± 5	+ 6.1	+11.7 ± 0.5
"	p.r.		50				50						+ 6.1			
Pul-Ark-1[y]	w.r.									4.06		-62	+15.9	55 ± 5[kk]	+ 8.5[ii]	+22.0 ± 1.3
Pul-Ark-3	w.r.		50[z]			50				3.58		-61 ± 2	+14.4	55 ± 5	+ 8.5	+19.4 ± 1.0
"	w.r.[aa]									3.95		-59	+15.6			
"	clay (h.p.)					75	25			5.65		-63	+19.6			
But-Cal-1	w.r.					80	20		W120 S540	6.10	14	-77 ± 3	+16.4	84 ± 8	+ 8.3	+18.0 ± 1.0
"	<20μ					80	20		S550	6.09		-79 ± 2	+15.9			
"	p.r.		60					40[bb]					+ 8.3			
Lak-Cal-3	w.r.	15	15		20	25	25			4.72		-63 ± 1	+16.8	65 ±6[kk]	+ 8.5[ii]	+21.3 ±1.0
"	<20μ	15	15	5	20	25	20			3.70	10	-73 ± 3	+15.6			
L.A.-Cal-2	w.r.		50		30		20			0.79		-60	+11.4	34 ± 5	+ 8.3	+17.5 ±1.5
"	p.r.												+ 8.3			
L.A.-Cal-4	w.r.		35		50		15		S150 W750	1.21		-61	+12.0	54 ± 6	+ 8.3	+15.2 ±0.7
"	<20μ								S150 W750				+18.9			
L.A.-Cal-6	w.r.	20	50		30					0.60		-58	+ 8.4			
"	<20μ	15	35		50					2.10		-69	+13.9	54 ±6	+ 8.5	+18.6 ± 1.2
"	w.r.[cc]	20	70		10								+ 8.5			
Mon-Cal-1	w.r.	20	60			20										
"	w.r.[aa]	20	45			35				1.77		-56	-13.2	40 ±5	+10.0	+18.1 ± 1.0
"	<20μ	15	15			70				4.55		-58	+15.9	74 ±7	+10.0	+18.1 ± 0.8
"	w.r.[cc]	25	70				5						+10.8			
Mon-Cal-3	w.r.	8	12		40	40			M520	4.17		-78	+16.7	82 ± 8	+ 8.5[ii]	+19.1 ± 0.5
S.D.-Cal-1	w.r.	✓	✓	Hbl	Vm	✓			W110 M550	2.73		-66	+14.2	40 ± 5[kk]	+ 8.5[ii]	+23.0 ± 1.9
S.D.-Cal-2	w.r.	✓	✓	Hbl	Hyb	✓			W500	2.37		-60	+15.1	40 ± 5[kk]	+ 8.5[ii]	+25.3 ± 2.0
S.L.O.-Cal-1	w.r.	✓	✓	✓		✓			M520	4.76		-71	+15.7	60 ±6[kk]	+ 8.5[ii]	+20.7 ±1.3
S.C.-Cal-1	w.r.	18	42	10		30			W120 W520	2.22		-66 ±5	+13.9	35 ± 5	+ 8.5[ii]	+24.1 ± 2.2
"	<20μ	5	15			60	20		M120 M550	4.39	8	-57 ± 1	+18.4			
Tul-Cal-1	<20μ	✓	✓	✓		✓	Chl						+11.6			
"	20CP <20μ	✓	✓	✓		✓	Chl		M510		2.27	-91 ±2				
Tul-Cal-2	<20μ	✓				✓							+15.3			
"	20CP <20μ	✓	✓			✓					5.10	-94 ± 1				
Tul-Cal-3	<20μ	✓	✓			✓	Hyb			5.20		-81	+14.1	74 ±7[kk]	+ 8.5[ii]	+16.2 ± 0.8
"	20CP <20μ	✓	✓			✓	Hyb		M530	3.75		-83				
Tul-Cal-4	<20μ	✓	✓			✓	Hyb	Hbl	M500	4.51		-81	+12.1	65 ±6[kk]	+ 8.5[ii]	+14.1 ±0.5
"	20CP <20μ	✓	✓			✓	Hyb	Hbl		3.96		-72				
Tul-Cal-5	<20μ	✓	✓			✓	Hyb			5.54		-86	+12.7	74 ±7[kk]	+ 8.5[ii]	+14.2 ±0.6
"	20CP <20μ	✓	✓			✓	Hyb		M550	4.41		-102				

SURVEY OF QUATERNARY WEATHERED ZONES (CONTINUED)

Sample No.	Desc.	Percent of Sample Q	F	M	Mo	K	O_a	O_b	D.T.A. peaks	H_2 yield μm/mg	wt. % Fe_2O_3	δD	δC^{18} bulk	wt. % Ox_{clay} ∞	δO^{18} p.r.	δO^{18} clay calculated pp
Tui-Cal-6	< 20μ									4.71		-88	+12.7	65 ±6 kk	+ 8.5 ii	+15.5 ±0.7
	20CP < 20μ	√	√			√	Hyb		M530	3.54		-98 ±2				
Tui-Cal-7	< 20μ	√	√	√		√	Hyb			3.52		-92	+10.9	50 ±5 kk	+ 8.5 ii	+13.4 ±0.5
	20CP < 20μ	√	√	√		√	Hyb		W50	1.70		-100 ±2				
Tui-Cal-8	< 20μ	√	√	√	√	√	Hyb			3.54		-84	+17.2			
	20CP < 20μ	√	√	√	√	√	Hyb		W120 W550	1.99		-76 ±5				
Bou-Col-1	w.r.	20	30		25	25				1.86		-107 ±2	+12.9	54 ±5	+ 8.5 i	+16.7 ±0.8
"	clay (h.p.)									1.68		-106 ±3	+ 7.5			
Min-Col-1	clay (h.p.)	5	15	10	60		10		M150	1.48		-98 ±2	+ 8.6	62 ±6	+ 8.8	+ 8.5 ±0.2
	w.r.		25	15	45		20								+ 7.7	
	w.r.		25	15	45		20								+ 8.8	
Lit-Conn-2	w.r.	20	10	5	40		25			2.15		-58				
D.K.-Ga-17	w.r.									1.31		-66	+12.3			
Kau-Haw-1	w.r.					√				3.90	28.6	-54 ±1	+15.8	57 ±6 kk	+ 6.4	+23.0 ±1.7
Kau-Haw-2	w.r.					25		75 dd		13.35	8.6	-27 ±1	+15.1			
Maui-Haw-1	w.r.					√				4.52	18.4	-67	+20.9	67 ±7 kk	+ 6.4	+28.2 ±2.3
Maui-Haw-2	w.r.						50	50 dd		9.00	18.4	-34 ±1	+17.8			
Maui-Haw-3	w.r.		√			√				4.21	14.0	-53 ±1	+18.4	62 ±6 kk	+6.4	+26.1 ±1.9
Maui-Haw-4	w.r.					√				4.84	15.4	-62	+20.5	71 ±7 kk	+6.4	+26.5 ±2.0
Maui-Haw-5	w.r.		√			√				4.19	7.8	-55	+17.1	62 ±6 kk	+6.4	+23.9 ±1.7
Maui-Haw-6	w.r.		√			√				3.55	7.7	-51 ±1	+14.9	52 ±5 kk	+6.4	+23.2 ±2.4
Maui-Haw-7	w.r.					√				6.72	8.1	-55 ±4	+21.3	88 ±9 kk	+6.4	+23.4 ±2.1
Maui-Haw-8	w.r.					√				6.41	9.6	-60 ±1	+20.9	88 ±9 kk	+6.4	+22.9 ±2.0
Maui-Haw-9	w.r.		√			√				5.24	7.4	-54	+19.8	76 ±8 kk	+6.4	+24.4 ±2.0
Maui-Haw-10	w.r.		√							3.56	9.0	-52	+14.3	52 ±5 kk	+6.4	+22.0 ±2.1
Boi-Ida-4	w.r.	15	35	10				40 ee		1.42		-137	+ 3.2	43 ±5 kk	-4.0	+ 2.0 ±0.2
"	< 20 μ	5	15	10				70 ee		2.21		-133	+ 1.6	72 ±7 kk	-4.0	+ 0.6 ±0.4
"	p.r. cc	20	50	15			15						+ 4.0			
Boi-Ida-5	w.r.	15	50	10				25 ee	W150	1.01		-135	- 4.2	27 ±5	-6.1	+ 1.3 ±1.3
"	< 20μ	10		10				80 ee	W130 W300	2.97		-153	- 3.0	82 ±8	-6.1	- 2.3 ±0.4
"	p.r. cc	15	50	10			25			0.86		-152	- 6.1			
Cla-Ida-1	w.r.	20	60	15			5		W120 M570	0.73	9.0	-108 ±1				
"	< 20μ	15	15	20		40	10			3.32		-109 ±5				
Ida-Ida-1	w.r.		20		50	30				3.21		-120 ±7	+ 7.0	82 ±8	+8.5 ii	+ 7.4 ±0.6
"	< 20μ		20		50	30			M150 M520	3.61		-104 ±2	+ 8.2			
Lat-Ida-1	w.r.	√	√	√					M120 M500	2.59	9.0	-103				
"	< 20μ	√	√	√					W125 W530	3.28		-106 ±3				
Mad-Mis-1	w.r.	20	50			30				2.18		-70	+13.2	35 ±5	+8.5 ii	+22.1 ±1.9
"	< 20μ	10	20			60		Hyb		3.90		-77	+15.0	65 ±6	+8.5 ii	+18.6 ±1.0
"	R.F. cc	20	50			30				1.95		-65	+12.7			

SURVEY OF QUATERNARY WEATHERED ZONES (CONTINUED)

Sample No.	Desc.	Percent of Sample Q	F	M	Mo	K	O_a	O_b	D.T.A. peaks	H_2 yield µm/mg	wt. % Fe_2O_3	δD	δO^{18} bulk	wt. % Ox_{clay}	δO^{18} p.r.	δO^{18} clay calculated [pp]
Jef-Mon-1	w.r.	√	√	√					W150 W300	2.20		-161 ±2	+ 2.5			
"	< 20µ	20		20				60 [oo]	W140 W290 W530	3.11		-166 ±4	+ 1.2	82 ±8	+ 8.3	- 0.4 ±0.7
"	p.r. [cc]														+ 8.3	
L.a.C.-Mon-1	clay [ff]	20			80					2.00		-157	+ 8.3 ±0.5	83 ±8	+14.2	+ 6.9 ±0.6
"	clay [gg]	5	15		80					1.83		-130	+11.4 ±0.4	83 ±8	+14.2	+10.7 ±0.3
"	p.r. [cc]												+14.2			
L.a.C.-Mon-2	w.r.	20	25		50			Hol	S150 W800	1.06		-106 ±4	+ 9.7	53 ±5	+ 7.3	+11.9 ±0.5
"	p.r.	20	60	10				Hol	M150 W800				+ 7.3			
Mis-Mon-1	w.r.	40	30		15	15			M120 M570	1.74	3.0	-134 ±2	+ 5.0 ±0.3	33 ±5	+ 7.7	- 0.6 ±1.2
"	< 20µ	10	20		20	50			S125 M560	3.38		-142 ±1	+7.7 ±0.3	73 ±7	+ 7.7	+7.7
"	p.r.	40	55	5									+7.7			
Mid-N.J.-1 [y]	w.r.											- 77	+13.9 ±0.2			
Colf-N.M.-1	clay	30	15			40	15		M150 M550	2.87		- 79 ±1	+13.4	46 ± 5 [kk]	+ 8.5 [ii]	+19.2 ±1.2
Monr-N.Y.-1 [y]	w.r.									0.37		- 81	+12.8			
Rock-N.Y.-1	w.r.	25	40	5			30			2.50		- 66				
Clev-N.C.-1 [y]	w.r.									4.41		- 67	+ 12.3			
Clev-N.C.-2 [y]	w.r.									2.45		- 60	+ 14.1			
Com-Okl-1	p.r. [cc]	25	70		5					0.95		- 71	+ 8.4			
"	p.r. [hh]	5	60		25		10			0.82		- 64	+ 6.7			
"	R.F. (h.p.)	√	√										+12.8			
"	< 20µ	10	60	T				Hyb		1.05		- 64	+ 7.8			
"	p.r.	25	70	5									+ 7.4			
Gre-Okl-1	w.r.	25	75													
"	R.F. [cc]	25	75							0.42		- 58	+ 5.7			
"	< 20µ	25	25				10	40 [oo]		3.34		- 53	+13.4	49 ± 5 [kk]	+ 5.0	+22.3 ±1.8
"	p.r. [cc]	25	75										+ 5.0			
H.R.-Ore.-1	w.r.	20	40	10		20		Hbl	M125 M530	2.75		- 86 ±6	+10.9	42 ± 5 [kk]	+ 7.3	+16.1 ±1.4
"	p.r.												+ 7.3			
Lan-Ore-1	w.r.	25	T			60	10		M125 M560	4.65		- 80 ±2	+15.5	63 ±6	+ 6.5 [ii]	+21.0 ±1.4
"	< 20µ	35		5		50	10		M130 M550	3.71	11.0	- 88 ±1	+13.6			
Mari-Ore-1	w.r.	20	10			70				5.45	8.0	- 79 ±1	+14.7	73 ±7	+ 7.4	+17.5 ±1.0
"	< 20µ	20	20			50	10		W300 S550	4.25		- 85 ±1	+14.5			
"	p.r.												+ 7.4			
Mul-Ore-1	w.r. [ii]		20					Hal	W300 S520	4.36	14.0	- 75 ±1	+14.2	62 ± 6 [kk]	+ 6.5 [ii]	+19.1 ±1.1
"	< 20µ [ii]							Hal	S130 S530	6.00		- 44 ±1	+17.0	80 ± 8 [kk]	+ 6.5 [ii]	+19.7 ±1.4
"	w.r. [mm]							Hal			16.0		+17.1			
"	< 20µ [mm]		20					Hal					+12.8			

SURVEY OF QUATERNARY WEATHERED ZONES (CONTINUED)

Sample No.	Desc.	Percent of Sample Q	F	M	Mo	K	O_a	O_b	D.T.A. peaks	H_2 yield µm/mg	wt. % Fe_2O_3	δD	δO^{18} bulk	wt. % Ox_{clay} [pp]	δO^{18} p.r.	δO^{18} clay calculated [pp]
Mul-Ore-2	w.r.							Hal	S130 S540	5.94		- 46 ± 1	19.4	80 ± 8 [kk]	+ 6.5 [ll]	+22.8 ± 1.7
"	<20µ							Hal	S520	6.09	15.0	- 51 ± 1	18.2 ± 0.6			
"	p.r. [e]									2.15		- 47 ±	12.3			
Wash-Ore-1	w.r.							Hal	S130 S560	5.12		- 73 ± 2				
"	<20µ							Hal	S550	6.09		- 62 ± 2				
"	p.r.												7.1			
Wash-Ore-2	w.r.							Hal	S140 S550	5.10		- 79	15.1	71 ± 7 [kk]	+ 7.0	+18.7 ± 1.1
"	<20µ							Hal	S530	6.10	19.0	- 69 ± 2	15.9	85 ± 9 [kk]	+ 7.0	+17.6 ± 1.1
"	p.r. [cc]									2.11		- 66	9.7			
Yam-Ore-1	w.r.				40	40	20		S150 S550	4.36	15.0	- 83 ± 1	14.7 ± 0.4	83 ± 8	+ 8.5 [ii]	+16.0 ± 0.8
"	<20µ				20	60	20		M150 S500				15.0	84 ± 8	+ 8.5 [ii]	+16.3 ± 0.7
"	p.r. [cc]												9.9			
Lla-Tex-4	<20 µ	√	√		√	√			M150 M550	3.54		- 59 ± 2	20.4			
"	R.F. [aa]	10	25		65					1.79		- 56 ± 4	16.3	68 ± 7	+ 8.5 [ii]	+20.2 ± 1.2
Park-Wyo-1	w.r.	20	10		70				M150 W660	1.85		-113 ± 3	9.7	72 ± 7	+ 7.8	+ 0.5 ± 0.3
"	< 20µ	15	10		70	5			M150 W660	1.85		-111	+10.0	77 ± 8	+ 7.8	+10.7 ±0.3
"	p.r. [cc]	20	55		10	15							+ 7.8			
E.B.-Nica-1	w.r.							G	S320	10.17		- 36	+13.8			

ANTARCTIC SOILS

T.G.-Anta-1	w.r.									0.36		-158				
R.I.-Anta-1	w.r.									0.61		-151				
R.I.-Anta-2	w.r.									0.55		-121				
R.I.-Anta-3	w.r.									0.64		-129				

ANCIENT KAOLINITE DEPOSITS

Sample No. Description	Percent of Sample Q	F	M	Mo	K	I	O	D.T.A. peaks	H_2 yield µm/mg	wt.% Fe_2O_3	δD	δO^{18} bulk	wt. % Ox clay	δO^{18} contaminant	δO^{18} clay calculated
Ri.S.-Ark-1 Wilcox Fm, Eocene	50			15	35			M550	2.69		- 59	+19.2	51 ± 5	+13.0	+25.3 ± 1.2
Pike-Ark-1 Tokio Fm Upper Cretaceous	5				95			S550	7.19		- 54 ±2	+22.0	95 ± 9	+13.0	+22.4 ± 1.2
Pul-Ark-2 Wilcox Fm, Eocene	55		10		35			M550	2.90		- 60 ± 1	+17.3	42 ± 5	+13.0	+23.4 ± 1.2
Sal-Ark-2 Residual Eocene Weathering Surface		20 z	5	15	60			M550	4.42		- 57	+17.7	77 ± 8	+10.0	+20.1 ± 1.1
Hue-Col-1 Clay in Dakota Ss. Lower Cretaceous	40				60			S550	4.88		-116 ± 2	+13.5	62 ± 6	+13.0	+13.8 ± 0.1
Pue-Col-1 Clay in Dakota Ss. Lower Cretaceous	10				90			S550	6.61		-108 ± 3	+16.3	91 ± 9	+13.0	+16.7 ± 0.4
Cle-Ida-1 Sedimentary Deposit Miocene	20				80				6.33		-125 ± 1	+13.0	81 ± 8	+13.0	+13.0
Lat-Ida-2 Plastic Clay Deposit Miocene	10				90				6.19		-122 ± 2	+12.8	91 ± 9	+13.0	+12.8 ± 0.1
Lat-Ida-2 Siliceous Clay Deposit Miocene								S580	2.98		-131 ± 2	+12.9	42 ± 5	+13.0	+12.5 ± 0.1
Lat-Ida-2 Residual Weathered Zone Miocene	40	20			40			S580	3.10	1.0	-122	+ 8.8	42 ± 5	+10.0	+ 7.1 ± 0.4
N.P.-Ida-1 Clay Deposit Miocene	40		15		45			S550	3.32	4.0	-121	+12.5	47 ± 5	+13.0	+11.9 ± 0.1
Cal-Mis-1 Cheltennam Fm, Cherokee Group, Pennsylvania	5				95			S550	7.16		- 62 ± 1	+19.0	95 ± 9	+13.0	+19.5 ± 0.5
Fra-Mis-1 Cheltennam Fm, Cherokee Group, Pennsylvania					100			S550	7.36		- 45 ± 2	+20.2			
Fra-Mis-2 Cheltenham Fm, Cherokee Group, Pennsylvania								S550	6.95		- 44 ± 1	+20.3			
Gas-Mis-1 Cheltenham Fm, Cherokee Group, Pennsylvania	85				15			M550	1.01		- 33	+26.8			
Cas-Mon-1 Kootenai Fm Lower Cretaceous	50		5		45			M550	3.33		-119 ± 1	+15.5	52 ± 5	+13.0	+17.8 ± 0.5
Mid-N.J.-1 Raritan Fm Lower Cretaceous	30		10		60			S550	4.44		- 74	+18.6	72 ± 7	+13.0	+20.8 ± 0.8
Mid-N.J.-2 Sandy Clay, Raritan Fm Lower Cretaceous	25				75			S550	5.34		- 66	+18.4	77 ± 8	+13.0	+20.1 ± 0.8
Mid-N.J.-2 Clay, Raritan Fm Lower Cretaceous	10				90			S550	7.34		- 64 ± 2	+20.6	91 ± 9	+13.0	+21.4 ± 0.8
Cla-Ore-2 Clay in Tuffaceous Ss. Miocene	5				95			W110 S550	6.27		- 88 ± 3	+17.7	95 ± 9	+13.0	+18.0 ± 0.5
Mari-Ore-1 Clay altered from Tuff. Miocene							Hal	S120 S560	6.05	2.0	- 51 ± 4	+15.2			

ANCIENT KAOLINITE DEPOSITS (CONTINUED)

Sample No. Description	Percent of Sample Q	F	M	Mo	K	I	O	D.T.A. peaks	H_2 yield μm/mg	wt.% Fe_2O_3	δD	δO^{18} bulk	wt.% ^{oo} Ox_{clay}	δO^{18} contaminant	δO^{18}_{clay} pp calculated
Mari-Ore-3 Clay altered from Tuff. Miocene					70		30	M120 M550	5.49		- 67 ± 2	+19.4			+19.4
Aik-S.C.-N11-11 Clay Deposit Upper Cretaceous					100				7.50		- 57	+21.7			
Che-Tex-1 Wilcox Fm L. Eocene	20			15	65			S550	4.86		- 56 ± 1	+20.4	81 ± 8	+13.0	+21.8 ± 1.4
Che-Tex-2 Wilcox Fm L. Eocene	15				85			S550	5.94		- 56 ± 1	+19.6	86 ± 9	+13.0	+20.3 ± 0.5
Eas-Tex-1 Cisco Group Pennsylvanian	20				40	40		W550	3.77		- 50	+18.2	81 ± 8	+13.0	+19.5 ± 0.6
Ste-Tex-1 Cisco Group Pennsylvanian	30				25	45		M550	2.57		- 54 ± 1	+17.7	72 ± 7	+13.0	+19.5 ± 0.6
You-Tex-1 Cisco Group Pennsylvanian	25				40	35		M550	3.38		- 47 ± 1	+19.3	77 ± 7	+13.0	+21.2 ± 0.8
Ben-Ver-1 Clay Deposit Miocene	20		10		70			S550	5.40		- 90 ± 1	+19.5	72 ± 7	+13.0	+22.1 ± 0.9
Pie-Wash-1 Residual Weathering of Volcanic Mid Tertiary	15			5	80				5.60		- 98 ± 1	+13.9	86 ± 9	+10.0	+14.6 ± 0.5
Pie-Wash-3 Residual Weathering of Volcanic Mid Tertiary	20			15	65			M130 M580	5.55	12.0	- 92	+13.8 ± 0.1	81 ± 8	+10.0	+12.2 ± 0.2
Spo-Wash-1 Sedimentary Deposit Miocene	10				75		15	S550	6.17		-117	+13.4	81 ± 8	+13.0	+13.5 ± 0.1
Spo-Wash-2 Clay Deposit, Sedimentary Miocene					100				7.57		-110 ± 1	+14.3			
Spo-Wash-3 Residual Weathering Zone Miocene					100				7.02		-128 ± 1	+13.9			
RPFM3 Ancient Weathering Zone Pennsylvanian	40					60			1.62		- 84 ± 2	+13.2	60 ± 6	+10.0	+15.3 ± 0.6
RPFM7 Ancient Weathering Zone Pennsylvanian	35	15	20		10	20			1.16		- 83 ± 1	+14.8	50 ± 5	+10.0	+19.6 ±1.0
RPFM10 Ancient Weathering Zone Pennsylvanian	40	30	20			10			0.86		- 90 ± 3	+13.0	30 ± 5	+10.0	+20.0 ± 2.0
CH-13 Clay in Shale Paleocene	✓			✓	✓				1.95		-108	+14.5			

ILLITES

Sample No. Description	Percent of Sample Q	F	M	Mo	K	I	O	D.T.A. peaks	H_2 yield um/mg	wt. % Fe_2O_3	δD	δO^{18} bulk	wt. % ^{oo} Ox_{clay}	δO^{18} contaminant	δO^{18}_{clay} PP calculated
Coco-Ariz-5 Fossil Soil, w.r. Precambrian	50	10				40			1.13		- 79 ±5	+14.5	40 ±5	+13.0	+16.7 ±0.5
Coco-Ariz-5 Fossil Soil, Clay Precambrian	20	20				60			2.17		- 80	+16.4	60 ±6	+13.0	+18.7 ±0.5
Coco-Ariz-6 Bulk Fossil Soil Precambrian									2.26		- 59				
Coco-Ariz-6 Clay, Fossil Soil Precambrian						60	40		2.34		- 66	+16.4	60 ±6	+13.0	+18.7 ±0.5
S.B.-Cal-15 Fossil Soil Precambrian	40					60			1.78		-105				

MONTMORILLONITES

Coco-Ariz-7 Bentonite, Chinle Fm Triassic	15			85				M120 M550 W750	2.31		- 99 ±3	+15.0	85 ±8	+13.0	+15.3 ±0.3
Fer-Mon-1 Bentonite Shale Upper Cretaceous	30		10	40			20		1.17		- 90	+12.4	50 ±5	+10.0	+14.9 ±0.5
H.R.-Ore-2 Fossil Soil Oligocene		10		90				S160 M570	2.69	5.0	-108	+11.6	91 ±9	+ 7.5	+12.0 ±0.4
Was-Ore-3 Weathered Basaltic Glass Post Miocene				100				S120 W500 W770	2.51		- 95	+16.8			
Was-Ore-4 Weathered Basaltic Glass Post Miocene				100				S120 W500 W770	2.47		-100 ±1	+17.6			
Was-Ore-6 Fossil Soil Miocene		15		75			10 U	S140 W830	1.59	9.0	- 87	+10.0	79 ±8	+ 7.5	+10.7 ±0.3
Was-Ore-8 Fossil Soil Miocene		45		40			15 U	M125	0.87		-115	+ 8.8	45 ±5	- 7.5	+10.4 ±0.4
Was-Ore-9 Red Clay, Fossil Soil Miocene	5	5		90					2.03		- 97				
Was-Ore-9 Yellow Clay, Fossil Soil Miocene				100				S150 M530	3.00	8.0	- 87 ±4	+ 9.5			
Was-Ore-10 Fossil Soil Oligocene	10			45	45			M130 S580	4.87	10.0	-112	+10.3	91 ±9	+10.0	+10.4 ±0.1
Nio-Wyo-1 Bentonitic Shale Upper Cretaceous	30	20	5	45					1.33		- 80	+14.8	54 ±5	+13.0	+16.2 ±0.5
Nio-Wyo-1 Weathered Bentonitic Shale Upper Cretaceous	30	10	5	45			10					+16.1			
Nio-Wyo-2 Bentonitic Shale Upper Cretaceous	5	10		85					2.23		- 94	+16.7	86 ±9	+ 7.5	+18.3 ±1.2
Nio-Wyo-2 Weathered Bentonitic Shale Upper Cretaceous	5			95					2.43		- 85	+17.7			
Wes-Wyo-1 Bentonite Upper Cretaceous		10		90				S120 M700	2.51		-113 ±2	+17.9 ±0.1	91 ±9	- 7.5	+19.0 ±1.1
TW-10-116 Oceanic Montmorillonite				100				S120 S800	2.57		- 62 ±1	+21.6			
TW-1-50-F-M Oceanic Montmorillonite	5	5		80			10 U	S120 W800	1.98		- 63	+22.9	83 ±8	+ 7.5	+26.1 ±1.9
TW-1-G Basaltic Glass												+ 4.4			
Carr II DR-9-L-M Oceanic Montmorillonite				80			20 U	S120 W800	1.85		- 75	+22.6	83 ±8	+ 7.5	+25.8 ±1.9
68 ATo 20 Bentonite Upper Cretaceous		5		60	35				3.64		- 85	+12.4	95 ±9	+10.0	+12.5 ±0.1
SB-1a Supergene Green Clay Tertiary	5			70	25				4.19		- 84	+17.4			
SB-3b Supergene White Clay Tertiary	15			40	45				4.61		- 80	+16.7			
SB-3b Supergene Light Green Clay Tertiary	15			85					2.37		- 63	+16.6	85 ±8	+10.0	+17.8 ±0.7
SC-12 Bentonite Paleocene	✓			✓					2.75		-130	+11.2			

SHALES

Sample No. Description	Q	F	I	Chl	$CO_3^=$	O	CO_2 yield µm/mg	H_2 yield µm/mg	δD	δO^{18} bulk	δO^{18} carbonate
Inyo-Cal-5 Ordovician Shale	20		40	5	25	10	2.30	0.90	- 69 ± 1	+14.5	+16.7
B.C.-Can-1 Cambrian Shale	20		40	40			0.12	2.49	- 54 ± 1	+13.5	
B.C.- Can-3 Precambrian Shale	40		45	15			0.07	1.97	- 64 ± 3	+13.0	
She-Ind-1 Silurian Shale	20		10	10	60		6.11				+28.1
Mis-Mon -3 Precambrian Shale	20	10	35	35			1.12	1.54	- 67 ± 1	+15.4	
Mis-Mon -4 Precambrian Shale	30	15	40	15			0.03	1.46	- 65	+15.0	
Mis-Mon -4 Fragments in Soil	35	20	40	5		10	0.16	0.66	- 80	+14.9	
Mis-Mon -4 Soil	35	20	15	5		25	2.07	2.15	- 99	+14.0	
Pow-Mon -7 Upper Cretaceous Shale	20	10	50	20			0.17	2.69	-102 ± 2	+14.4	
Liv-N.Y.-1 Moscow Shale Devonian	20		20	20	40		4.51	1.71	- 63	+14.9	+24.0
Monr-N.Y.-2 Vernon Shale Silurian	45		10		45		4.38	0.67	- 61		+22.3
Ham-Ohio-1 Eden Shale Ordovician							0.94	2.31	- 48		+24.5

GLACIAL LAKE CLAYS

8:3 Glacial Lake Clay Illinoian, Pleistocene	40	10	15	20	15		1.74	1.99	- 63		+24.3
8:4 Glacial Lake Clay Illinoian, Pleistocene	✓	✓	✓	✓	✓			1.79	- 56		+24.0
10:4 Glacial Lake Clay Pre Illinoian, Pleistocene	✓	✓	✓	✓	✓			2.58	- 49		

PERLITES

Ben-Wash-1 Perlite Eocene								1.71	-150 ± 1	+12.0	
Chel-Wash-1 Perlite Eocene								2.36	-118 ±3	+13.4	
Pie-Wash-4 Perlite Eocene								3.07	- 98 ±1	+13.0	
Pie-Wash-5 Perlite Eocene								3.14	-114 ± 2	+12.0	

Meteoric Water Samples From Small Streams and Springs

Sample No.	δD	δO^{18}	Sample No.	δD	δO^{18}
Iny-Cal-1		-16.6	Mis-Mon-1		-15.8
L.A.-Cal-4, lake		- 1.9	Bak-Ore-1		-16.1
Mar-Cal-1	-36	- 4.6	Gra-Ore-1	-113	
Mon-Cal-2		- 5.3	H.R.-Ore-2	-100	-12.9
Mon-Cal-4		- 6.2	Kla-Ore-2		-13.2
S.L.O.-Cal-1		- 5.1	Kla-Ore-4		-12.9
S.C.-Cal-1		- 5.1	Mul-Ore-3		- 9.6
Boi-Ida-1	-133		Til-Ore-1		- 7.4
Lat-Ida-1		-15.8	Was-Ore-1	- 93	-12.1
Jef-Mon-2	-137	-17.5	Wash-Ore-1	- 67	- 9.0

FOOTNOTES AND ABBREVIATIONS TO TABLE 4-1

[a] Muscovite separate contained kaolinite

[b] Biotite separate contained kaolinite

[c] Biotite purified by paper shaking, kaolinite still present (~10%)

[d] Biotite purified by ultrasonic cleaning, kaolinite still present (~10%)

[e] Biotite separate contained kaolinite and hydrobiotite

[f] Biotite purified by paper shaking and handpicking, kaolinite still present (~10%)

[g] Biotite cleaned ultrasonically three times with 10% Calgon solution, kaolinite still present (~10%)

[h] Gibbsite quantity assumed to be the remainder

[i] Gibbsite quantity estimated using the H_2 yield

[j] Gibbsite and Chlorite quantities roughly estimated assuming that they constitute the remainder

[k] Biotite separate displays very fine clay adhering to surfaces

[l] Biotite purified using ultrasonic cleaning with 10% Calgon solution

[m] Sample contains abundant organic matter

[n] Petrographic thin sections used to estimate quantities.

[o] Feldspar weathered

[p] Handpicked gray clay (M-1) from the bulk sample

[q] Handpicked brown clay (M-2) from the bulk sample

[r] Hornblende largely altered to montmorillonite

[s] Handpicked clay containing a mixture of brown (M-2) and gray clay (M-1)

[t] Weathered feldspar

[u] Includes all mafic minerals plus glass, assumed to be the remainder

[v] See Figure 5-15 for detailed description

[w] Chlorite assumed to be the remainder

[x] Sample contains a considerable quantity of amorphous clay

[y] Bulk soils, δO^{18} values taken from Taylor and Epstein (1964)

[z] Nepheline

[aa] Very weathered portion

[bb] Non feldspar minerals of a basalt

[cc] Slightly weathered

[dd] Gibbsite assumed to be the remainder, qualitative X-ray information only

[ee] Amorphous Al-Si-Fe hydroxide, identified by D.T.A., assumed to be the remainder

[ff] Brown clay

[gg] Gray clay

[hh] Outer weathered surface of the parent rock

[ii] Upper soil zone near the surface

[ii] Parent rock granitic, assumed δO^{18} of parent rock

[kk] Percentage estimated solely on the basis of the hydrogen yield assuming one weathering product

[ll] Parent rock basaltic, assumed δO^{18}

[mm] Intensely weathered rock several feet below the surface

[nn] Amorphous clay, quantity assumed to be the remainder

[oo] Weight percent of the total oxygen of the bulk sample in the clay mineral or hydroxide fraction

[pp] δO^{18} of the clay mineral or hydroxide and member calculated by material balance

Q - quartz
F - feldspar
M - mica
Mo - montmorillonite
K - kaolinite
Hal - halloysite
G - gibbsite
Chl - chlorite
Hbl - hornblende
Ilm - ilmenite

Mu - muscovite
B - biotite
Hyb - hyrobiotite
Vm - vermiculite
R.Fr. rock fragment
O - other
O_a - remainder of the sample, minerals not identified
O_b - other minerals, see abbreviations or footnotes
w.r. - whole rock

p.r. - fresh parent rock
<20μ - 20 micron size fraction
200P - size fraction passing through a 200 mesh screen
h.p. - hand picked
D.T.A. - differential thermal analysis
W100-weak endothermic peak at 100°C
M100-moderate endothermic peak at 100°C
S550-strong endothermic peak at 550°C
μm/mg - micromoles per milligram
T - trace amount present

✓ - qualitative identification only
wt. % - weight percent
Ox - oxygen
I - illite

Figure 4-1. The δD values of all the Quaternary soil samples, ancient kaolinites, montmorillonites, illites, and shales arranged according to mineralogy, geographic location, and age. The degree of shading of each data-point indicates the proportion of parent rock (open) to weathering product (black) in each sample. The following symbols are used to indicate the types of clay minerals or hydroxides in each sample.

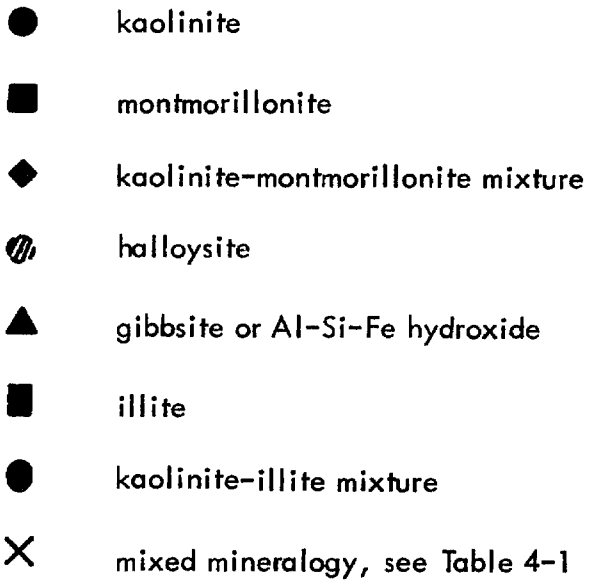

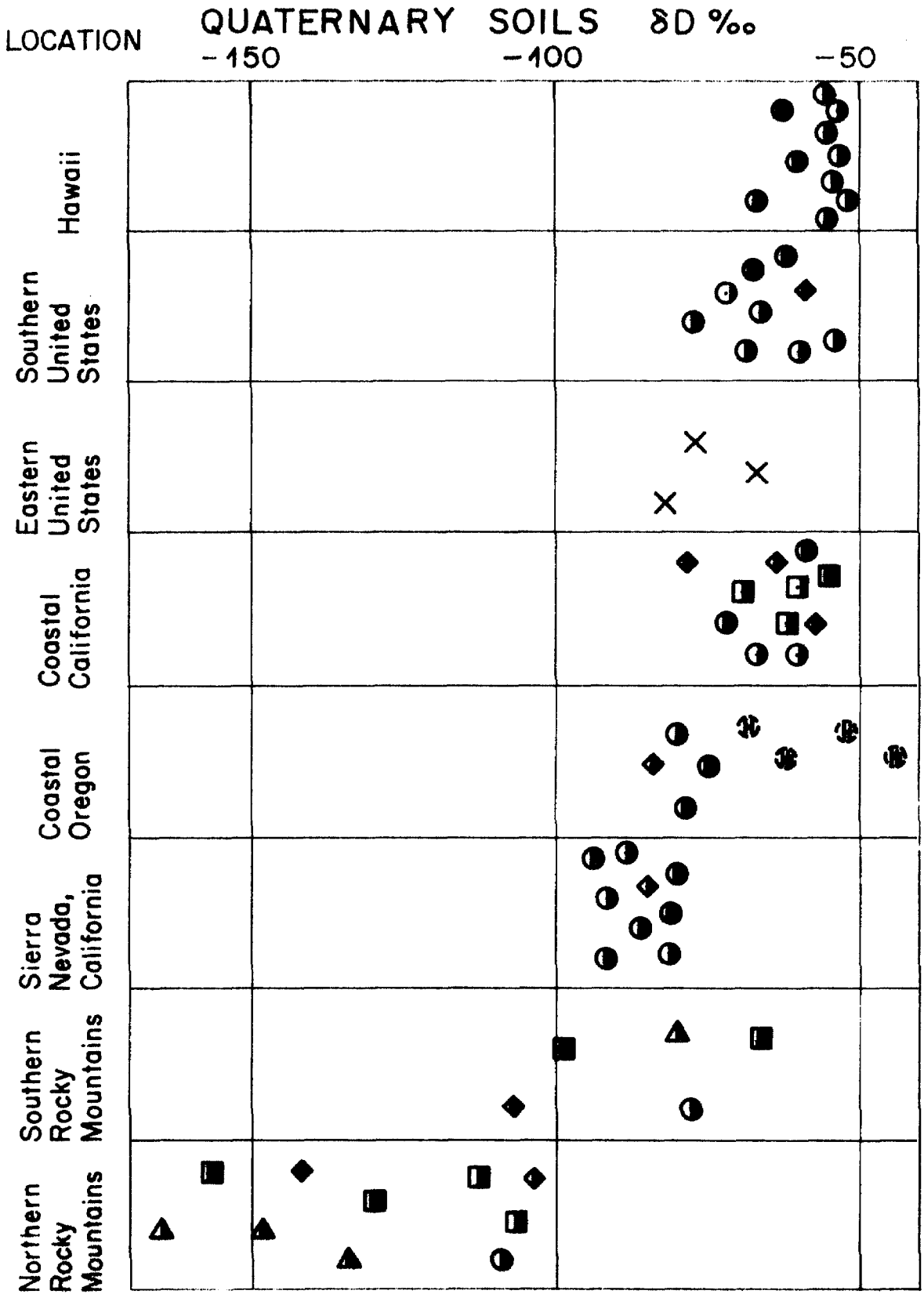
LOCATION
QUATERNARY SOILS δD ‰
-150
-100
-50
Hawaii
Southern United States
Eastern United States
Coastal California
Coastal Oregon
Sierra Nevada, California
Southern Rocky Mountains
Northern Rocky Mountains

Figure 4-1

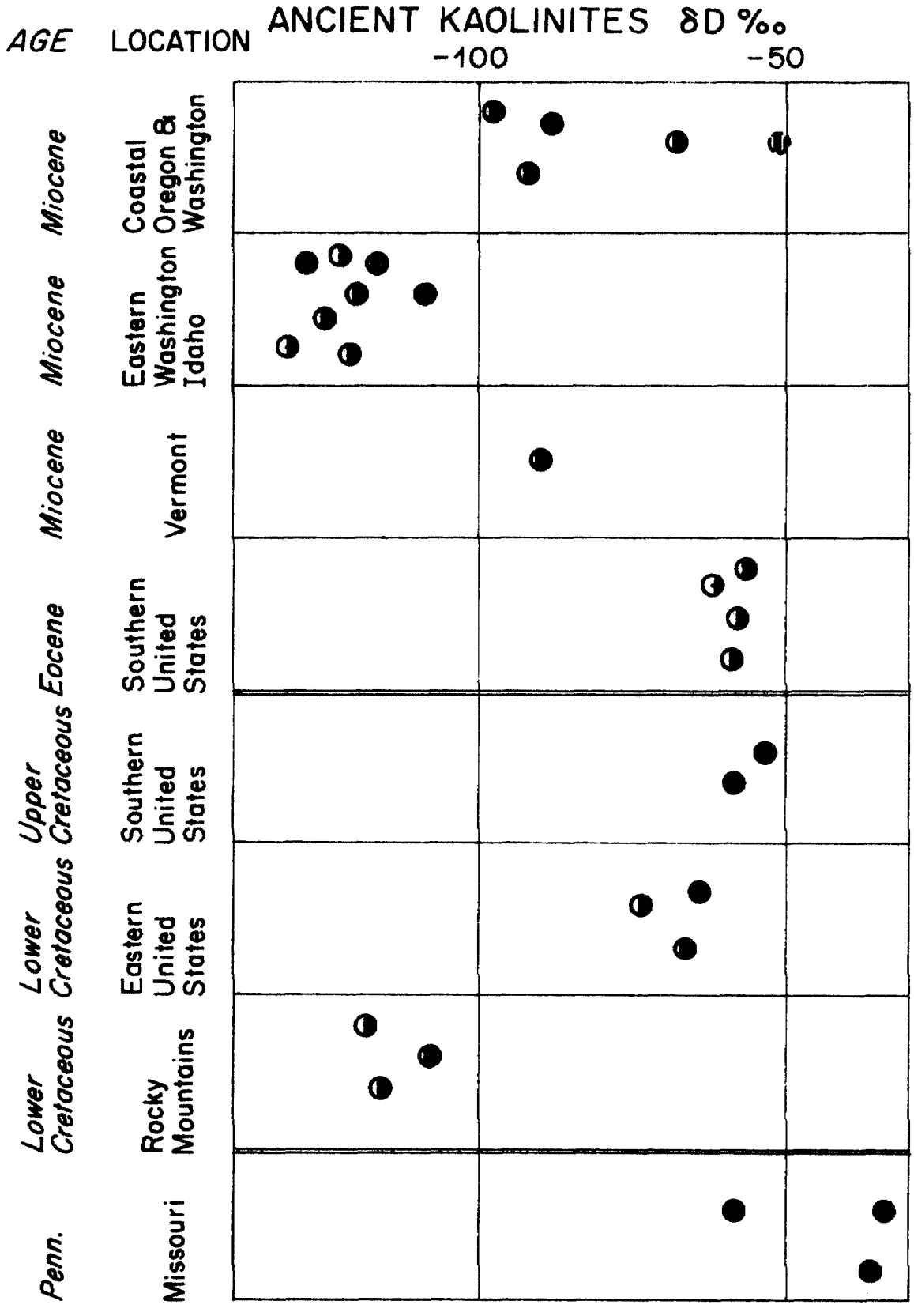
ANCIENT KAOLINITES δD ‰
-100
-50
AGE
LOCATION
Miocene
Coastal Oregon & Washington
Miocene
Eastern Washington Idaho
Miocene
Vermont
Eocene
Southern United States
Upper Cretaceous
Southern United States
Lower Cretaceous
Eastern United States
Lower Cretaceous
Rocky Mountains
Penn.
Missouri

Figure 4-1

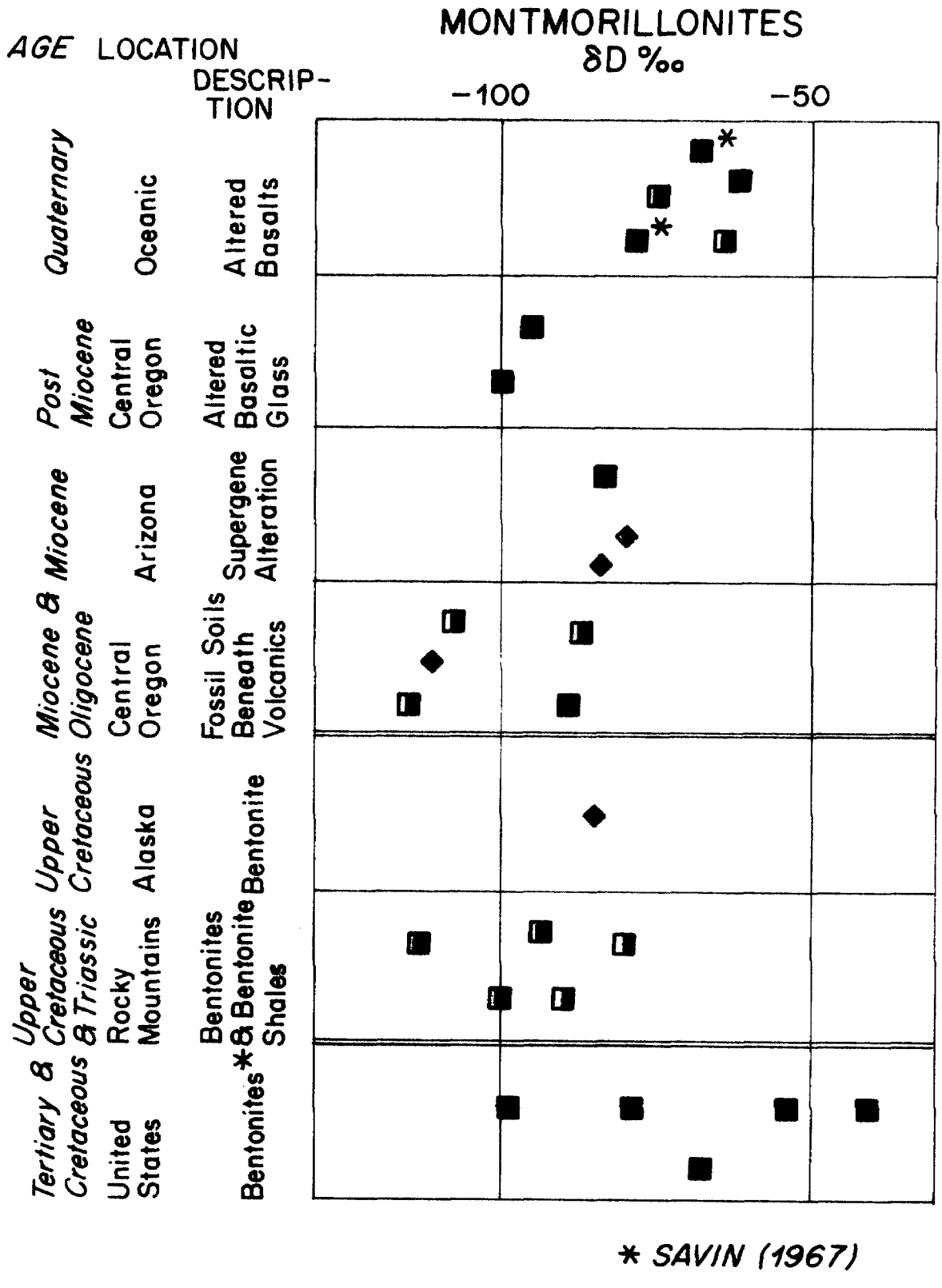
MONTMORILLONITES
δD ‰
−100
−50
AGE
LOCATION
DESCRIP-TION
Quaternary
Oceanic
Altered Basalts
Post Miocene
Central Oregon
Altered Basaltic Glass
Miocene
Arizona
Supergene Alteration
Miocene & Oligocene
Central Oregon
Fossil Soils Beneath Volcanics
Upper Cretaceous
Alaska
Bentonite
Upper Cretaceous & Triassic
Rocky Mountains
Bentonites & Bentonite Shales
Tertiary & Cretaceous
United States
Bentonites*
* SAVIN (1967)

Figure 4-1

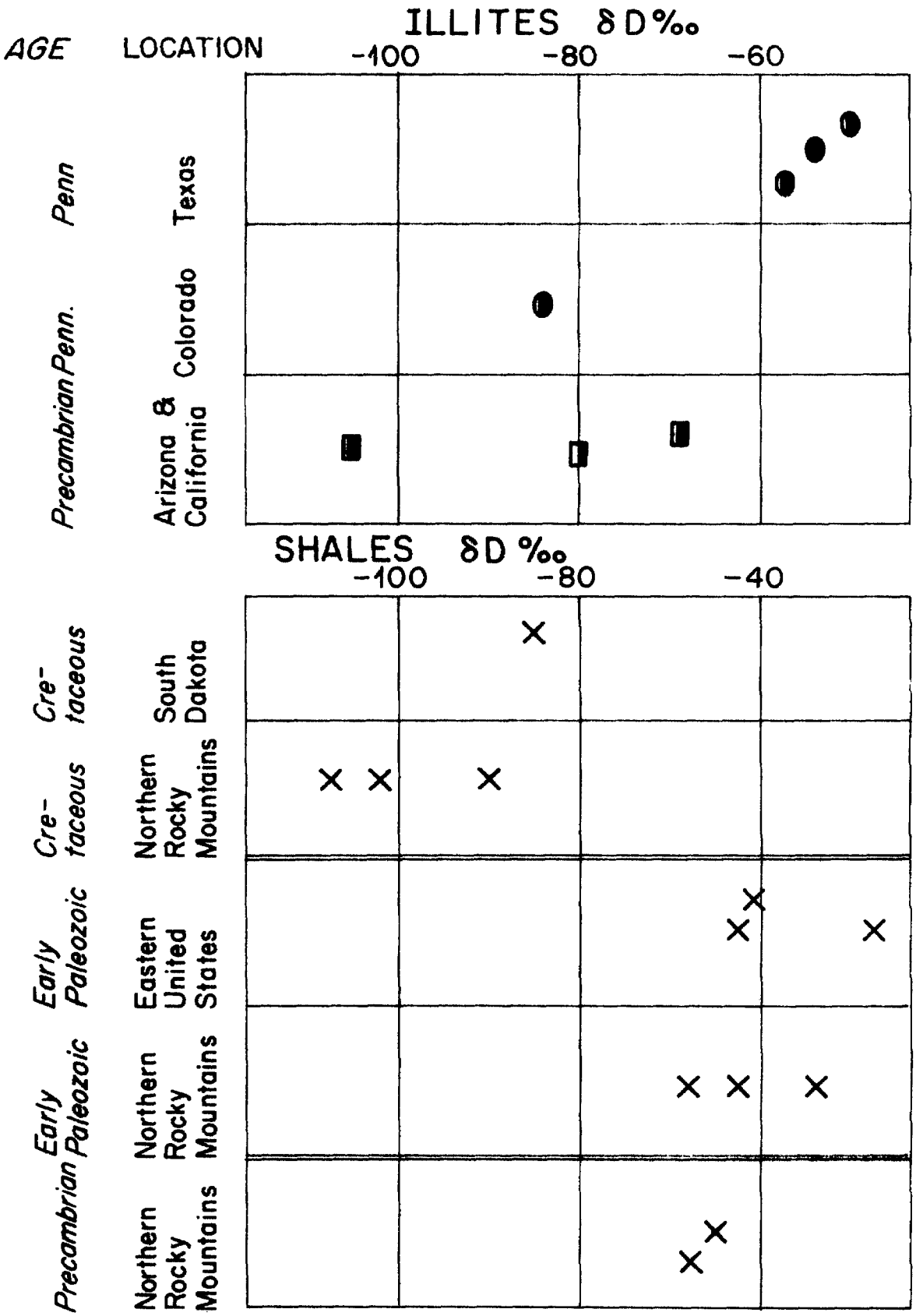
ILLITES δD‰
AGE
LOCATION
-100
-80
-60
Precambrian Penn.
Penn
Arizona & California
Colorado
Texas
SHALES δD ‰
-100
-80
-40
Precambrian
Early Paleozoic
Early Paleozoic
Cre-taceous
Cre-taceous
Northern Rocky Mountains
Northern Rocky Mountains
Eastern United States
Northern Rocky Mountains
South Dakota

Figure 4-1

Figure 4-2. The δO^{18} values of all the Quaternary soil samples, ancient kaolinites, montmorillonites, illites, and shales arranged according to mineralogy, geographic location, and age. The degree of shading of each data-point indicates the proportion of parent rock (open) to weathering product (black) in each sample. The following symbols are used to indicate the types of clay minerals or hydroxides in each sample.


kaolinite


montmorillonite


kaolinite–montmorillonite mixture


halloysite


gibbsite or Al–Si–Fe hydroxide

illite


kaolinite–illite mixture


mixed mineralogy, see Table 4-1

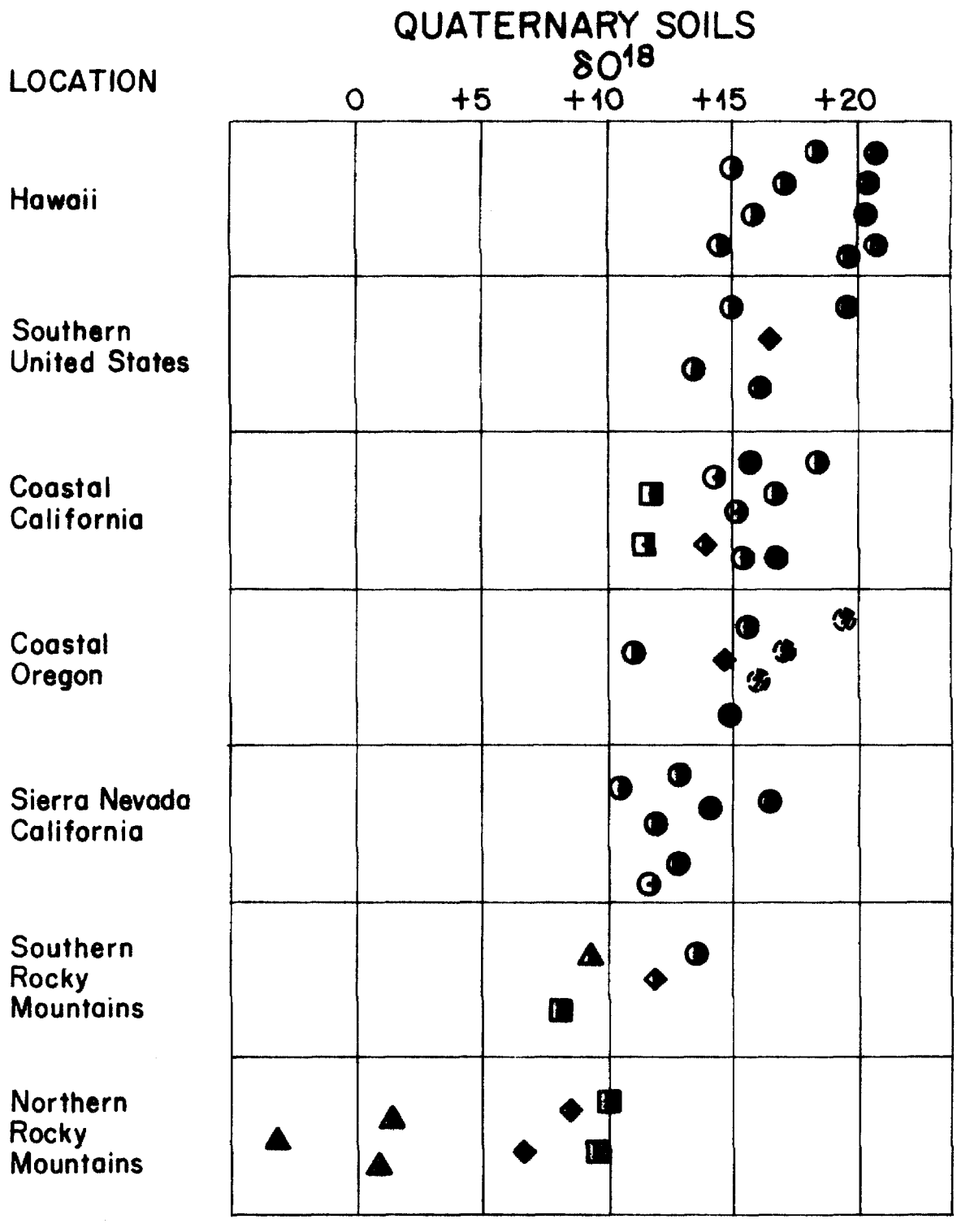
QUATERNARY SOILS
δO^{18}
LOCATION
0
+5
+10
+15
+20
Hawaii
Southern United States
Coastal California
Coastal Oregon
Sierra Nevada California
Southern Rocky Mountains
Northern Rocky Mountains

Figure 4-2

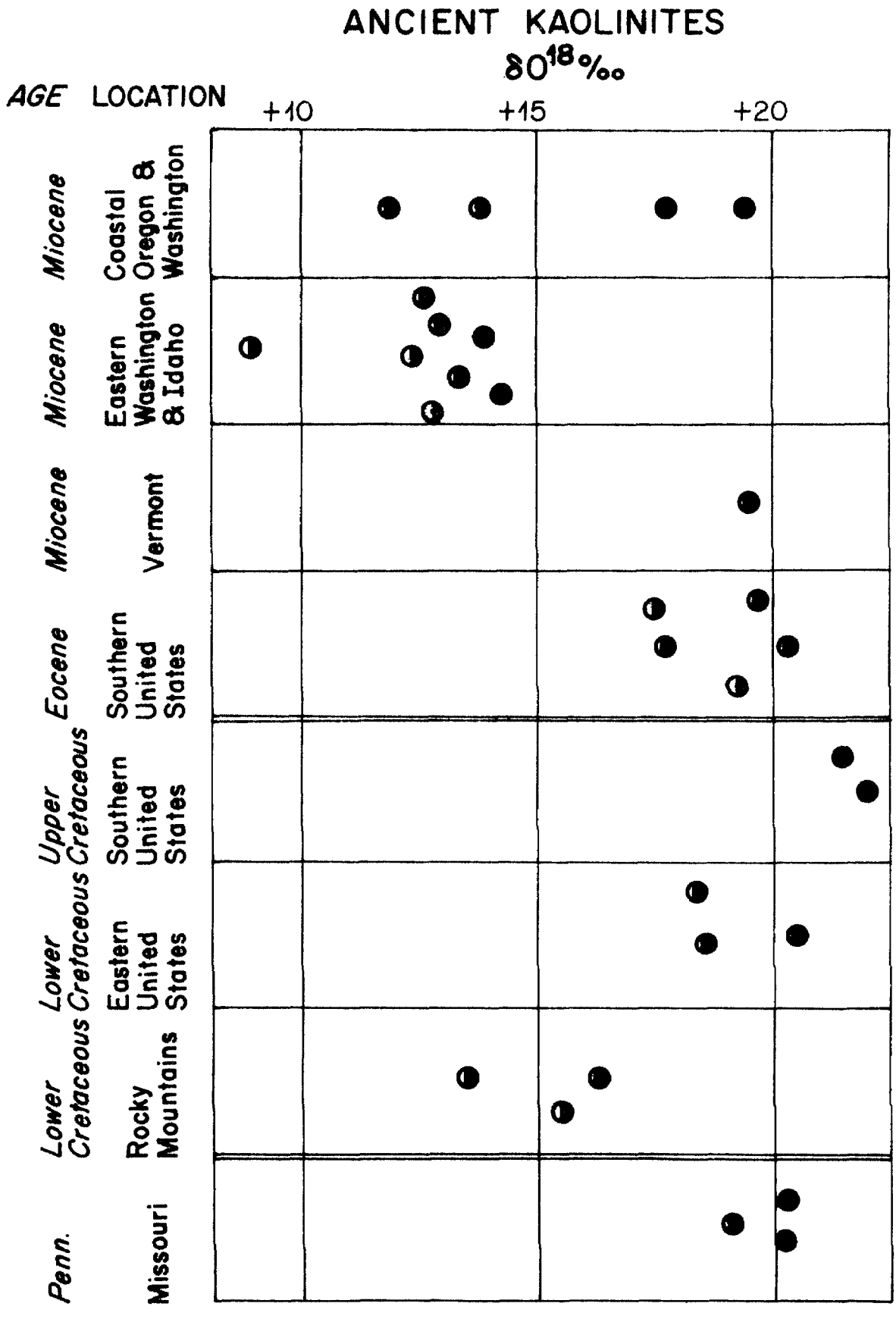
ANCIENT KAOLINITES
δO^{18}‰
AGE
LOCATION
+10
+15
+20
Miocene
Coastal Oregon & Washington
Miocene
Eastern Washington & Idaho
Miocene
Vermont
Eocene
Southern United States
Upper Cretaceous
Southern United States
Lower Cretaceous
Eastern United States
Lower Cretaceous
Rocky Mountains
Penn.
Missouri

Figure 4-2

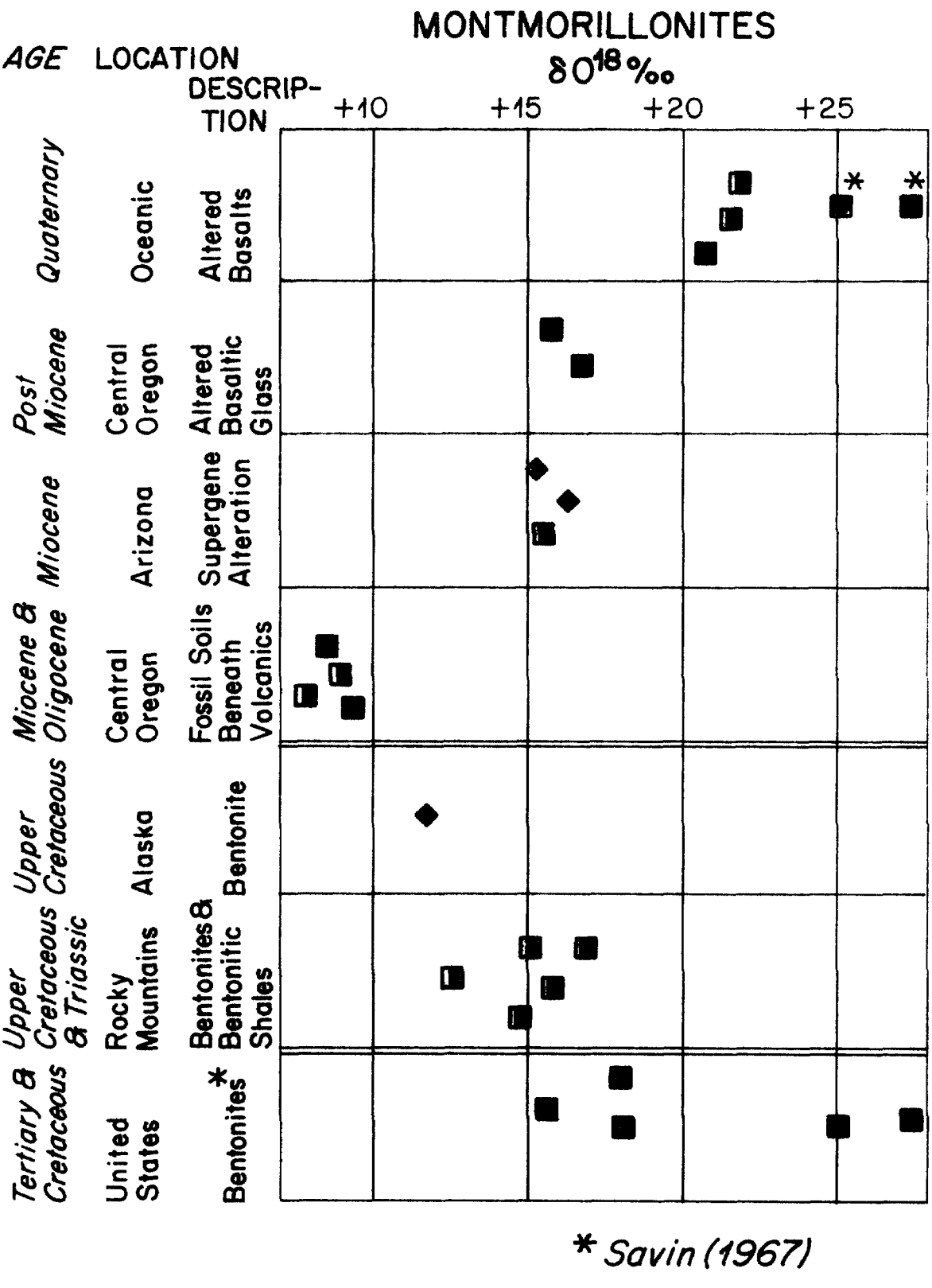
MONTMORILLONITES
δO18 ‰
+10
+15
+20
+25
AGE
LOCATION
DESCRIP-TION
Quaternary
Oceanic
Altered Basalts
Post Miocene
Central Oregon
Altered Basaltic Glass
Miocene
Arizona
Supergene Alteration
Miocene & Oligocene
Central Oregon
Fossil Soils Beneath Volcanics
Upper Cretaceous
Alaska
Bentonite
Upper Cretaceous & Triassic
Rocky Mountains
Bentonites & Bentonitic Shales
Tertiary & Cretaceous
United States
Bentonites*
* Savin (1967)

Figure 4-2

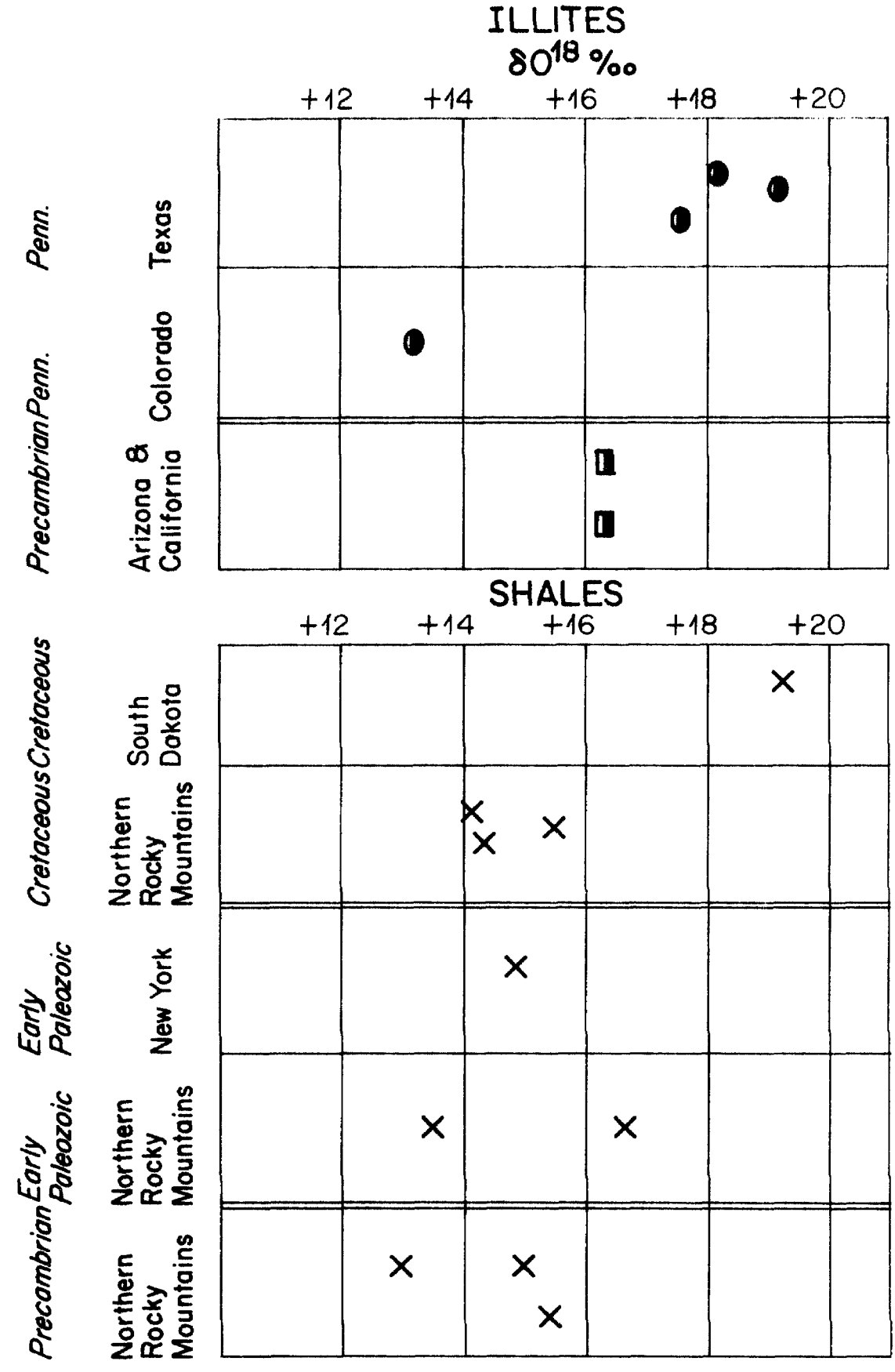
ILLITES
δO18 ‰
+12
+14
+16
+18
+20
Precambrian
Penn.
Penn.
Arizona & California
Colorado
Texas
SHALES
+12
+14
+16
+18
+20
Precambrian
Early Paleozoic
Early Paleozoic
Cretaceous
Cretaceous
Northern Rocky Mountains
New York
Northern Rocky Mountains
Northern Rocky Mountains
South Dakota

Figure 4-2

V. DETAILED ISOTOPIC STUDIES OF WEATHERING PROFILES

5.1 General statement

Detailed isotopic studies were undertaken on seven different weathering profiles, three on igneous or metamorphic parent rocks, and four on sedimentary parent rocks. Four different mineralogical types were studied, characterized by abundant kaolinite, gibbsite, montmorillonite and/or halloysite. The isotopic compositions of most of the weathering products and some of the minerals from the underlying parent rocks were studied from the fresh parent rock up to the A zone of the soil.

Locations of the seven profiles are given in Figure 5-1. They are scattered throughout the United States, encompassing a variety of climates from semi-arid to sub-tropical. The range of elevations is 500 to 6000 feet above sea level. The localities were chosen to cover a wide range in the intensity of weathering and type of vegetative cover. They include: (1) the Elberton, Georgia kaolinite profile formed on a Precambrian granite; (2) the Big Sur, California montmorillonite profile formed on a Mesozoic gneissic quartz diorite; (3) the Spokane, Washington halloysite-nontronite profile formed on the Miocene Columbia River basalt; (4a,b,c) three poorly-developed profiles developed on Upper Cretaceous shales (Pierre shale or its equivalent) in Fergus County, Montana; Stanley County, South Dakota; and Jefferson County, Colorado; (5) the Missoula, Montana profile developed on a Precambrian Belt Series shale.

5.2 Elberton, Georgia kaolinite profile

The Elberton profile (New Comolli Quarry, elevation 700 feet, Elbert

Figure 5-1. Map of the United States, showing the locations of the seven weathering profiles studied in detail.

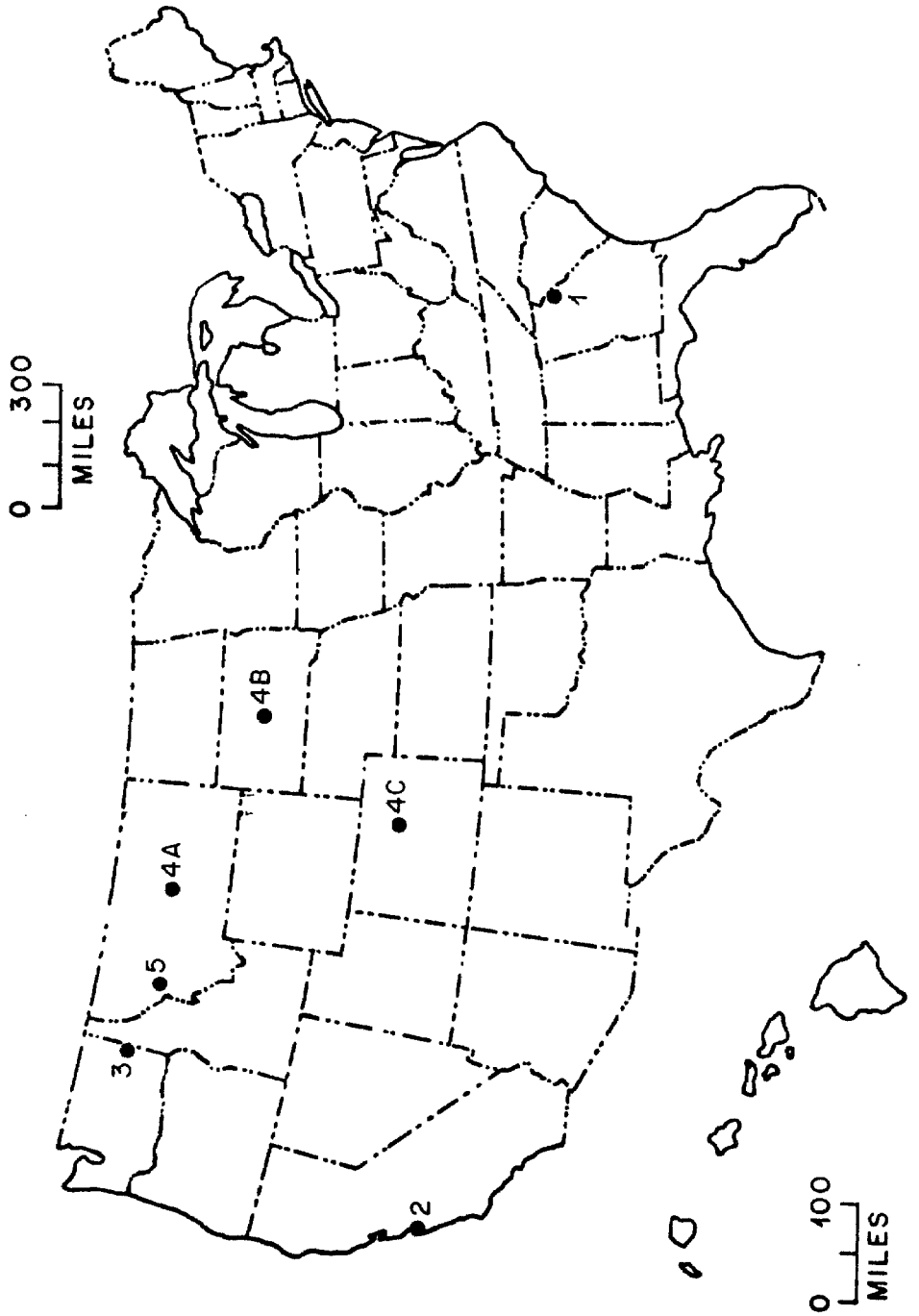
0 300
MILES
1
2
3
4A
4B
4C
5
0 100
MILES

County, Georgia, Figure 5-2, see Appendix I for the exact location), the O^{18} relationships of which were originally studied by Taylor and Epstein (1964), is characterized by intense kaolinite weathering of a medium to fine grained granite. The climate is subtropical, with a temperature range of 7° to 27°C (mean monthly) and a total rainfall of about 45 to 55 inches, with a seasonal maximum in the summer. The quarry is located in a region of rolling topography covered with a mixed broadleaf and coniferous forest.

Samples were collected from ten different horizons within the soil profile, from fresh granite deep in the quarry to the uppermost organic-rich A zone. A field description of the profile (obtained from L.T. Silver) is given in Table 5-1 and Figure 5-2.

Mineralogical descriptions of the samples are given in Table 4-1 and Figure 5-3, together with the isotopic data obtained on the bulk samples and on various mineral separates. Petrographic descriptions of six of the samples are given in Table 5-2 and X-ray diffraction patterns are shown in Appendix II.

Parent rock minerals: The δO^{18} values of the minerals quartz, feldspar, biotite and muscovite in the fresh rock represent equilibrium at magmatic temperatures (see Figures 1-1 and 5-3). If these minerals were to undergo oxygen isotopic re-equilibration with the local meteoric waters ($\delta O^{18} \approx -5‰$, calculated from δD values of meteoric waters, Friedman, 1964) at Earth-surface temperatures (10° to 25°C) during weathering, their δO^{18} values would increase drastically (see Figure 1-1). Two of these minerals, quartz and biotite, display essentially no change in their δO^{18} values from the fresh rock up into the most intensely weathered zone (see Figure 5-3), indicating that no exchange has occurred. Based on the whole-rock δO^{18} values, it is very likely that the feldspars also retain their original δO^{18} values;

TABLE 5-1

Descriptions of the Samples from the Elberton, Georgia Profile

G-E-Eg-1 *

A medium- to fine-grained quartz monzonite (average grain size 1 mm) containing 30% quartz, 30% plagioclase (oligioclase), 30% K-feldspar (microcline), 4 - 6% biotite, 2 - 3% muscovite and 2% accessory minerals.

G-E-Eg-15-1 *

Same as above.

G-E-Eg-15-2 *

Somewhat fissile, yellow-stained, altered quartz monzonite; quartz unaltered; plagioclase crystals broken up with kaolinite alteration along cracks and surfaces; K-feldspar crystals mostly unaltered, a few crystals broken up with kaolinite alteration along surfaces; biotite partially altered to hydrobiotite and some kaolinite; muscovite relatively unaltered.

G-E-Eg-15-3 *

Gray saprolite; quartz grains show some rounding of edges; plagioclase greatly altered to kaolinite, with almost all crystals broken up; K-feldspar moderately altered to kaolinite, many crystals broken up with alteration along cracks and surfaces; biotite largely altered to hydrobiotite, some edges altered to kaolinite; muscovite grains slightly altered and broken.

TABLE 5-1 (continued)

G-E-Eg-15-4 * ⊗

Residual fragments from a pink saprolite; similar to 15-3 except that: plagioclase almost completely altered to kaolinite with only scattered crystal fragments remaining; K-feldspar largely altered to kaolinite with almost all crystals broken up; biotite completely altered to hydrobiotite.

G-E-Eg-15-5 * ⊗

Similar to 15-4 except that: quartz sometimes broken up, muscovite partially altered to hydromuscovite.

G-E-Eg-15-6 * ⊗

Similar to 15-4 except that very little feldspar remains.

G-E-Eg-20-1

Deep red clay zone, some rootlets; c.g./c ratio# < 0.2 .

G-E-Eg-20-2

Yellow-brown granular soil; c.g./c ratio# > 2; root materials very abundant; rock fragments in most cases have not been moved more than a few inches.

TABLE 5-1 (continued)

G-E-Eg-20-3

Dark brown granular soil; c.g./c ratio# > 2; many rootlets; local spots of red oxidized clay; scattered rock fragments may have been transported a few inches.

* Thin sections used.

⊗ These thin sections represent rock fragments in the bulk sample.

c.g./c ratio = volume ratio of medium grained quartz and feldspar to clay-size fraction.

Figure 5-2. Detailed sketch of the Elberton, Georgia weathering profile. Sample 1 , fresh granite, was collected 30 feet below sample 15-1.

Figure 5-3. δD and δO^{18} contents of bulk samples and minerals from the Elberton profile. Quartz, biotite and muscovite were analyzed directly. Kaolinite and gibbsite values were determined by material balance calculations.

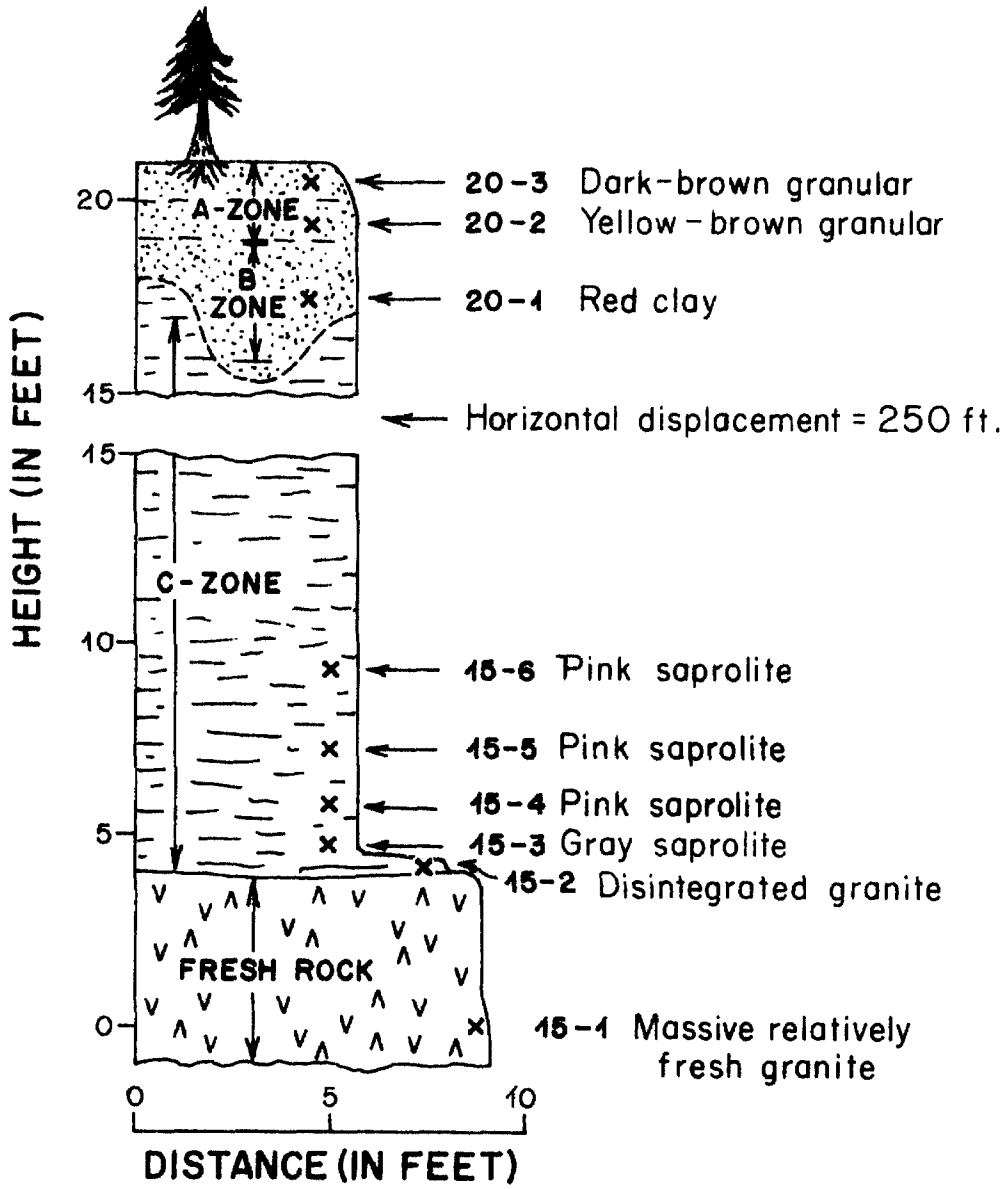
20-3 Dark-brown granular
20-2 Yellow-brown granular
20-1 Red clay
Horizontal displacement = 250 ft.
15-6 Pink saprolite
15-5 Pink saprolite
15-4 Pink saprolite
15-3 Gray saprolite
15-2 Disintegrated granite
15-1 Massive relatively fresh granite
A-ZONE
B ZONE
C-ZONE
FRESH ROCK
HEIGHT (IN FEET)
DISTANCE (IN FEET)
20
15
10
5
0
0
5
10

Figure 5-2

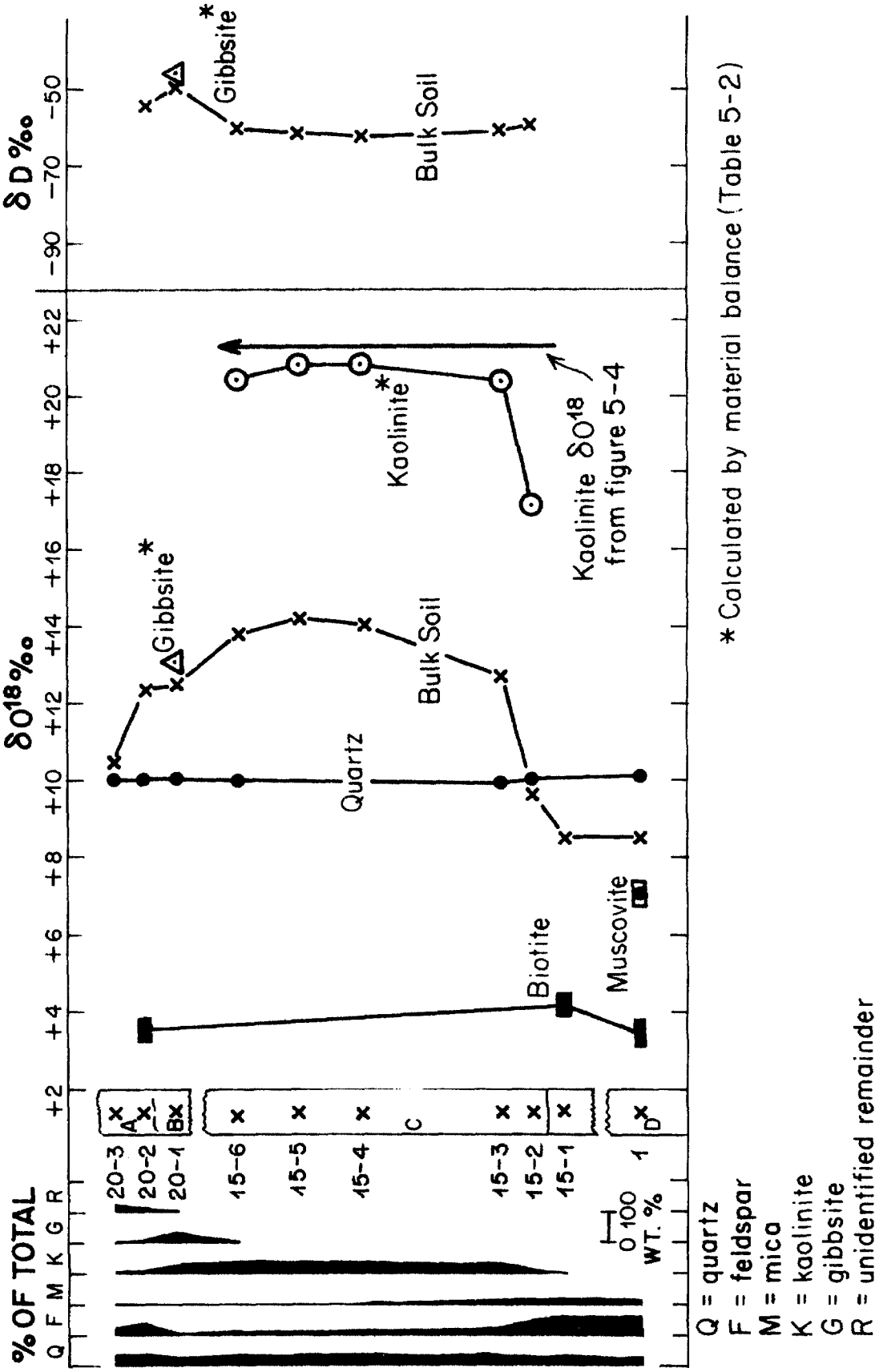
% OF TOTAL
Q F M K G R
δO18‰
δD ‰
+2 +4 +6 +8 +10 +12 +14 +16 +18 +20 +22
-90 -70 -50
20-3
20-2
20-1
15-6
15-5
15-4
15-3
15-2
15-1
A
B
C
D
0 100
WT. %
Quartz
Biotite
Muscovite
Gibbsite*
Bulk Soil
Kaolinite*
Kaolinite δO18 from figure 5-4
Gibbsite*
Bulk Soil
* Calculated by material balance (Table 5-2)
Q = quartz
F = feldspar
M = mica
K = kaolinite
G = gibbsite
R = unidentified remainder

Figure 5-3

however, no δO^{18} analyses were obtained on pure feldspars from the soil profile, because even the slightly weathered rock shows appreciable kaolinitic alteration of feldspar (see Figure 5-3).

The failure of the δO^{18} of the parent minerals to equilibrate with meteoric waters in the weathering environment is consistent with the observation that these minerals are not in chemical equilibrium with K^+, Na^+, H^+ and silica in local ground waters (see Figures 5-5 to 5-7). Because of the dynamics of ground water flow and the slow rates of dissolution of silicates, initially pure rainwaters commonly do not reach cation or anion concentrations high enough to be in equilibrium with feldspars (see Feth et al., 1964). Silica concentrations supersaturated with respect to quartz are commonly observed in local ground waters, which suggests that at Earth-surface temperatures quartz - $[SiO_2]aq.$ equilibration rates are also very slow. In contrast to the behavior of parent-rock minerals, it will be shown in the next few paragraphs that the weathering products are apparently in both isotopic and chemical equilibrium with the weathering environment.

C - zone: The δO^{18} values of the bulk samples from the C-zone vary directly with the kaolinite contents of the samples (see Figure 5-3). Most of the kaolinite has formed by alteration of the feldspars, and the plagioclase is more highly altered than the K-feldspar.

Inasmuch as the δO^{18} contents of quartz and biotite (and probably feldspar and muscovite as well) do not change throughout the weathering profile, the δO^{18} content of kaolinite in the C-zone may be calculated by material balance (Table 5-2). The δO^{18} values of kaolinite calculated in this fashion are shown on Figure 5-3.

TABLE 5-2

MATERIAL BALANCE CALCULATIONS OF THE δD AND δO^{18} CONTENT OF KAOLINITE AND GIBBSITE

Sample No. (ft. above fresh rock)	δO^{18} bulk	wt. % Quartz	wt. % Feldspar	wt. % Mica	wt. % Kaolinite	δO^{18} calculated Kaolinite	wt. % Gibbsite	δO^{18} calculated Gibbsite [a]	wt. % Weathering Products	Percent of Total Weathering Products: Kaolinite	Gibbsite	δD bulk	δD Kaolinite	δD calculated Gibbsite
20-1, bulk	+ 12.5	30	10	5	25		30	+10.2	55	45	55			
20-1, 400P	+ 15.5	20	5	5	30		40	+15.9	75	43	57	-49		-46
15-6, bulk	+ 13.8	40	15	5	40	+ 19.8			40					
15-6, kaolinite separate	+ 19.4	15			85	+ 20.0			85	100	0	-60	-60	
15-5, bulk	+ 14.2	40	15	5	40	+ 20.8			40	100	0	-61	-61	
15-4, bulk	+ 13.9	40	20	5	35	+ 20.9			35	100	0	-62	-62	
15-3, bulk	+ 12.7	35	25	10	30	+ 20.4			30	100	0	-62	-62	
15-2, bulk	+ 9.6	30	50	10	10	+ 17.1			10	100	0	-59	-59	
15-1, bulk	+ 8.5	30	60	10										
						+ 20.4 [b]		+ 13.1 [c]					-61 [d]	

[a] For purposes of calculation ilmenite and their accessory minerals small in quantity were ignored

[b] Average δO^{18} of kaolinite excluding 15-2

[c] Average δO^{18} of gibbsite

[d] Average δD of kaolinite

Figure 5-4 is a plot of δO^{18} content against weight percent kaolinite for the bulk soil samples from the C-zone. The weight percent kaolinite in this case is determined by the yield of H_2O released during the hydrogen extraction procedure. Kaolinite is a very hydrous mineral compared to the other constituents in the C-zone; hence the hydrogen yield is a very accurate and direct measure of the kaolinite content. The isotopic composition of pure kaolinite can thus be obtained by extrapolating the data in Figure 5-4 to 100% clay. The extrapolated δO^{18} value from Figure 5-4 ($+21.3‰$) is close to the average of the values calculated in Table 5-2 ($+20.4‰$).

The agreement of the two methods leads us to believe that the kaolinite in the Elberton profile has a relatively uniform δO^{18} of $+20.9 \pm 1.0$ throughout the C-zone. This δO^{18} value contrasts sharply with the δO^{18} contents of the parent minerals. Using the above δO^{18} value, and assuming the δO^{18} of local ground waters to be $-5‰$, an oxygen isotope fractionation factor between kaolinite and water can be calculated as follows:

$$\alpha^{ox}_{kaolinite\text{-}H_2O} = \frac{\left(\frac{O^{18}}{O^{16}}\right)_{kaolinite}}{\left(\frac{O^{18}}{O^{16}}\right)_{water}} = \frac{1 + \delta K/1000}{1 + \delta H_2O/1000} = \frac{1 + 20.9/1000}{1 - 5/1000} = 1.0260$$

This value is in good agreement with that of Savin and Epstein (1970a) (see Table 1-1). This strongly suggests that the kaolinite is in oxygen isotopic equilibrium with local ground waters.

The δD content of the C-zone samples ($\delta D = -61$) to a very close approximation also gives the δD of the kaolinite, because the contribution from the micas and traces of Al-Fe hydrates is very small. The measured δD is uniform through-

Figure 5-4. δO^{18} content of bulk weathered rock samples and a kaolinite concentrate from the Elberton profile plotted as a function of the weight percent kaolinite. The weight percent kaolinite was determined by measurement of the amount of water released during hydrogen isotopic extraction procedures.

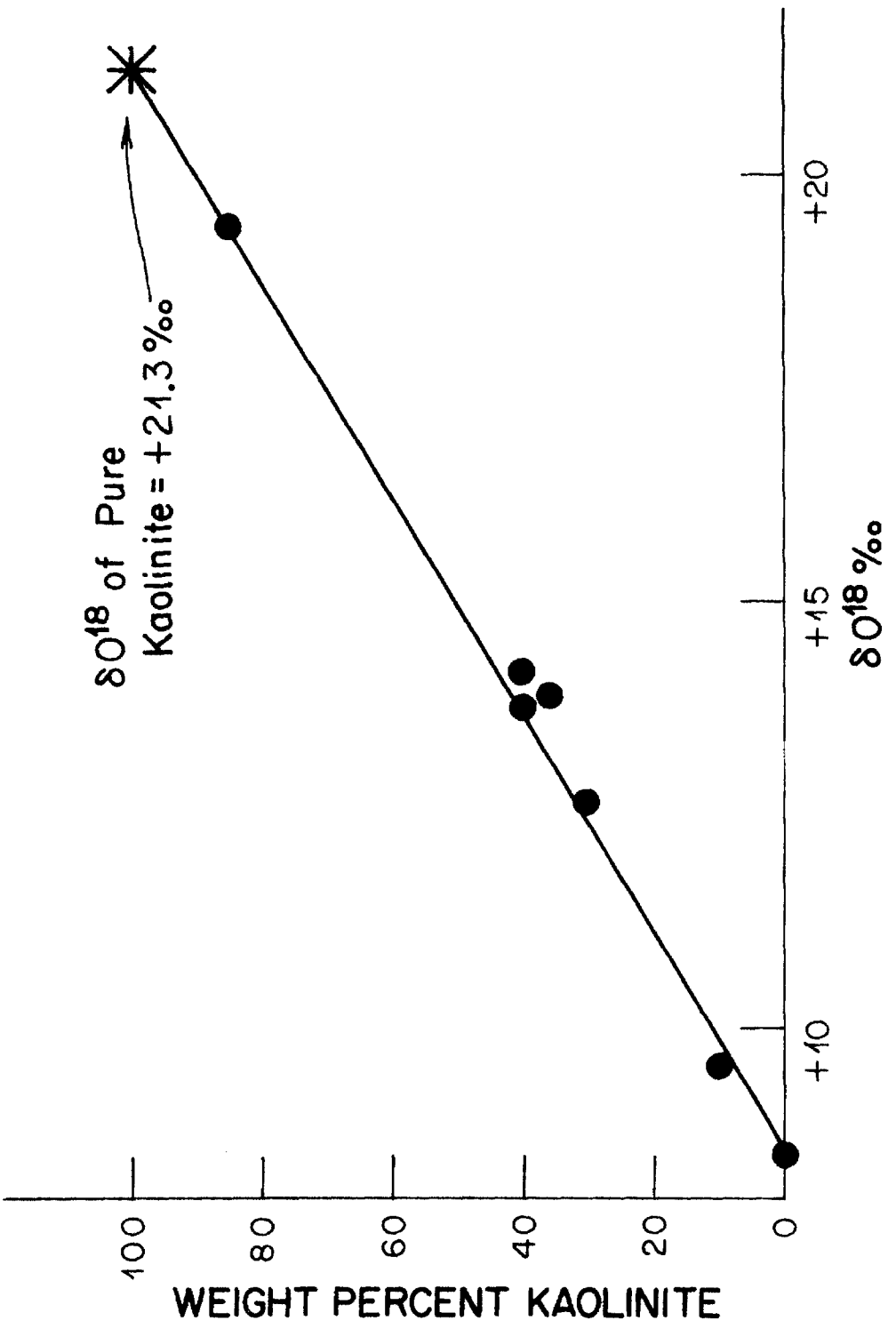
δO18 of Pure
Kaolinite = +21.3‰
+20
+15
+10
δO18 ‰
100
80
60
40
20
0
WEIGHT PERCENT KAOLINITE

Figure 5-4

Figure 5-5. Equilibrium stability fields of quartz and amorphous silica gel at 15° to 25°C, 1 atmosphere pressure. Constructed from solubility constants given by Garrels and Christ (1965). Also shown are the values of log [Na^+], log [SiO_2] and pH typical of ground waters in crystalline rocks of northern Georgia (Savin, 1964). These ground waters straddle the quartz and H_4SiO_4 fields of the diagram.

Figure 5-6. Equilibrium stability fields of albite, sodium montmorillonite, kaolinite and gibbsite at 15° to 25°C and 1 atmosphere pressure (based on equilibrium constants given by Hess, 1966). Also shown are the values of log [Na^+], log [SiO_2] and pH typical of ground waters in crystalline rocks of northern Georgia (Sever, 1964). These ground waters lie completely within the kaolinite field of the diagram.

Figure 5-7. Equilibrium stability fields of potassium feldspar, illite, kaolinite and gibbsite at 15° to 25°C and 1 atmosphere pressure (based on equilibrium constants given by Hess, 1966). Also shown are the values of log [K^+], log [SiO_2] and pH typical of ground waters from crystalline rocks of northern Georgia (Sever, 1964). These ground waters straddle the kaolinite and illite fields of the diagram.

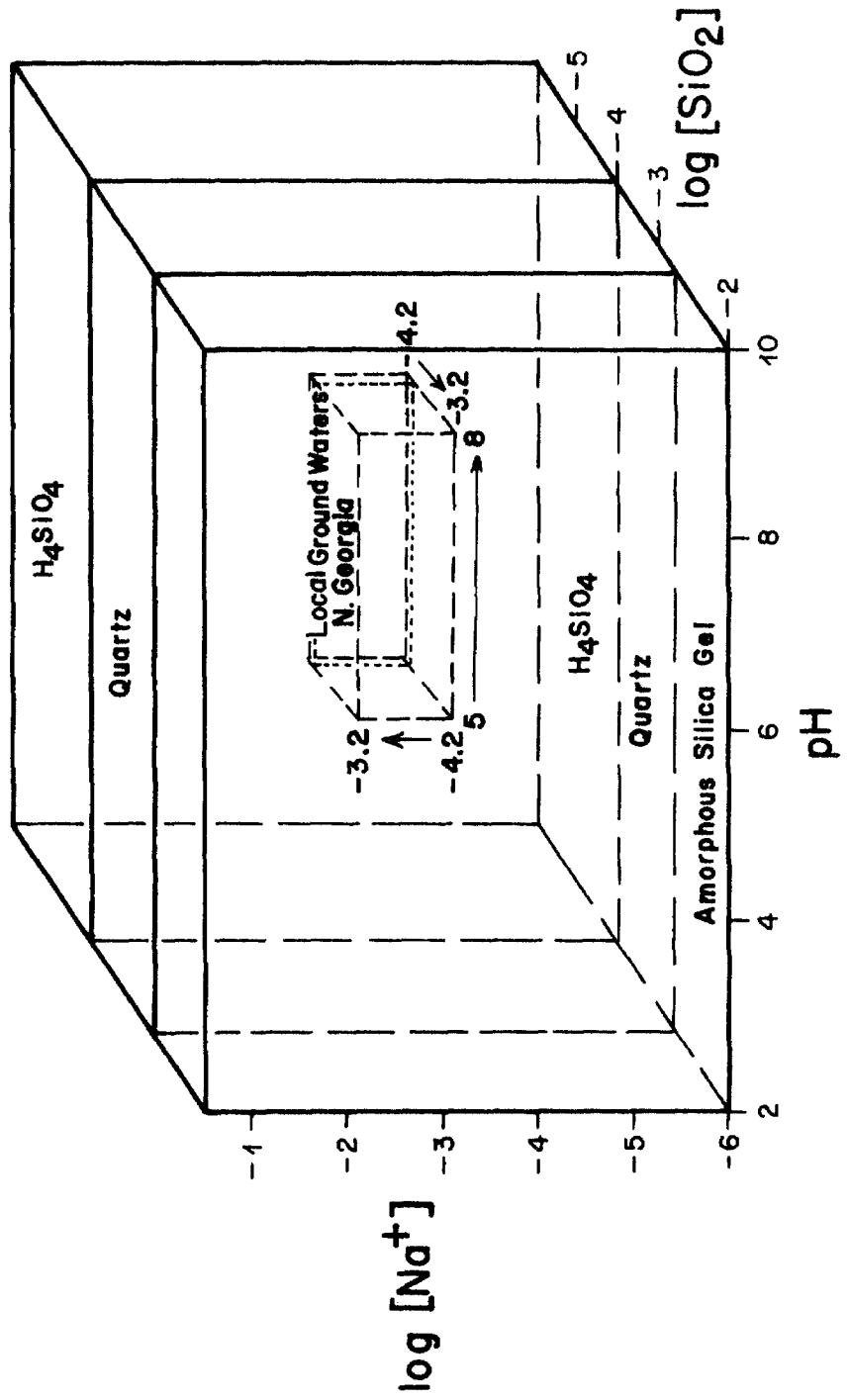
log [SiO2]
-5
-4
-3
-2
pH
2
4
6
8
10
log [Na+]
-1
-2
-3
-4
-5
-6
H4SiO4
Quartz
Amorphous Silica Gel
Local Ground Waters
N. Georgia
-4.2
-3.2
8
5

Figure 5-5

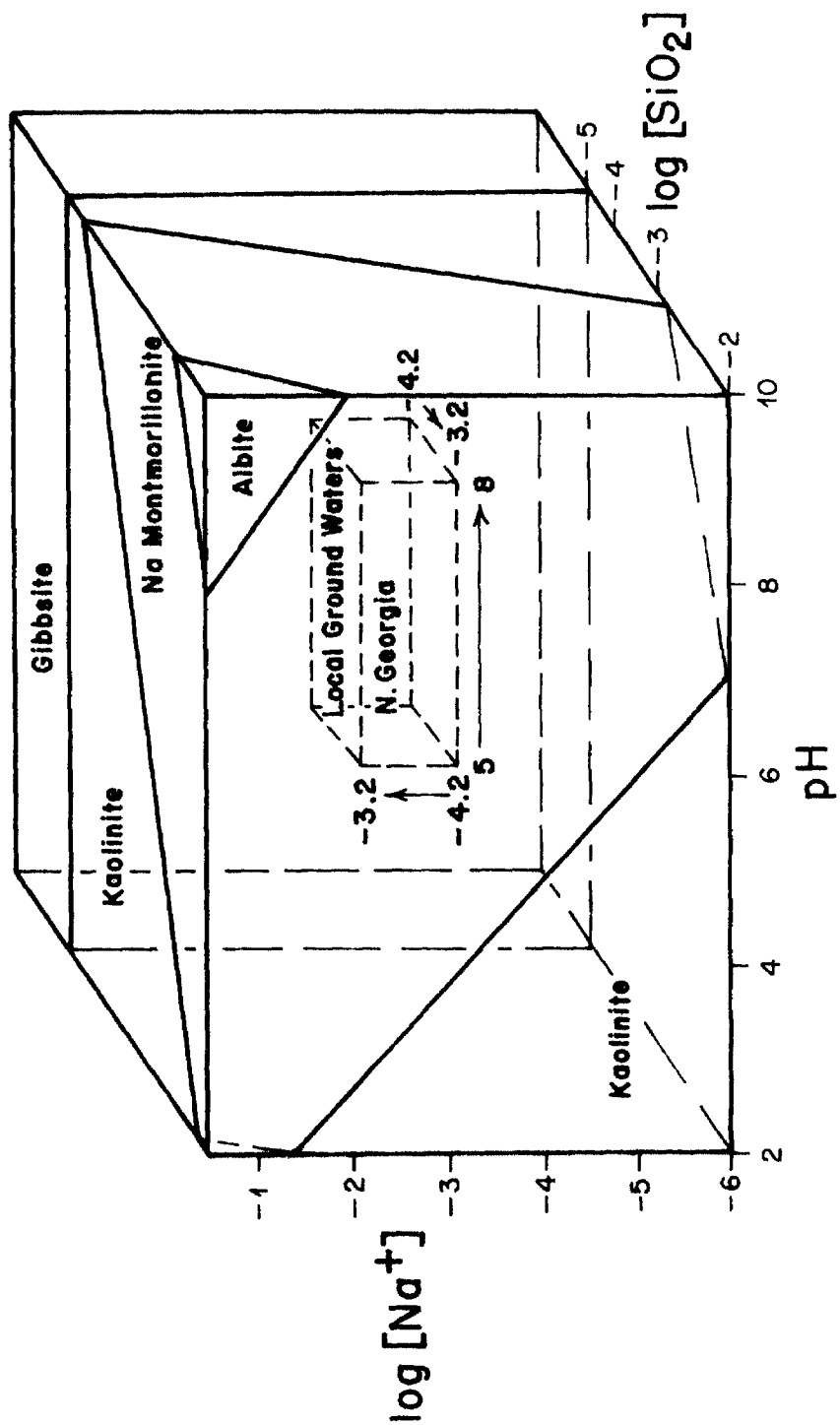
Gibbsite
Na Montmorillonite
Albite
Kaolinite
Kaolinite
Local Ground Waters
N. Georgia
-3.2
-4.2
-4.2
-3.2
5
8
log [Na+]
log [SiO2]
pH
-1
-2
-3
-4
-5
-6
-5
-4
-3
-2
2
4
6
8
10

Figure 5-6

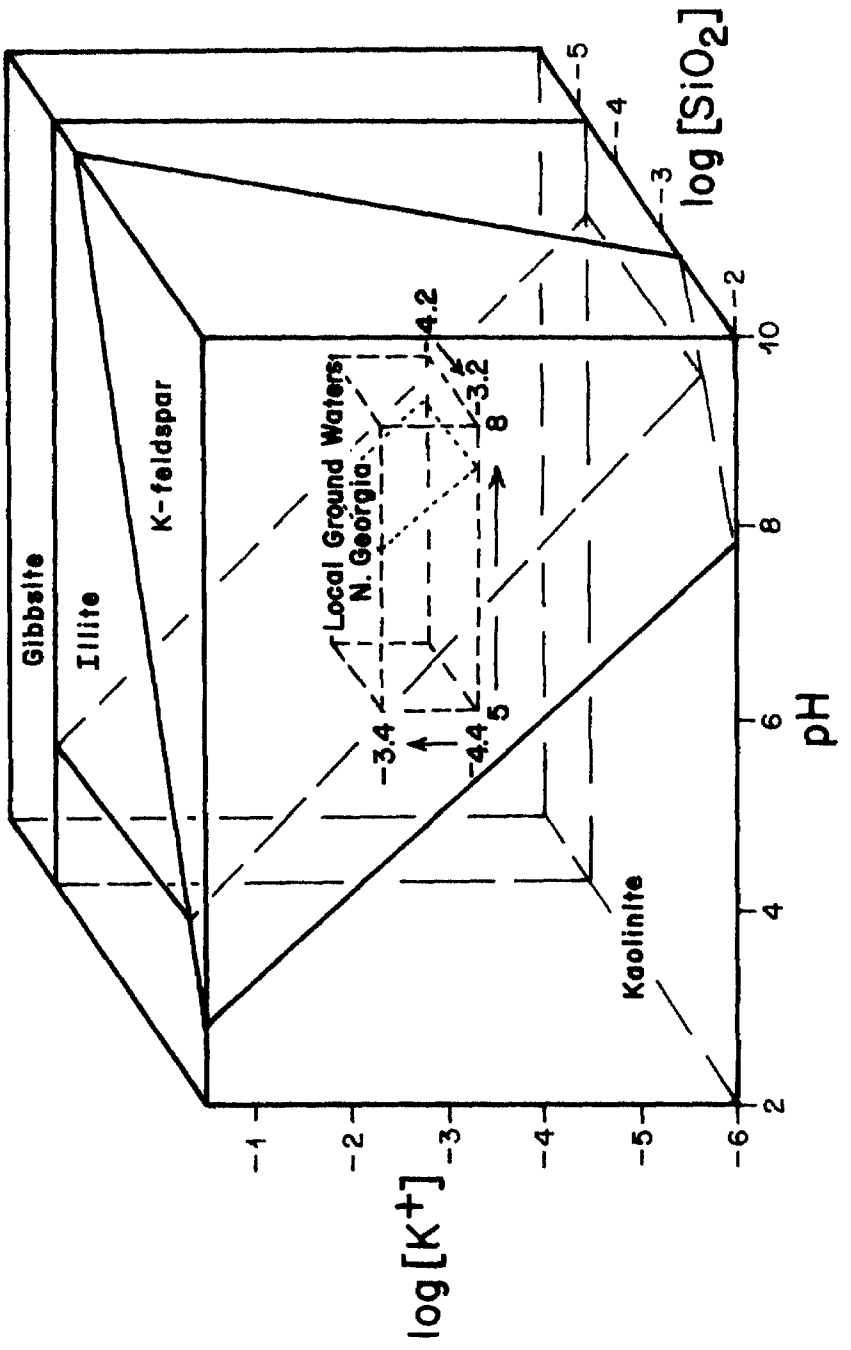
Gibbsite
Illite
K-feldspar
Kaolinite
Local Ground Waters
N. Georgia
-4.2
-3.2
-3.4
-4.4
8
5
log [K+]
log [SiO2]
pH
-1
-2
-3
-4
-5
-6
-5
-4
-3
-2
10
8
6
4
2

Figure 5-7

out the entire C-zone and is identical to the δD of the 85% pure kaolinite separate from sample 15-6, in which quartz was the only contaminant. Using the above δD value of kaolinite and $\delta D = -30‰$ for local ground waters (Friedman, 1964), a hydrogen isotope fractionation factor between kaolinite and water can be calculated as follows:

$$\alpha^{hy}_{kaolinite\text{-}H_2O} = \frac{1 - {}^{61}/_{1000}}{1 - {}^{30}/_{1000}} = 0.968$$

This value is in good agreement with that of Savin and Epstein (1970a) (see Table 1-1). This strongly suggests that the kaolinite is in hydrogen isotopic equilibrium with local ground waters.

Further evidence that the kaolinite is in hydrogen and oxygen isotopic equilibrium with local ground waters is indicated by the fact that this kaolinite plots almost exactly on Savin and Epstein's (1970a) kaolinite line (Figure 5-11).

Examination of Figures 5-6 and 5-7 illustrates that kaolinite is also in apparent chemical equilibrium with ground waters found in crystalline rocks of northern Georgia.

A- and B-zones: Samples 20-1 to 20-3 are located in the uppermost zones of the profile, 20-1 in the B-zone and 20-2 and 20-3 in the A-zone. The bulk δO^{18} content decreases from the C-zone to the B-zone (see Figure 5-3) despite the increase in the total amount of weathering products (from 40 to 55%). Inasmuch as the only new mineral present in abundance in the B-zone is gibbsite (30 to 40% of the sample), this decrease in O^{18} suggests that gibbsite must be distinctly lower

in O^{18} than coexisting kaolinite. Using a value of $+20.9‰$ for kaolinite, the δO^{18} of the gibbsite in sample 20-1 was calculated by material balance (Table 5-2).

The calculation was done for both the bulk sample and for the <400 mesh size fraction. The two calculations are in reasonable agreement considering the errors involved. The average δO^{18} of the two determinations is $+13.1$. If the gibbsite is assumed to be in isotopic equilibrium with local meteoric waters, the fractionation factor between gibbsite and water can be estimated, using $\delta O^{18} = -5$ for the local meteoric waters.

$$\alpha^{ox}_{\text{gibbsite-}H_2O} = \frac{1 + {}^{13.1}/_{1000}}{1 - {}^{5}/_{1000}} = 1.018$$

The δD values of samples 20-1 and 20-2 are higher than those in the C-zone, suggesting that gibbsite has a higher δD than kaolinite. From material balance calculations in Table 5-2 the pure gibbsite is estimated to have a $\delta D = -46‰$. Using this value and a $\delta D = -30‰$ for local meteoric waters the hydrogen isotopic fractionation factor between gibbsite and water, $\alpha^{hy}_{\text{gibbsite-}H_2O}$, is determined to be 0.984.

The gibbsite in sample 20-1 coexists with quartz and feldspar. Figures 5-5 and 5-6 illustrate that gibbsite is thermodynamically incompatible with quartz and feldspar under equilibrium conditions. It therefore appears that rainwaters percolating into the B-zone are sufficiently deficient in silica that gibbsite is a stable phase (see Figures 5-6 and 5-7). Such weathering conditions tend to eliminate feldspar, biotite and quartz from the system rather than resulting in a change in their δO^{18} content.

The decrease in δO^{18} from sample 20-1 to 20-3 is a reflection of the decrease in abundance of weathering products in 20-3. The δO^{18} approaches a value characteristic of a mixture of quartz, some feldspar and very little clay, which is in fact what is observed by X-ray analysis. As was pointed out earlier, the δO^{18} of quartz and biotite does not change in going from the fresh rock to the A-zone. The δO^{18} of the feldspar in the A-zone also does not appear to have exchanged significantly with the local waters; otherwise, the δO^{18} of the bulk sample would not decrease from 20-1 to 20-3.

5.3 Big Sur, California montmorillonite profile

The Big Sur profile (roadcut, 800 foot elevation, 1.5 miles from the Pacific Coast, 6 miles due north of Point Sur, Monterey County, California, Figure 5-8, see Appendix I for the exact location) was formed by intense montmorillonitic weathering of a non-uniform, coarse-grained hornblende-quartz diorite gneiss. The marine temperate to subtropical dry climate is characterized by an annual temperature range of 3° to 24°C (mean monthly) and a total rainfall of 25 to 45 inches, with a seasonal maximum in the winter. The topography is rugged with dense Mediterranean scrub vegetative cover.

Figure 5-8 shows a detailed sketch of the roadcut from which the samples were collected. Samples 1 to 11 all came from the roadcut. Sample 12, the parent rock, was collected several hundred yards further east where fresher rock could be found. Table 5-3 gives a brief description of each sample.

Quantitative estimates of the mineral constituents are given in Table 4-1 and Figure 5-11 together with the isotopic data obtained on the bulk samples and on various mineral separates. Petrographic descriptions of samples 9 and 12

TABLE 5-3

Descriptions of the Samples from the Big Sur, California Profile

Mon-Cal-1-12 *

Slightly weathered, coarse grained (~5mm) hornblende, quartz-diorite gneiss containing plagioclase - 50% (oligioclase - andesine), quartz - 25% , hornblende-15%, chlorite - 10% ; hornblende partially altered to Fe-rich chlorite; plagioclase altered slightly along cleavage planes to montmorillonites.

Mon-Cal-1-9 *

Residual friable boulder of hornblende, quartz-diorite gneiss; quartz unaltered, plagioclase slightly more altered along cleavage planes and edges to montmorillonite; hornblende largely altered to a red-brown montmorillonite and some chlorite.

Mon-Cal-1-10

Yellow-brown saprolite; abundant residual coarse-grained plagioclase and quartz; c.g./c ratio # ≈ 2.

Mon-Cal-1-11

Light green and yellow saprolite; moderately abundant medium to fine grained plagioclase and quartz; c.g./c ratio # ≈ 1.

TABLE 5-3 (continued)

Mon-Cal-1-8

Gray, yellow and brown varicolored saprolite; moderately abundant medium to coarse grained plagioclase and quartz; c.g./c ratio # $\approx$ 1.

Mon-Cal-1-7

Yellow and brown saprolite; residual cobble; abundant medium to coarse grained plagioclase and quartz; c.g./c ratio # $\approx$ 1.5 .

Mon-Cal-1-6

Dark brown and gray clay zones 1/2 to 2 inches thick with occasional fragments of quartz and feldspar; c.g./c ratio # < 0.3 .

Mon-Cal-1-4

Dark brown and gray clay zones 1/2 to 2 inches thick with moderately abundant plagioclase and quartz; c.g./c ratio # < 0.5 .

Mon-Cal-1-3

Brown clay with rare plagioclase and quartz; c.g./c ratio # < 0.2 .

Mon-Cal-1-2

Brownish-gray clay with rare plagioclase and quartz; c.g./c ratio # < 0.2 .

TABLE 5-3 (continued)

Mon-Cal-1-1

Dark brown to black granular soil with abundant plagioclase and quartz; c.g./ c ratio# ≈ 1.

* Thin sections used.

\# c.g./c ratio = volume ratio of coarser grained feldspar and quartz to clay-sized fraction.

Figure 5-8. A detailed sketch of the Big Sur, California weathering profile. The A-zone is a dark brown organic-rich soil containing a moderate abundance of residual feldspar and quartz grains. The B-zone contains 65 to 85% gray and brown clay with the remainder consisting of residual quartz and feldspar grains. The C-zone contains 30 to 65% brown and gray clay with abundant residual feldspar, quartz and rare hornblende grains. The 3 x 5 inch cards a, b, c and d shown in the photographs, Figures 5-9 and 5-10, are shown in this sketch.

Figure 5-9. A photograph of the Big Sur, California weathering profile. The 3 x 5 inch cards a, b, c and d are also shown in Figure 5-8. Note the heavy vegetative cover above the soil profile and the abundance of roots in the A-zone.

Figure 5-10. A closeup photograph at the boundary between the B and C zones in the Big Sur, California weathering profile. The 3 x 5 inch card is also shown in Figures 5-8 and 5-9. Note the 1 to 2 inch thick clay-rich lens in the C-zone.

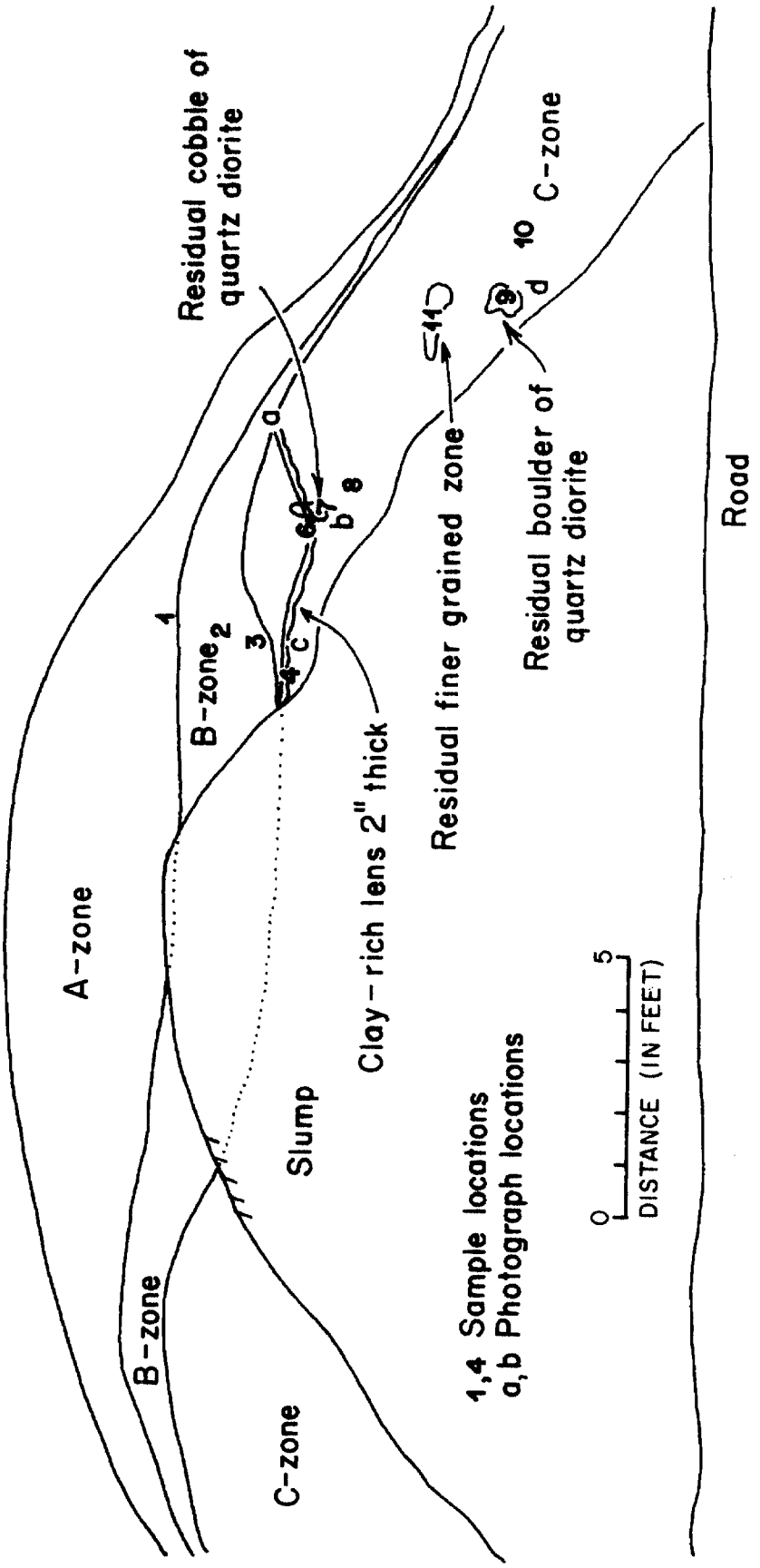
Residual cobble of quartz diorite
A-zone
B-zone
B-zone
C-zone
Slump
Clay-rich lens 2" thick
Residual finer grained zone
Residual boulder of quartz diorite
C-zone
Road
1,4 Sample locations
a,b Photograph locations
0
5
DISTANCE (IN FEET)

Figure 5-8

Figure 5-9

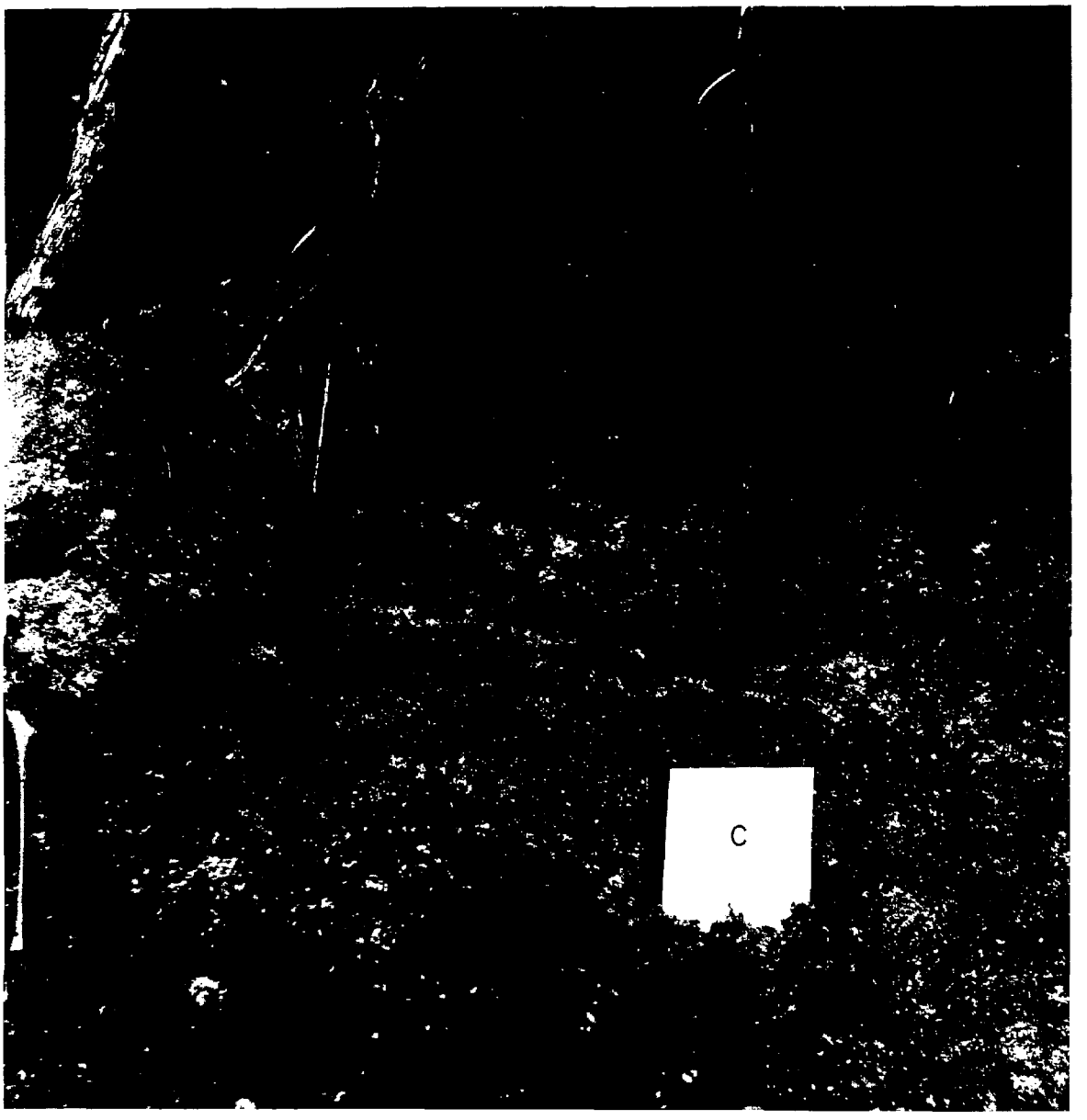

Figure 5-10

Figure 5-11. δD and δO^{18} contents of bulk samples and minerals from the Big Sur, California profile. Quartz, feldspar and hornblende were analyzed directly. The M-1 and M-2 montmorillonite separates were analyzed directly. The δO^{18} values of the pure M-1 and M-2 montmorillonites were calculated by material balance. Sample 12, relatively fresh quartz-diorite gneiss, was collected about 1000 feet east of the detailed profile.

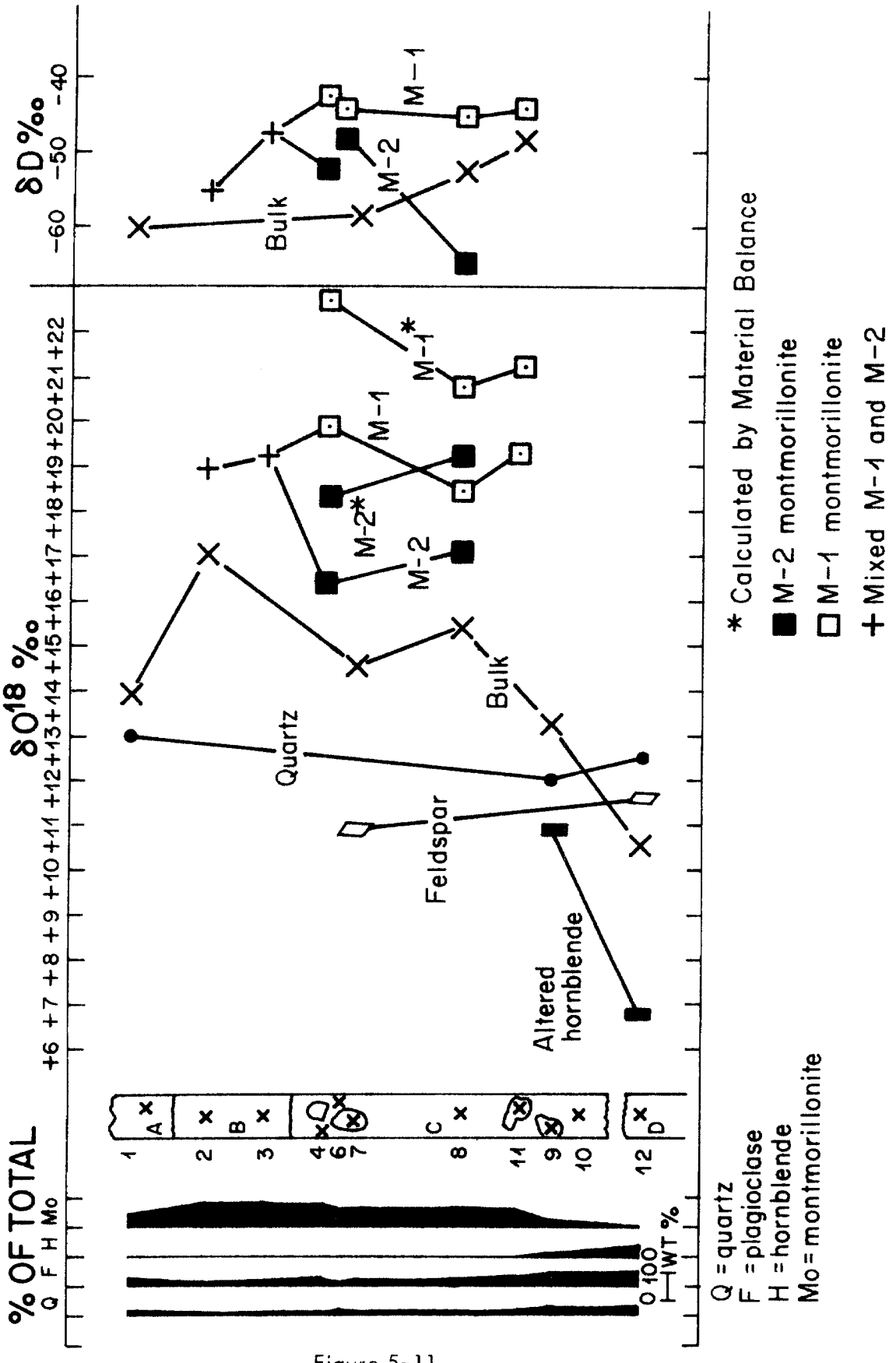
% OF TOTAL
Q F H Mo
δO18 ‰
+6 +7 +8 +9 +10 +11 +12 +13 +14 +15 +16 +17 +18 +19 +20 +21 +22
δD ‰
-60 -50 -40
Quartz
Feldspar
Altered hornblende
Bulk
M-1
M-2
M-1*
M-2*
A
B
C
D
1
2
3
4
6
7
8
11
9
10
12
0 100 WT %
Q = quartz
F = plagioclase
H = hornblende
Mo = montmorillonite
* Calculated by Material Balance
M-2 montmorillonite
M-1 montmorillonite
Mixed M-1 and M-2

Figure 5-11

are given in Table 5-3, and X-ray diffraction patterns for two samples are shown in Appendix II.

Parent minerals: The δO^{18} content of the minerals quartz, plagioclase and hornblende in the relatively fresh parent rock (sample 12) are shown in Figure 5-11. Quartz and feldspar display very little change (less than 1‰) in δO^{18} going from the fresh rock to intensely weathered horizons. This small variation may be due to imperfect separation of quartz and feldspar or to inhomogeneties in the δO^{18} of the parent rock. Hornblende weathers very readily; it is completely gone from all samples except (1) the relatively fresh rock (sample 12) where it is partially altered to chlorite, and (2) a single residual, weathered boulder (sample 9) where it is largely altered to montmorillonite and chlorite. The δO^{18} content of the altered hornblende in sample 9 is drastically different from that in sample 12, presumably as a result of the very high δO^{18} value of the montmorillonite.

Weathered horizons: As was observed in the Elberton profile, the δO^{18} content of the bulk soil in the Big Sur profile closely parallels the clay content. Two distinctly different montmorillonites are present, a gray montmorillonite (designated M-1) and a brown montmorillonite (designated M-2). Visual inspection suggests that M-1 results from the alteration of feldspar, and M-2 results from the alteration of hornblende. The two montmorillonites have identical X-ray patterns (see Appendix II). The only chemical difference observed between the two clays is their iron content. M-1 clays have Fe_2O_3 contents of 3.5 to 4.5% by weight, whereas M-2 clays have 6.5 to 8.5% . Mixing of the clays occurs in the B-zone of the soil so physical separation of the two clays is confined to the C-zone.

Handpicked separates of relatively pure M-1 and M-2 clays were analyzed

isotopically. The δO^{18} values are plotted in Figure 5-11. These samples contain about 75% clay, the impurities being mainly quartz and feldspar. These M-1 and M-2 clay concentrates show distinct differences in δO^{18} content, M-1 being about 2 to 3 per mil higher in O^{18} than M-2.

Figure 5-12 is a plot of δO^{18} versus weight percent Fe_2O_3 for the clay concentrates. The δO^{18} content increases with decreasing Fe_2O_3 content, but there is too much scatter in the data to determine the δO^{18} contents of the pure end members (assuming that they are a Fe-rich nontronite and an Fe-poor beidellite). There is an indication, however, that $\alpha^{ox}_{\text{nontronite-}H_2O} < \alpha^{ox}_{\text{beidellite-}H_2O}$.

The δO^{18} contents of pure M-1 and M-2 clays are calculated by material balance in Table 5-4 and illustrated in Figure 5-11. The difference between the average δO^{18} contents of M-1 and M-2 is 2.8‰ which corresponds to a 3.0 weight percent difference in Fe_2O_3. This large observed difference in δO^{18} contents, considering the relatively small difference in observed Fe_2O_3 contents, indicates that small chemical differences may have large effects on δO^{18} contents of clay minerals formed at low temperatures.

Using a δO^{18} value of local ground water equal to -6‰ (calculated from δD of meteoric waters from coastal Monterey County, Friedman, 1964) and the average δO^{18} values of M-1 and M-2 from Table 5-3, the oxygen isotopic fractionation factors between these montmorillonites and water can be calculated as follows:

$$\alpha^{ox}_{(M-1)-H_2O} = 1.0277 \quad ; \qquad \alpha^{ox}_{(M-2)-H_2O} = 1.0248$$

These values are in reasonable agreement with those of Savin and Epstein (1970a ,

TABLE 5-4

Material Balance Calculations of the δO^{18} Content of M-1 and M-2 Montmorillonites

Sample No. clay type	δO^{18} bulk	wt. %[a] Quartz	wt. %[b] Feldspar	wt. % Montmorillonite	Calculated δO^{18} M-1	Calculated δO^{18} M-2	wt. % Fe_2O_3 M-1	wt. % Fe_2O_3 M-2	δD
4, M-1	+ 19.8	7	18	75	+ 22.7		4.2		-42
4, M-2	+ 16.4	7	18	75		+ 18.2		6.6	-51
8, M-1	+ 18.3	7	18	75	+ 20.7		4.5		-45
8, M-2	+ 17.0	7	20	73		+ 19.2		8.4	-65
11, M-1	+ 19.2	5	15	80	+ 21.2		3.8		-44
				Average =	+ 21.5	+ 18.7	4.5	7.5	

[a] Used δO^{18} = + 12.5 for quartz

[b] Used δO^{18} = + 11.6 for feldspar

Figure 5-12. The δO^{18} content of handpicked M-1 and M-2 montmorillonites from the Big Sur, California profile, plotted as a function of the weight percent Fe_2O_3 in the sample.

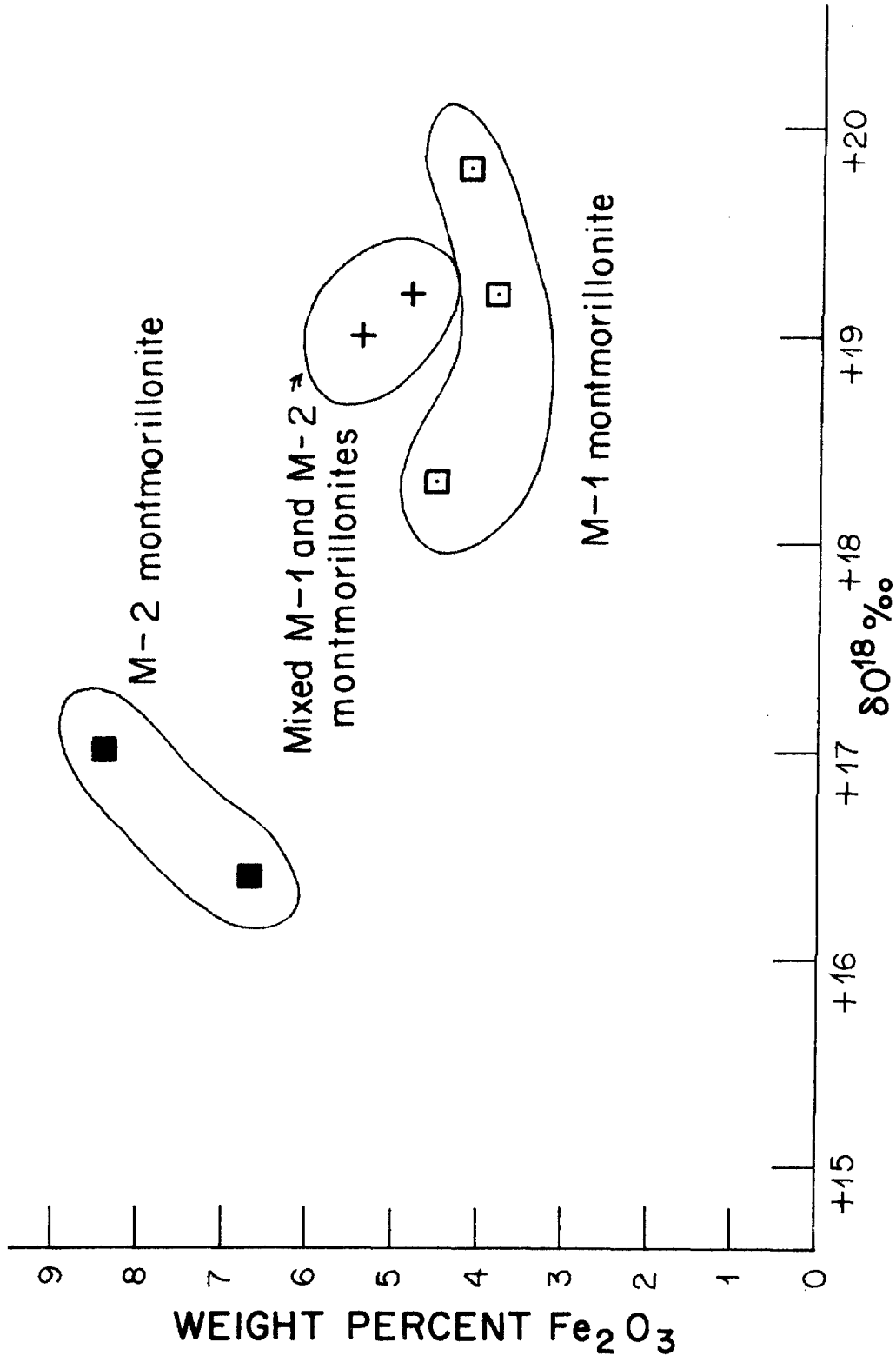
M-2 montmorillonite
Mixed M-1 and M-2 montmorillonites
M-1 montmorillonite
WEIGHT PERCENT Fe_2O_3
δO^{18} ‰
0
1
2
3
4
5
6
7
8
9
+15
+16
+17
+18
+19
+20

Figure 5-12

Table 1-1).

Figure 5-11 shows that the M-1 clay has a distinctly higher δD value than the M-2 clay. However, the differences from one sample horizon to the next are variable.

The bulk sample δD values seem to reflect the dominant clay type (see Figure 5-11), either M-1 or M-2. The clay in the bulk sample 11 is predominantly M-1 clay. In bulk sample 8 there is a mixture of M-1 and M-2. In bulk sample 7, a residual boulder where hornblende has been completely altered to clay but where considerable feldspar remains, the clay is mostly M-2. In bulk sample 1, organic matter is mixed with M-1 and M-2 clays.

Because montmorillonite is the only hydrous mineral of importance in the M-1 and M-2 separates, the δD values reflect the δD of the pure M-1 and M-2 clays. The difference between the average δD values of the M-1 and M-2 clays is about 10‰. As was discussed in Chapter III, the δD values of montmorillonites are not perfectly dependable because of hydrogen exchange between OH and interlayer water during the extraction procedure. However, if the degree of exchange for M-1 and M-2 clays are similar, the relative δD values of the two clays should be the same as the measured ratios. This suggests that $\alpha^{hy}_{beidellite-H_2O} > \alpha^{hy}_{nontronite-H_2O}$.

The δO^{18} and δD values of the pure M-1 and M-2 clays (from Table 5-3) are plotted on a δD versus δO^{18} plot in Figure 5-13. The values plot very near the kaolinite line and quite distant from the montmorillonite line (both lines are from Savin and Epstein, 1970a). However, since any exchange effects occurring during the experimental procedures would produce abnormally high δD values, the true data-points conceivably ought to be placed slightly below the kaolinite line.

Figure 5-13. δD and δO^{18} contents of M-1 and M-2 montmorillonites from the Big Sur, California profile plotted on a δD versus δO^{18} diagram. δO^{18} values were calculated by material balance, taken from Table 5-3. Also shown is the kaolinite from the Elberton profile. The kaolinite and montmorillonite lines of Savin and Epstein (1970a) are shown for reference.

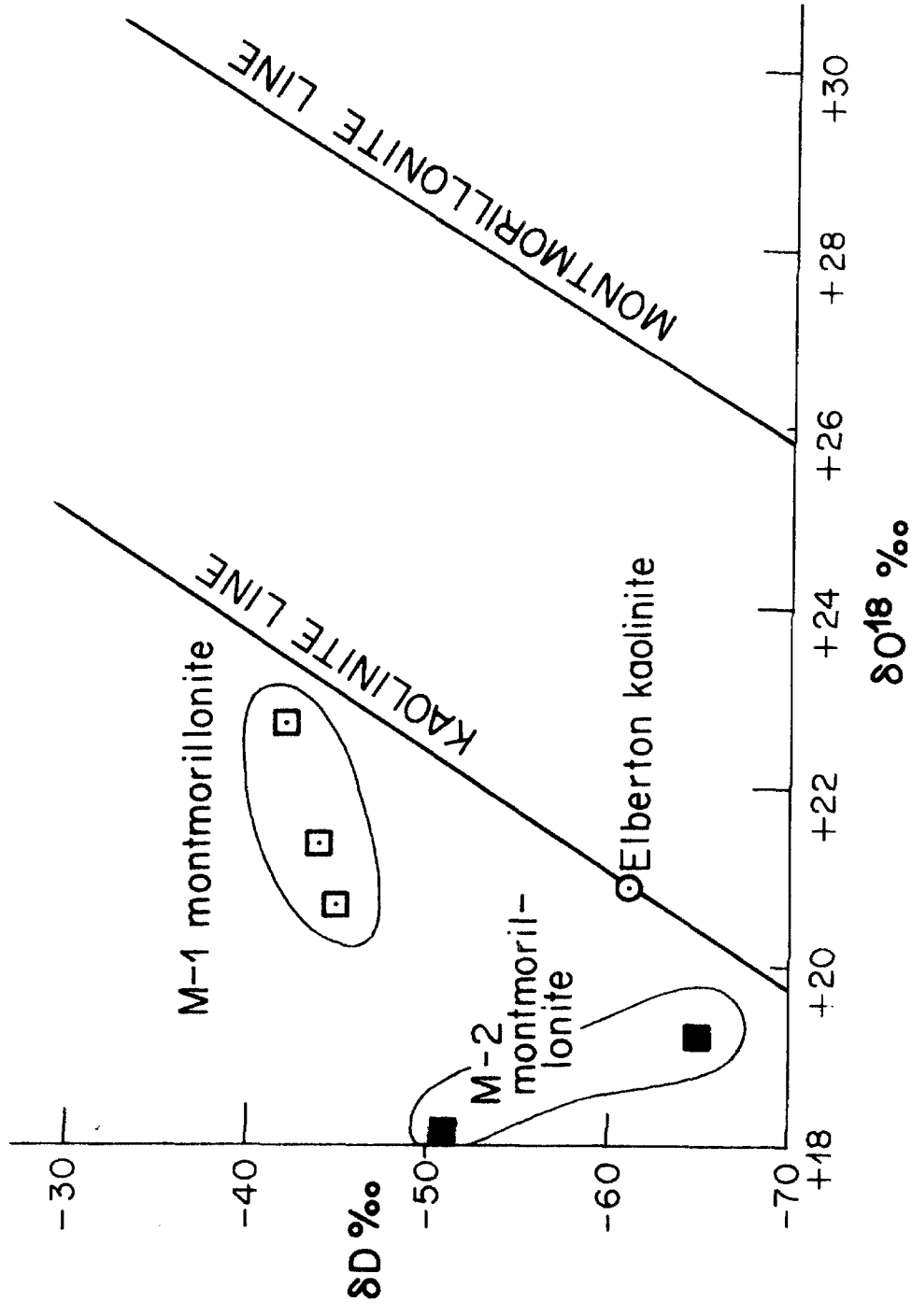
MONTMORILLONITE LINE
KAOLINITE LINE
M-1 montmorillonite
M-2 montmoril-lonite
Elberton kaolinite
-30
-40
-50
-60
-70
δD ‰
+18
+20
+22
+24
+26
+28
+30
δO18 ‰

Figure 5-13

5.4 Spokane County, Washington halloysite profile

The Spokane County profile (roadcut, elevation 300 feet, Mica Creek, Washington, see Appendix I for the exact location) is characterized by intense halloysite weathering of a vesicular basalt. The profile was formed during Miocene time under a wet temperature climate (Hosterman, 1969).

Samples were collected from eleven different horizons within the soil profile from fresh basalt to the uppermost clay-rich horizon. A description of the profile (Hosterman, 1969) is given below.

> The saprolite formed from the Columbia River Basalt is composed of 80 to 95 percent halloysite and 5 to 20 percent ilmenite and limonite. The basalt texture is preserved and is even accented by the uniformly disseminated grains of blue-black ilmenite against the white clay.
>
> Five gradational zones can be recognized in a typical section of basalt saprolite. These five zones can be seen in the outcrop of basalt saprolite on the main road at Mica Creek (SW 1/4 SW 1/4 SW 1/4 sec. 3, T. 23 N., R. 45 E.) Figure 5-14 shows the variations in content of SiO_2, Al_2O_3, Fe_2O_3, TiO_2, and CaO of the five zones. The upper zone of basalt saprolite is pale brown and is composed of halloysite and ilmenite; some of the ilmenite is altered to limonite. The cracks are filled with grains of quartz and muscovite that have been transported from the overlying Latah Formation through ground-water movement. This results in the SiO_2 content of the upper zone being high and the Al_2O_3 content being low (fig. 5-14). The second zone is also composed of halloysite and ilmenite, but since little or no limonite is present, the color is light bluish gray to light gray. All vesicles and cracks are filled with white halloysite. This zone has the lowest SiO_2 content and the highest Al_2O_3 and TiO_2 content. The third zone is weak yellow from the small amount of nontronite present. Halloysite and ilmenite are the main constituents, and halloysite fills most of the vesicles. The SiO_2 content is a little higher than zone 2, and the Al_2O_3 and TiO_2 contents are a little lower than zone 2 (fig. 5-14). Zone 4 is pale olive to light olive gray because of the greater amount of nontronite. Other minerals present are halloysite and ilmenite, with nontronite filling the cracks and vesicles. A few laths of plagioclase are present, but most of them are altered to halloysite. The fifth zone is light gray basalt that is virtually unaltered. This zone is considerably higher in Fe_2O_3 than any of the other zones (fig. 5-14). The contact with the overlying clay is surprisingly sharp.

Mineralogical descriptions of the samples are given in Table 4-1 and Figure 5-15, together with the isotopic data obtained on the bulk samples and the halloysite and ilmenite mineral separates.

The δO^{18} value of the unweathered basalt, $+7.0‰$, is typical of basalts and gabbros throughout the world (Taylor, 1968). Residual ilmenites from three different horizons of the weathering profile display only a slight variation in δO^{18}. Their δO^{18} values are characteristic of igneous ilmenites (Taylor, 1968), although these values are known to be slightly high because the ilmenite separates contained 5 - 10% halloysite contaminant.

As was the case with the two previous profiles, the δO^{18} contents of the intensely weathered rock samples show a direct correlation with the clay contents (see Figure 5-15). The δO^{18} values of the bulk samples B to H reflect primarily a mixture of halloysite and ilmenite. Note that the δO^{18} values of these bulk samples are intermediate to the δO^{18} values of the ilmenite separate and the halloysite separate. The δO^{18} values of the bulk samples I and J reflect a mixture of the clay minerals halloysite and nontronite, and the residual igneous minerals plagioclase, pyroxene and ilmenite.

The δD contents of the bulk samples (samples B to H contain halloysite, samples I and J contain nontronite and halloysite) vary in an erratic manner from -70 to -102.

As was pointed out in Chapter III, halloysite hydroxyl exchanges hydrogen isotopes at room temperature with interlayer water. Assuming interlayer water in Pasadena has a $\delta D = -50‰$ and that the fractionation factor between interlayer water and hydroxyl is 0.970, halloysites wholly exchanged with Pasadena atmospheric vapor would have δD values equal to $-80‰$. The observed δD values of the samples

Figure 5-14. Variation of the chemical composition of the bulk samples as a function of depth in the basalt saprolite from a roadcut at Mica Creek, near Spokane, Washington (after Hosterman, 1969).

Figure 5-15. δD and δO^{18} contents of bulk samples and pure halloysite and ilmenite mineral separates in the Spokane, Washington profile.

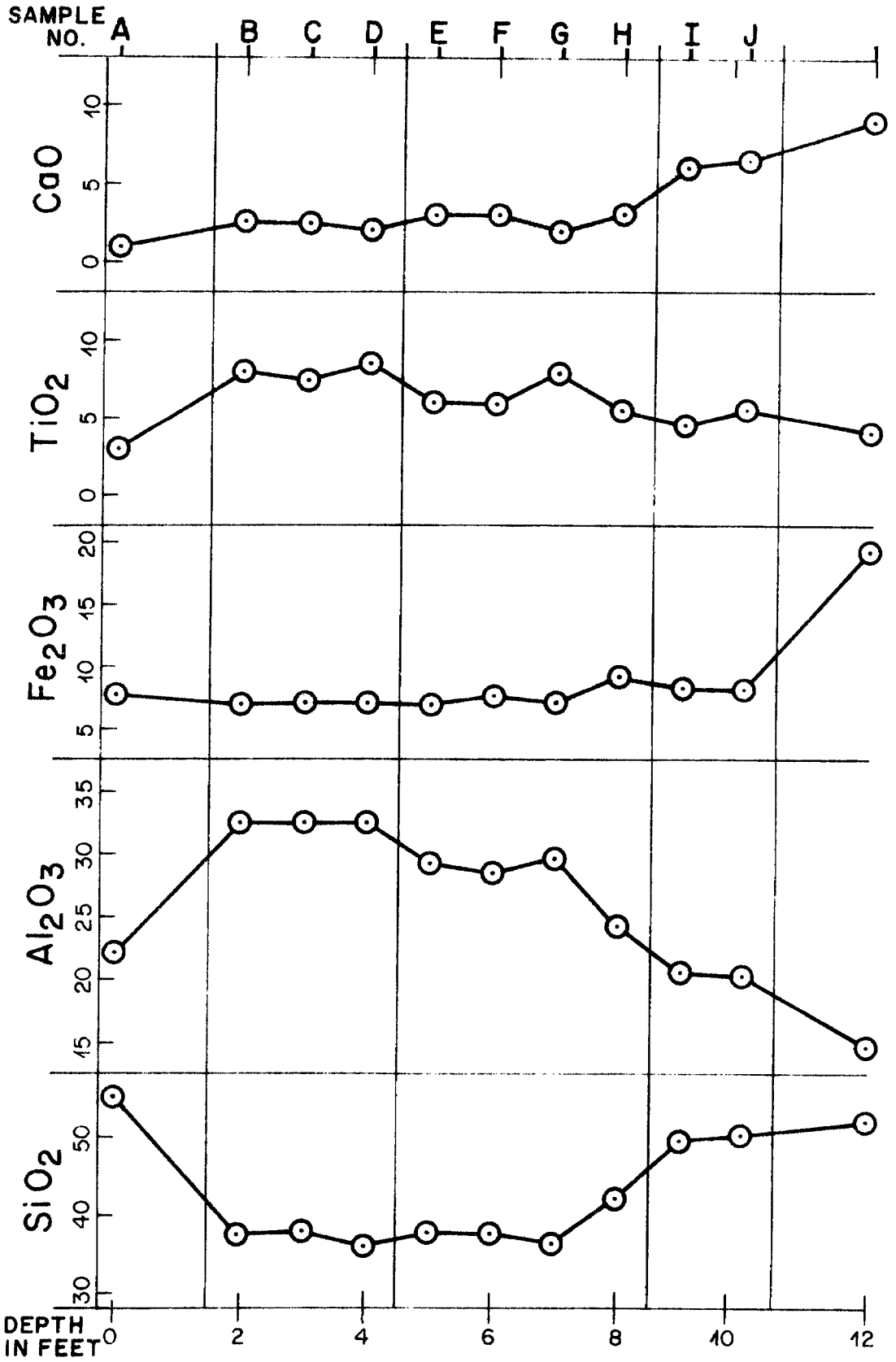
SAMPLE NO.
A
B
C
D
E
F
G
H
I
J
CaO
0
5
10
TiO2
0
5
10
Fe2O3
5
10
15
20
Al2O3
15
20
25
30
35
SiO2
30
40
50
DEPTH IN FEET
0
2
4
6
8
10
12

Figure 5-14

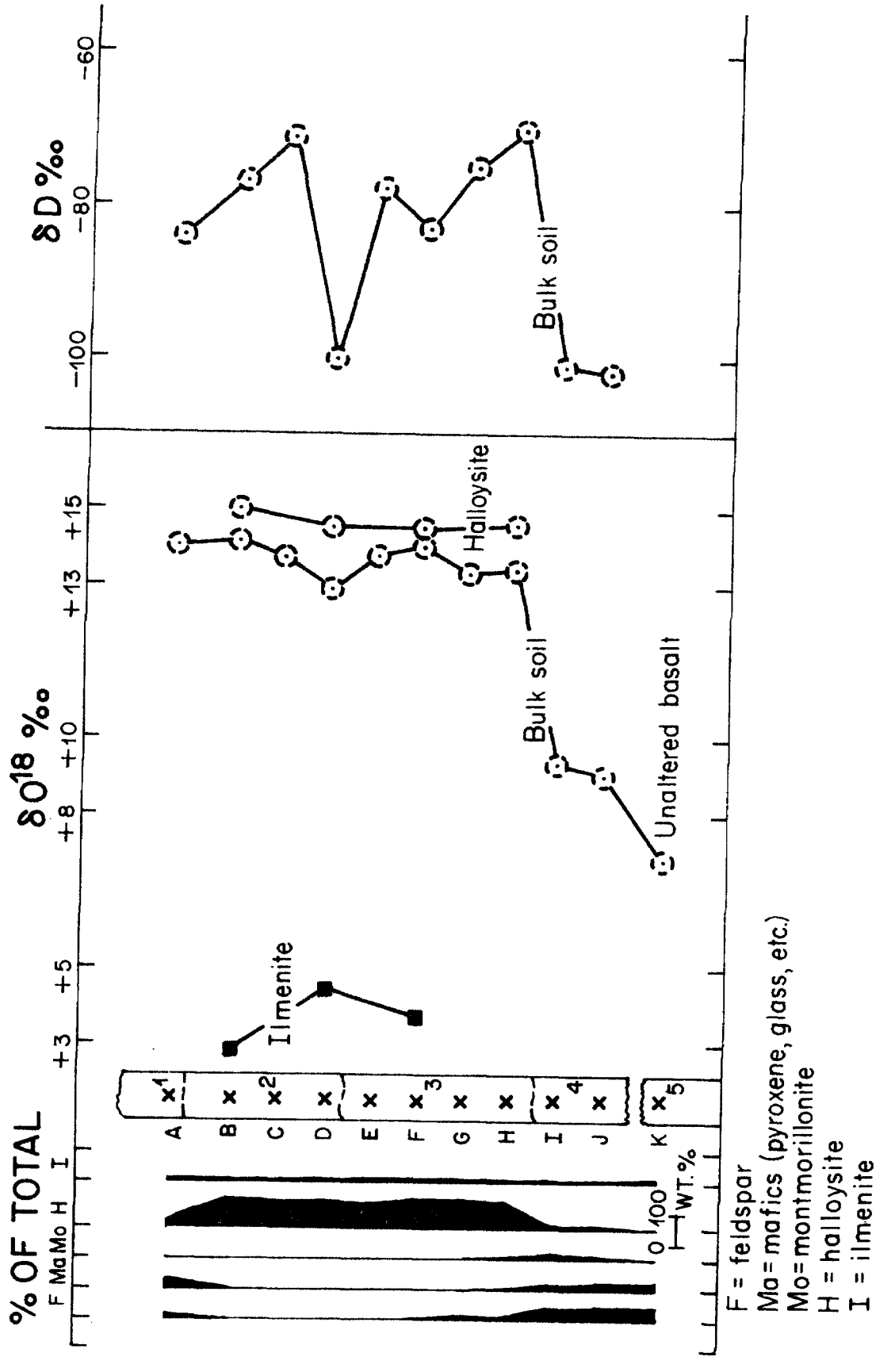
δD ‰
-60
-80
-100
Bulk soil
δO18 ‰
+15
+13
+10
+8
+5
+3
Halloysite
Bulk soil
Unaltered basalt
Ilmenite
A
B
C
D
E
F
G
H
I
J
K
x1
x2
x3
x4
x5
% OF TOTAL
F Ma Mo H I
0 100
WT.%
F = feldspar
Ma = mafics (pyroxene, glass, etc.)
Mo = montmorillonite
H = halloysite
I = ilmenite

Figure 5-15

Figure 5-16. The δD and δO^{18} contents of Miocene halloysites from the Spokane, Washington profile, compared with kaolinites of similar origin and age from the Spokane area, and plotted on a $\delta D - \delta O^{18}$ diagram. Savin and Epstein's (1970a) kaolinite line is shown for reference.

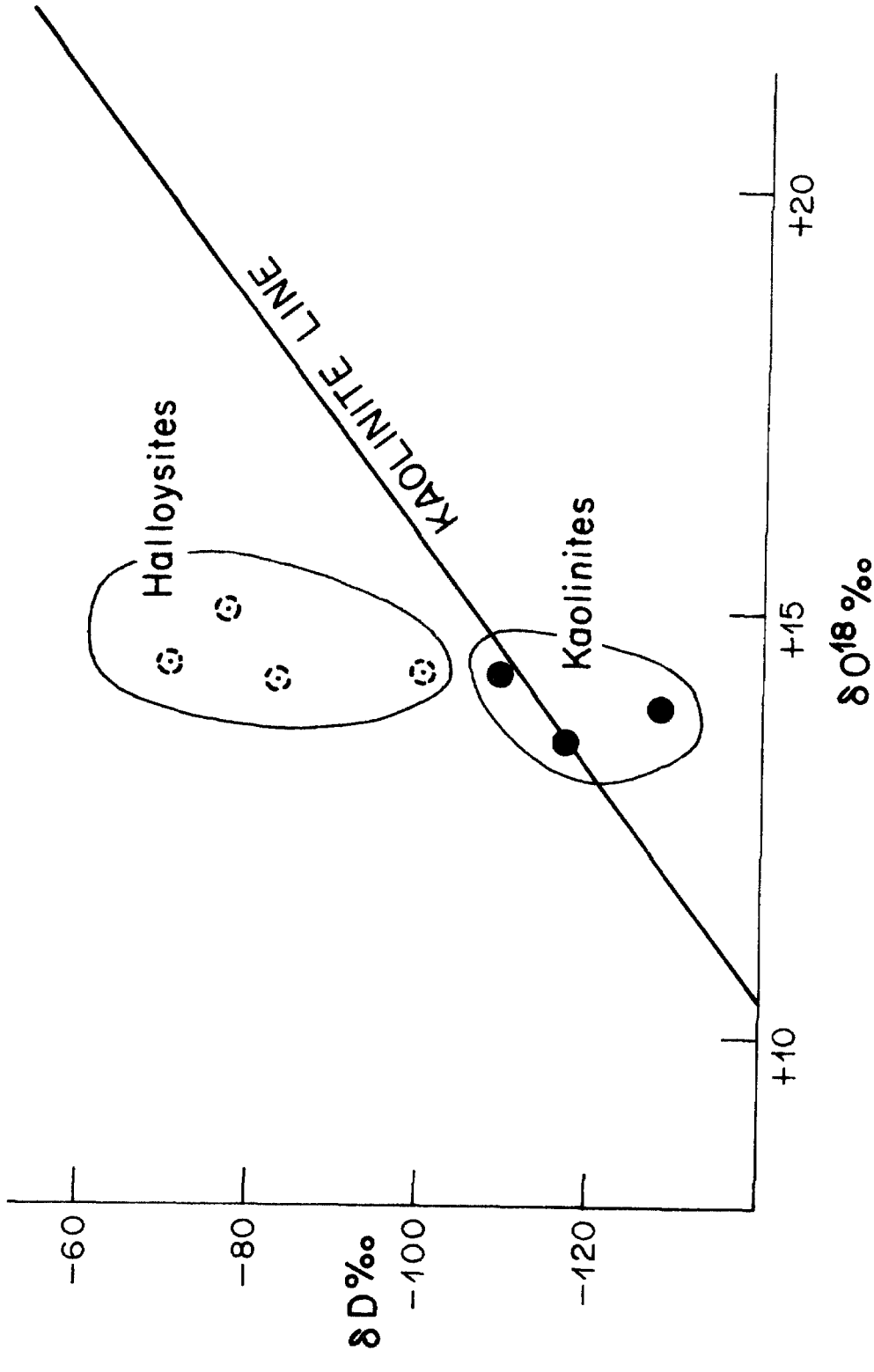
KAOLINITE LINE
Halloysites
Kaolinites
+20
+15
+10
δO18 ‰
−60
−80
−100
−120
δD‰

Figure 5-16

containing halloysite are compatible with at least partial isotopic exchange of this type.

Samples I and J have lower δD values than the other samples. This probably reflects the lower δD of the nontronite. Because the true δD of the halloysite is not accurately known, and because nontronite hydroxyl probably also undergoes some hydrogen isotope exchange with its interlayer water during heating and outgassing procedures, the δD value of the pure nontronite end member cannot be determined.

Figure 5-16 shows the isotopic values of (1) the four pure halloysite samples B, D, F and H, and (2) three kaolinite samples (Spo-Wash-1, 2, 3, Table 4-1) from the Spokane area plotted on a $\delta D - \delta O^{18}$ diagram. All of these clays were formed by weathering processes under similar climatic conditions during Miocene time. Because kaolinite and halloysite are chemically identical except for the interlayer water in halloysite, it is reasonable to expect that the original isotopic compositions of these samples should have been similar. Figure 5-16 illustrates that δO^{18} values of the two groups are indeed very similar, but that the δD values of the two groups are distinctly different. The halloysites have δD values 30 to 50‰ heavier than the δD values of the kaolinites. In addition, the δD and δO^{18} values of the kaolinites lie very near Savin and Epstein's (1970a) kaolinite line, suggesting that they are equilibrium values, whereas the halloysites are displaced above the kaolinite line. This suggests that the measured δD values of the halloysites are not preserved but represent exchange with interlayer water. The δO^{18} values of the halloysites, however, appear to have been partially preserved.

5.5 Pierre shale profiles

Three poorly developed Pierre shale profiles were studied: (1) roadcut

at an elevation of 5000 feet, Fergus County, Montana, (2) excavation site at an elevation of 1500 feet, Stanley County, South Dakota, and (3) open pit mine at an elevation of 5500 feet, Jefferson County, Colorado (see Appendix I for exact locations). The weathered zones are characterized by the leaching of carbonate and sulfur and the partial oxidation of iron. With the exception of one sample in which clay minerals are weathered to allophane (no. 3, Figure 5-18), no significant changes in silicate mineralogy occur from fresh shale to surface soil. The continental steppe climates in the three areas are characterized by an annual temperature range of -7° to +24°C (mean monthly) and a total rainfall of 10 to 20 inches, with a seasonal maximum in late spring. The generally flat lying topography is covered with sparse prairie grasses.

Samples were collected from three to five different horizons in each soil profile, from fresh shale at the base of the excavated cuts to the uppermost soil horizon. Detailed descriptions of two of the profiles, (1) and (2), are given by Tourtelot (1962). Descriptions and isotopic results for each of the profiles are given in Figures 5-17, 5-18 and Tables 4-1 and 5-5.

The δO^{18} and δD values of the samples from profiles (1) and (2) show almost no change in going from fresh shale to the soil horizon. There is only a slight correlation between the δO^{18} values and the intensity of weathering in a given profile. This fact suggests that little or no isotopic exchange has occurred during the weathering process.

The δO^{18} and δD values of the fresh shale and the slightly weathered shale in profile (3) are also nearly identical. Very little isotopic exchange appears to have taken place as a result of this degree of weathering. However, the intensely weathered shale, in which montmorillonite, illite, and feldspar are altered to an

Figure 5-17. δD and δO^{18} contents of bulk samples from poorly developed soil profiles on the Claggett shale (Pierre shale equivalent), Fergus County, Montana; and the Pierre shale, Stanley County, South Dakota.

Figure 5-18. δD and δO^{18} contents of bulk samples from a poorly developed soil profile on a Pierre shale equivalent, Jefferson County, Colorado.

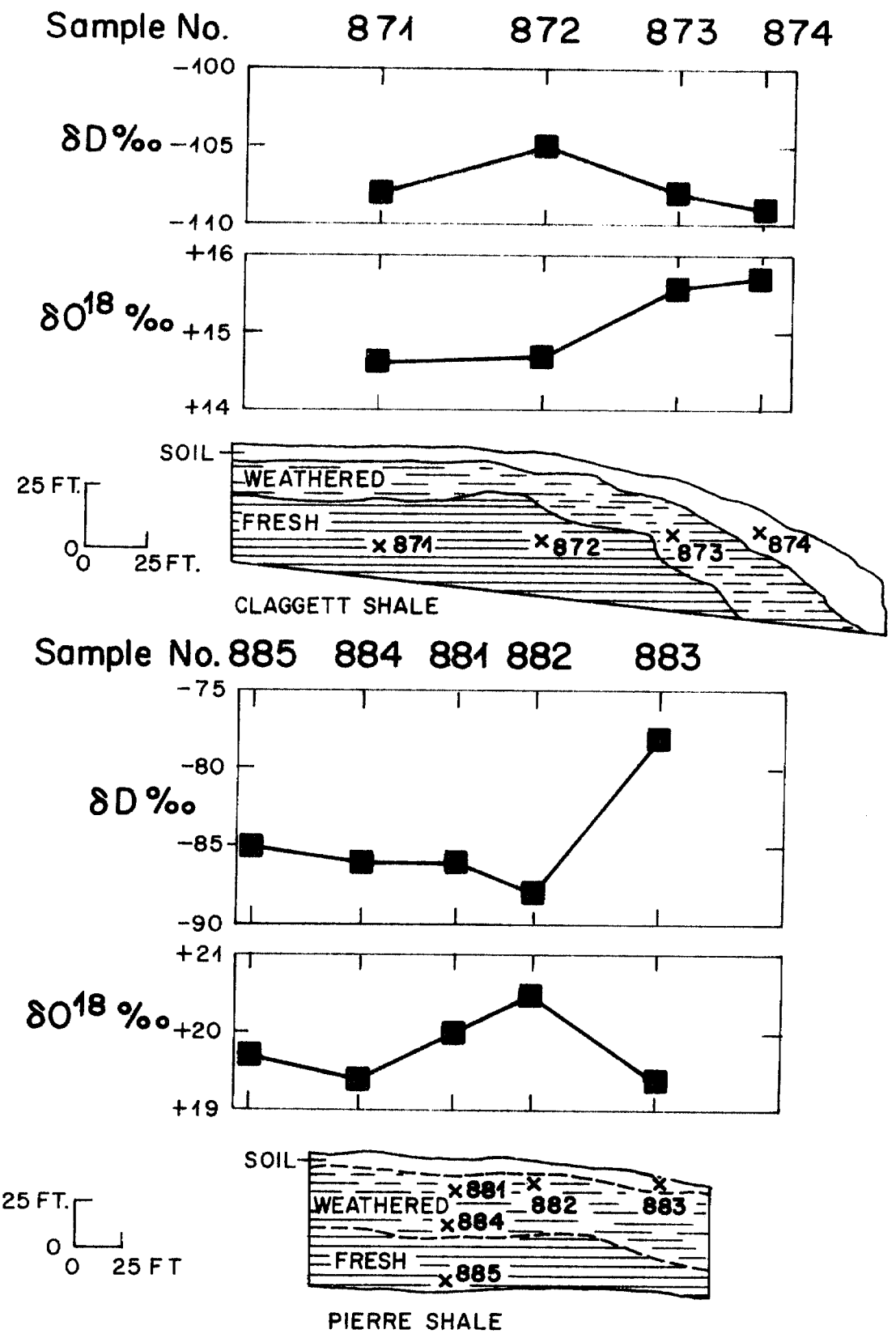
Sample No. 871 872 873 874
-100
δD‰ -105
-110
+16
δO18 ‰ +15
+14
SOIL
WEATHERED
FRESH
25 FT.
0
0 25FT.
×871
×872
×873
×874
CLAGGETT SHALE
Sample No. 885 884 881 882 883
-75
-80
δD‰
-85
-90
+21
δO18 ‰ +20
+19
SOIL
WEATHERED
FRESH
25 FT.
0
0 25 FT
×881
×882
×883
×884
×885
PIERRE SHALE

Figure 5-17

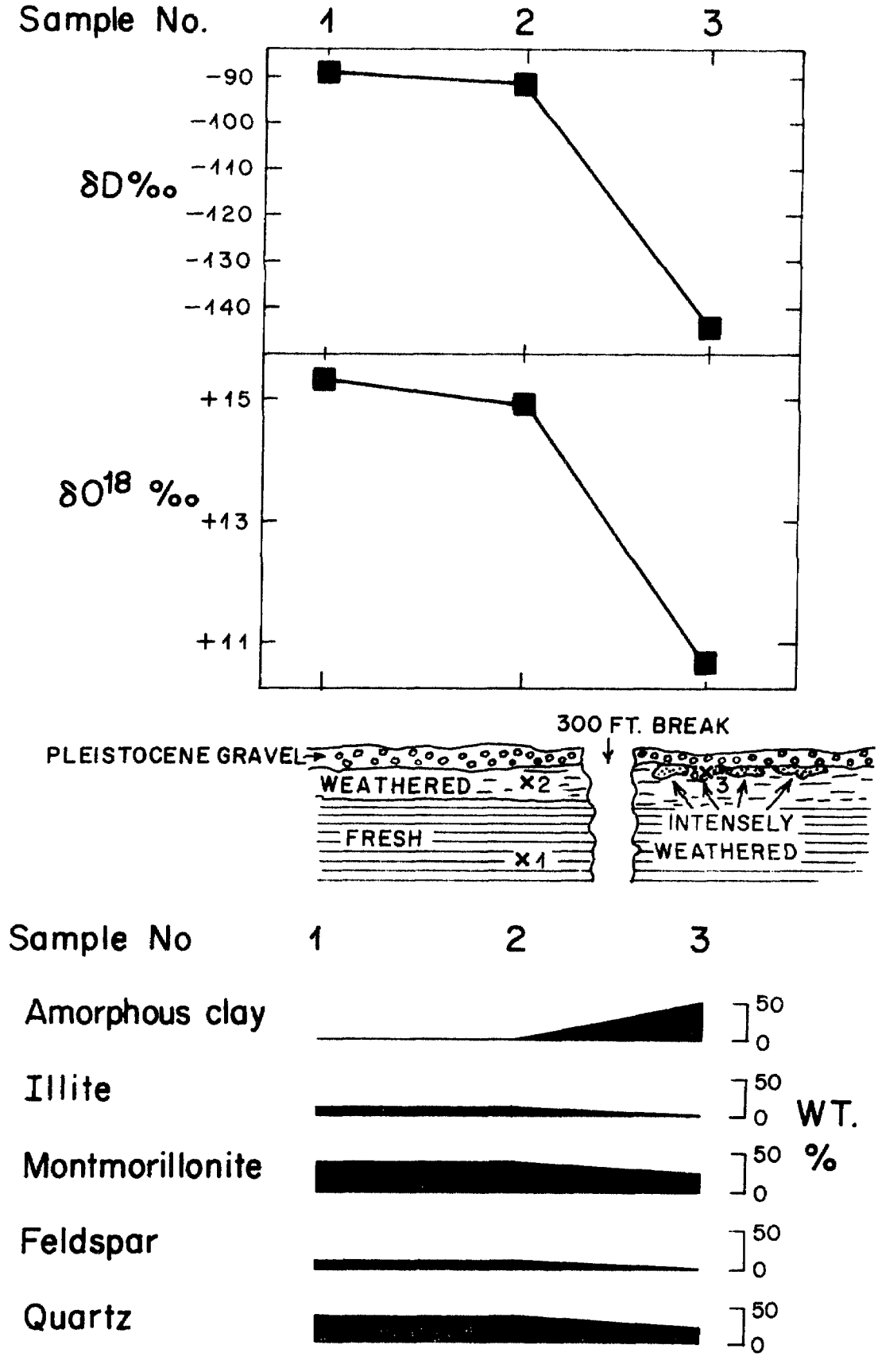
Sample No.
1
2
3
-90
-100
-110
-120
-130
-140
δD‰
+15
+13
+11
δO18 ‰
300 FT. BREAK
PLEISTOCENE GRAVEL
WEATHERED
x2
FRESH
x1
x3
INTENSELY
WEATHERED
Sample No
1
2
3
Amorphous clay
Illite
Montmorillonite
Feldspar
Quartz
50
0
WT.
%

Figure 5-18

TABLE 5-5

Mineralogical and Chemical Descriptions of the Claggett and Pierre Shale Profiles (after Tourtelot, 1962)

	Claggett Shale Profile			
Sample No. :	871	872	873	874
Chemical Components				
wt. % Fe_2O_3	5.10	5.01	6.17	5.74
wt. % CaO	1.25	1.11	0.23	0.90
wt. % CO_2	0.14	0.04	0.03	0.02
wt. % SO_3 (acid soluble)	3.00	3.03	0.46	0.17
Minerals				
wt. % Quartz	15	18	17	17
wt. % Feldspar	4	3	3	2
wt. % Clay Minerals	60	60	70	70
wt. % Other	21	19	10	11
Clay Minerals				
wt.% Kaolinite	8	6	5	6
wt.% Chlorite	4	4	0	0
wt.% Illite (1)	20	17	16	19
wt.% Montmorillonite (2)	20	20	24	22
wt. % Mixed Layer (1) and (2)	48	53	55	53

TABLE 5-5 (continued)

Pierre Shale Profile					
Sample No. :	885	884	881	882	883
Chemical Components					
wt. % Fe_2O_3	3.18	3.28	5.44	5.71	5.67
wt.% CaO	2.35	1.97	0.94	1.01	1.54
wt. % CO_2	2.40	1.82	0.03	0.05	0.31
wt.% SO_3 (acid soluble)	0.12	0.26	1.10	0.29	0.10
wt. % S (acid insoluble)	0.49	0.66	0.00	0.02	0.02
Minerals					
wt.% Quartz	19	17	17	18	15
wt.% Feldspar	1	2	1	1	2
wt.% Clay Minerals	75	65	75	70	75
wt.% Other	5	16	7	11	8
Clay Minerals					
wt.% Kaolinite	2	4	0	0	1
wt.% Chlorite	3	2	1	?	?
wt.% Illite (1)	18	15	15	20	17
wt.% Montmorillonite (2)	33	28	30	39	44
wt.% Mixed Layer (1) and (2)	44	51	54	41	38

amorphous clay, shows distinct differences in both δD and δO^{18} from the fresh shale. These changes are undoubtedly due to the formation of the new amorphous clay mineral. This amorphous clay probably formed in equilibrium with the very light meteoric waters that would be expected at elevations of 5000 feet in Colorado.

The isotopic results from these three profiles suggest that exposure of clay minerals to very large amounts of water over thousands of years results in little or no isotopic exchange, as long as no mineralogical changes occur. However, recrystallization and formation of new clay minerals definitely can involve changes in both D/H and O^{18}/O^{16}.

5.6 Missoula, Montana profile

The Missoula profile (roadcut, 5500 foot elevation, Missoula County, Montana, see Appendix I for the exact location) is very poorly developed. A soil several inches thick consists of organic matter and fragments of the underlying Precambrian Belt Series shale. The cold, mountainous climate is characterized by an annual temperature range of -8° to +16°C (mean monthly) and a total rainfall of 10 to 20 inches without any distinct seasonal maximum. The rugged topography is covered by coniferous forests.

Three samples were collected: the fresh shale, shale fragments in the soil, and the bulk soil itself. A mineralogical description of the samples is given in Table 4-1 and illustrated in Figure 5-19, along with isotopic values of the bulk samples.

The shale fragments appear to be only slightly weathered compared to the fresh shale. The only mineralogical difference between the fresh rock and the shale fragments in the soil is a lower chlorite content in the fragments. If we assume

Figure 5-19. δD and δO^{18} contents of bulk samples from a poorly developed soil profile on a Belt Series shale, Missoula County, Montana.

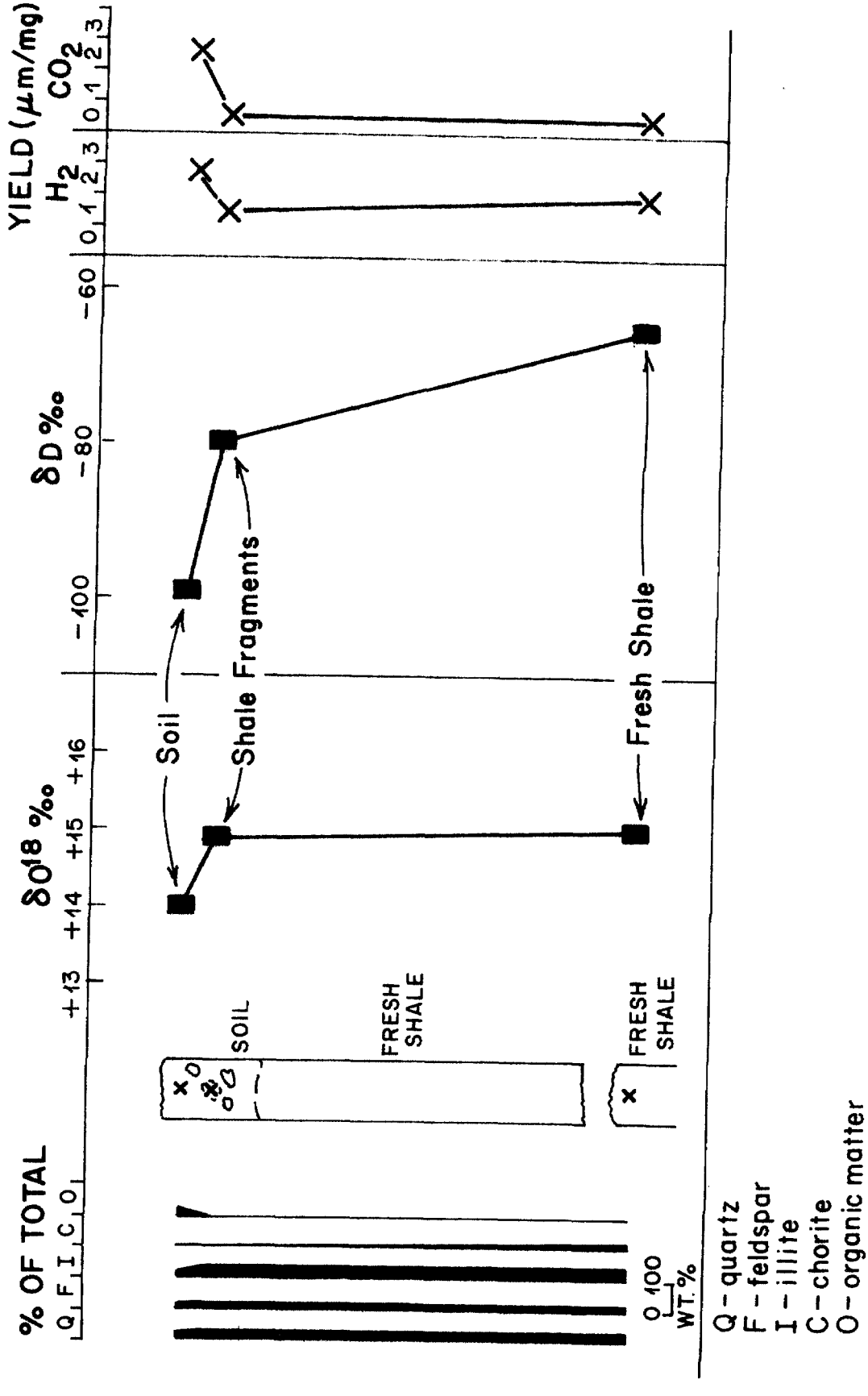
YIELD (μm/mg)
CO2
H2
δD ‰
δO18 ‰
Soil
Shale Fragments
Fresh Shale
% OF TOTAL
SOIL
FRESH SHALE
FRESH SHALE
WT.%
Q - quartz
F - feldspar
I - illite
C - chorite
O - organic matter

Figure 5-19

that the fragments were originally mineralogically identical to the fresh shale, the chlorite in the fragments has been selectively weathered (note the decrease in H_2 yield going from fresh shale to the fragments). The difference in δO^{18} between the fresh shale and the fragments is barely outside analytical error. This is in keeping with the very slight change in bulk mineralogy. The change in δD, however, is appreciable, probably because the change in mineralogy involves chlorite, the most hydrous mineral in the shale. The process of selective alteration of chlorite has apparently been accompanied by hydrogen isotope exchange of the remaining chlorite and illite. Another (more unreasonable) interpretation is that there is an abnormally large hydrogen isotope fractionation between chlorite and illite in the fresh shale.

A more significant change in δO^{18} and δD is observed in going from the shale fragments to the bulk soil. The decrease in δO^{18} probably reflects a further change in the bulk mineralogy, involving the alteration of illite. No new clay minerals appear in sufficient abundance to be identified by X-ray, although a small amount of amorphous clay is probably present. The most abundant new material in the soil is organic matter, as revealed by the sudden sympathetic increase in both H_2 and CO_2 yield. The organic matter is probably responsible for the observed low δD values of the bulk sample, although very little is known about the δD content of organic matter in soils.

S. Epstein (personal communication) has observed that for a given type of plant, δD values show a correlation with the δD values of local meteoric waters. However, this is complicated by the fact that the difference between the δD of the plant and the δD of the meteoric water is dependent on the nature of the plant.

The isotopic results from the Missoula profile suggest that isotopic

changes in parent-rock clay minerals do not take place as a result of exposure to large quantities of isotopically light waters, except where weathering has caused the destruction of or recrystallization of a clay mineral in the parent rock.

VI. ISOTOPIC SURVEY OF QUATERNARY SOILS FROM THE UNITED STATES

Let us now examine the general variations in δD and δO^{18} of soils and their coexisting waters in the United States, to determine whether clear-cut isotopic correlations exist between these materials.

The δD and δO^{18} distribution of meteoric waters in North America is shown by approximate contours in Figure 6-1. The δO^{18} values shown in parentheses were calculated using the formula $\delta D = 8\,\delta O^{18} + 10$ (Craig, 1961a). Two effects dominate the observed distribution, elevation and latitude. Elevation changes are mainly responsible for the variations in tropical and temperate regions and latitude effects become more prominant near the Arctic circle. The two effects are basically related to the prevailing air temperatures, the higher elevations and latitudes having colder climates. Localities at low elevations in inland basins and those in the rain shadows of mountain ranges generally do not fit such a simple picture. The δD and δO^{18} values therefore do not correlate perfectly with mean annual temperatures, or even with the average temperatures of the rainy season in a given locality.

A large number of active soils or weathered zones were collected throughout the United States. Igneous parent rocks were selected in order to insure that the clay minerals or hydroxides formed were not inherited from the parent rock. The most-weathered, organic-free portions of the soils or weathered zones were selected.

Detailed descriptions of individual samples may be found in Appendix I. Isotopic, mineralogical and chemical data are given in Table 4-1.

Figure 6-1. Approximate contours of δD (-30 to -130‰) and δO^{18} (-5.0 to -17.5‰) of present-day meteoric waters in North America, based mainly on data by Friedman (1964), and unpublished data this report. δO^{18} values calculated using Craig's (1961a) relationship ($\delta D = 8\delta O^{18} + 10$).

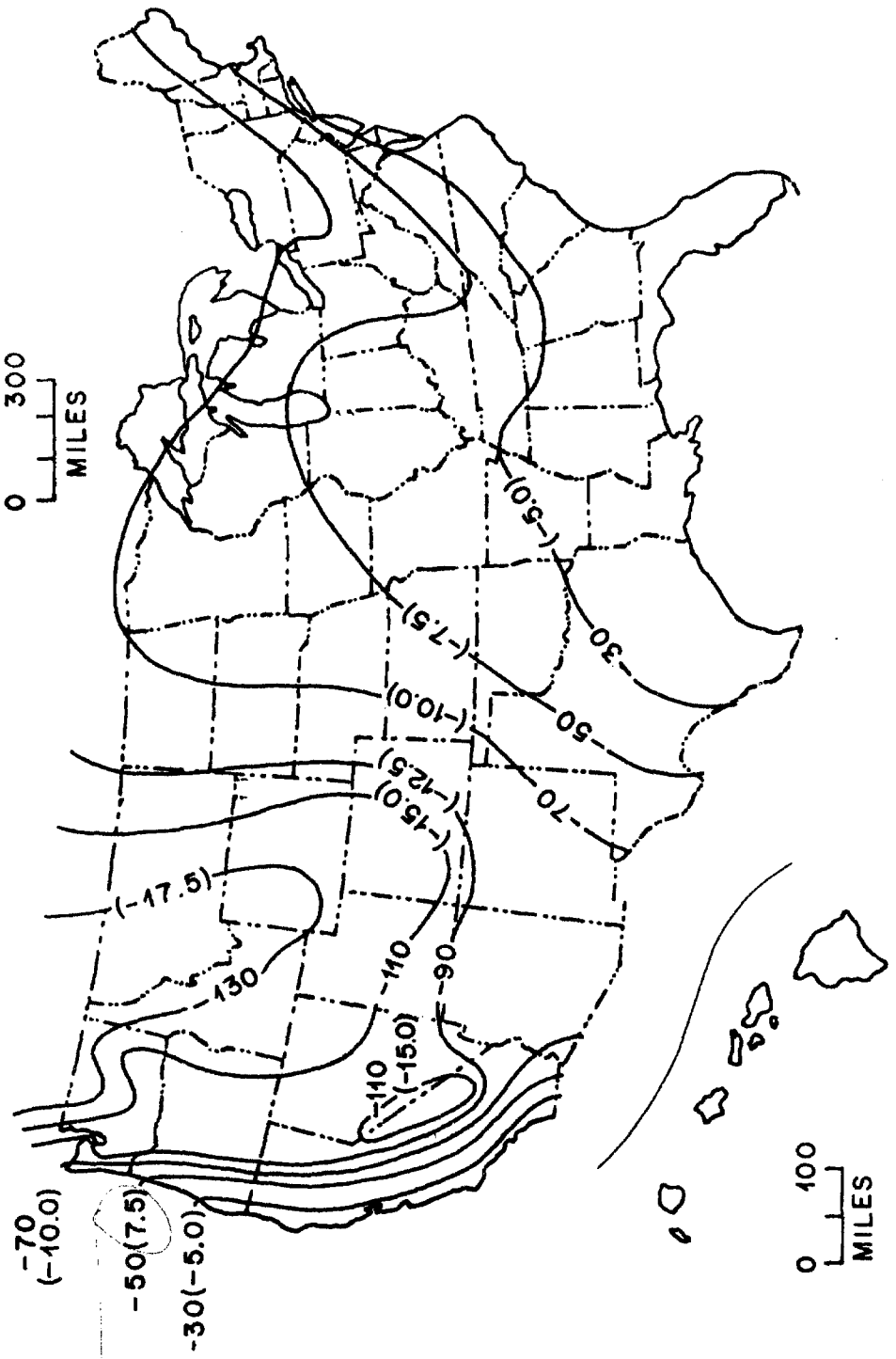
0 300
MILES
(-5.0)
(-7.5)
(-10.0)
(-12.5)
(-15.0)
(-17.5)
30
50
70
90
110
130
-110
(-15.0)
-70
(-10.0)
-50(7.5)
-30(-5.0)
0 100
MILES

Figure 6-1

The ages of the clays in the weathered zones are undoubtedly variable, because production and removal rates are different in each location. Age determinations on soils or weathered zones are full of assumptions. It is thought, however, that the analyzed soils have in large part been formed during the Holocene and/or Pleistocene.

Figure 6-2 shows the δD contents of the bulk soils on a map of the United States. The δD values are almost wholly a reflection of the δD values of weathering products because the igneous parent rocks have low hydrous mineral contents.

Comparison of this figure with Figure 6-1 shows that the correlation between the δD values of meteoric waters and the δD values of bulk soils is good. As anticipated, the δD values of the soils are generally 10 to 40‰ lighter than the corresponding δD values of the local meteoric waters.

The samples from Hawaii, coastal California and coastal Oregon exhibit a progressive change in δD with latitude. The average δD of the Hawaii samples, excluding the two gibbsite samples, is -56; the average δD of the coastal California samples is -64; and the average δD of the coastal Oregon samples, excluding the halloysites, is -78.

The coastal California samples average about 25‰ heavier than the western Sierra Nevada samples, illustrating the effect of a change in elevation from 500-1000 feet to 2500-4500 feet. The soil samples from the Pacific Northwest show a progressive change of 80‰ in δD as one moves inland, corresponding to an elevation change from 500-1500 feet to 5000-6000 feet. The local meteoric waters display a corresponding change in δD values. Although far less data have been obtained, a progressive change in the δD values of soils is also observed in

Figure 6-2. A map of the United States, showing the δD contents of all Quaternary soils analyzed in this study.

Figure 6-3. Two east-west topographic profiles through the northern and southern United States, showing the δD values of Quaternary soils analyzed in this study.

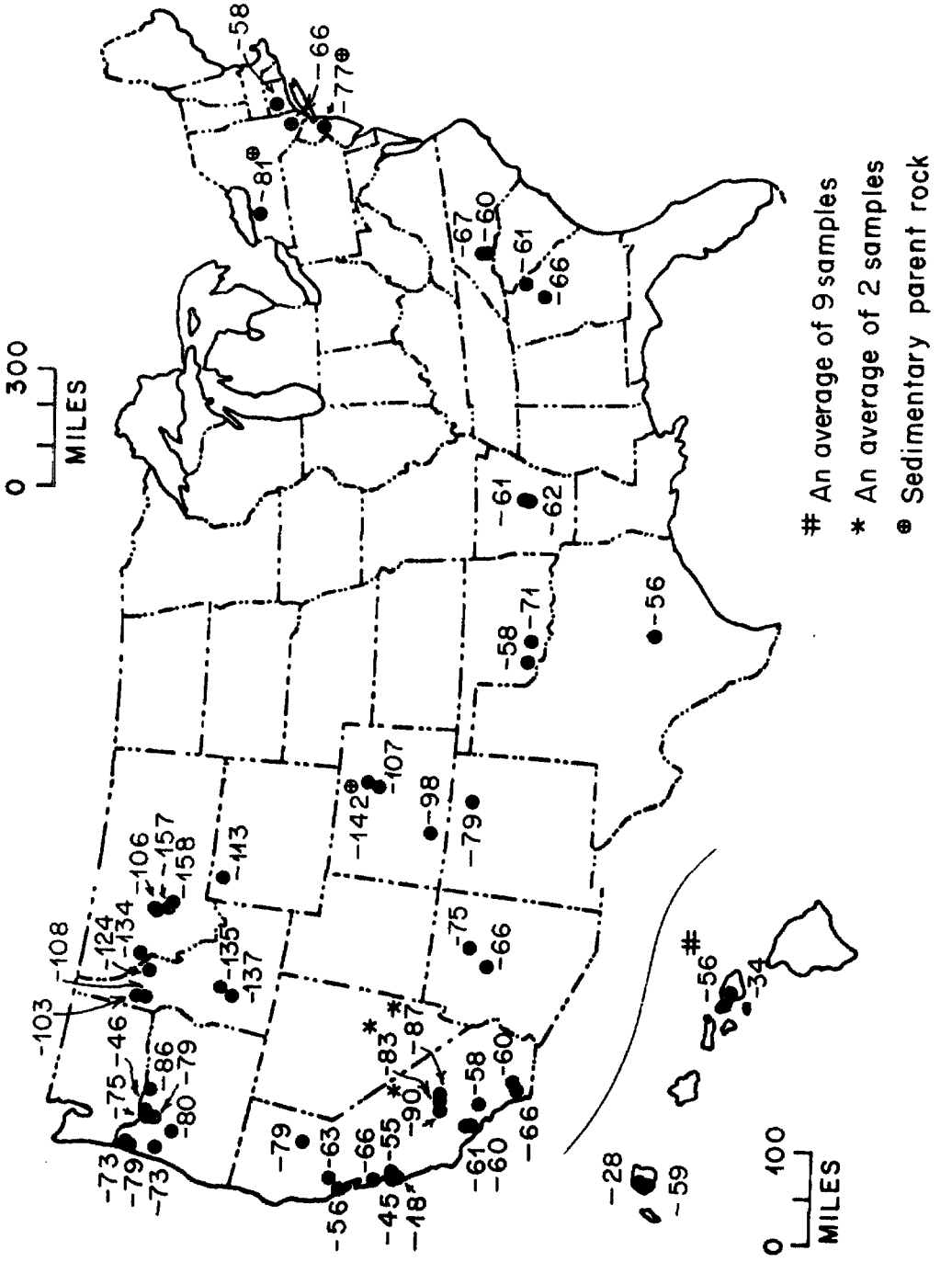
0 300
MILES
0 100
MILES
An average of 9 samples
* An average of 2 samples
⊕ Sedimentary parent rock

Figure 6-2

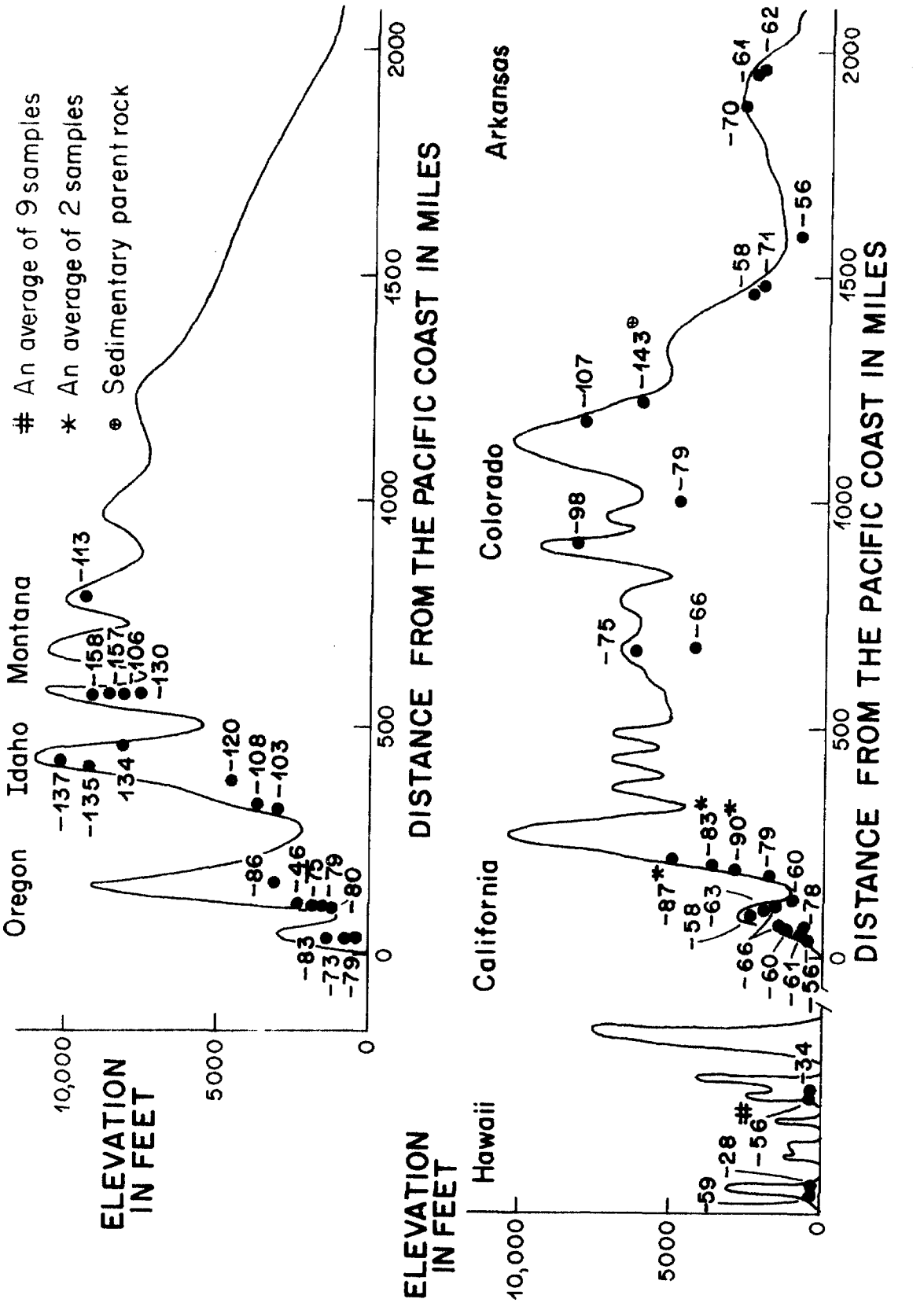
Oregon
Idaho
Montana
An average of 9 samples
* An average of 2 samples
⊕ Sedimentary parent rock
ELEVATION IN FEET
10,000
5000
0
DISTANCE FROM THE PACIFIC COAST IN MILES
0
500
1000
1500
2000
-137
-135
134
-158
-157
-106
-130
-113
-120
-108
-103
-86
-46
-75
-79
-80
-83
-73
-79
Hawaii
California
Colorado
Arkansas
-59
-28
-56#
-34
-87*
-58
-63
-83*
-90*
-79
-66
-60
-61
-56
-78
-75
-98
-107
-66
-143⊕
-79
-58
-71
-70
-64
-62
-56

Figure 6-3

going from coastal California or the Gulf of Mexico to Colorado.

Figure 6-3 illustrates the δD values of the soils on two east-west topographic profiles, one extending from the Oregon coast to the north central United States, and the other extending from Hawaii to Arkansas (and including California and Colorado). The systematic variation of δD of the soil samples with elevation is further emphasized in this figure.

The δO^{18} contents of the weathering products from the bulk soils were calculated by material balance (see Table 4-1). These δO^{18} values are shown on a map of the United States in Figure 6-4 and shown on two east-west topographic profiles in Figure 6-5. The same general correlations observed for δD values of the bulk soils are also observed for these calculated δO^{18} values.

Figure 6-6 is a plot of δD versus δO^{18} for all the bulk Quaternary soil samples and clay-rich separates except a few soil samples from western Oregon which contain halloysite. Except for two samples, the hydrogen isotopic values of these halloysites are consistently higher in δD than are kaolinites from Quaternary soils in the same general region. Because the δD values of these halloysites probably represent exchanged values (see sections 3.1 and 5.4), they are not plotted in Figure 6-6.

As mentioned earlier in this chapter, the δD contents of the Quaternary bulk soil samples are primarily a reflection of the δD of the clay minerals in the soils. The δO^{18} contents are determined by the relative amounts of both clay minerals and parent rock in each sample.

Figure 6-6 shows that samples with a high parent rock content plot closer to the region of δO^{18} of common igneous rocks, as expected. The more clay-rich samples plot closer to the kaolinite line of Savin and Epstein (1970a).

Figure 6-4. A map of the United States showing the δO^{18} values (determined by material balance, Table 4-1) of the clay minerals and hydroxides in Quaternary soils.

Figure 6-5. Two east-west topographic profiles showing the δO^{18} values (determined by material balance) of clay minerals and hydroxides in Quaternary soils.

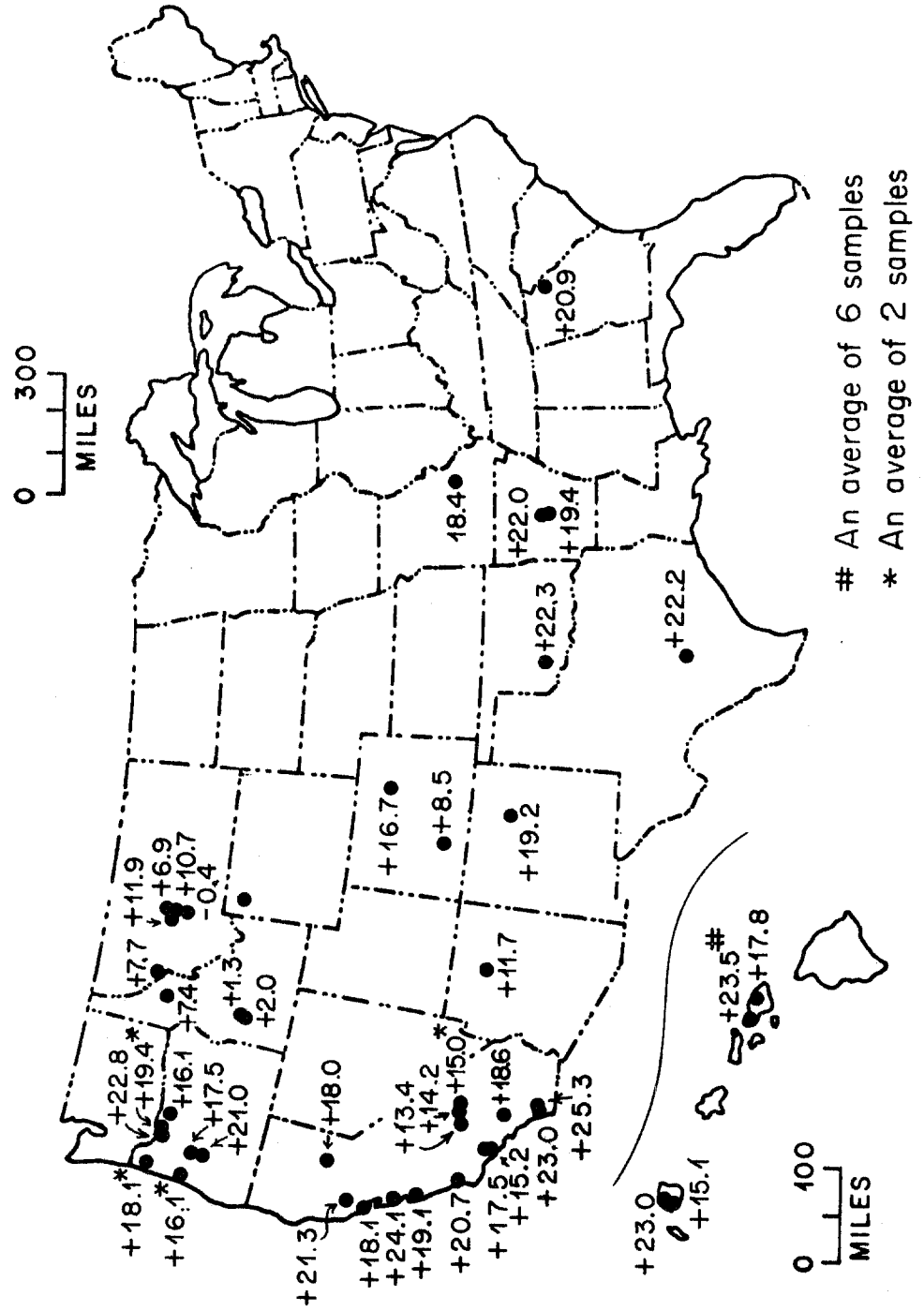
0 300
MILES
+20.9
18.4
+22.0
+19.4
+22.3
+22.2
+16.7
+8.5
+19.2
+11.7
+11.9
+6.9
+10.7
-0.4
+7.7
+7.4
+1.3
+2.0
+22.8
+19.4*
+16.1
+17.5
+21.0
+18.0
+13.4
+14.2
+15.0*
+18.6
+25.3
+18.1*
+16.1*
+21.3
+18.1
+24.1
+19.1
+20.7
+17.5
+15.2
+23.0
+23.0
+15.1
+23.5#
+17.8
An average of 6 samples
* An average of 2 samples
0 100
MILES

Figure 6-4

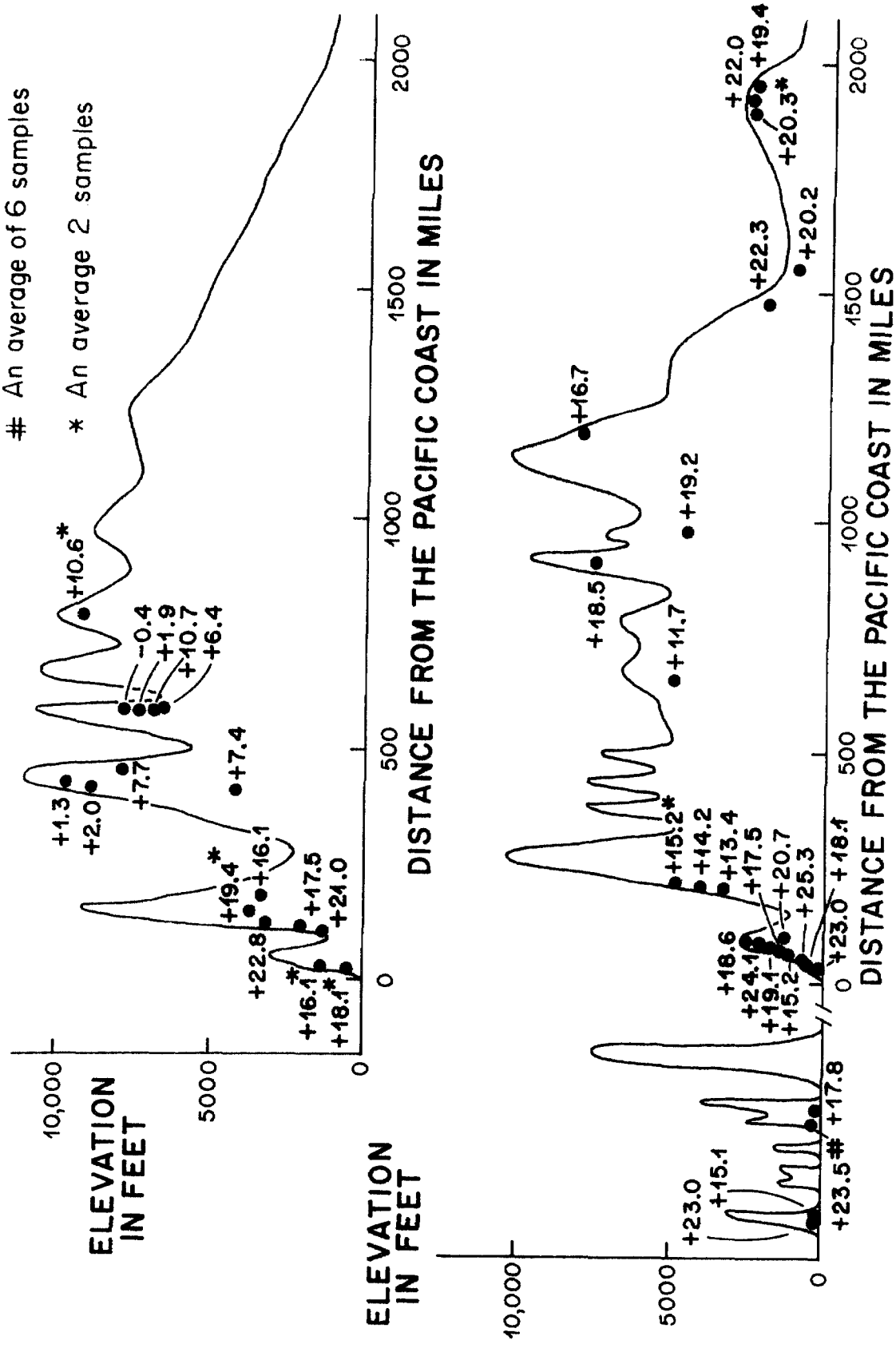
An average of 6 samples
* An average 2 samples
ELEVATION IN FEET
10,000
5000
0
0
500
1000
1500
2000
DISTANCE FROM THE PACIFIC COAST IN MILES
+1.3
+2.0
+7.7
+10.6*
-0.4
+1.9
+10.7
+6.4
+7.4
+19.4*
+16.1
+22.8
+16.1*
+17.5
+24.0
+18.1*
+16.7
+18.5
+19.2
+11.7
+15.2*
+14.2
+13.4
+17.5
+20.7
+25.3
+18.6
+24.1
+19.1
+15.2
+23.0
+18.1
+22.0
+19.4
+20.3*
+22.3
+20.2
+23.0
+15.1
+23.5#
+17.8

Figure 6-5

Figure 6-6. A δD versus δO^{18} diagram for all analyzed Quaternary soils, except those containing halloysite, of the United States. Some sample localities are represented by isotopic values of the bulk soil sample as well as a clay-rich fraction of the bulk soil. Savin and Epstein's (1970a) kaolinite line is shown for reference. A region of δO^{18} values of common igneous rocks is also shown (Taylor, 1968). The degree of shading of each data-point indicates the proportion of parent rock (open) to weathering product (black) in each sample. The five samples labeled "Sierra Nevada" are from the western slope of the Sierra Nevada mountains, California.

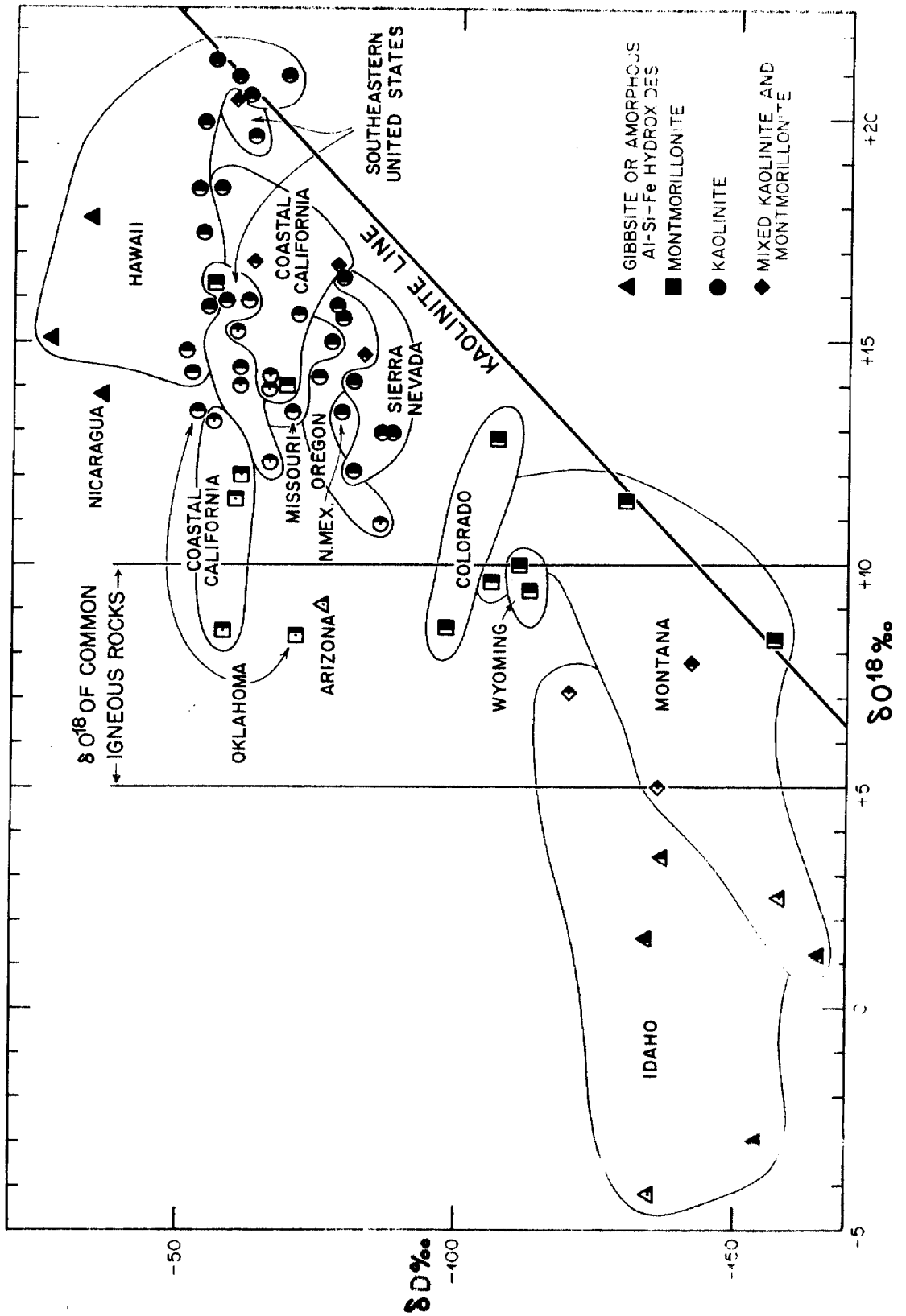
KAOLINITE LINE
SOUTHEASTERN UNITED STATES
HAWAII
COASTAL CALIFORNIA
SIERRA NEVADA
NICARAGUA
COASTAL CALIFORNIA
MISSOURI
OREGON
N.MEX.
COLORADO
OKLAHOMA
ARIZONA
WYOMING
MONTANA
IDAHO
δ O18 OF COMMON IGNEOUS ROCKS
GIBBSITE OR AMORPHOUS Al-Si-Fe HYDROXIDES
MONTMORILLONITE
KAOLINITE
MIXED KAOLINITE AND MONTMORILLONITE
δD‰
δO18 ‰
-50
-100
-150
-5
+5
+10
+15
+20

Figure 6-6

Generally, taking into consideration the effect or δO^{18} parent-rock minerals in the soil, the δD and δO^{18} values of the samples plot in a zone essentially parallel to the meteoric water line. Furthermore the samples show a geographic distribution which corresponds to the geographic distribution of meteoric waters.

Figure 6-7 is a plot of the δD of the bulk soils (basically the δD of the clay minerals or hydroxides in the soils) versus the δO^{18} of the clay minerals or hydroxides in the soils determined by material balance calculations. The weathering products in the soils are distinguished in terms of their mineralogy (by symbol notations) and locality. The δD and δO^{18} of meteoric waters from corresponding localities are also shown.

Tie lines are drawn connecting the δD and δO^{18} values of a typical water from a given region to the δD and δO^{18} values of clay minerals or hydroxides in the soils from that region. In general the δD values of the clay minerals or hydroxides in the soils are 10 to 40‰ lighter than the δD values of the corresponding meteoric waters. The δO^{18} values of the clay minerals in the soils are generally 20 to 30‰ heavier than the δO^{18} of corresponding meteoric waters. The δO^{18} of the hydroxides in the soils are generally 15 to 20‰ heavier than the δO^{18} of the corresponding waters.

The measured differences between the δD and δO^{18} contents of clay minerals or hydroxides and those of meteoric waters agree quite well with the kaolinite isotopic fractionation factors suggested by Savin and Epstein (1970a) and the isotopic fractionation factors for gibbsite determined in section 5-2. This agreement suggests that a close approach to isotopic equilibrium is generally attained in weathering environments.

Figure 6-7. Figure 6-7 is a δD versus δO^{18} diagram of clay minerals and hydroxides from Quaternary soil zones of the United States. The δO^{18} values were determined by material balance calculations. The isotopic compositions of meteoric waters from several localities are also shown (data from Friedman, 1964; and this report). Tie lines are drawn connecting typical isotopic values of meteoric waters from one locality to the region of isotopic values of soils from that locality. Craig's (1961a) meteoric water line and Savin and Epstein's (1970a) kaolinite and montmorillonite lines are shown for reference.

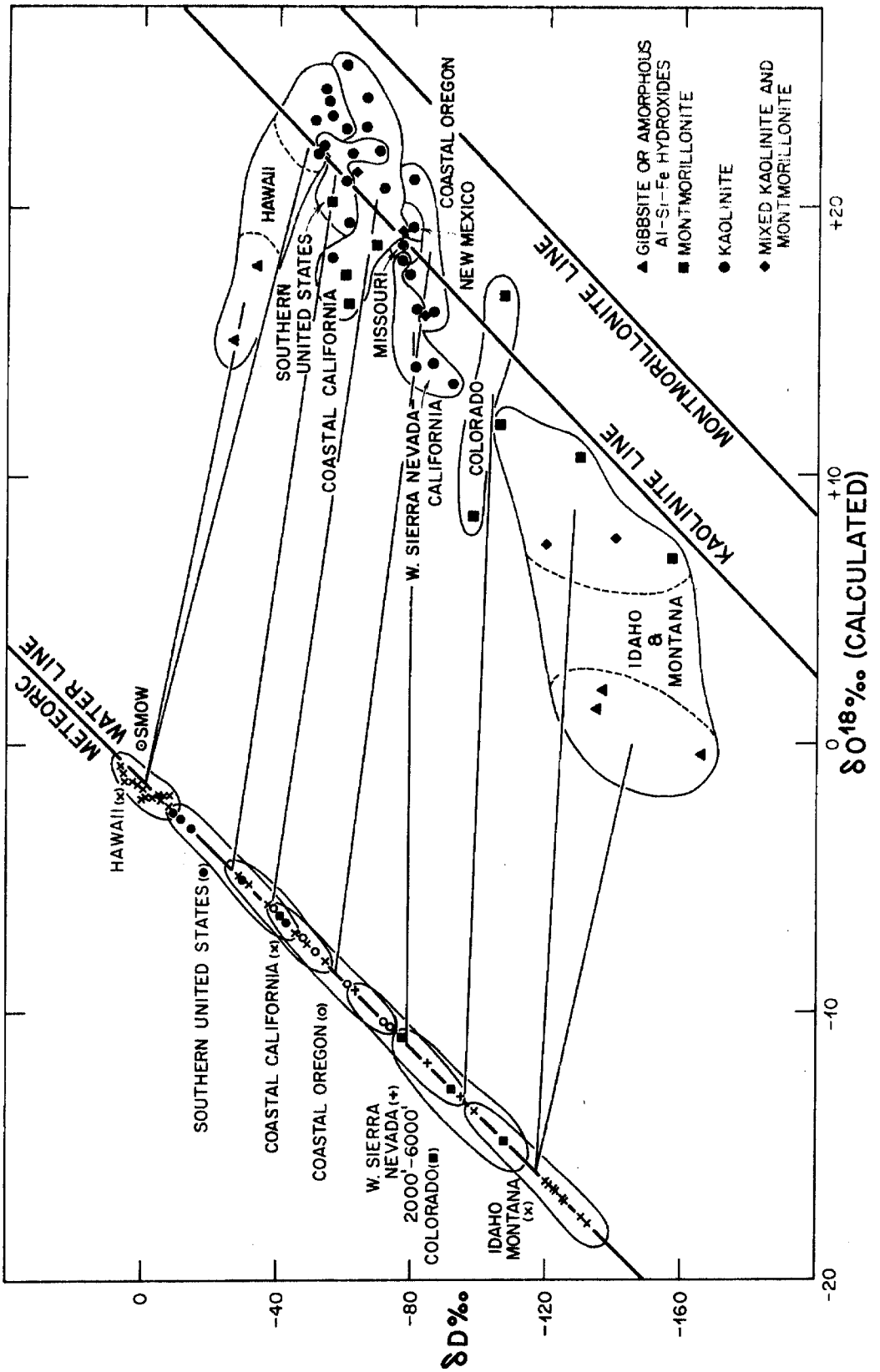
METEORIC WATER LINE
SMOW
HAWAII (x)
SOUTHERN UNITED STATES (●)
COASTAL CALIFORNIA (x)
COASTAL OREGON (○)
W. SIERRA NEVADA (+) 2000'-6000'
COLORADO (■)
IDAHO MONTANA (x)
HAWAII
SOUTHERN UNITED STATES
COASTAL CALIFORNIA
MISSOURI
W. SIERRA NEVADA
CALIFORNIA
COLORADO
NEW MEXICO
COASTAL OREGON
IDAHO & MONTANA
KAOLINITE LINE
MONTMORILLONITE LINE
▲ GIBBSITE OR AMORPHOUS Al-Si-Fe HYDROXIDES
■ MONTMORILLONITE
● KAOLINITE
◆ MIXED KAOLINITE AND MONTMORILLONITE
δD‰
δO18‰ (CALCULATED)
0
-40
-80
-120
-160
+20
+10
-10
-20

Figure 6-7

The clay minerals shown in Figure 6-7 can be divided into three groups, the koalinites, the montmorillonites, and the mixed kaolinite-montmorillonite group. The kaolinites tend to be more common in warmer coastal areas, and the montmorillonites are more predominant in the dry inland regions. This segregation is undoubtedly the result of differences in climatic conditions. Montmorillonites require a high pH and high activities of alkali and silica. Kaolinites require a lower pH and lower alkali and silica activities (see Figure 5-6).

In warm, wet regions vegetation is abundant and humic acids from decaying plant remains and carbon dioxide from plant roots tend to keep the pH low. An abundant supply of water tends to keep alkali and silica activities low. Thus kaolinites are favored by such climates.

In dry, inland regions the vegetation is sparse and pH is controlled more by rock-water interaction. The supply of water is lower and alkali and silica activities can reach higher levels in the ground waters. Thus montmorillonite formation is favored.

Although the isotopic compositions of kaolinites as a group generally differ from the isotopic composition of the montmorillonites as a group (due to climatic effects), the two clays seem to exhibit very similar isotopic behavior. The isotopic compositions of the kaolinites and montmorillonites, as well as mixtures of the two clays, all plot in the vicinity of the kaolinite line. In addition, where both kaolinites and montmorillonites do happen to form within single climatic regions (e.g., California and southern United States) they exhibit similar isotopic values.

These observations might suggest that the isotopic fractionation factors

for these two minerals are more similar than Savin and Epstein's (1970a) kaolinite and montmorillonite lines would suggest, or that one or both of the following factors may be of importance: (1) the montmorillonites of these Quaternary soils have chemical compositions appreciably different from the montmorillonites investigated by Savin and Epstein (1970a); (2) the montmorillonites in Quaternary soils are formed at higher temperatures than the bentonites and oceanic montmorillonites investigated by Savin and Epstein (1970a).

The chemical composition of montmorillonite is known to have an important effect on the O^{18}/O^{16} and D/H isotopic compositions of montmorillonites (see section 5.3). Such chemical effects conceivably could cause the montmorillonites of Quaternary soils to plot in the vicinity of the kaolinite line.

Montmorillonites formed by subaerial weathering are generally found only in warm dry climates or climates with a long dry season. If the montmorillonites form during the warm summer months, the temperatures might be relatively high compared to montmorillonites formed in oceans or lakes. Such a temperature difference is in the right direction to cause the montmorillonites of Quaternary soils to plot closer to the kaolinite line. This point will be discussed in more detail in Chapter VIII and Chapter X.

As an example of the isotopic variations in soils in a single region, let us examine in more detail the isotopic results obtained on Hawaiian soils. Figure 6-8 shows the bulk soils from Hawaii plotted on a $\delta D - \delta O^{18}$ diagram. The δD values are exceedingly uniform in the kaolinite-rich samples, and the δO^{18} values vary directly with the clay content of the samples. The most clay-rich samples plot in the vicinity of the kaolinite line. Thus, even though these samples were collected from a variety of locations on two different islands, all the kaolinites

Figure 6-8. A δD versus δO^{18} diagram for kaolinite- and gibbsite-rich soils from Maui and Kauai. Symbols are filled to represent proportion of clay or hydroxide, open to represent parent rock. Savin and Epstein's (1970a) kaolinite line is shown for reference.

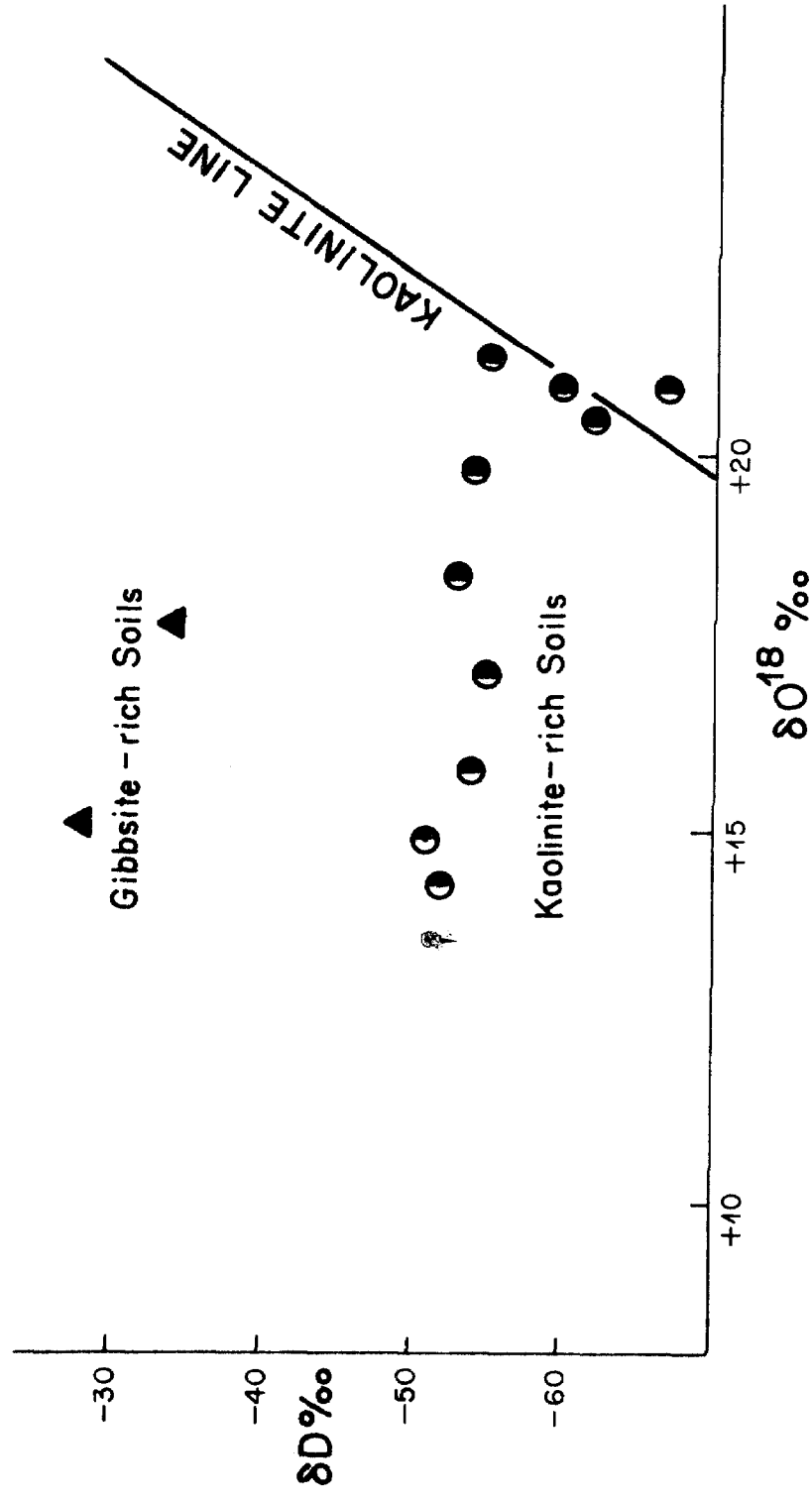
KAOLINITE LINE
Gibbsite-rich Soils
Kaolinite-rich Soils
δD‰
δO18 ‰
-30
-40
-50
-60
+10
+15
+20

Figure 6-8

from Hawaii appear to be exceedingly uniform in both δD and δO^{18}. This uniformity is undoubtedly a result of the relatively uniform climate and the small isotopic variation in meteoric waters in the low coastal areas of the Hawaiian Islands.

Two samples which are relatively pure gibbsites display δD and δO^{18} values distinct from the kaolinites. Because both the kaolinites and gibbsites were formed from isotopically similar meteoric waters (all samples are from low coastal elevations in Hawaii) the data indicate that gibbsite has a lower preference for O^{18} and a higher preference for deuterium than kaolinite (in agreement with data from the Elberton profile, section 5.2).

The δD and δO^{18} values of (1) gibbsites from Hawaii, Nicaragua and Georgia, and (2) the amorphous Al-Si-Fe hydroxides from Idaho and Montana have been shown in the above discussion and in section 5.2 to be distinctly different from the isotopic values of clay minerals in the same areas. This indicates that the mineral-H_2O isotopic fractionation factors for <u>all</u> these hydroxides are relatively similar and distinct from those of clay minerals.

Figure 6-9 shows data points for all the gibbsites analyzed in this study. The δO^{18} values were calculated by material balance in those cases where noticeable amounts of parent rock were present in the sample. Although considerable scatter in isotopic values occurs, the samples plot along a line parallel to the meteoric water line but noticeably above the kaolinite line. The fractionation factors calculated in section 5.2 for gibbsite-H_2O are used to determine a gibbsite line (see Appendix I, Savin, 1967) in Figure 6-9. The isotopic values of the samples show a reasonable distribution about this line suggesting that the fractionation factors are basically correct. The samples display variable iron contents (see Table 4-1), which may in part account for some of the scatter observed in

Figure 6-9. A δD versus δO^{18} diagram for gibbsites or Al-Si-Fe amorphous hydroxides from Quaternary soils in Hawaii (Haw), Nicaragua (Nica), Georgia (Ga), Idaho (Ida) and Montana (Mont). All of these samples appear on Figure 6-6 except the Georgia sample; it represents a calculated value for the gibbsite-rich B-zone of the Elberton soil. The δO^{18} values of the Idaho and Montana samples were calculated by material balance as outlined in text. Savin and Epstein's (1970a) kaolinite line is shown for reference. A gibbsite line was constructed using $\alpha^{hy}_{gibbsite-H_2O} = 0.984$ and $\alpha^{ox}_{gibbsite-H_2O} = 1.018$. Note that these α's do not necessarily apply to Fe hydroxides, as it is possible that they lie along the gibbsite line as a result of cancelling effects of Fe content in α^{ox} and α^{hy} (see discussion in section 10.1). For example, a $\alpha^{hy}_{Fe(OH)_3-H_2O} \approx 0.940$ and a $\alpha^{ox}_{Fe(OH)_3-H_2O} \approx 1.014$ would also produce a line essentially coincident with the gibbsite line shown.

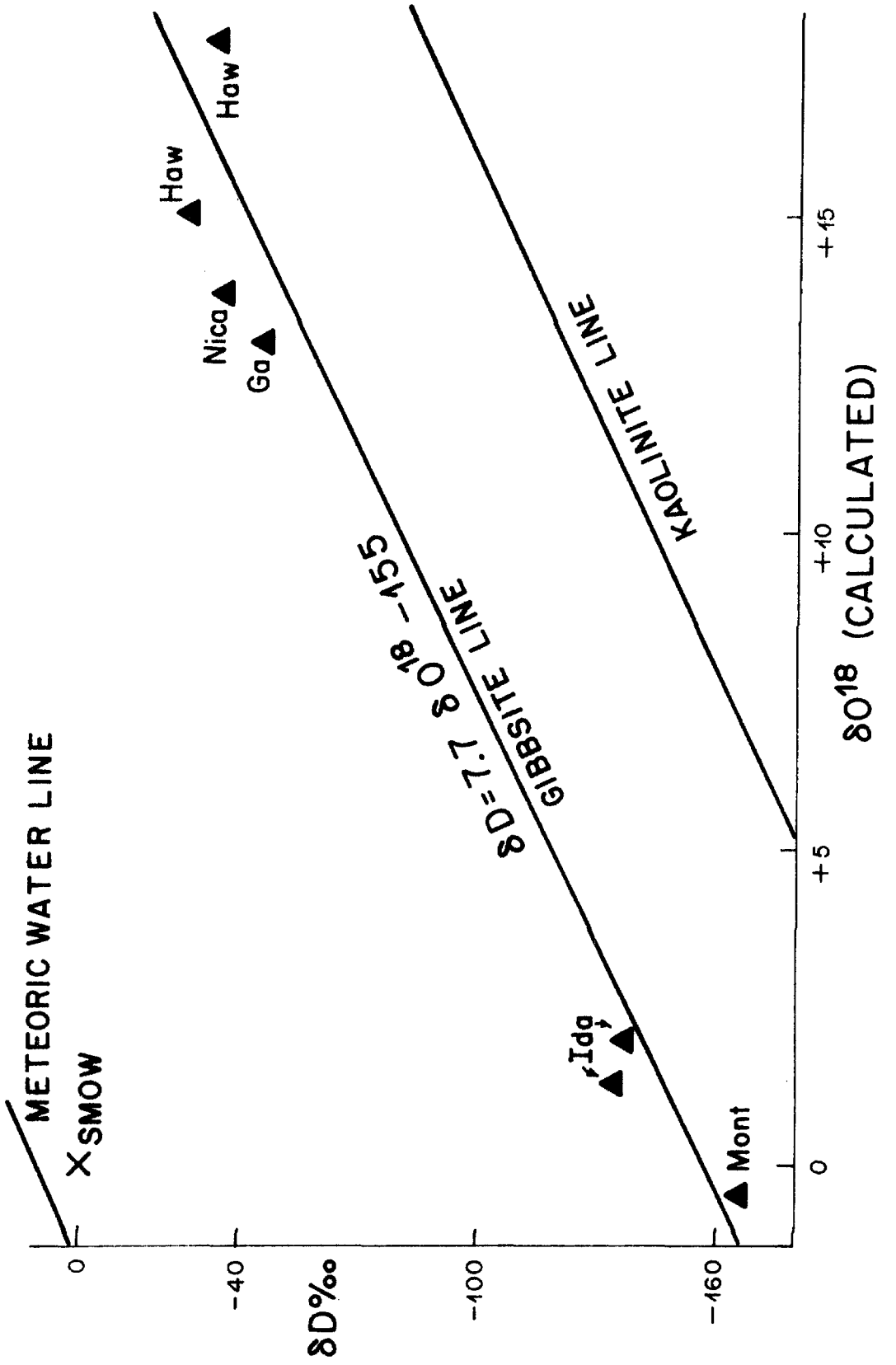
METEORIC WATER LINE
SMOW
δD=7.7 δO18 -155
GIBBSITE LINE
KAOLINITE LINE
Haw
Haw
Nica
Ga
Ida
Mont
0
-40
-100
-160
δD‰
0
+5
+10
+15
δO18 (CALCULATED)

Figure 6-9

the data. However, no systematic correlation between isotopic values and iron content (as weight percent Fe_2O_3) is observed.

The range of isotopic values of weathering products in Quaternary soils of the United States is -30 to -165 for δD and +25 to -3 for δO^{18}. However, because the rates of production of clay minerals are strongly dependent on both temperature and the availability of moisture (warm and wet climates are more conducive to clay formation), most of the weathering products in the continental United States have δD values from -30 to -100 and δO^{18} values from +15 to +25. This general range of isotopic values for weathering products is probably valid for the Earth as a whole, because the present investigation has covered almost the total spectrum of climatic conditions. In addition, if the isotopic composition of the ocean has been relatively unchanged over geologic time, this range probably also applies to the past. However, the average δD and δO^{18} values of weathering products may have been heavier in the past because during most of geologic history, climates were probably somewhat warmer than the present-day climate.

Sediments throughout the world are made up not only of weathering products but also of erosional products. Erosional products are basically materials mechanically transported from parent rocks to a site of deposition, without undergoing appreciable isotopic or chemical exchange with the weathering environment. Therefore, the isotopic composition of sediments will reflect both the isotopic compositions of the weathering products and those of the erosional products, depending on the relative proportions of each. Drainage systems which have their sources in regions of cold, dry climates will carry a relatively small proportion of weathering products compared to regions with warm, wet climates. Therefore, even though the weathering products in the former areas will be abnormally low in

δO^{18} and δD, the bulk sediments will not necessarily exhibit such values. Nonetheless, it is probably safe to conclude that the bulk δO^{18} and δD values of sediments derived from temperate and tropical areas where igneous and metamorphic rocks are exposed to weathering and erosion will be higher in δO^{18} and δD than sediments derived from analogous rock types in colder areas. This could have importance with regard to tracing the source areas of various types of sedimentary rocks.

VII. ANCIENT KAOLINITE AND ILLITE DEPOSITS

Many ancient kaolinite deposits are described in the geologic literature because of their economic value. Some of these kaolinite deposits represent residual weathering zones. Others are sedimentary deposits which represent clays transported from their original weathering sites.

In many instances the intensity of weathering has been so severe that essentially monomineralic kaolinite zones have formed or kaolinite occurs in pseudomorphs after feldspar. In other instances alluvial processes have undoubtedly concentrated kaolinite during transport so that nearly pure kaolinite deposits result. The impurities present are most commonly quartz, feldspar or flint.

Abundant kaolinite deposits were formed in the Tertiary, Cretaceous and Pennsylvanian Periods. The association of the kaolinites with fossil plant remains and lignite is common. From these plant remains it can be inferred that the climatic conditions must have been warm and moist.

Some of the kaolinite deposits sampled in the present work contain illite as well as kaolinite. Detailed descriptions of sample localities are given in Appendix I. Mineralogical descriptions and δD and δO^{18} isotopic results are given in Table 4-1.

A plot of δD versus δO^{18} for the kaolinite deposits is given in Figure 7-1. All the samples displayed are kaolinite deposits in which geologic evidence points to an origin by weathering processes. They therefore must have formed at Earth-surface temperatures. Most of the samples show no geologic evidence of

Figure 7-1. A $\delta D - \delta O^{18}$ diagram for ancient kaolinite and illite deposits (primarily of residual weathering origin). The degree of shading of each data-point indicates the proportion of impurities such as quartz, feldspar and/or flint (open) to kaolinite or illite (black) in each sample. The kaolinite line of Savin and Epstein (1970a) is shown for reference.

Figure 7-2. A $\delta D - \delta O^{18}$ diagram for kaolinites of various ages that have a purity greater than 80%. The two Quaternary samples include the kaolinite from the Elberton, Georgia profile (δO^{18} calculated, see section 5.2) and the most kaolinite-rich soil from Hawaii. A least squares line is drawn through the data points for all Quaternary, Tertiary and Cretaceous samples. Note how closely the least squares line coincides with the kaolinite line of Savin and Epstein (1970a), clearly indicating the validity of the assumptions utilized by Savin and Epstein in constructing their line.

Figure 7-3. A $\delta D - \delta O^{18}$ diagram of kaolinites and illites of various ages, with the δO^{18} values corrected by material balance calculations for impurities. Savin and Epstein's (1970a) kaolinite line is shown for reference.

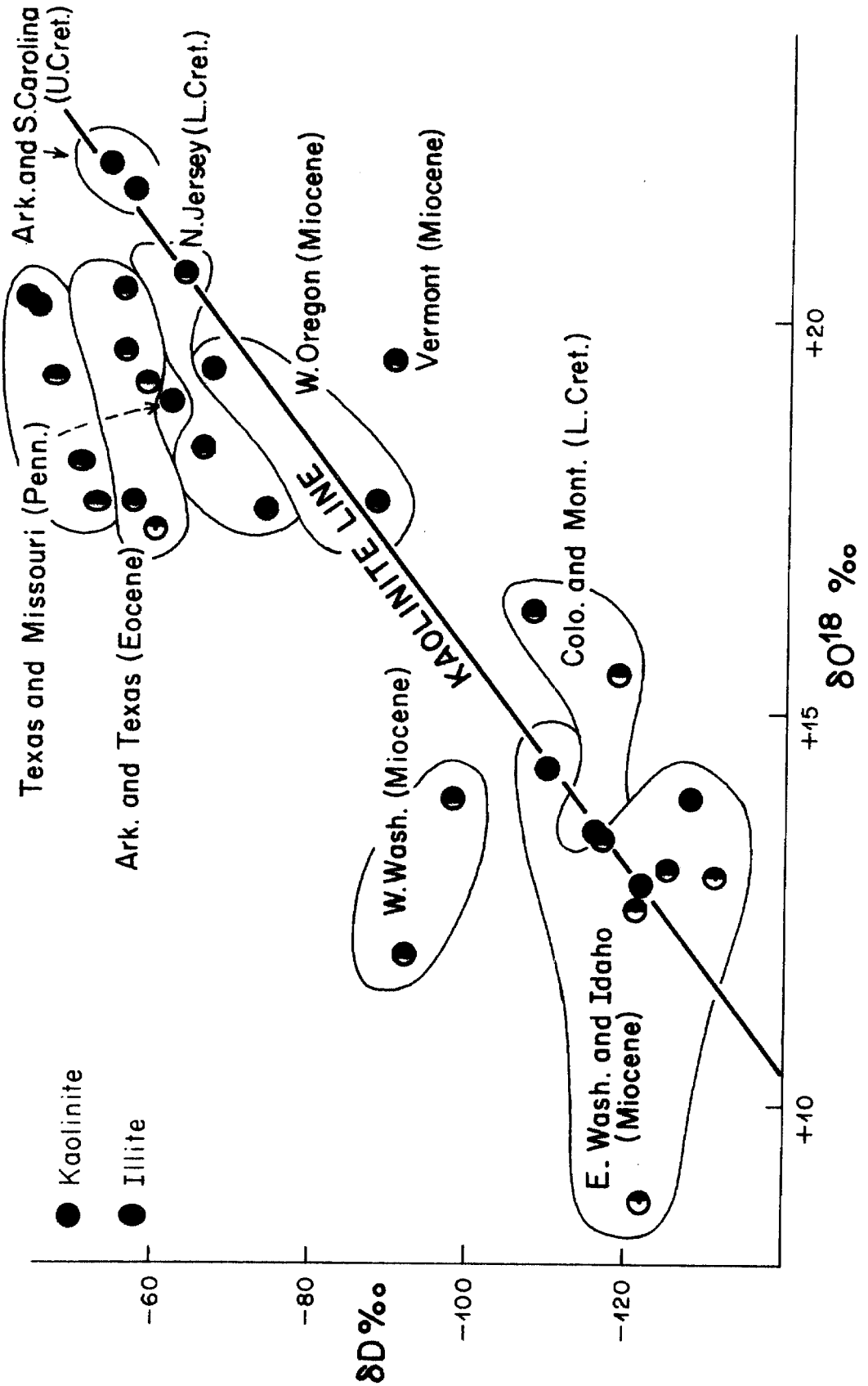
Kaolinite
Illite
Texas and Missouri (Penn.)
Ark. and Texas (Eocene)
Ark. and S.Carolina (U.Cret.)
N.Jersey (L.Cret.)
W.Oregon (Miocene)
Vermont (Miocene)
KAOLINITE LINE
W.Wash. (Miocene)
Colo. and Mont. (L.Cret.)
E. Wash. and Idaho (Miocene)
-60
-80
-100
-120
δD‰
+10
+15
+20
δO18 ‰

Figure 7-1

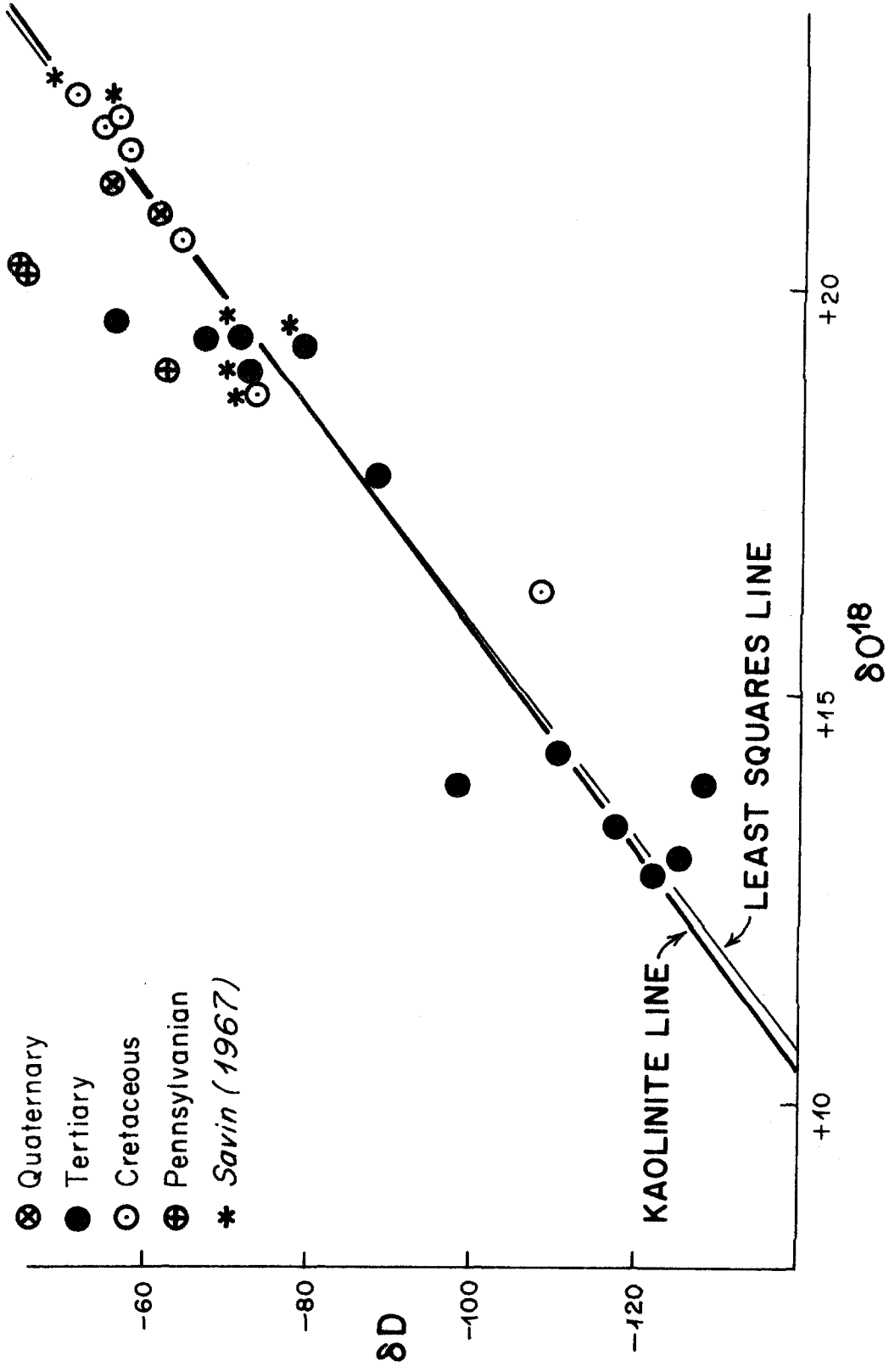
Quaternary
Tertiary
Cretaceous
Pennsylvanian
Savin (1967)
KAOLINITE LINE
LEAST SQUARES LINE
δD
δO18
-60
-80
-100
-120
+10
+15
+20

Figure 7-2

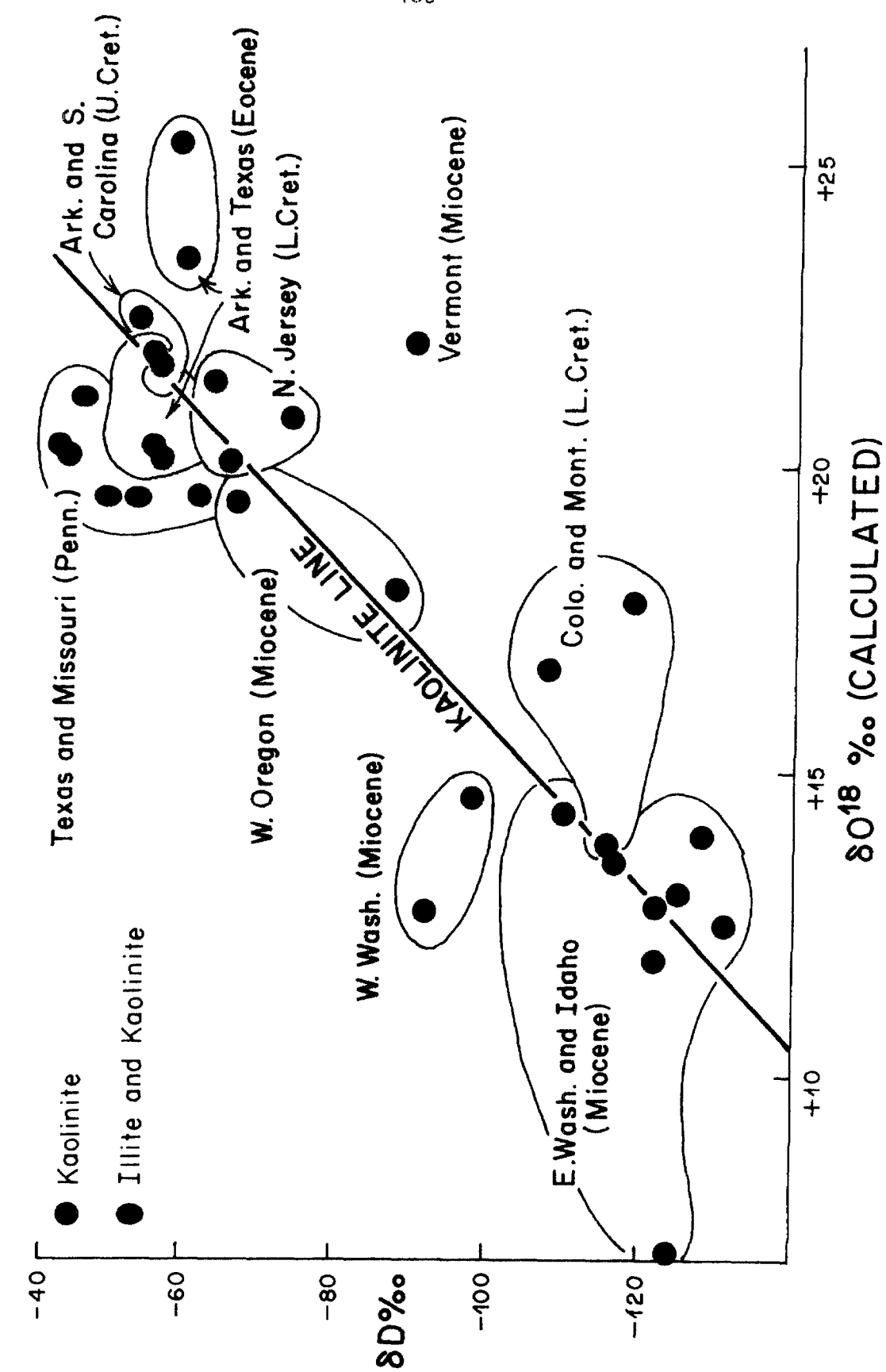
Kaolinite
Illite and Kaolinite
Texas and Missouri (Penn.)
Ark. and S. Carolina (U.Cret.)
Ark. and Texas (Eocene)
N. Jersey (L.Cret.)
Vermont (Miocene)
W. Oregon (Miocene)
KAOLINITE LINE
W. Wash. (Miocene)
Colo. and Mont. (L.Cret.)
E.Wash. and Idaho (Miocene)
-40
-60
-80
-100
-120
δD‰
+10
+15
+20
+25
δO18 ‰ (CALCULATED)

Figure 7-3

having been buried any more than a few hundred feet. A few have undergone burial of at most 2000 feet. Some of the samples are known to have suffered post-depositional leaching, but usually this took place soon after burial. The presence of illite in a few samples may indicate that some have undergone post-depostional diagenetic alteration.

The deposits occur in formations having a great range in porosity, from clay-rich shales to sandstones with lenses of clay, to residual weathering zones. It is certain that most of the deposits have been exposed to large quantities of meteoric water both during and subsequent to their formation.

Figure 7-1 shows that the δD and δO^{18} isotopic compositions of the kaolinites are distributed roughly along the kaolinite line of Savin and Epstein (1970a). The locations of the deposits and their ages are shown. The purity of the samples is indicated by the amount of shading in the sample points.

The displacement of the samples from the kaolinite line seems to be primarily a function of the amounts of impurities in the samples. This can be seen by comparing Figure 7-1 with Figure 7-2; the latter shows only samples containing 80% or more kaolinite.

Figure 7-3 and Table 4-1 show the isotopic compositions of the kaolinites, with δO^{18} values corrected by material-balance calculation for the δO^{18} of co-existing quartz or parent rock. Inasmuch as the δO^{18} values of the impurities were not directly measured, such values had to be estimated. Quartz from the sedimentary deposits was assumed to have $\delta O^{18} = +13$, a reasonable mean δO^{18} value for quartz from various sources. For residual deposits, δO^{18} values of parent-mineral impurities were set equal to +10 or + 7.5, depending on the parent-rock type. Although these calculations improve many of the δO^{18} values and thus

force the kaolinite isotopic values into better conformity with the kaolinite line, a number of samples were even further displaced from the kaolinite line. This suggests that parent-rock δO^{18} values are in fact more variable than those assumed.

Table 7-1 shows the calculation of δO^{18} values of quartz by material balance in the Eocene Wilcox formation, assuming a constant δO^{18} ($^{+}21.4$) for the kaolinite. This is a reasonable assumption because the kaolinites were all formed under similar weathering conditions in the south-central United States. Therefore, even for this single formation, the δO^{18} values of the quartz are variable.

There are other possible explanations why kaolinite samples might be displaced from the kaolinite line. A few samples plotted in Figure 7-2 fall below the kaolinite line. Such apparent isotopic anomalies can be explained if hydrogen isotope exchange between kaolinite and water occurs at a greater rate than oxygen isotope exchange. The younger meteoric waters in these localities would almost certainly have had lower δD than the waters from which the kaolinites were originally formed; hence, hydrogen isotope exchange without accompanying oxygen exchange would move the samples below the kaolinite line.

Another possibility is that the farther one moves down and to the left along the kaolinite line, the lower is the average temperature of the meteoric waters from which the kaolinites are formed. This results in a larger $\alpha^{ox}_{\text{kaolinite - } H_2O}$, causing the isotopic values of such samples to be displaced to the right and below the kaolinite line.

A least squares plot ($\delta D = \underline{7.7}\ \delta O^{18} - \underline{222}$) for all the samples except those of Pennsylvanian age (these may have reequilibrated with H_2O at a higher temperature than 15° to 25°C) is shown in Figure 7-2. Note that the slope is

TABLE 7-1

Material Balance Calculations of the δO^{18} of Quartz in the Eocene Wilcox Formation of Arkansas and Texas

Sample No.	wt. % Quartz	δO^{18} Bulk Sample	Calculated δO^{18} * of the Quartz
H.S.-Ark-1	50 ± 5	+19.2	+ 16.7 ± 0.5
Pul-Ark-2	60 ± 6	+17.3	+14.3 ± 0.8
Che-Tex-1	20 ± 5	+20.4	+ 15.6 ± 1.3
Che-Tex-2	15 ± 5	+19.6	+ 7.1 ± 5.0

* calculated assuming the δO^{18} of the kaolinite (together with a small amount of montmorillonite in two cases) equals +21.4. This is the best estimated value using a δD for kaolinite equal to -58‰, and assuming that the kaolinite plots on the kaolinite line.

slightly steeper than the slope of Savin and Epstein's (1970a) kaolinite line. This least-squares line may be more representative of the actual distribution of kaolinite δD and δO^{18} values because of the temperature effect mentioned above.

The three samples of Pennsylvanian age in Figure 7-2 plot above the kaolinite line. Also, all the samples of Pennsylvanian age in Figure 7-3 (in which corrections for impurities have been made) plot above the kaolinite line. Many of these samples contain illite in addition to kaolinite. All of these samples probably suffered exchange and/or recrystallization under mild diagenetic conditions. Isotopic exchange at higher temperatures could result in such a shift in a $\delta D - \delta O^{18}$ plot. Another possible but unlikely interpretation is that the isotopic composition of the Pennsylvanian oceans was different from the present-day oceans.

One of the major objectives of this study was to examine the feasibility of determining paleoclimates from oxygen and hydrogen isotope analyses of ancient weathering clay deposits. The determination of δD and δO^{18} values of ancient meteoric waters is strongly dependent upon the preservation of the isotopic compositions of the clays. As was pointed out above, some kaolinite deposits may have undergone sufficient post-depositional hydrogen isotope exchange to shift the analyses below the kaolinite line. Despite this problem, the isotopic values of the ancient kaolinites are generally sufficiently different from those of Quaternary soils that it is certain that isotopic values can be preserved in favorable cases.

Figure 7-4 shows how the isotopic compositions of Quaternary soils from Idaho, Montana and Colorado compare with kaolinites of Miocene and Lower Cretaceous age from the same general areas. Taking into account isotopic effects due to impurities and mineralogical differences, the Quaternary soils as a group have lower δD and δO^{18} values than the ancient kaolinites. It was shown in

Figure 7-4. A $\delta D - \delta O^{18}$ diagram comparing isotopic values of Quaternary soils from Idaho, Montana and Colorado with those of Miocene and Lower Cretaceous kaolinites from Idaho, Montana, Colorado and eastern Washington. The degree of shading of each data-point indicates the proportion of impurities such as quartz, feldspar and flint (open) to weathering products (black) in each sample. Savin and Epstein's (1970a) kaolinite line is shown for reference.

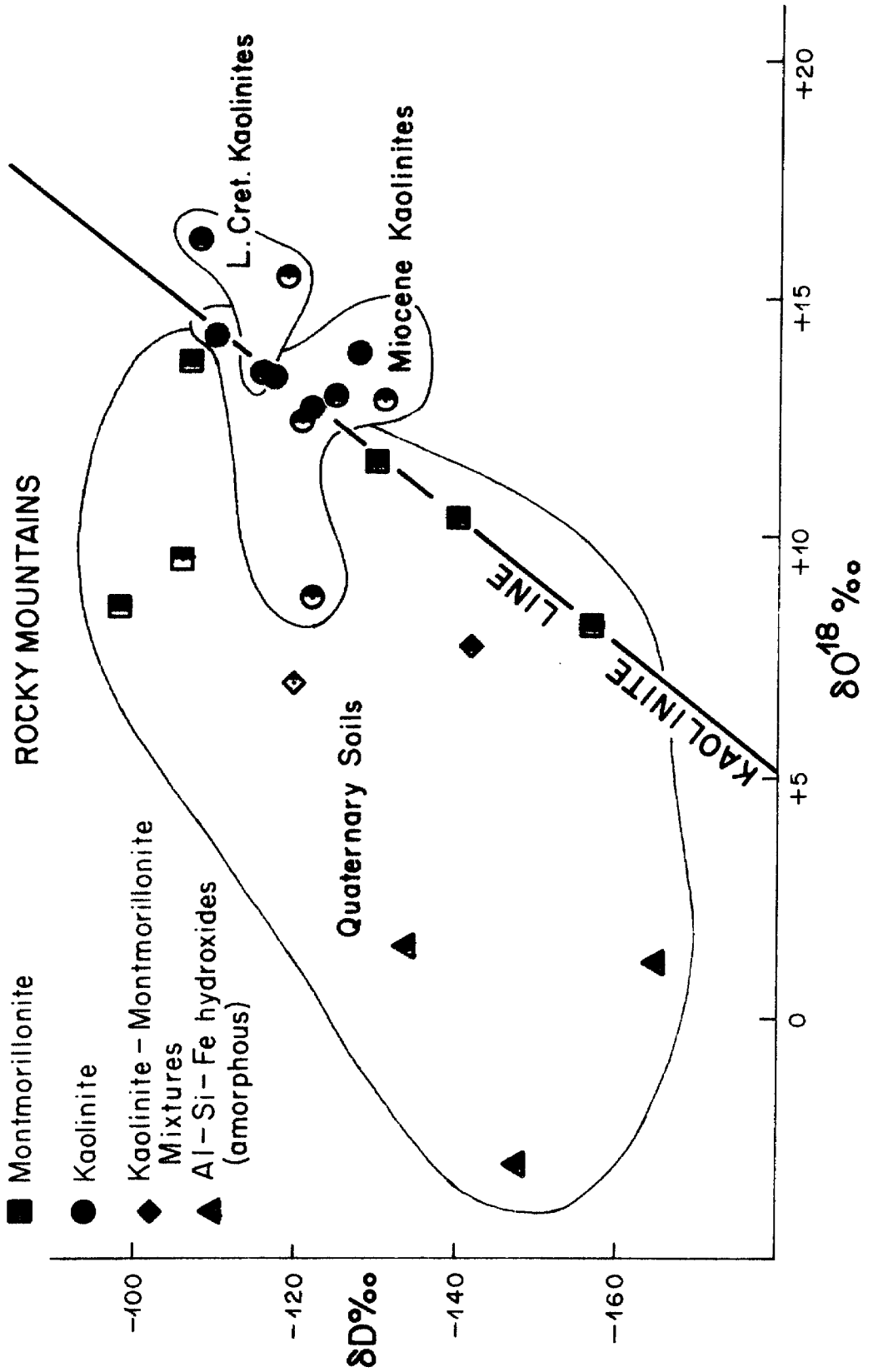
ROCKY MOUNTAINS
Montmorillonite
Kaolinite
Kaolinite – Montmorillonite Mixtures
Al – Si – Fe hydroxides (amorphous)
L. Cret. Kaolinites
Miocene Kaolinites
Quaternary Soils
KAOLINITE LINE
−100
−120
−140
−160
δD‰
0
+5
+10
+15
+20
δO18 ‰

Figure 7-4

Chapter VI that isotopic data on these Quaternary soils reflect the δD and δO^{18} values of present-day meteoric waters. The ancient kaolinites, therefore, appear to reflect meteoric waters isotopically heavier in δD and δO^{18} than present-day waters, suggesting warmer climates in those periods. Geological, paleontological and paleobotanical evidence, as well as δO^{18} studies of carbonates in ocean sediments (Emiliani, 1964), would generally support the idea of warmer climates in the Tertiary and Cretaceous Periods. Because isotopic exchange with Quaternary waters would tend to lower the δD and δO^{18} values of the ancient kaolinites in these regions, these kaolinite isotopic values should be viewed as minimum values.

Figure 7-5 compares isotopic data on Quaternary soils from the southern United States and Hawaii with Eocene, Upper Cretaceous, and Pennsylvanian kaolinites from the southern United States. Taking into account isotopic effects due to impurities, the isotopic values of the Quaternary soils are very similar to those of the ancient kaolinites. This was expected because the present-day climate of the southern United States and Hawaii are probably not very different from the paleoclimates in these areas. The variation of climate with age mentioned in the previous discussion probably existed in the southern United States, too, but the differences would be much greater in inland regions at high elevations and high latitudes. At lower latitudes near warm oceans such as the Gulf of Mexico these differences are small. However, if the small differences that do exist in isotopic values (see Figure 7-6) are real the Eocene and Upper Cretaceous kaolinites have heavier δD and δO^{18} values and appear to have formed in slightly warmer climates than the present-day climate of the southern United States.

The Pennsylvanian kaolinites and illites are more noticeably distinct from

Figure 7-5. A $\delta D - \delta O^{18}$ diagram comparing isotopic values on Quaternary soils from the southern United States and Hawaii with those of kaolinites and illites of various ages from the southern United States. The degree of shading of each data-point indicates the proportion of impurities such as quartz, feldspar and flint (open) to weathering products (black) in each sample. Savin and Epstein's (1970a) kaolinite line is shown for reference.

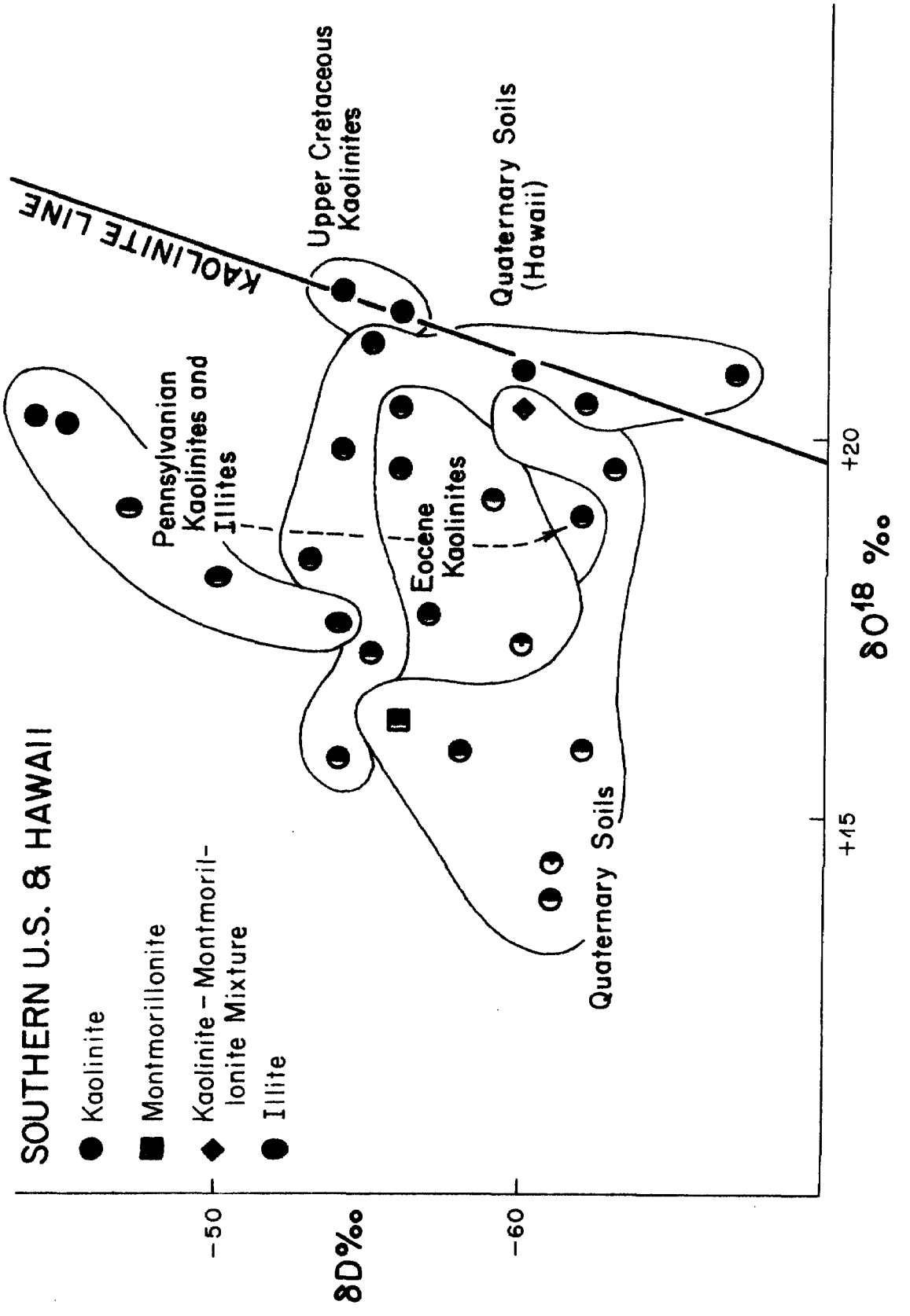
SOUTHERN U.S. & HAWAII
Kaolinite
Montmorillonite
Kaolinite – Montmorillonite Mixture
Illite
KAOLINITE LINE
Upper Cretaceous Kaolinites
Quaternary Soils (Hawaii)
Pennsylvanian Kaolinites and Illites
Eocene Kaolinites
Quaternary Soils
−50
−60
δD‰
+15
+20
δO18 ‰

Figure 7-5

the Quaternary soils. As was pointed out above these isotopic values may reflect diagenetic alteration are higher temperatures. If this diagenetic alteration occurred during Paleozoic time it is very encouraging to see that such effects are still preserved.

Because there are observable differences in the isotopic values of Quaternary soils and ancient kaolinites the isotopic values of the kaolinites (particularly the δD values, as they reflect only the clay minerals in the samples) may be used to calculate the isotopic values of ancient meteoric waters. The δD values of some Tertiary meteoric waters have been calculated in Figure 7-6, assuming complete preservation of the kaolinites. A $\alpha^{hy}_{kaolinite-H_2O} = 0.970$ was assumed to make the calculations.

The δ D values of specific kaolinites are plotted on a map of the United States in Figure 7-6. Some of these values were taken from data by Sheppard et al. (1969) on supergene kaolinites. The calculated δ D values of Tertiary waters are encircled, and roughly estimated contours are drawn. The solid, shaded areas represent locations of Tertiary marine sedimentation. The speckled areas represent locations of lake sediments or continental alluvial deposits of Tertiary age. There is insufficient isotopic data from any specific period to allow further subdivision of the Tertiary. Therefore the isotope data can represent conditions in the Tertiary in only a generalized way.

The distribution of the calculated isotopic values of Tertiary meteoric waters appear to show patterns somewhat different from today (compare Figures 7-6 and 6-1). The contour patterns in Figure 7-6 are grossly similar to present-day patterns, but the gradients between contours are more gentle. If the contours represent the distribution of the δD values of meteoric waters in the Tertiary, it

Figure 7-6. A map of the United States, showing the δD values of kaolinites of Tertiary age. Numbers encircled are calculated δD values of meteoric waters of Tertiary age, assuming $\alpha^{hy}_{kaolinite\text{-}H_2O} = 0.970$. Rough contours have been drawn showing the calculated distribution of δD in Tertiary meteoric waters.

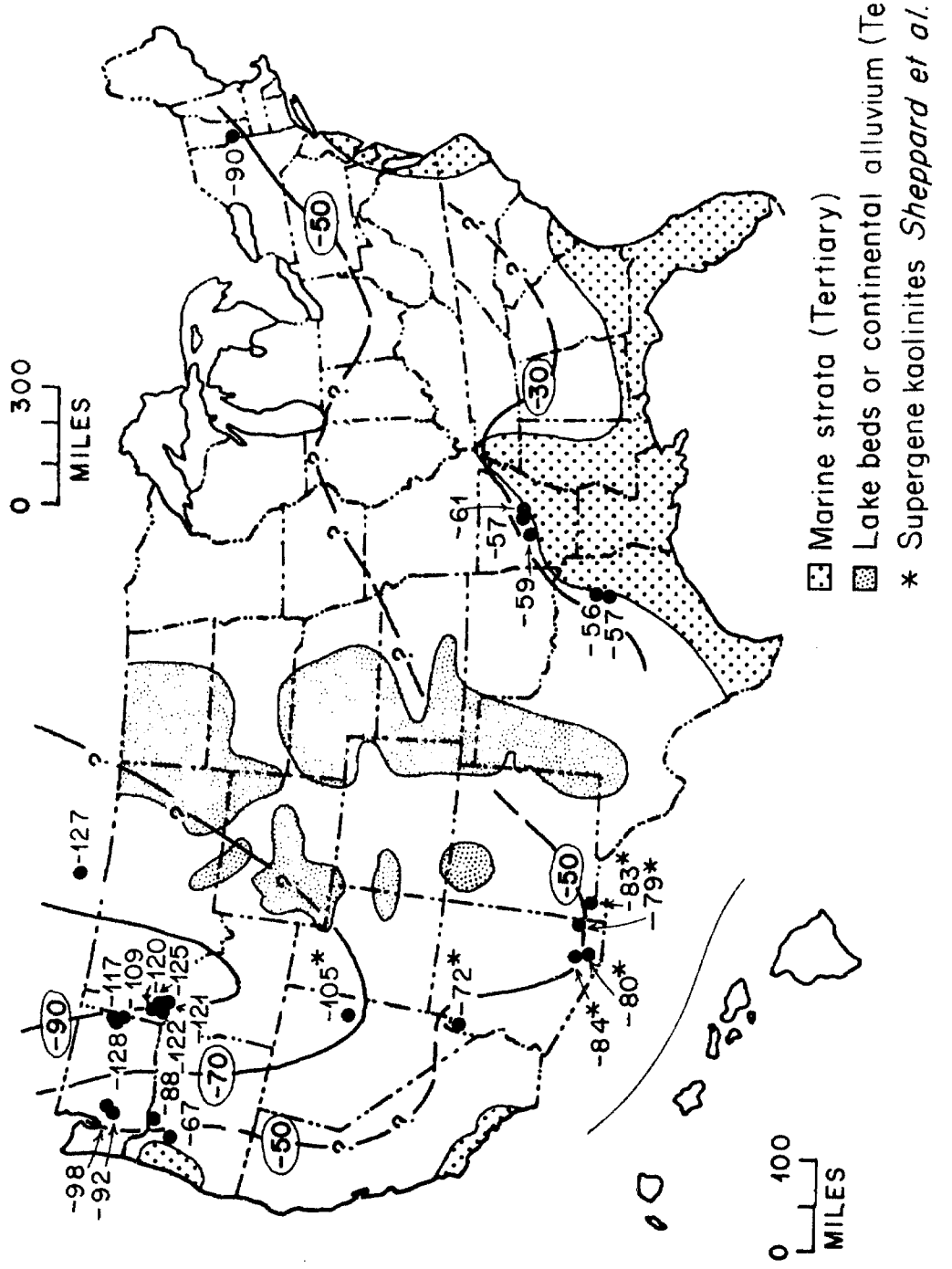
0 300
MILES
-90
-50
-30
-61
-57
-59
-56
-57
-127
-117
-109
-120
-125
-121
-128
-122
-88
-67
-70
-105*
-72*
-50
-83*
-79*
-84*
-80*
-98
-92
Marine strata (Tertiary)
Lake beds or continental alluvium (Tertiary)
* Supergene kaolinites Sheppard et al. (1969)
0 100
MILES

Figure 7-6

would appear that the configuration of the continent and the major topographic features were roughly similar to the present day, although the average elevation of the continent may have been lower. The more gentle gradients can probably be explained as being due to less extreme climatic differences between the coastal and inland regions.

Because of isotopic exchange effects mentioned previously, the δD values shown in Figure 7-6 are minimum values. This perhaps suggests that the actual δD values of Tertiary meteoric waters were even heavier than those given in Figure 7-6. However, it must be remembered that the isotopic values may reflect only conditions in either the summer seasons or perhaps in the rainy seasons, because the rate of clay formation would be greatest under warm and wet climatic conditions. Clearly, careful correlation of geologic, paleontological and paleobotanical data, together with considerably more isotopic data, will be necessary to better ascertain variations of δD and δO^{18} in ancient meteoric waters.

Figures 7-7 and 7-8 show the δD values of kaolinites and illites of Cretaceous and Pennsylvanian ages, respectively, plotted on maps of the United States. Contours of the δD values of meteoric waters of those ages have not been drawn because of an insufficient number of data points. However, by using $\alpha^{hy}_{\text{kaolinite-}H_2O} = 0.970$ to determine the δD values of meteoric waters of those ages, it can be seen that Cretaceous and Pennsylvanian δD values were apparently heavier than those of present-day meteoric waters. More analyses of such ancient clays conceivably could allow the construction of maps of the δD values of Cretaceous and Pennsylvanian meteoric waters. First, however, more definite proof must be obtained that the isotopic results on such kaolinites represent pristine, unaltered values.

Figure 7-7. A map of the United States, showing the δD values of kaolinites of Cretaceous age.

Figure 7-8. A map of the United States, showing the δD values of kaolinites and illites of Pennsylvanian age.

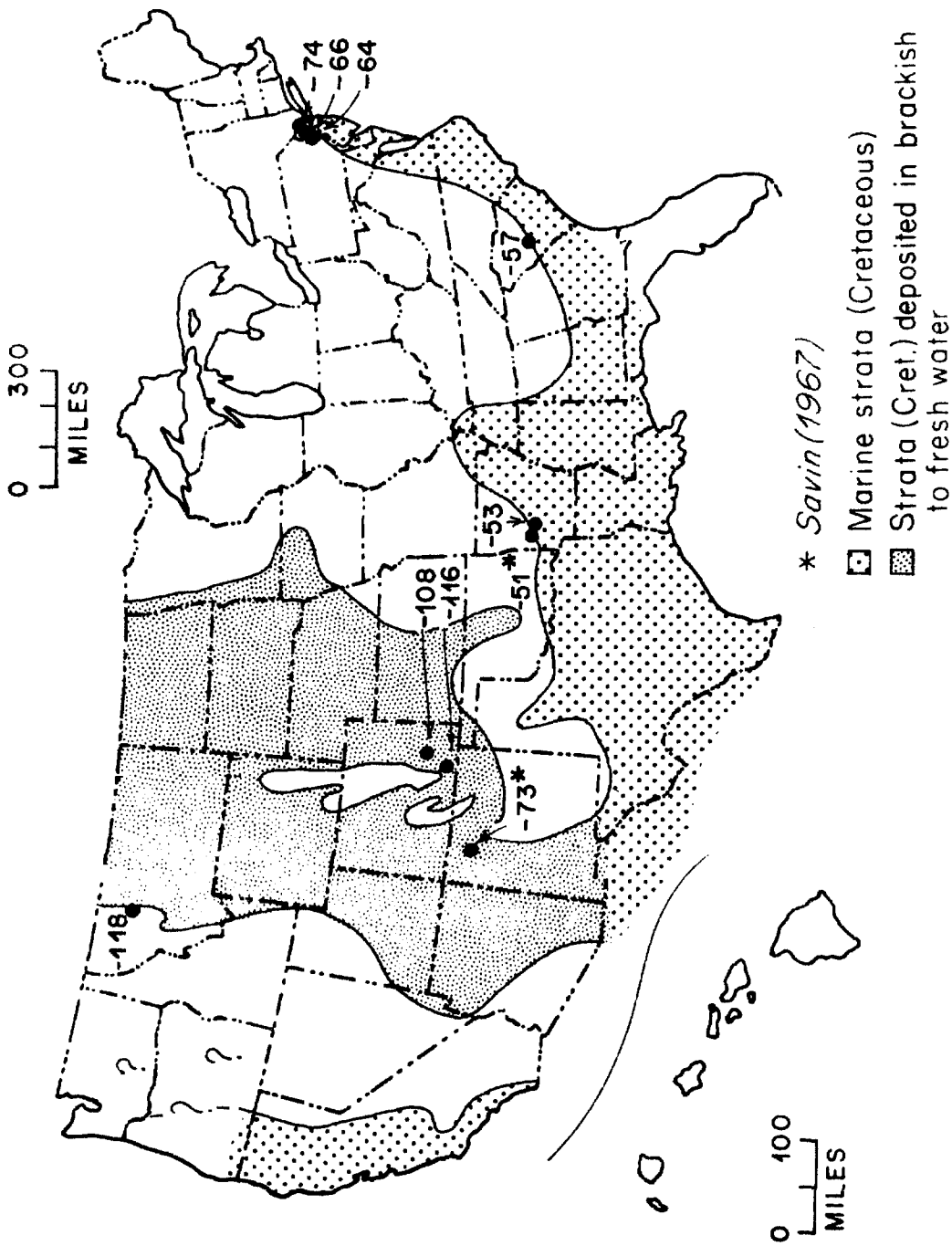
0 300 MILES
-74
-66
-64
-57
-53
-108
-116
-51*
-73*
-118
? ? ?
* Savin (1967)
Marine strata (Cretaceous)
Strata (Cret.) deposited in brackish to fresh water
0 100 MILES

Figure 7-7

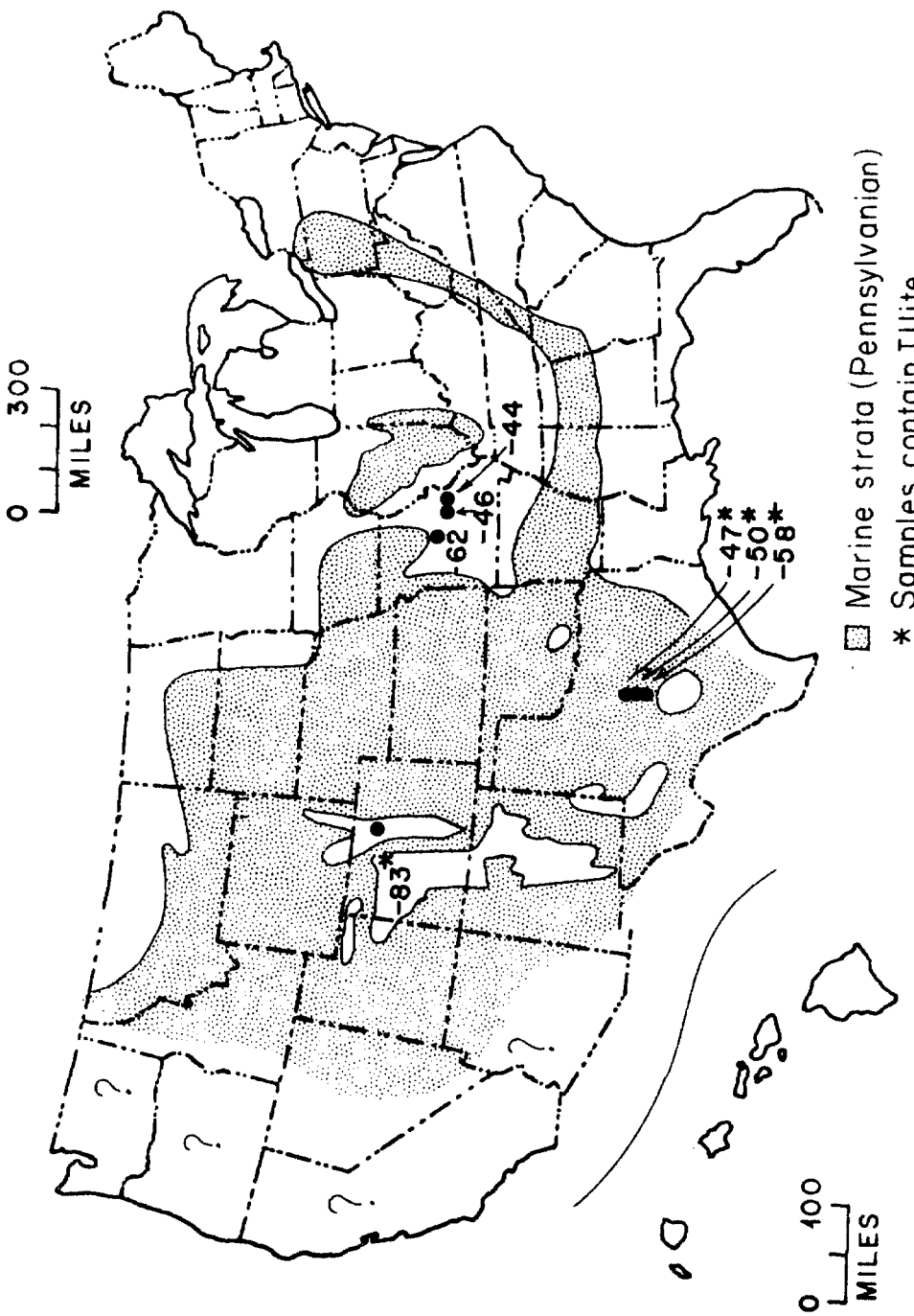
0 300
MILES
-44
-46
62
-47*
-50*
-58*
83
Marine strata (Pennsylvanian)
* Samples contain Illite
0 100
MILES

Figure 7-8

VIII. MONTMORILLONITES

The montmorillonites considered in this chapter have very diverse origins. The various types are listed below.

Oceanic dredge hauls: Montmorillonites formed by alteration of deep ocean basalts or basaltic glasses during subaqueous weathering processes. Temperatures of formation are 0° to 5°C, unless hydrothermal activity is involved.

Bentonites: Montmorillonitic alteration of volcanic ash deposited in shallow marine, brackish, or fresh waters. The alteration could result from contact with these waters and/or from post-depositional alteration by interstitial pore waters. The temperature of alteration conceivably could range from 0° to 100°C, but most samples probably formed at 10° to 30°C. All the bentonites have been exposed to meteoric waters since their formation.

The bentonites here classified as "marine" were formed near the shorelines of the Gulf of Mexico and the Pacific Ocean in marine formations. The bentonites here classified as "brackish-water" were deposited in shallow inland seas with narrow passageways to the open ocean and/or they occur in a sequence of strata which includes alternate marine and nonmarine formations. The bentonites here classified as "fresh-water" were deposited in fresh water lakes.

The marine, brackish or fresh character of the waters in which the bentonites were formed was inferred from geological and paleontological data given by Tourtelot (1962), Gill and Cobban (1966), Reeside (1957), Daugherty (1941) and Kerr and Kulp (1949).

Bentonite shales: Bentonites with admixtures of detrital sediments derived from subaerial weathering and erosion.

Quaternary subaerial weathering products: Soils or rocks altered by surface ground waters, usually under seasonal, arid or semi-arid climatic conditions. Temperatures of alteration should range from 0° to 30°C.

Altered basaltic glass (pillow lavas) : Montmorillonites probably formed by the alteration of the outer glass rinds of pillow lavas by subaerial weathering processes. Temperatures of formation are probably from 0° to 30°C.

Fossil montmorillonite soils buried by lava flows: Ancient soils formed by subaerial weathering processes. Temperature of formation ranges from 0° to 30°C. Reequilibration of soils at higher temperatures during cooling of overlying lavas is likely because the soils are only a few feet thick. Also, pillow structures exist in some of the lavas, suggesting an abundant supply of water. Temperatures of re-equilibration may perhaps be as high as 350°C.

Hypogene montmorillonites: Montmorillonites formed by the alteration of aluminosilicate rocks by ascending hydrothermal waters. Temperatures of formation range from 50° to 350°C.

Supergene montmorillonites: Montmorillonitic alteration of aluminosilicate rocks by descending meteoric waters that have reacted with sulfide minerals. Temperatures of formation are probably from 20° to 50°C.

Detailed descriptions may be found in Appendix I and the cited references. Information on mineral impurities, differential thermal analyses and isotopic data are given in Tables 4-1 and 5-3.

Savin and Epstein (1970a) determined the δD and δO^{18} contents of two types of low-temperature montmorillonites, from oceanic dredge hauls and

from bentonites. They observed a large scatter in isotopic values compared with kaolinites. In addition, the correlation of δD and δO^{18} between meteoric waters and montmorillonites was very poor. They therefore chose the samples whose origin was best understood and constructed a tentative montmorillonite line for 25°C, using $\alpha^{hy}_{\text{montmorillonite-}H_2O} = 0.938$ and $\alpha^{ox}_{\text{montmorillonite-}H_2O} = 1.0273$. Their montmorillonite line is shown in Figure 8-1 along with all of the isotopic data on montmorillonites from this study, from Savin and Epstein (1970a), and from Sheppard et al.(1969).

In considering the isotopic data on montmorillonites, six factors are important: (1) the isotopic compositions of the waters in which the montmorillonites were formed; (2) the temperatures of formation or reequilibration of the montmorillonites; (3) the chemical compositions of the montmorillonites (see section 5-3); (4) the amounts and isotopic compositions of impurities in the samples; (5) post-formational isotopic exchange between the montmorillonites and interstitial pore waters; and (6) the effects of hydrogen isotope exchange between interlayer water and hydroxyl during the laboratory extraction procedures (see Chapter III).

As can be seen by comparing Figure 7-1 and 7-2 with Figure 8-1, the scatter in δD and δO^{18} values of montmorillonites is much greater than the scatter in the isotopic values of kaolinites. This is to be expected because of the analytical problems connected with hydrogen isotope analyses of montmorillonites.

However, Figure 8-2 illustrates that systematic variations in δO^{18} and δD values can be found when comparing montmorillonites of similar origins.

The marine bentonites as a group display δO^{18} and δD values distinctly heavier than the isotopic values of bentonites formed in fresh or brackish waters.

Figure 8-1. A $\delta D - \delta O^{18}$ diagram for montmorillonites of a variety of origins. All montmorillonites analyzed to date are plotted on the diagram, except for a few mixed kaolinite-montmorillonite hypogene clays of Sheppard et al (1969) and the very impure montmorillonitic soils of the present work. The degree of shading of each data-point indicates the proportion of impurities (open) to montmorillonite (black) in each sample. The impurities are mainly quartz and feldspar. The kaolinite and montmorillonite lines of Savin and Epstein (1970a) are shown for reference.

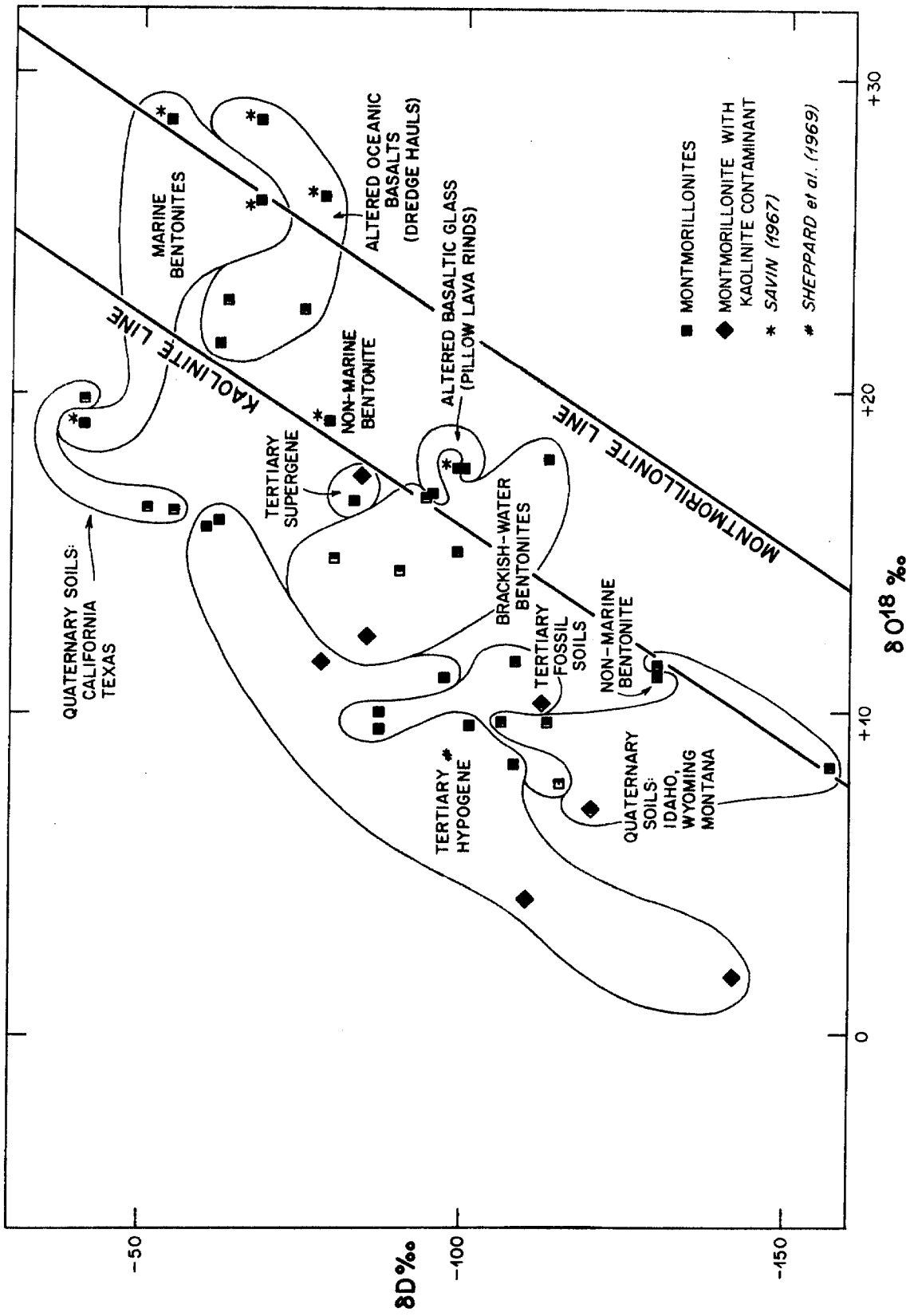
MARINE BENTONITES
ALTERED OCEANIC BASALTS (DREDGE HAULS)
ALTERED BASALTIC GLASS (PILLOW LAVA RINDS)
NON-MARINE BENTONITE
KAOLINITE LINE
MONTMORILLONITE LINE
TERTIARY SUPERGENE
BRACKISH-WATER BENTONITES
TERTIARY FOSSIL SOILS
NON-MARINE (BENTONITE
QUATERNARY SOILS: CALIFORNIA TEXAS
TERTIARY # HYPOGENE
QUATERNARY SOILS: IDAHO, WYOMING MONTANA
MONTMORILLONITES
MONTMORILLONITE WITH KAOLINITE CONTAMINANT
* SAVIN (1967)
# SHEPPARD et al. (1969)
-50
-100
-150
δD‰
+30
+20
+10
0
δO18 ‰

Figure 8-1

Figure 8-2. A $\delta D - \delta O^{18}$ diagram of bentonites and altered pillow lava rinds or basalt fragments from marine, brackish-water and nonmarine environments. The δO^{18} values of these montmorillonite samples were corrected by material balance calculations for any impurities. Savin and Epstein's (1970a) kaolinite and montmorillonite lines are shown for reference.

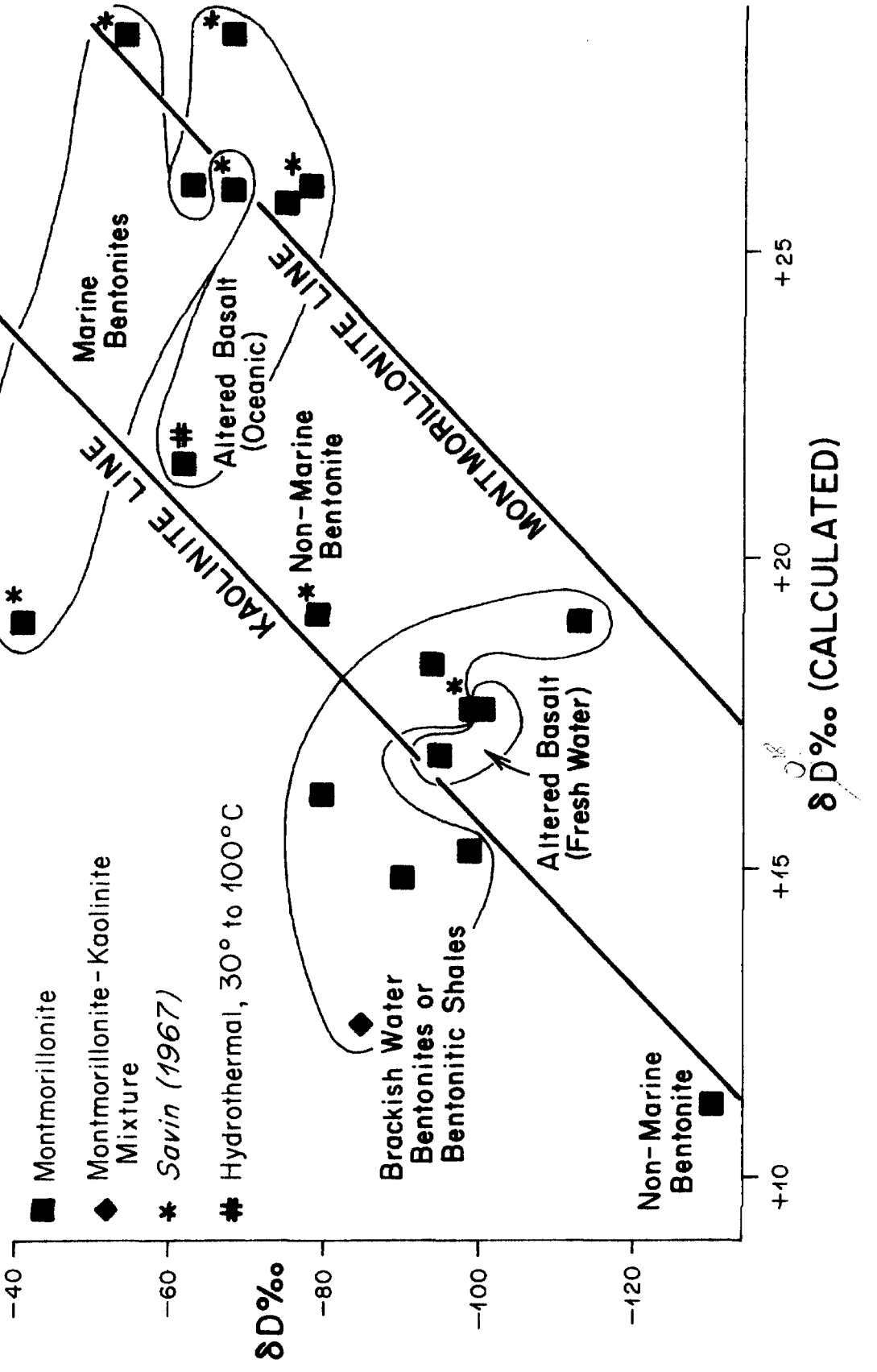
Montmorillonite
Montmorillonite-Kaolinite Mixture
Savin (1967)
Hydrothermal, 30° to 100°C
δD‰
−40
−60
−80
−100
−120
+10
+15
+20
+25
δD‰ (CALCULATED)
KAOLINITE LINE
MONTMORILLONITE LINE
Marine Bentonites
Altered Basalt (Oceanic)
Non-Marine Bentonite
Brackish Water Bentonites or Bentonitic Shales
Altered Basalt (Fresh Water)
Non-Marine Bentonite

Figure 8-2

These isotopic differences parallel the differences in isotopic composition between the marine and the brackish or fresh waters in which the alteration of volcanic ash to montmorillonite took place. The major isotopic effects in bentonites are thus due principally to variations in the δD and δO^{18} of the coexisting waters. This alteration, however, could have taken place either before or after burial by other sediments.

The scatter in δO^{18} and δD values within a single group of bentonites, either those of marine origin or those of brackish-water origin, might in part be attributed to different temperatures of formation of each sample.

Figure 8-2 also illustrates that montmorillonites formed as alteration products of basaltic material in an oceanic environment are distinctly heavier in δD and δO^{18} values than those of montmorillonites of nearly identical origin formed in fresh water environments. This undoubtedly reflects the different isotopic compositions of ocean waters and fresh waters. A single isotopically anomalous montmorillonite sample formed by alteration of basalt in the oceanic environment is shown in Figure 8-2 (TW-10-116). The sample is reported as being of hydrothermal origin (Banks and Melson, 1966). It plots well to the left of the others, consistent with a higher temperature origin.

The montmorillonites formed by the alteration of basaltic glass in fresh water (pillow lava rinds) plot farther to the left of the montmorillonite line than do the oceanic samples of similar origin. This very likely reflects a difference in the temperatures of formation of the two groups: the oceanic montmorillonites probably formed at 0° to 5°C, and the fresh-water montmorillonites formed at 15° to 30°C. Such temperature differences can be responsible for large changes in the equilibrium montmorillonite-H_2O isotopic fractionation factors, and the positions of various

samples on a $\delta D - \delta O^{18}$ plot are consistent with these temperature differences (see Figure 1-1). For example, a temperature change from 0° to 20°C is estimated (Figure 1-1) to produce a change of 4 per mil in δO^{18} in the montmorillonite in equilibrium with a given water.

Figure 8-3 further illustrates the effect of temperature on the δD and δO^{18} content of montmorillonites. The higher temperature hypogene montmorillonites plot distinctly to the left of all montmorillonite samples from Quaternary soils, altered basaltic glass and the supergene zones of porphyry copper deposits. The fossil soils buried by lava flows have isotopic values generally intermediate to the above groupings. This is to be expected if the fossil soils have undergone different degrees of reequilibration with meteoric waters during the cooling of the lava flows.

Both the hypogene montmorillonites and the Quaternary soils as groups display a range of δD and δO^{18} values parallel to the meteoric water line. This range of values is consistent with the formation of these montmorillonites in the presence of meteoric waters.

Figure 8-5 also illustrates the effects of temperature on the δO^{18} values of montmorillonites. These montmorillonites have several characteristics in common: (1) they were formed from a single rock type, namely basalt; (2) they are located in a restricted geographic area (see Figure 8-4); and (3) they are of similar ages, namely mid-Tertiary. The montmorillonites of fossil soils buried by lava flows display distinctly lower δO^{18} values than the montmorillonites of the altered rinds of pillow lavas. This is consistent with the different temperatures to which these montmorillonites have been subjected, as the latter samples represent low-temperature weathering of basaltic glass after the cooling of the pillow basalts.

Figure 8-3. A $\delta D - \delta O^{18}$ diagram of montmorillonites from Quaternary soils, Tertiary supergene deposits, Tertiary fossil soils buried by lava flows, and altered rinds of Miocene pillow lavas. The δO^{18} values of these montmorillonite samples were corrected by material balance calculations for any impurities. Savin and Epstein's (1970a) kaolinite and montmorillonite lines are shown for reference.

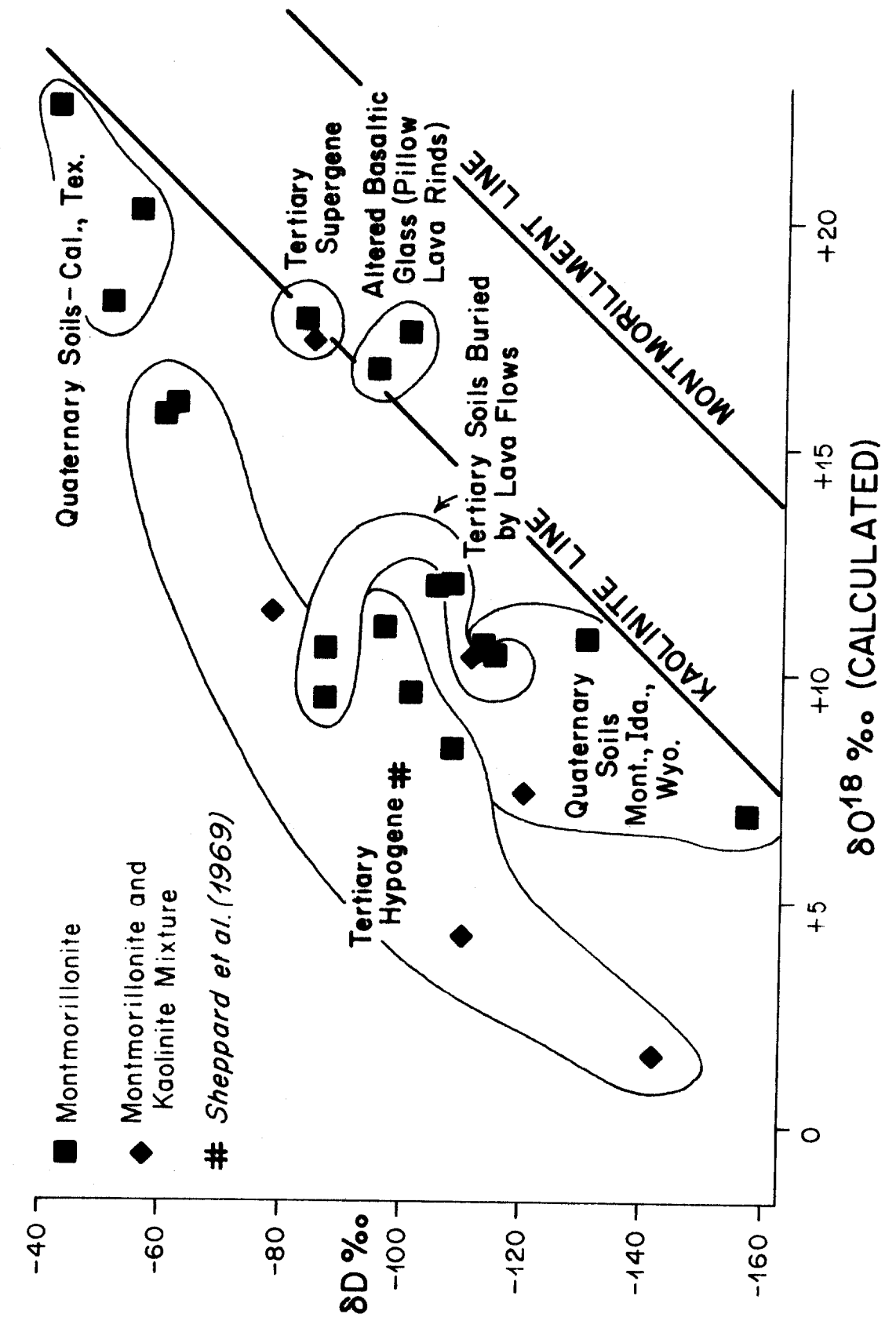
Montmorillonite
Montmorillonite and Kaolinite Mixture
Sheppard et al. (1969)
Quaternary Soils-Cal., Tex.
Tertiary Supergene
Altered Basaltic Glass (Pillow Lava Rinds)
Tertiary Soils Buried by Lava Flows
Tertiary Hypogene #
Quaternary Soils Mont., Ida., Wyo.
MONTMORILLONITE LINE
KAOLINITE LINE
δD ‰
δO18 ‰ (CALCULATED)
-40
-60
-80
-100
-120
-140
-160
0
+5
+10
+15
+20

Figure 8-3

Figure 8-4. A map of northcentral Oregon, showing the locations of montmorillonite samples shown in Figure 8-5.

Figure 8-5. A $\delta D - \delta O^{18}$ diagram for montmorillonites from fossil soils buried by lava flows and altered rinds of pillow lavas; both groups are of mid-Tertiary age from north-central Oregon. The δO^{18} values of the montmorillonite samples have been corrected for impurities by material balance calculations. The numbers above the data-points refer to locations of the samples shown in Figure 8-4. Savin and Epstein's (1970a) kaolinite line is shown for reference.

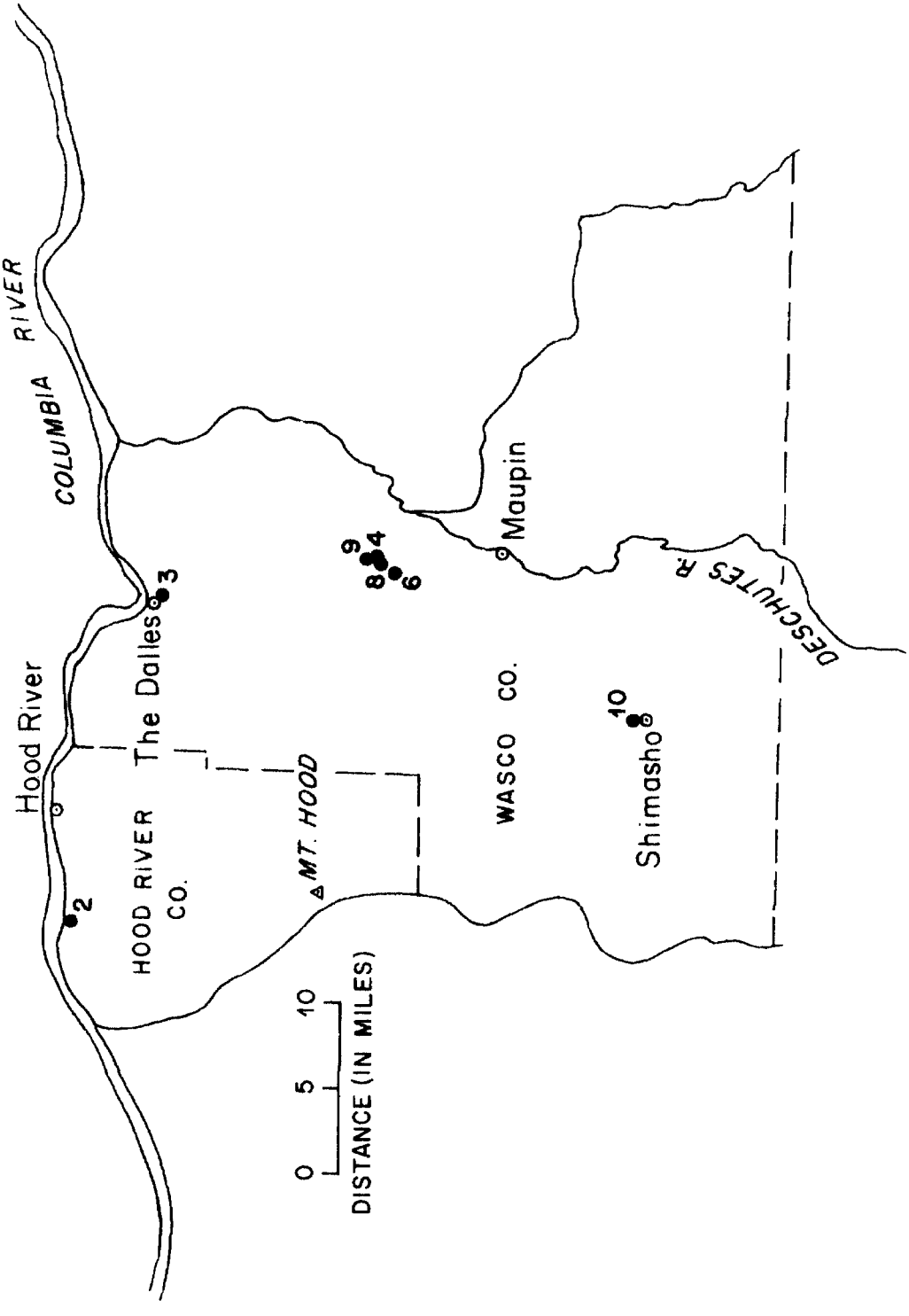
COLUMBIA RIVER
Hood River
The Dalles
Maupin
DESCHUTES R.
HOOD RIVER CO.
MT. HOOD
WASCO CO.
Shimasho
2
3
4
6
8
9
10
0
5
10
DISTANCE (IN MILES)

Figure 8-4

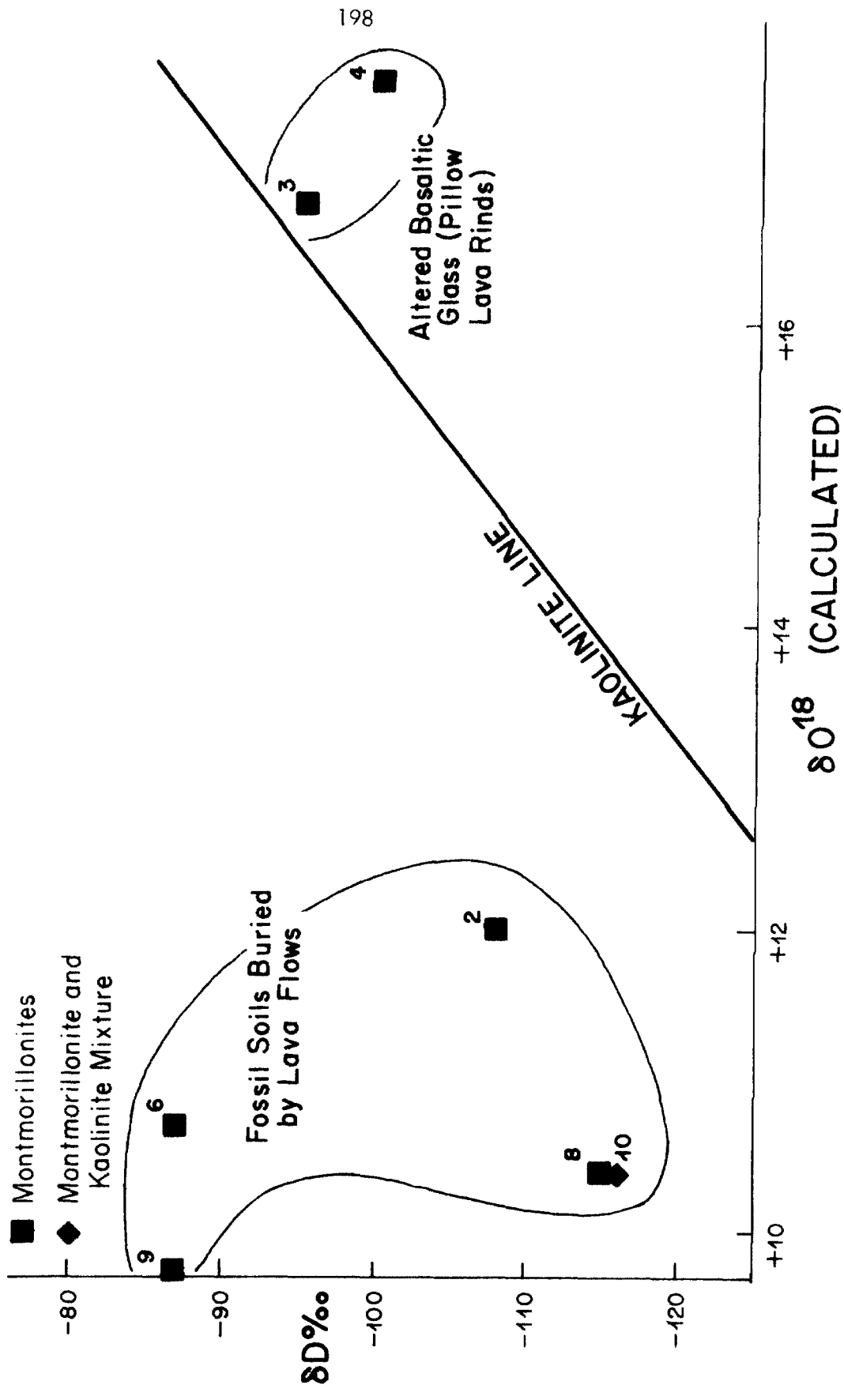
Montmorillonites
Montmorillonite and Kaolinite Mixture
Fossil Soils Buried by Lava Flows
Altered Basaltic Glass (Pillow Lava Rinds)
KAOLINITE LINE
δD‰
δO18 (CALCULATED)
-80
-90
-100
-110
-120
+10
+12
+14
+16
2
3
4
6
8
9
10

Figure 8-5

If we assume that the montmorillonites from the pillow lava rinds and the fossil soils buried by lava flows equilibrated with H_2O's having similar δO^{18} values and that the montmorillonites from the pillow lava rinds formed at 20°C (a reasonable Earth-surface temperature), from Figure 1-1 we can calculate the temperature of reequilibration of the fossil soils. The δO^{18} values of the above two montmorillonite groups (see Figure 8-5) differ by 6‰ . Making the above assumptions, this difference would suggest (see Figure 1-1) that the fossil soils reequilibrated at 60° to 70°C.

The δD values of the two groups of montmorillonites delineated in Figure 8-5 do not show any systematic differences. The fossil soils, which were all formed on Oligocene or Miocene volcanics and later covered by volcanics of the same age, show a large range of δD values. This range conceivably could be the result of temperature variations during isotopic reequilibration, or to evaporative effects when the hot lavas came into contact with the wet soils.

Up to this point the question of isotopic exchange of ancient montmorillonites with recent meteoric waters has been for the most part ignored. Figure 8-6 contrasts the δD and δO^{18} values of montmorillonites from Quaternary soils with those of Upper Cretaceous bentonites. Both groups are located in the same geographic area.

The bentonites, as a group, display distinctly higher δD and δO^{18} values than the Quaternary soils, suggesting that the observed isotopic values of the bentonites represent preserved values. Inasmuch as the bentonites probably formed in brackish waters, their present isotopic values are similar to their presumed original values. If isotopic exchange between the bentonites and Quaternary meteoric waters has taken place, the exchange has only been partial. If

Figure 8-6. A $\delta D - \delta O^{18}$ diagram comparing the isotopic compositions of montmorillonites from Quaternary soils of Idaho, Montana and Wyoming with the isotopic values of Cretaceous brackish-water bentonites and bentonite shales from Montana and Wyoming. The δO^{18} values of the montmorillonite samples were corrected for impurities using material balance calculations. The kaolinite and montmorillonite lines of Savin and Epstein (1970a) are shown for reference.

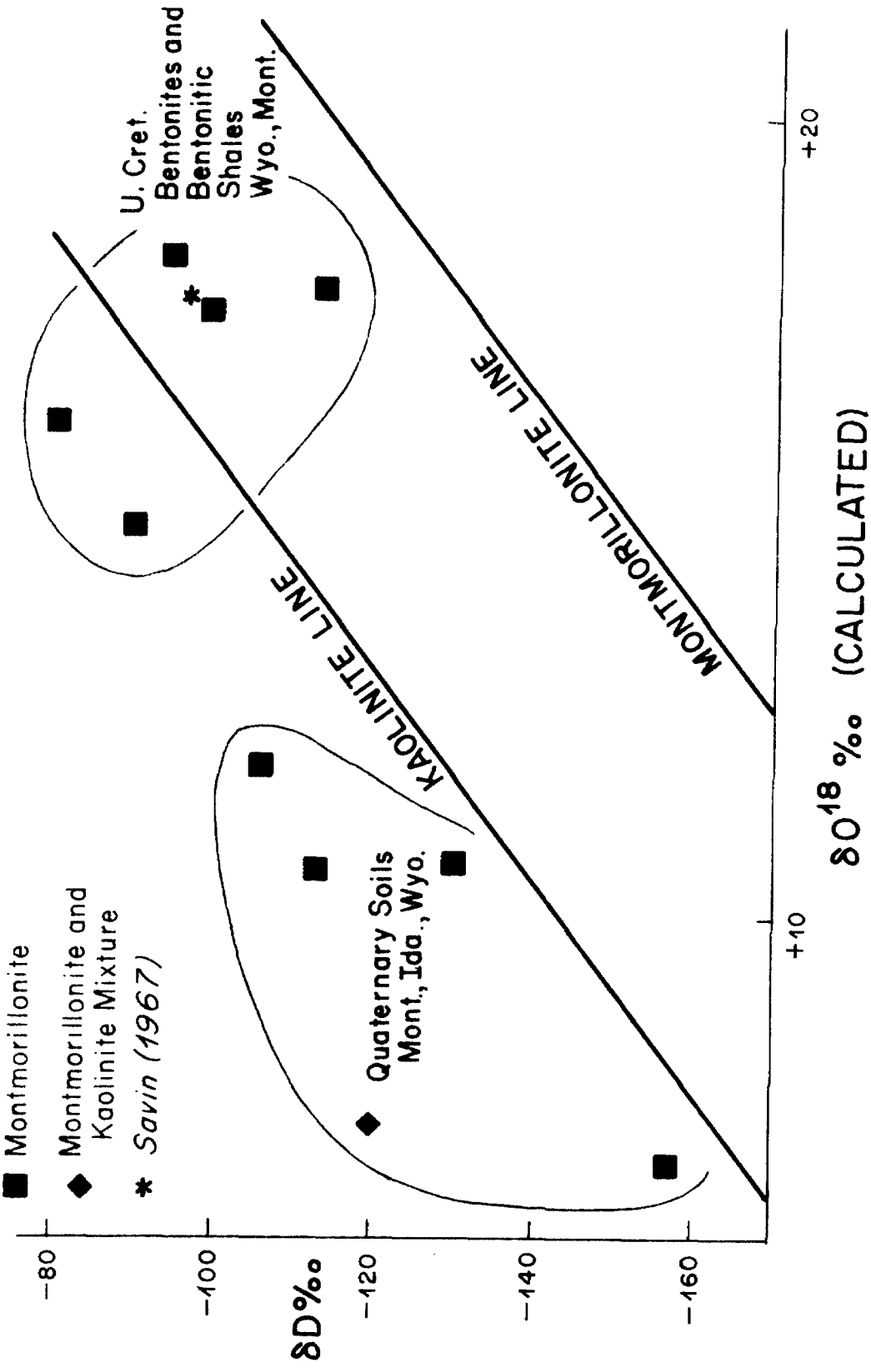
Montmorillonite
Montmorillonite and Kaolinite Mixture
Savin (1967)
U. Cret. Bentonites and Bentonitic Shales Wyo., Mont.
Quaternary Soils Mont., Ida., Wyo.
KAOLINITE LINE
MONTMORILLONITE LINE
δD‰
δO18 ‰ (CALCULATED)
-80
-100
-120
-140
-160
+10
+20

Figure 8-6

partial isotopic exchange has occurred it means that the observed δD and δO^{18} values of the bentonites are minimum values in the sense that the original values must have been this high or higher.

As has been shown in the preceding discussion, there is appreciable scatter in the isotopic compositions of montmorillonites. However, when montmorillonites of a particular type are considered, systematic variations as a function of water isotopic composition, temperature of formation, and chemical composition (see section 5.3) can be observed. More careful study of montmorillonite isotopic compositions in the framework of detailed chemical and geological information undoubtedly will lead to a more thorough understanding of the environmental conditions of the formation of various types of montmorillonites.

As a result of more thorough studies it is anticipated that a family of montmorillonite lines conceivably can be drawn on a $\delta D - \delta O^{18}$ plot, similar to the one proposed by Savin and Epstein (1970a). These lines will differ systematically as a function of the temperatures of formation of the montmorillonites and as a function of chemical composition of the montmorillonites.

IX. SHALES AND GLACIAL LAKE CLAYS

Shales are consolidated deposits of clay-sized particulate matter generally containing small amounts of organic matter, carbonates, sulfides, and other salts. The clay-sized particulate matter is largely composed of clay minerals, quartz, and feldspar. The clay minerals in a shale may be detrital, authigenic, or diagenetic in origin.

In this study several shales with a low organic content were studied for their total δO^{18} content, their total δD content, and the δO^{18} value of their carbonate fraction. The δD of the whole rock and the δO^{18} of the carbonate were also analyzed in three glacial lake clays from the eastern United States.

Detailed descriptions of the samples may be found in Appendix I and the cited references. Mineralogical and isotopic data are given in Table 4-1.

Figure 9-1 illustrates the δD and δO^{18} contents of shales of Cretaceous, Lower Paleozoic and Precambrian ages. The isotopic compositions of the shales plot into two groups, the Lower Paleozoic and Precambrian shales with a dominantly illite-chlorite clay mineralogy, and the Cretaceous shales with a dominantly montmorillonite clay mineralogy. The δD values of the Lower Paleozoic and Precambrian shales are distinctly heavier than the δD values of the Cretaceous shales. Also the δO^{18} values of the Cretaceous shales display a much greater range than those of the Lower Paleozoic and Precambrian shales.

Figure 9-2 shows that the δD values of Lower Paleozoic and Precambrian shales show no correlation with present-day latitude or elevation. Some of the shales with the heaviest δD values are from Montana and British Columbia, and

Figure 9-1. A $\delta D - \delta O^{18}$ diagram of Lower Paleozoic, Precambrian and Cretaceous shales from North America. Savin and Epstein's (1970a) kaolinite line is shown for reference.

Figure 9-2. A δD diagram of Precambrian, Lower Paleozoic, and Cretaceous shales, and Pleistocene glacial-lake clays from North America.

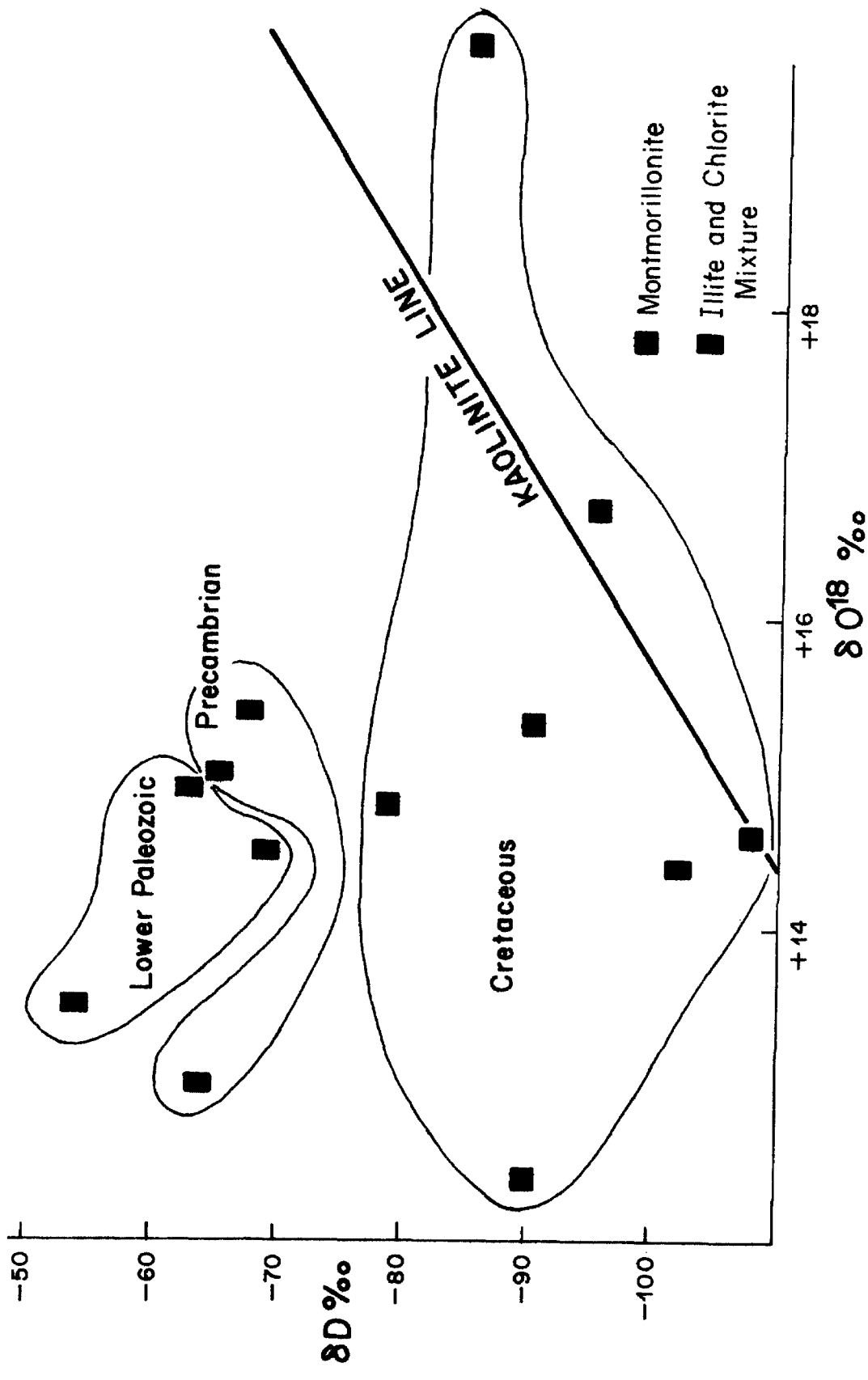
KAOLINITE LINE
Montmorillonite
Illite and Chlorite Mixture
Lower Paleozoic
Precambrian
Cretaceous
δD ‰
δO18 ‰
-50
-60
-70
-80
-90
-100
+14
+16
+18

Figure 9-1

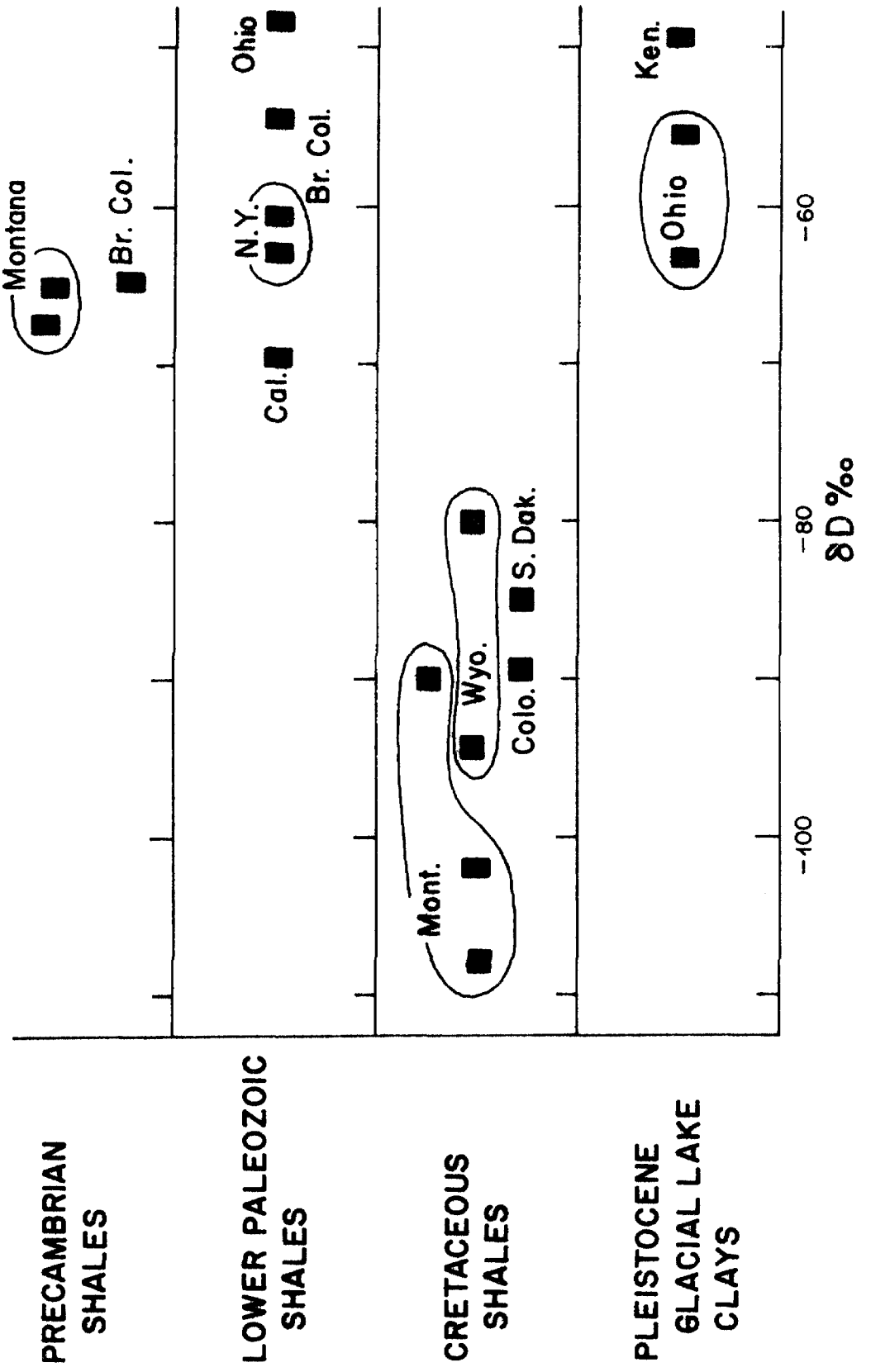
PRECAMBRIAN SHALES
LOWER PALEOZOIC SHALES
CRETACEOUS SHALES
PLEISTOCENE GLACIAL LAKE CLAYS
Montana
Br. Col.
Cal.
N.Y.
Ohio
Br. Col.
Mont.
Wyo.
Colo.
S. Dak.
Ohio
Ken.
-100
-80
-60
δD ‰

Figure 9-2

they have δD values similar to those from Ohio and New York. Yet the δD values of present-day meteoric waters in the two areas differ by 50‰ to 90‰ (see Figure 6-1). This indicates that these Lower Paleozoic and Precambrian shales have not suffered appreciable hydrogen isotope exchange with either present-day, Holocene or Pleistocene meteoric ground waters. Although it is somewhat less certain, exchange with Tertiary meteoric ground waters probably can also be ruled out (see Figure 7-6).

Figure 9-3 is a $\delta D - \delta O^{18}$ plot comparing the isotopic compositions of Lower Paleozoic, Precambrian, and Cretaceous shales from Wyoming, Montana, and British Columbia with the isotopic values of Quaternary soils from Wyoming, Montana and Idaho. The δD and δO^{18} values of the shales are quite distinct from those of Quaternary soils. In addition it should be noted that the older shales which might be expected to have suffered the greatest degree of isotopic exchange with meteoric waters display the largest isotopic differences from Quaternary soils. These data strongly suggest that the shale isotopic values are basically preserved and represent environmental conditions very different from equilibration with present-day meteoric waters.

The Cretaceous shales for the most part contain a mixture of montmorillonite, illite, quartz, feldspar, carbonate, and traces of other minerals. The montmorillonite probably resulted from the alteration of volcanic ash in brackish waters. The carbonate (when it occurs) is probably of biogenic origin. The quartz, feldspar and illite are probably detrital. All of these materials have been subjected to at least mild diagenetic conditions.

The δD values of these shales are primarily due to their constituent montmorillonite. They probably represent equilibration of the montmorillonite

Figure 9-3. A $\delta D - \delta O^{18}$ diagram comparing the measured isotopic compositions of clay-rich or hydroxide-rich Quaternary soils from Idaho, Montana, and Wyoming with the isotopic compositions of Cretaceous, Lower Paleozoic, and Precambrian shales from Montana, Wyoming, and British Columbia. In the case of the Quaternary soils the degree of shading of each data-point indicates the proportion of parent rock (open) to weathering product (black) in each sample. Savin and Epstein's (1970a) kaolinite line is shown for reference.

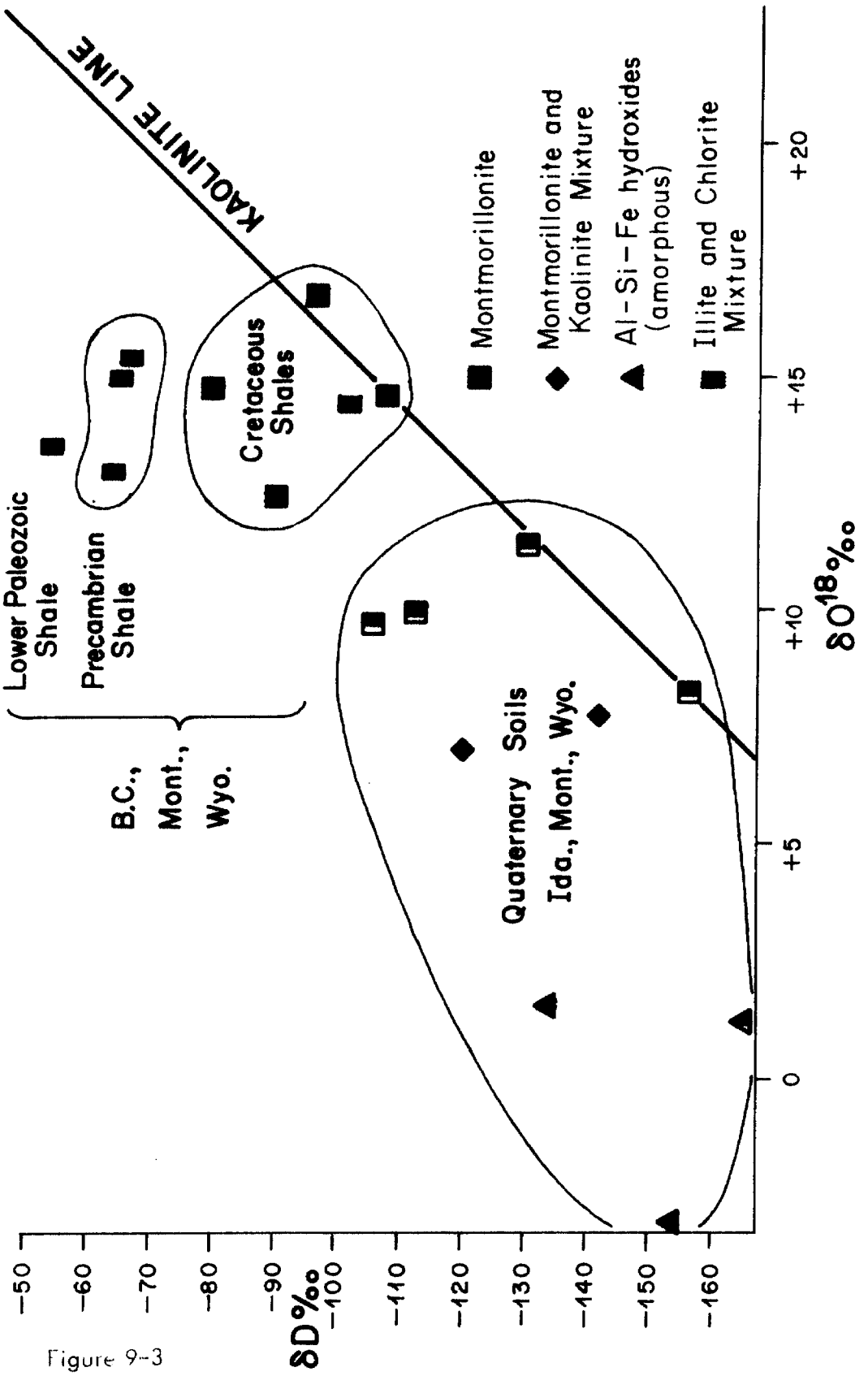
KAOLINITE LINE
Lower Paleozoic Shale
Precambrian Shale
B.C., Mont., Wyo.
Cretaceous Shales
Quaternary Soils
Ida., Mont., Wyo.
Montmorillonite
Montmorillonite and Kaolinite Mixture
Al-Si-Fe hydroxides (amorphous)
Illite and Chlorite Mixture
δD‰
δO18‰
−50
−60
−70
−80
−90
−100
−110
−120
−130
−140
−150
−160
0
+5
+10
+15
+20

Figure 9-3

with brackish waters at the time of deposition or at some later time under mild diagenetic conditions. The variations in δO^{18} of the shales are due to a variety of different causes, reflecting the diversity of origins of the oxygen-bearing minerals.

The Lower Paleozoic and Precambrian shales contain a mixture of illite, chlorite, quartz and in some instances carbonate. The illite and chlorite may be detrital or (more likely) may represent the end products of diagenesis. The quartz is probably detrital. The carbonate (when it occurs) probably has a biologic origin. All of these shales have suffered some degree of diagenesis, particularly the Precambrian and Cambrian shales from Montana and British Columbia.

The δD values of these older shales conceivably could reflect diagenetic equilibration of illite and chlorite with marine pore waters. In any case the δD values of the waters with which these clays equilibrated must have been heavier than -55 to -70‰, and probably near 0‰, inasmuch as at equilibrium at low temperatures, all known clay mineral-H_2O hydrogen isotope fractionation factors are less than unity.

The δO^{18} values of these older shales, as was the case with the Cretaceous shales, reflect the diversity in δO^{18} of the oxygen-bearing minerals. The smaller range in δO^{18} of the older shales compared to the Cretaceous shales (see Figure 9-1) may reflect more isotopically uniform sources of oxygen-bearing minerals or a more isotopically uniform pore water (oxygen reservoir) with which the minerals equilibrated during diagenesis.

The δO^{18} values of the carbonate fraction of the Lower Paleozoic shales display a 9‰ range (Figure 9-4). The lightest of these is located in the Inyo Mountains of California where present-day meteoric waters have a $\delta O^{18} \sim -15.0$‰

(see Figure 6-1). The others are located in eastern United States where the present-day meteoric waters are somewhat heavier ($\sim -7.5‰$). These observed carbonate δO^{18} values are compatible with isotopic exchange between present-day ground waters and the carbonates at 15° to 25°C (see Figure 1-1).

The δD values of these same shales (Figure 9-4) do not show any obvious correlation with the δO^{18} values of the carbonate fraction. This suggests that although the carbonate fraction of the shales may undergo significant isotopic exchange with meteoric waters, the clay mineral fraction does not suffer significant hydrogen isotopic exchange with the meteoric waters.

The δD values of the carbonate fraction of the glacial lake clays are very similar to the δO^{18} values of the Lower Paleozoic shales of eastern United States. The δO^{18} values of glacial melt waters were undoubtedly lighter (possibly -10 to $-20‰$) than present-day values (-5 to $-10‰$). Carbonate in equilibrium with glacial melt waters at 0°C having a $\delta O^{18} = -15 \pm 5‰$ would have a $\delta O^{18} = +19 \pm 5‰$ (see Figure 1-1) somewhat lighter than the observed δO^{18} values. This suggests that possibly the carbonates in the glacial lake clays have reequilibrated with present-day meteoric waters at 15° to 25°C, or that the carbonate δO^{18} values of the shales represent equilibration with Pre-Pleistocene meteoric waters and the glacial lake clays are merely mechanically transported shale material in which the carbonate has undergone little or no exchange with glacial melt waters.

The mineralogy of the Lower Paleozoic shales and the glacial lake clays are nearly identical; they both contain predominantly illite, chlorite, quartz and carbonate. The δD values of the glacial clays are identical to those of the Lower Paleozoic shales. Despite the fact that the clay minerals must have been

Figure 9-4. A δD (clay minerals) - δO^{18} (carbonates) diagram of Lower Paleozoic shales and glacial lake clays. The shale samples contain 10 to 50 weight percent carbonate.

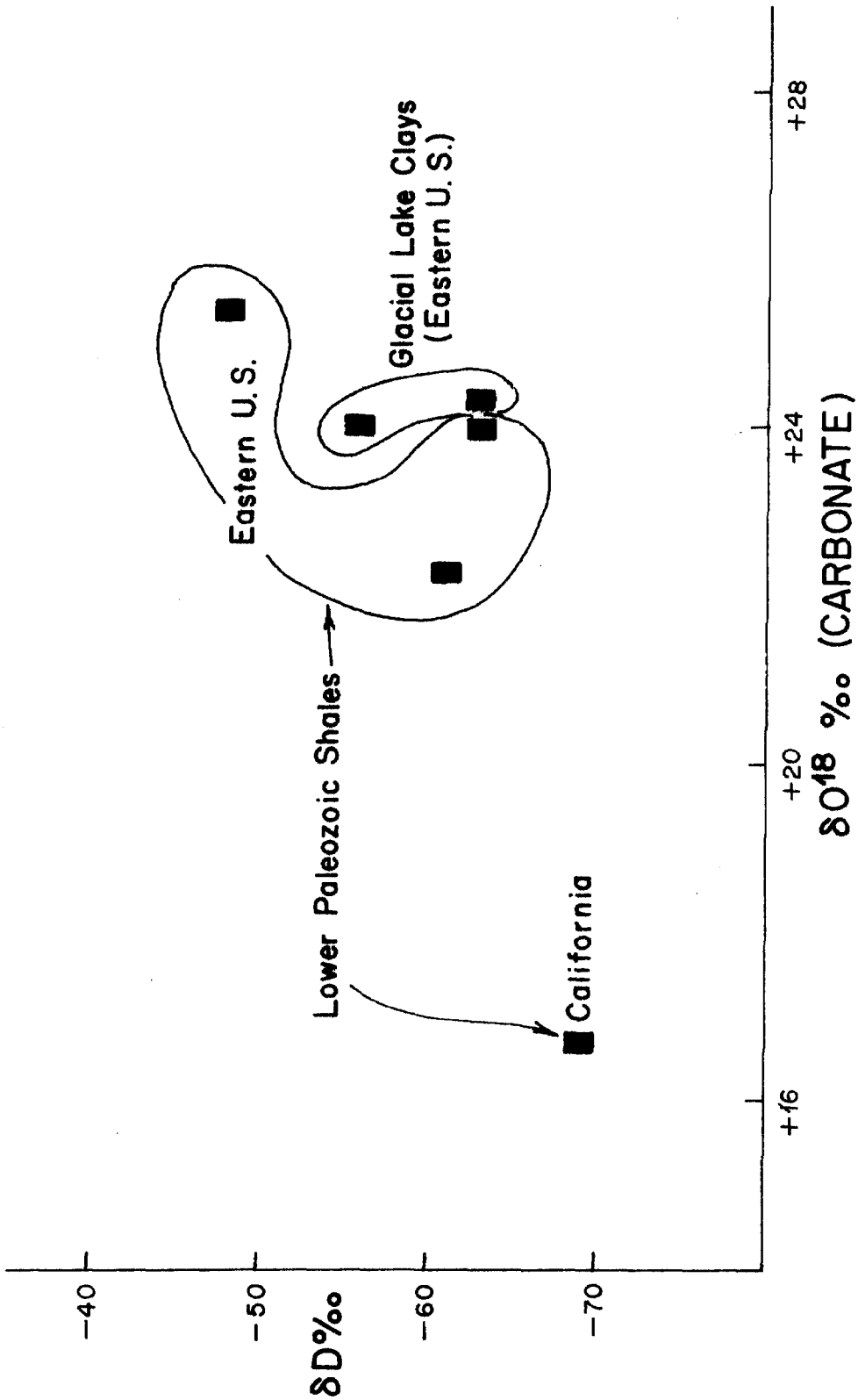
Eastern U.S.
Glacial Lake Clays
(Eastern U.S.)
Lower Paleozoic Shales
California
−40
−50
−60
−70
δD‰
+16
+20
+24
+28
δO18 ‰ (CARBONATE)

Figure 9-4

exposed to very light glacial melt waters ($\delta D = -70$ to $-150‰$) they do not appear to have suffered significant hydrogen isotopic exchange.

X. SUMMARY AND CONCLUSIONS

10.1 Mineral-H_2O fractionation factors for kaolinite, montmorillonite and gibbsite

The hydrogen and oxygen isotopic fraction factors for kaolinite-H_2O and montmorillonite-H_2O at sedimentary temperatures were estimated by Savin and Epstein (1970a) to be:

$$\alpha^{ox}_{\text{kaolinite-}H_2O} = 1.027 \qquad \alpha^{hy}_{\text{kaolinite-}H_2O} = 0.97$$

$$\alpha^{ox}_{\text{montmorillonite-}H_2O} = 1.027 \qquad \alpha^{hy}_{\text{montmorillonite-}H_2O} = 0.94$$

The hydrogen and oxygen isotopic fractionation factors between gibbsite [$Fe/(Fe + Al)$ = 5 - 25%] and water at Earth-surface temperatures have been estimated in this study to be:

$$\alpha^{ox}_{\text{gibbsite-}H_2O} = 1.018 \qquad \alpha^{hy}_{\text{gibbsite-}H_2O} = 0.984$$

Utilizing these fractionation factors, equations relating the δD and δO^{18} values of kaolinites, montmorillonites, and gibbsites may be determined. These equations plot as straight lines on a $\delta D - \delta O^{18}$ diagram, approximately parallel to Craig's (1961a) meteoric water line (see Figure 10-1).

δD and δO^{18} analyses of kaolinite-rich samples formed at Earth-surface temperatures from the Elberton, Georgia profile, many Quaternary soils, and many ancient kaolinite deposits all completely confirm the validity of Savin and Epstein's (1970a) kaolinite line and their estimation of isotopic fractionation factors for the

Figure 10-1. $\delta D - \delta O^{18}$ diagram showing Savin and Epstein's (1970a) kaolinite and montmorillonite lines and a gibbsite line estimated from data in this report. Also shown are two montmorillonite bands, one for Fe-rich oceanic montmorillonites formed at 0° to 5°C by submarine weathering processes and the other for Fe-poor montmorillonites formed at 15° to 30°C by subaerial weathering processes.

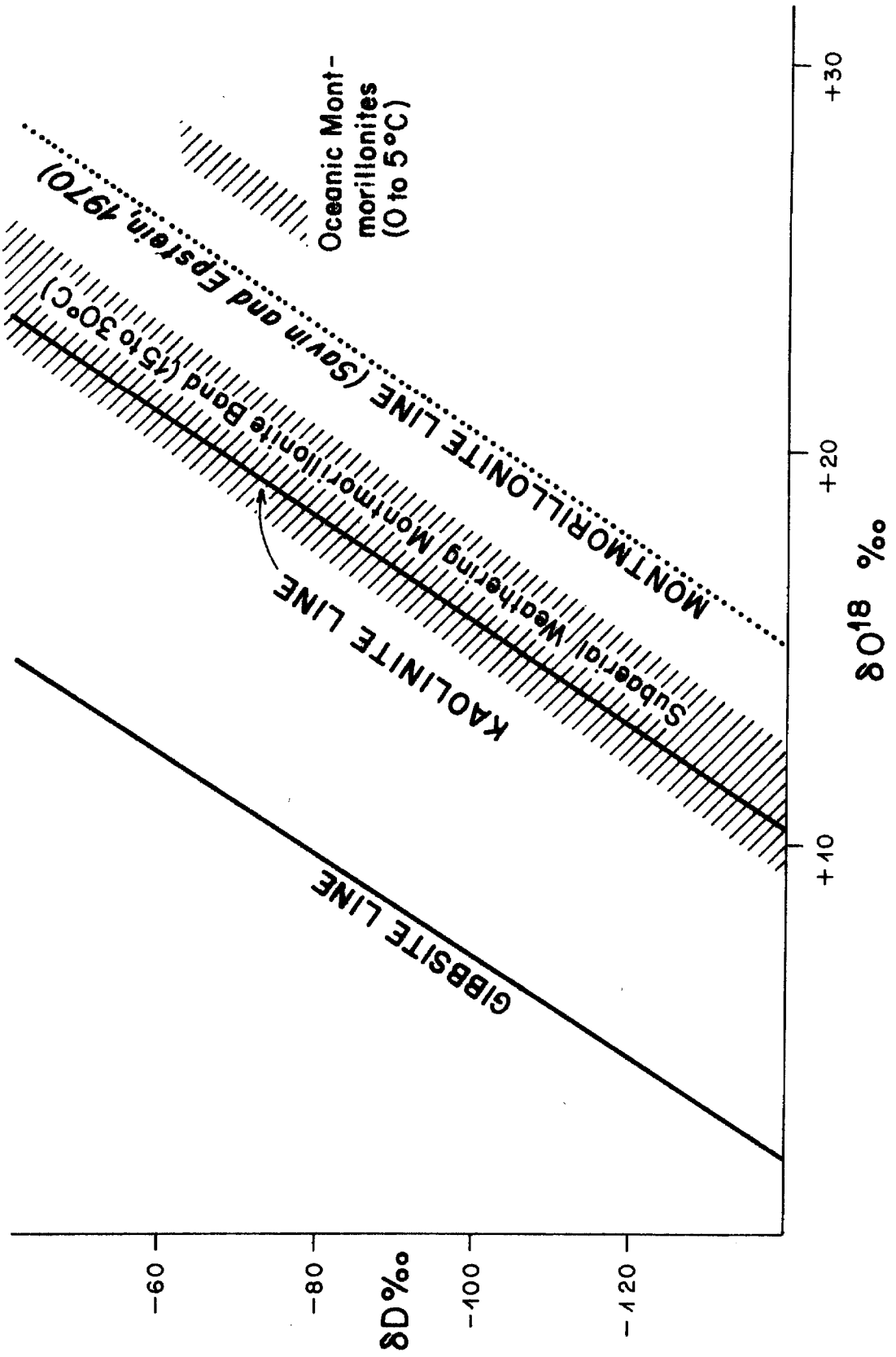
Oceanic Mont-
morillonites
(0 to 5°C)
MONTMORILLONITE LINE (Savin and Epstein 1970)
Subaerial Weathering Montmorillonite Band (15 to 30°C)
KAOLINITE LINE
GIBBSITE LINE
δD‰
−60
−80
−100
−120
δO18 ‰
+10
+20
+30

Figure 10-1

kaolinite-H_2O system at Earth-surface temperatures.

δD and δO^{18} analyses of a variety of montmorillonites in the present study indicate that the fractionation factors for the montmorillonite-H_2O system derived by Savin and Epstein (1970a) are not generally applicable to most montmorillonites. The isotopic data from montmorillonites display a much greater scatter than kaolinites, presumably as a result of (1) the greater range of chemical compositions of montmorillonites compared to kaolinites, (2) the greater range of the temperatures of formation of montmorillonites, and (3) the possibility that the D/H ratios determined for montmorillonite OH are contaminated during heating and outgassing procedures.

For the sake of illustration two montmorillonite "bands" are shown in Figure 10-1. The oceanic montmorillonite "band" is located using $\alpha^{ox}_{\text{montmorillonite-}H_2O} = 1.027$ and $\alpha^{hy}_{\text{montmorillonite-}H_2O} = 0.93$, and represents the positions of relatively Fe-rich montmorillonites (samples TW-1-50-F-M and Carr II-DR-9-L-M have 11 and 22 weight percent Fe_2O_3 respectively, M. Bass, personal communication) formed by submarine weathering of basalts at 0° to 5°C. The α's were selected on the basis of the observed isotopic values of these submarine montmorillonites and those of ocean water.

The subaerial weathering montmorillonite "band" is centered on a line having $\alpha^{ox}_{\text{montmorillonite-}H_2O} = 1.027$ and $\alpha^{hy}_{\text{montmorillonite-}H_2O} = 0.97$. The band represents the relatively Fe-poor montmorillonites (average of 3 to 4 weight percent Fe_2O_3 for the Big Sur montmorillonites) that are typically formed by the subaerial weathering of granitic rock types at 15° to 30°C in relatively dry climates. These α's were selected on the basis of (1) the observed isotopic values of montmorillonites and local meteoric waters from the Big Sur weathering profile

and (2) the observation that the isotopic data on most weathering montmorillonites are distributed in the vicinity of the kaolinite line.

Isotopic data on the Big Sur profile suggest that an increase in Fe-content lowers both $\alpha^{ox}_{montmorillonite-H_2O}$ and $\alpha^{hy}_{montmorillonite-H_2O}$. This chemical variation probably has a greater effect on $\alpha^{hy}_{montmorillonite-H_2O}$ than on $\alpha^{ox}_{montmorillonite-H_2O}$, because the hydroxyls are all bonded directly to the octahedrally coordinated cation while a majority of the oxygens are bonded to tetrahedrally coordinated Si or Al. Any shifting of the montmorillonite line with changes in Fe content will depend on the relative changes in the two α's taken together. A simultaneous decrease in both α's can lead to essentially no shift of the montmorillonite line, because the two effects tend to cancel one another.

Therefore, although the separation of the subaerial weathering montmorillonite and submarine weathering montmorillonite "bands" (see Figure 10-1) can probably in part be explained as a result of differences in Fe-content, the most important effect is the difference of 25° to 30° C in the temperature of formation of the two groups. Increasing temperature lowers $\alpha^{ox}_{montmorillonite-H_2O}$ and raises $\alpha^{hy}_{montmorillonite-H_2O}$; these two effects reinforce one another, as they produce a shift to the left and upward on a $\delta D - \delta O^{18}$ diagram. An increase in temperature from 0° to 30°C would be accompanied by a change from about 1.030 to 1.024 in $\alpha^{ox}_{montmorillonite-H_2O}$ and from about 0.95 to 0.96 in $\alpha^{hy}_{montmorillonite-H_2O}$ (see Figures 1-1 and 1-2). This is just about enough to produce the separation of the two montmorillonite "bands" shown on Figure 10-1. Note that even though the separation of the two "bands" is ascribed essentially to a temperature effect, the two "bands" were constructed for a low

temperature, high Fe montmorillonite and a "high" temperature, low Fe montmorillonite both having an identical $\alpha^{ox}_{\text{montmorillonite-}H_2O}$ of 1.027 (because of the cancelling effects of temperature and Fe content on this α).

Bentonites probably are formed over a range of temperatures from 0° to 40° C because the alteration may take place from the time of ash deposition in an ocean or lake up to and including the time of burial and diagenesis. The Fe contents of bentonites are quite variable (Grim, 1968) but are similar to those of the Big Sur weathering montmorillonites.

Future determinations of the hydrogen and oxygen isotopic fractionation factors for the beidellite-H_2O (Al end member), nontronite-H_2O (Fe end member) and saponite-H_2O (Mg end member) will be necessary to accurately fix the positions of the several "montmorillonite" lines. The montmorillonite line of Savin and Epstein (1970a) probably should be discarded, as it does not really apply to any of the important montmorillonite occurrences in nature. It is useful only in that it represents a rough compromise between the isotopic values of oceanic and continental montmorillonites.

The hydrogen and oxygen isotopic fractionation factors for the gibbsite-H_2O system were estimated by isotopic studies of Quaternary soils containing Fe-rich gibbsites and amorphous Al-Si-Fe hydroxides (see Figure 10-1). Note that the $\alpha^{hy}_{\text{gibbsite-}H_2O}$ is higher than $\alpha^{hy}_{\text{kaolinite-}H_2O}$, even though both fractionation factors basically involve hydroxyl-water fractionations and the hydroxyls in both cases are bonded to aluminum ions. This implies that one cannot simply assign fractionation factors to hydroxyl-water independent of the mineral type involved. It is very likely that the major difference between gibbsite and kaolinite is brought about by differences in the degree of hydrogen bonding between the layers.

Gibbsite layers are much more strongly hydrogen bonded than kaolinite layers (Bragg et al., 1965, pp. 117 and 277). It is reasonable to expect that hydrogen bonding could have an effect on hydrogen isotopic fractionation factors inasmuch as noticeable shifts in infrared absorption spectra are produced by changes in hydrogen bonding (Nakamoto, 1963, p. 81).

Systematic variations of $\alpha^{ox}_{\text{montmorillonite-}H_2O}$ and $\alpha^{hy}_{\text{montmorillonite-}H_2O}$ with variations in the Fe/Al ratio in montmorillonites from the Big Sur weathering profile suggest that $\alpha^{ox}_{\text{Fe-hydroxide-}H_2O} < \alpha^{ox}_{\text{Al-hydroxide-}H_2O}$ and that $\alpha^{hy}_{\text{Fe-hydroxide-}H_2O} < \alpha^{hy}_{\text{Al-hydroxide-}H_2O}$. However, the gibbsites did not exhibit any systematic isotopic variations as a function of changes in the Fe/Al ratio. This may be the result of the fact that an increase in Fe/Al would tend to decrease $\alpha^{ox}_{\text{Fe-Al-hydroxide-}H_2O}$ and shift the gibbsite line to the left, but it could also decrease $\alpha^{hy}_{\text{Fe-Al-hydroxide-}H_2O}$ and shift the gibbsite line down, thus producing a partially cancelling effect.

10.2 Preservation of the hydrogen and oxygen isotopic compositions of clay minerals

In laboratory experiments, minerals which do not contain interlayer water (e.g., kaolinite) do not show any tendency to undergo significant hydrogen or oxygen isotopic exchange with water at room temperature. Clay minerals containing interlayer water that is not in direct contact with mineral hydroxyl (e.g., montmorillonite) also do not show significant hydrogen or oxygen isotopic exchange with water at room temperature. However, procedures used to remove this interlayer water can cause hydrogen contamination of the mineral hydroxyl. Clay minerals which contain interlayer water in direct contact with mineral hydroxyl (e.g.,

halloysite) do undergo rapid hydrogen isotopic exchange at room temperature. Data on natural halloysites in the present study completely confirms that halloysite does not preserve its δD values at Earth-surface temperatures. It is also likely that the hydroxyl oxygen is also easily exchanged.

At temperatures of 100° to 200°C, it may be inferred that the rates of hydrogen and oxygen isotopic exchange with water become important for all clay minerals. Isotopic data on montmorillonites and, in particular, kaolinites are of use in geologic studies, but in the case of halloysites, these are probably of limited use.

Because laboratory experiments cannot in general indicate to what degree isotopic exchange between clay minerals and water occurs over very long periods of time, isotopic data on natural samples in conjunction with geologic information must be used to evaluate the problem of isotopic exchange over geologic time periods. The following statements argue in favor of isotopic preservation of various clay minerals:

(1) Detailed isotopic studies on three different Quaternary soils developed on Cretaceous shales have shown that the montmorillonite and illite in the shale have not undergone significant hydrogen or oxygen isotopic exchange with large quantities of rainwater that must have percolated through these soils over periods of at least several hundred years.

(2) Isotopic studies on Pleistocene glacial lake clays indicate that illite and chlorite do not undergo hydrogen isotopic exchange even under conditions of intimate contact (glacial scouring and erosion) with waters that must have been very deficient in deuterium.

(3) The δD and δO^{18} values of ancient kaolinite deposits from the northern Rocky Mountains are distinctly higher than those of clay-rich Quaternary soils from the same region.

(4) Two Jurassic kaolinites analyzed by Sheppard et al. (1969), one from British Columbia and the other from Alaska, have $\delta D = -80$ and $-78‰$ respectively; these clays certainly have not exchanged appreciably with present-day meteoric waters.

(5) The δD and δO^{18} values of ancient bentonites from the northern Rocky Mountains are higher than those of montmorillonite-rich Quaternary soils from the same geographic region.

(6) The hydrogen isotopic values of Precambrian and Lower Paleozoic shales from the northern Rocky Mountains are higher than those of Cretaceous shales from the same region, which are in turn higher than those of Quaternary soils from this area.

(7) The hydrogen isotopic values of Lower Paleozoic shales from the eastern United States are identical to those of Lower Paleozoic and Precambrian shales from British Columbia and Montana, thus showing no correlation with the δD values of present-day meteoric waters.

(8) Although the δO^{18} values of the carbonate fraction of some Lower Paleozoic shales are so light that they almost certainly have exchange with meteoric water, no such lowering is observed for the δD of the clay minerals in the shales.

To sum up, all the ancient samples discussed above display δD and/or δO^{18} values which are much too high to be in equilibrium with present-day or Pleistocene meteoric waters (or in some cases, even with Tertiary meteoric waters). These observations suggest that many types of clay minerals found in a variety of

rock types appear to have preserved isotopic values over very long periods of time. The preservation of isotopic values in shales may be related to the fact that they are somewhat impermeable and thus less susceptible to isotopic exchanges.

In a few instances, ancient kaolinites, particularly the Lower Cretaceous kaolinites from the Rocky Mountains and a Miocene kaolinite from a fault zone in Vermont appear to have undergone some D/H exchange with isotopically light meteoric waters, while undergoing a lesser or negligible degree of oxygen isotopic exchange. This is suggested by the fact that the isotopic values plot on the low D/H, high O^{18}/O^{16} side of Savin and Epstein's (1970a) kaolinite line.

These kaolinites occur in lenses or as the matrix in permeable sandstones, in sandy shales, or in one case in a fault zone. It is reasonable that they might have exchanged with very large amounts of water over long periods of time. Perhaps higher temperatures prevailed during burial to promote exchange. Also, if the waters had a low pH, one might expect more exchange than normal even at low temperatures (see Sheppard et al., 1969, p.767).

The original D/H ratio of the above kaolinites can be estimated on the basis of two possible models: (1) hydrogen isotopic exchange without accompanying oxygen isotopic exchange or (2) hydrogen isotopic exchange and oxygen isotopic exchange of only the hydroxyl oxygens. Both models would imply a shift below the kaolinite line, and such models suggest that the original δ D values of the Cretaceous kaolinites from the Rocky Mountains would have been about -80 to -95 ‰ and the original δ D values of the kaolinite from Vermont would be about -60 to -70‰ . These corrected values are much more like the δD values of other Cretaceous and Miocene kaolinites from other locations in the United States. They also are more compatible with the warmer climates that probably existed in

the Lower Cretaceous and the Miocene.

The Tertiary halloysites from the Spokane, Washington profile have distinctly higher D/H ratios than nearby kaolinites of the same age. Most of the Quaternary halloysites from western Oregon have distinctly higher D/H ratios than those of Quaternary kaolinites from the same region.

These observations may cast some doubt on the usefulness of the isotopic data obtained by Savin and Epstein (1970a) and Sheppard et al. (1969) on halloysites. The one halloysite which Savin and Epstein (1970a) analyzed had a $\delta D = -60‰$ and a $\delta O^{18} = +22.0‰$; these values place it on the kaolinite line, as if it were a preserved equilibrium value. However, this might be coincidence, inasmuch as a halloysite in equilibrium with Pasadena water vapor has a $\delta D = -80‰$, assuming $\alpha^{hy}_{halloysite\text{-}H_2O} = 0.970$, partial isotopic exchange with Pasadena water vapor might not produce a noticeable change in its δD value.

Because not all the hydroxyl hydrogen in halloysites is in contact with interlayer water, partial preservation of D/H ratios may be possible. We may also note that the δD values of the halloysites of Sheppard et al., (1969) range from -80 to $-110‰$, again only slightly displaced from a $\delta D = -80‰$ for halloysite in equilibrium with Pasadena water vapor. It is suggested here that unless it can be shown that a particular halloysite definitely preserves its δD values (i.e., because it is perhaps well crystallized), there is no point in measuring the hydrogen isotope ratios of natural halloysites.

10.3 Isotopic evidence for climatic conditions during the Tertiary

Ancient kaolinites, in particular those of Tertiary age, have isotopic values that suggest they formed approximately in equilibrium with ancient meteoric

waters (i.e., they lie on the kaolinite line). This allows us to calculate the isotopic compositions of these ancient meteoric waters. Using the δD values of kaolinites of Tertiary ages from many locations in the United States, and a $\alpha^{hy}_{kaolinite\text{-}H_2O}$ of 0.970, an approximate contour map of the δD values of mid- and early-Tertiary meteoric waters was constructed for the United States (see Figure 7-6). The distribution of δD values for these Tertiary meteoric waters is similar to the present-day distribution except that the contrast in δD values between coastal and high inland regions is less extreme. This indicates that the general topography in the United States during the Tertiary was essentially similar to that of the present except that elevations were perhaps lower and some mountain barriers were probably less prominent. Also the climatic differences between coastal and inland regions were probably less extreme.

One area of particular interest is the Washington-Oregon-Idaho area. The Mid- to Upper-Miocene kaolinites of this area show a progressive change in δD from -65 to -125‰ in going inland from the coast. This corresponds to a change in the δD of meteoric water from about -35 to -95‰, compared with the present range of -50 to -130‰.

Although kaolinite is forming in abundance in western Oregon and Washington today, apparently little or no kaolinite is forming in eastern Washington and northern Idaho. This is a result of the low amount of rainfall and extreme range of climatic conditions that now exists in eastern Washington and northern Idaho. The abundance of Miocene kaolinites in eastern Washington and northern Idaho therefore indicate that the amount of rainfall in this area during the Miocene must have been much greater than today, perhaps suggesting the absence of the Cascades as a major topographic barrier to Pacific storms. The range of -75 to

-95‰ for δD suggested for the Miocene meteoric waters of eastern Washington and northern Idaho could indicate a cool temperate climate in an area of moderate elevation, assuming that the distance from the Pacific coast is similar to that of the present-day. The absence of the High Cascade Range during the Miocene might be sufficient to allow such climatic conditions.

Axelrod (1964) studied the remains of Mid-Miocene Trapper Creek flora in the Idavada volcanics of southern Idaho. The following statements of Axelrod (1964) indicate that the isotopic and paleobotanical data are in excellent agreement. "The fossil plants resemble trees and shrubs that contribute to living conifer-hardwood forests in the humid cool temperate parts of western North America, eastern North America and northeast Asia." Also he said that "The climate was cool temperate. Precipitation was about 45-50 inches yearly, well distributed seasonally, and snow was rare. Temperatures were moderately warm in summer and cool in winter." In addition he said " The altitude of the Trapper Creek flora is calculated at approximately 3000 feet."

Another area of particular interest is the southern United States. The Lower Eocene kaolinites in the Wilcox formation have $\delta D = -55$ to $-60‰$ almost indistinguishable from the $\delta D = -58$ to $-63‰$ of kaolinites from Quaternary soils in this region. These isotopic data suggest that the climate during the Lower Eocene was very similar to, or perhaps slightly warmer than today's climate. A detailed paleobotanical study by Berry (1924) of Early Tertiary flora suggests that the Lower Eocene climate was warm temperate to subtropical, the same as the present-day climate in good agreement with the isotopic data.

A third area of interest is the Arizona and New Mexico area. Mid-Tertiary supergene kaolinites and montmorillonites in this region have $\delta D = -62$ to

-80‰ (Silver Bell deposit, Table 4-1; Sheppard et al., 1969), suggesting that the δD values of meteoric waters were -30 to -50‰, somewhat heavier than today's waters. The water table during the Mid-Tertiary is known to have been much higher than the present one (Livingston et al., 1968) suggesting a much wetter and therefore perhaps more temperate climate. Heavier δD values for the meteoric waters of the Mid-Tertiary are compatible with a moist temperate climate, perhaps intermediate between the cool-temperate climate of the Pacific Northwest during the Miocene and the warm-temperate to subtropical climate of southern United States during the Lower Eocene.

10.4 Isotopic criteria for distinguishing clay minerals of different origins

On the basis of hydrogen and oxygen isotopic data alone, a variety of clay minerals of different origins may be distinguished from one another.

Hypogene clay minerals: On a $\delta D - \delta O^{18}$ graph hypogene kaolinites and montmorillonites (Sheppard et al., 1969) plot closer to the meteoric water line than all other clay minerals known at the present time. This is mainly a result of their higher-temperature origin. Some clay minerals in soils buried and heated by lava flow also plot well to the left of the kaolinite line.

Clay minerals formed by subaerial weathering processes: On a $\delta D - \delta O^{18}$ diagram, kaolinites and montmorillonites formed by weathering processes plot in the vicinity of the kaolinite line. In particular pure kaolinites plot almost exactly on this line. Isotopically these materials cannot be distinguished from supergene clay minerals.

Hydroxides formed by weathering processes: Aluminum and iron hydroxides formed by subaerial weathering processes have isotopic values which plot in the vicinity of the gibbsite line. Although none have been analyzed as yet, submarine gibbsites and Fe-hydroxides might be expected to plot to the right of the gibbsite line, whereas those of hydrothermal origin would plot to the left.

Montmorillonites formed by submarine weathering processes: Montmorillonites formed by submarine weathering processes have a limited range of isotopic values, and their δO^{18} values are heavier than those of all other clay minerals.

Bentonites: Bentonites have isotopic values which overlap those of montmorillonites formed by weathering processes. Therefore, from a purely isotopic point of view they are indistinguishable from such clays. However, bentonites of a marine origin have heavier δD and δO^{18} values than those of nonmarine or brackish-water origin.

Illites: Illites have isotopic values which generally plot on the low δO^{18} - high δD side of the kaolinite line. This is in agreement with geologic data which suggest a diagenetic origin for most illites, as burial and diagenesis generally occur at temperatures somewhat higher than those prevailing at the Earth's surface.

Ocean sediments: The new data in the present study essentially confirm the interpretation of Savin and Epstein (1970b) regarding the origin of the clay minerals in ocean sediments.

(kaolinites) The δD and δO^{18} values calculated by Savin and Epstein (1970b) for kaolinites in ocean sediments are compatible with an origin

by tropical subaerial weathering processes.

(montmorillonites) The δD and δO^{18} values calculated by Savin and Epstein (1970b) for the montmorillonites in ocean sediments are similar to those of average continental bentonites or bentonite shales, or to those of average montmorillonites formed by subaerial weathering processes. In a few specific cases the δD and δO^{18} values of certain ocean sediments very rich in montmorillonite are compatible with an origin by submarine weathering processes.

(illites) The δD and δO^{18} values calculated by Savin and Epstein (1970b) for the illites in ocean sediments are similar to those of illites in shales. Thus, almost all the clay minerals in oceanic sediments have isotopic compositions compatible with their derivation from subaerial weathering and erosion of continental materials.

BIBLIOGRAPHY

Axelrod, D. J., The Miocene Trapper Creek flora of southern Idaho, Calif. Univ. Publ. Geol. Sci. 51, 148 p., 1964 .

Banks, H.H. and W.G. Melson, Saponite from the Mid Atlantic Ridge, Lat. 22°N (abstract), Geol. Soc. Amer. Spec. Paper 101, p. 9-10, 1966 .

Berry, E.W., The middle and upper Eocene floras of southeastern North America, U.S.G.S. Prof. Paper, 92, 206 p., 1924 .

Bragg, S.L., G.F. Claringbull and W.H. Taylor, Crystal Structure of Minerals, Cornell University Press, Ithaca, New York, 1965 .

Bramlette, M.N., Geology of the Arkansas bauxite region, Ark. Geol. Sur. Info. Circ., 8, 68 p., 1936.

Brosgé, W.P. and C. L. Whittington, Geology of the Umiat-Maybe Creek region, Alaska, U.S.G.S. Prof. Paper, 303H, p. 534, 1966.

Burt, F.A., The origin of the Bennington kaolins, Rep. of the Vermont St. Geol., 16, p. 65-84, 1927-8 .

Clayton, R. N., I Friedman, D.L. Graf, T.K. Mayeda, W.F. Meents and N. F. Shimp, The Origin of saline formation waters, 1, isotopic composition, J. of Geophys. Res., 71, p. 3869-3882, 1966.

Clayton, R.N. and T. D. Mayeda, The use of bromine pentafluoride in the extraction of oxygen from oxides and silicates for isotopic analysis, Geochim. et Cosmochim. Acta, 27, p. 43, 1963.

Clayton, R.N., J.R. O'Neil, T.D. Mayeda, unpublished data, 1967.

Craig, H., Isotopic standards for carbon and oxygen and correction factors for mass spectrometric analysis of carbon dioxide, Geochim. et Cosmochim. Acta, 12, p. 133 (1957).

Craig, H., Isotopic variations in meteoric waters, Science, 133, p. 1702-1703, 1961a.

Craig, H., Standard for reporting concentrations of deuterium and oxygen-18 in natural waters, Science, 133, p. 1833-1844, 1961b.

Daugherty, L.H., The upper Triassic flora of Arizona, Carnegie Inst. Wash. Public. 526, p. 1-108, 1941.

Emiliani, C., T. D. Mayeda, Oxygen isotopic analysis of some molluscon shells from fossil littoral deposits of Pleistocene age, Amer. Jour. Sci., 262, p. 107-113, 1964.

Epstein, S., The variations of the O^{18}/O^{16} ratio in nature and geologic implications, Researches in Geochemistry, John Wiley and Sons, New York, 1959.

Epstein, S., Variations of the O^{18}/O^{16} of fresh waters and ice, Nat. Acad. Sci, Nat. Res. Council Publ. 400, p. 20-28, 1956.

Epstein, S. and T. Mayeda, Variations in the O^{18} content of water from natural sources, Geochim. et Cosmo. Acta 4, p. 213-224, 1953.

Epstein, S. and H.P. Taylor, Variation of O^{18}/O^{16} in minerals and rocks, Researches in Geochemistry, John Wiley and Sons, New York, 1967.

Feth, J.H., C.E. Roberson and W.L. Polzer, Sources of mineral constituents in water from granitic rocks, Sierra Nevada, California and Nevada, U.S.G.S. Water Supply Paper, 1535-I, 170 p., 1964.

Fisher, C.A., Clays in the Kootenai formation near Belt, Montana, U.S.G.S. Bull., 340, p. 418, 1908.

Friedman, I., Deuterium content of natural waters and other substances, Geochim. et Cosmochim. Acta, 4, p. 89-103, 1953.

Friedman, I., The variation of the deuterium content of natural waters in the hydrologic cycle, Reviews of Geophysics, 2, p. 177-224, 1964.

Garlick, D., Oxygen isotope ratios in coexisting minerals of regionally metamorphosed rock, Ph.D. thesis, Calif. Inst. of Tech., 1964 .

Garlick, D., The stable isotopes of oxygen, Handbook of Geochemistry, Springer-Verlag, New York, 1969.

Garrels, R.M. and C. L. Christ, Solutions, Minerals and Equilibria , Harper and Row, New York, 1965.

Gill, J.R. and W. A. Cobban, The Red Bird section of the upper Cretaceous Pierre shale in Wyoming, U.S.G.S. Prof. Paper, 393-A, 1966.

Glover, S.L., Clays and shales of Washington, Wash. Geol. Surv. Bull., 24, p. 208-213, 1941.

Grim, R.E., Clay Mineralogy, McGraw-Hill, New York, 1968 .

Halevy, E., The exchangeability of hydroxyl groups in kaolinite, Geochim. et Cosmochim. Acta, 28, p. 1139-1145, (1964).

Herald, P. G. and G.R. Heyl, Kaolin deposits of south Pike county, Arkansas, Ark. Geol. Surv. Bull, 7, 1942.

Hess, P., Phase equilibria of some minerals in the K_2O-Na_2O-Al_2O_3-SiO_2-H_2O system at 25° C and 1 atmosphere, Amer. Jour. Sci., 264, p. 289-309, 1966.

Hosterman, J.W., Clay deposits of Spokane county, Washington, U.S.G.S. Bull., 1270, 96p., 1969 .

Hosterman, J.W., Geology of the clay deposits in parts of Washington and Idaho, Clays and Clay Minerals, Proc. of 7th Nat. Conf., Pergamon Press, New York, p. 285-292, 1961.

Huntting, M.T., Perlite and other volcanic glass occurrences in Washington, St. of Wash., Report of Invest., 17, 1949.

Kerr, P.F. and J.L. Kulp, Reference clay localities--United States, API. Project 49, Prelim. Rept. No.2, 1949.

Kirshenbaum, I., Physical Properties and Analysis of Heavy Water, McGraw-Hill, New York, 438 p., 1951.

Ledoux, R.L. and J.L. White, Infrared studies of OH groups in expanded kaolinite, Science, 143, p. 244, 1964a.

Ledoux, R.L. and J.L. White, Infrared studies of selected deuteration of kaolinite and halloysite at room temperature, Science, 145, p. 47, 1964b.

Livingston, D.E., R.L. Mauger and P.E. Doman, Geochronology of the emplacement, enrichment, and preservation of Arizona porphyry copper deposits, Econ. Geol. 63, p. 30-36, 1968.

Longwell, C.R., H.D. Miser, R.C. Moore, K. Bryan and S. Paige, Rock formations in the Colorado Plateau of southeastern Utah and northern Arizona, U.S.G.S. Prof. Paper, 132, p. 1-23, 1923-1924.

McAuliffe, C.D., M.S. Hall, L.A. Dean and S. B. Hendricks, Exchange reactions between phosphates and soils, Soil Sci. Soc. Proc., 12, p. 119-123, 1947.

McCrea, J.M., The isotopic chemistry of carbonates and a paleotemperature scale, J. Chem. Phys., 18, p. 849-857, 1950.

McKinney, C.R., J.M. McCrea, S. Epstein, H. A. Allen and H.C. Urey, Improvements in mass spectrometers for the measurement of small differences in isotopic abundance ratios, Rev. Sci. Inst., 21, p. 724-730, 1950.

McQueen, H.S., Geology of the fire clay districts of east central Missouri, Missouri Geol. Surv. and Water Resources, 28, 244 p., 1943.

Nakamoto, K., Infrared Spectra of Inorganic and Coordination Compounds, John Wiley, New York, p. 71-140, 1963.

Nier, A.O., A mass spectrometer for isotope and gas analysis, Rev. Sci. Instr., 18, p. 398-411, 1947.

O'Neil, J.R., R.N. Clayton, T.K. Mayeda, Oxygen isotope fractionation in divalent metal carbonates, Jour. Chem. Phys., 51, p. 5547-5558, 1969.

O'Neil, J.R. and H.P. Taylor, Jr., Oxygen isotope fractionation between muscovite and water, (abstract), Jour. Geophys. Res., 74, p. 6012-6022, 1969.

O'Neil, J.R. and H.P. Taylor, Jr., The oxygen isotope and cation exchange chemistry of feldspars, Amer. Mineralogist, 52, p. 1414-1437, 1967.

Pliler, R. and J.A.S. Adams, The distribution of thorium, uranium, and potassium in a Pennsylvanian weathering profile, Geochim. et Cosmochim. Acta, 26, p. 1137-1146, 1962.

Plummer, F.B., H.B. Bradley, F.K. Pence, Clay deposits of the Cisco group of north-central Texas, Univ. of Texas Public., 4915, p. 13-20, 1949.

Reeside, J.B., Paleoecology of the Cretaceous seas of the western interior of the United States, Geol. Soc. Amer. Mem., 67 (2), p. 505-542, 1957.

Ries, H., H. B. Kümmel, G.N. Knapp, The clays and clay industry, Geol. Sur. of New Jersey, Final Report of the St. Geol., 6, p. 174-7, 1904.

Rex, R.W., J. K. Syers, M.L. Jackson and R.N. Clayton, Aeolian origin of quartz in soils of Hawaiian Islands and in Pacific pelagic sediments, Science, 163, p. 277-279, 1969.

Romp, L.A., The exchange of hydrogen by deuterium in hydroxyls of kaolinite, Jour. Phys. Chem., 60, p. 987-988, 1956.

Roy, D.M. and R. Roy, Hydrogen-deuterium exchange in clays and problems in the assignment of infrared frequencies in the hydroxyl region, Geochim et Cosmochim. Acta 11, p. 72-85, 1957.

Savin, S.M., Oxygen and hydrogen isotope ratios in sedimentary rocks and minerals, Ph.D. Thesis, Calif. Inst. of Tech., 1967.

Savin, S.M. and S. Epstein, The oxygen and hydrogen isotope geochemistry of clay minerals, Geochim. et Cosmochim. Acta, 34, p. 25-42, 1970a.

Savin, S.M. and S. Epstein, The oxygen and hydrogen isotope geochemistry of ocean sediments and shales, Geochim. et Cosmochim. Acta, 34, p. 43-63, 1970b.

Sever, C.W., Geology and ground water resources of crystalline rocks, Dawson Co., Georgia, Geor. Geol. Surv. Info. Circ., 30, 1964.

Sharp, R.P., Ep-Archean and Ep-Algakion erosion surfaces, Grand Canyon, Arizona, Geol. Soc. Am. Bull., 51, p. 1235-1269, 1940.

Sheppard, S.M.F., R.L. Nielsen, H.P. Taylor, Jr., Oxygen and hydrogen isotope ratios of clay minerals from porphyry copper deposits, Econ. Geol., 64, p. 755-777, 1969.

Sheppard, S.M.F. and H.P. Taylor, Jr., Hydrogen isotope exchange and equilibrium studies in the kaolinite-water system, manuscript in preparation, 1970.

Skeels, F.H., The clays of Idaho, St. of Idaho, Bur. of Mines and Geol. Bull., 2, 74 p., 1920.

Stengel, H.B. and F.K. Pence, Characteristics of Texas ball clay near Troup, Univ. of Texas Public., 5019, 51 p., 1950.

Taylor, H.P., Jr., The oxygen isotope geochemistry of igneous rocks, Contrib. Mineral. and Petrol., 19, p. 1-71 (1968).

Taylor, H.P., Jr. and S. Epstein, Oxygen isotope analyses of tektites, soils, and impact glasses, in Isotopic and Cosmic Chemistry, Craig, Miller and Wasserburg, eds., North-Holland Publ. Co., Amsterdam, p. 181-199, 1964.

Taylor, H.P., Jr. and S. Epstein, Relationship between O^{18}/O^{16} ratios in coexisting minerals of igneous and metamorphic rocks, Part I, Principles and experimental results, Bull. Geol. Soc. Amer., 73, p. 461-480, 1962.

Taylor, H.P., Jr. and S. Epstein, Relationship between O^{18}/O^{16} ratios in coexisting minerals of igneous and metamorphic rocks, Part II, Application to petrological problems, Bull. Geol. Soc. Amer., 73, p. 675-693, 1962.

Tourtelot, H.A., Preliminary investigation of the geologic setting and chemical composition of the Pierre shale, Great Plains Region, U.S.G.S. Prof. Paper, 390, 74 p., 1962.

Urey, H.C., The thermodynamic properties of isotopic substances, Jour. Chem. Soc., p. 562-581, 1947.

Waagé, K.M., Refractory clays of south-central Colorado, U.S.G.S. Bull., 993, 101 p., 1953.

Warshaw, C.M. and R. Roy, Classification and a scheme for the identification of layer silicates, Geol. Soc. Amer. Bull., 72, p. 1455-1492, 1961.

Williams, N.F. and Plummer, N., Clay resources of the Wilcox group in Arkansas, St. of Ark., Div. of Geol., Info. Circ., 15, 98 p., 1951.

Wilson, H. and R. C. Treasher, Refractory clays of western Oregon, Ore. Dept. of Geol. and Mineral Res. Bull., 6, 95 p., 1938.

APPENDIX I

ABBREVIATIONS TO APPENDIX I

Sample Collections:

R.P.S.	-	collected by Robert P. Sharp
H.P.T.	-	collected by Hugh P. Taylor
M.N.B.	-	supplied by Manuel N. Bass
M.S.	-	collected by Michael Stephens
R.E.C.	-	collected by Roy E. Cameron
L.T.S.	-	collected by Leon T. Silver

Sample No. Code (Locations):

States or Countries

Anta	-	Antarctica	N.J.	-	New Jersey
Ariz	-	Arizona	N.M.	-	New Mexico
Ark	-	Arkansas	N.Y.	-	New York
Cal	-	California	N.C.	-	North Carolina
Col	-	Colorado	Ohio	-	Ohio
Conn	-	Connecticut	Okl	-	Oklahoma
Ga	-	Georgia	Ore	-	Oregon
Haw	-	Hawaii	S.C.	-	South Carolina
Ind	-	Indiana	S.D.	-	South Dakota
Ida	-	Idaho	Tex	-	Texas
Mis	-	Missouri	Wash	-	Washington
Mon	-	Montana	Can	-	Canada
Nica	-	Nicaragua			

Counties, Provinces and Quadrangles

Aik	-	Aiken	Coco	-	Coconino
Bak	-	Baker	Colf	-	Colfax
B.C.	-	British Columbia, Province	Com	-	Comanche
			D.K.	-	DeKalb
Benn	-	Bennington	Eas	-	Eastland
Ben	-	Benton	Elb	-	Elbert
Boi	-	Boise	Fer	-	Fergus
But	-	Butte	Fra	-	Franklin
Cal	-	Callaway	Gas	-	Gasconade
Cas	-	Cascade	Gra	-	Grant
Che	-	Cherokee	Gre	-	Greer
Chel	-	Chelan	Ham	-	Hamilton
Cla	-	Clackamus	H.R.	-	Hood River
Cle	-	Clearwater	H.S.	-	Hot Spring
Clev	-	Cleveland	Hue	-	Huerfano

Ida	-	Idaho	Pie	-	Pierce
Inyo	-	Inyo	Pike	-	Pike
Jef	-	Jefferson	Pue	-	Pueblo
Kla	-	Klamath	Pul	-	Pulaski
L.A.	-	Los Angeles	R.I.	-	Ross Island, Quadrangle
L.a.C.	-	Lewis and Clark	Rock	-	Rockland
Lak	-	Lake	Sal	-	Saline
Lan	-	Lane	S.B.	-	Santa Barbara
Lat	-	Latah	S.C.	-	Santa Cruz
Lit	-	Litchfield	S.D.	-	San Diego
Liv	-	Livingstone	She	-	Shelby
Lla	-	Llano	S.L.O.	-	San Luis Obispo
Mad	-	Madison	Spo	-	Spokane
Mar	-	Marin	Stan	-	Stanley
Mari	-	Marion	Ste	-	Stephens
Mid	-	Middlesex	T.C.	-	Taylor Glacier, Quadrangle
Min	-	Mineral	Til	-	Tillamook
Mis	-	Missoula	Tul	-	Tulare
Mon	-	Monterey	Was	-	Wasco
Monr	-	Monroe	Wash	-	Washington
Mul	-	Mulnomar	Wes	-	Weston
Nio	-	Niobrara	Yam	-	Yamhill
N.P.	-	Nez Perce	You	-	Young
Park	-	Park			

APPENDIX I

SAMPLE LOCATIONS AND DESCRIPTIONS

Detailed Profiles

Mon-Cal-1 : roadcut, C of NE1/4, sec. 5, T18S, R1E, about 6 mi. N of Pt. Sur, elev. ~800 ft. (section 5.3)

Jef-Col-1 : from open pit mine 3.2 mi. S of Marshall on Colorado Rt. 93, elev. ~ 6000 ft. (section 5.5)

Elb-Ga-1 : New Comolli Quarry, end of a dirt road 0.4 mi. S of j'n of Ga. Rt. 17 and Ga. Rt. 72, NE of Elberton, Ga. (L.T.S.)

Fer-Mon-1 : roadcut, NW1/4 sec. 31, T18N, R19E. (section 5.5)(H. Tourtelot)

Mis-Mon-4 : W side of US Rt. 12, SE1/4 NW1/4 sec. 26, T12N R20W. (section 5.6) (H. P. T.)

Stan-S.D.-1 : spillway excavation, NE1/4 sec. 31, T6N, R30E. (section 5.5) (H. Tourtelot)

Spo-Wash-5 : roadcut at Mica Creek, SW1/4 SW1/4 SW1/4 sec. 3, T23N, R45E. (section 5.4) (J.W. Hosterman)

Quaternary Soils and Weathered Zones

Coco-Ariz-2 : E side of interstate 17 at Mundo Park exit, 18 mi. S. of Flagstaff; elev. 6300 ft.; alteration of a Tertiary vesicular basaltic flow to a red-brown clay sampled about 15 ft. below the ground surface.

Coco-Ariz-3 : S. side of Arizona Rt. 180, 21.7 miles NW of j'n of 180 and U.S.66; elev. ~ 8000 ft. ; red-brown clay alteration along a joint in a Quaternary basalt flow.

Pul-Ark-1 : Fourche Mtn; residual soil from syenite. (Taylor and Epstein, 1964)

Pul-Ark-3 : E. side of Arkansas Rt. 367, 2.5 mi. S. of bridge over Fourche Creek, from the boundary of the B and C soil zones, developed on syenite; sampled about 3 ft. below the ground surface; see photo #1 .

But-Cal-1 : SW side of Calif. Rt. 32; 7 mi. NE of Chico, elev. ~1960 ft.; red clay from a soil formed on a Tertiary andesite flow, sampled about 2 ft. below the ground surface.

Photograph #1 : Pul-Ark-3
(The numeral 1 is on a 3 x 5 in. card)

Lak-Cal-3 : roadcut, C. of sec. 5, T12N, R7W; S. end of Clear Lake, elev. ~ 2380 ft., C-zone of a soil on Quaternary andesite, sampled about 2 ft. below the ground surface.

L.A.-Cal-2 : roadcut 0.5 mi. N. of Cornell, W. Santa Monica Mtns., elev. ~ 900 ft.; C-zone of a soil developed on a Miocene andesite, sampled about 2 ft. below the ground surface.

L.A.-Cal-4 : roadcut 0.2 mi. W. of Cornell, W. Santa Monica Mtns., elev. ~ 1000 ft., C-zone of a soil developed on a Miocene andesite, sampled about 2 ft. below the ground surface.

L.A.-Cal-6 : roadcut, NW 1/4 sec. 14, T3N, R11W, Acton Q.; elev. ~ 5840 ft.; C-zone of a soil on a Mesozoic granodiorite, sampled about 6 ft. below the ground surface.

Mar-Cal-1 : W. side of the road to Pt. Reyes, 2.2 mi. N. of Pt. Reyes Station; elev. ~10 ft.; C-zone of a soil on Mesozoic quartz diorite, sampled about 15 ft. below the ground surface.

Mon-Cal-3 : W. side of U.S. 1, NW Pt. Sur. Q., 1.5 mi. S. of Sobernanes Pt.; elev. ~ 100 ft.; poorly developed B-zone of a soil developed on a Mesozoic quartz diorite, sampled about 3 ft. below the ground surface.

S.D.-Cal-1 : roadcut, NW 1/4 sec. 19 T11S R3W, 0.5 mi. NW of the C. of the town of Vista; elev. ~400 ft.; poorly developed B-zone of a red-brown soil on a Mesozoic tonalite, sampled about 2 ft. beneath the ground surface.

S.D.-Cal-2 : roadcut, sec. 20, T11S, R2W, 1 mi. NE of Calif. Rt. 395, elev. ~1350 ft.; poorly developed B-zone of a soil developed on a Mesozoic granodiorite, sampled about 1 ft. below the ground surface.

S.L.O.-Cal-1 : S. side of road, S 1/2, NE 1/4, SE 1/4, sec. 18, T29S, R14E, San Luis Obispo Q.; elev. ~1775 ft.; poorly developed B-zone of a soil on a Mesozoic granodiorite, sampled about 1 ft. below the ground surface.

S.C.-Cal-1 : W. side of Calif. Rt. 9, 4 mi. N. of Santa Cruz; elev. ~500 ft.; brown clay from clay-rich lense in the B-zone of a soil developed on a Mesozoic quartz diorite, sampled about 2 ft. below the ground surface.

Tul-Cal-1 : base of an uprooted tree, sec. 24, T19S, R30E, Mineral King Q.; elev. ~7200 ft.; soil in the roots of a fallen tree developed from a granitic cobbly gravel, sampled about 1 ft. below the ground surface.

Tul-Cal-2 : roadcut, W 1/2, SW 1/4, NE 1/4, sec. 34 T19S, R30E, Camp Nelson Q.; elev. ~5900 ft.; red-brown moderately developed B-zone of a soil on a Mesozoic granite, sampled about 3 ft. below the ground surface.

Tul-Cal-3 : S. side of dirt road E. of paved road, C. of sec. 1, T20S,R30E, Camp Nelson Q.; elev.~6400 ft.; a light brown poorly developed B-zone of a soil on a Mesozoic granite sampled about 2 ft. below the ground surface.

Tul-Cal-4 : S. side of paved road, N1/2, NE1/4, NW1/4, sec. 11, T20S, R30E, Camp Nelson Q.; elev.~ 5300 ft.; a dark brown soil in granitic cobbly gravel, sampled about 4 ft. below the ground surface.

Tul-Cal-5 : N. side of paved road, NE1/4, NW1/4, NE1/4, sec. 10, T20S, R30E, Camp Nelson Q,; elev.~ 4600 ft.; moderately developed red-brown B-zone of a soil on a Mesozoic granodiorite, sampled about 3 ft. below the ground surface.

Tul-Cal-6 : N. side of paved road, NE1/4 NE1/4 NE1/4 sec. 8, T20S, R30E, Camp Nelson Q.; elev.~3200 ft.; moderately developed C-zone of a soil on a Mesozoic granodiorite sampled about 3 ft. below the ground surface.

Tul-Cal-7 : SE side of Bear Creek road, NE1/4, NE1/4 sec. 12, T20S,R29E, Springville Q.; elev.~ 2000 ft.; moderately developed red-brown consolidated B-zone of a soil on a Mesozoic tonalite, sampled about 3 ft. below the ground surface.

Tul-Cal-8 : SW side of Ave. 176, S1/2, NW1/4, SW1/4, sec. 7, T21S, R29E, Springville Q.; elev.~ 900 ft.; poorly developed dark red-brown consolidated B-zone of a soil on a Mesozoic tonalite, sampled about 3 ft. below the ground surface.

Bou-Col-1 : S. side of Colorado Rt. 119, 1.8 mi. W. of j'n of 119 and Colorado Rt. 93; elev.~6100 ft.; clay-rich ground-water alteration zone in a Precambrian granite.

Min-Col-1 : NW side of U.S. 160, 1.1 mi. E. of Wolf Creek Pass Summit; elev. ~10,000 ft.; outer portion of spheroidally weathered boulder in Tertiary andesitic flow, sampled about 3 ft. below the ground surface.

Lit-Conn-2 : W. side of Connecticut Rt. 8; 4.5 mi. N. of j'n of Rt. 8 and Connecticut Rf. 20; elev. ~1000 ft.; clay-rich ground-water alteration zone in a Paleozoic gneiss, sampled 60 ft. below the ground surface.

D.K.-Ga-1 : Stone Mtn.; cultivated top soil developed on the granite. (Taylor and Epstein, 1964)

Kau-Haw-1 : W. side of road, 2 mi. N. of Koloa; elev. 450 ft.; saprolite developed on Quaternary basalt, sampled about 20 ft. below the ground surface. (R.P.S.)

Kau-Haw-2 : W. side of road, 2 mi. N. of Koloa; elev.~ 450 ft., veinlets of white clay in the saprolite developed on Quaternary basalt, sampled about 20 ft. below the ground surface. (R.P.S.)

Maui-Haw-1 : roadcut, 0.5 mi. W of Keanae, NE coast of Maui Is.; elev.~ 200 ft.; saprolite on a Quaternary basalt, sampled about 50 ft. below the ground surface. (R.P.S.)

Maui-Haw-2 : roadcut, 1.5 mi. due S. of Waipio Bay, NE coast of Maui Is.; elev.~500 ft.; saprolite on a Quaternary basalt, sampled about 10 ft. below the ground surface. (R.P.S.)

Maui-Haw-3 : roadcut, 1.2 mi. SW of Pauwela Pt., N. coast of Maui Is.; elev.~250 ft.; saprolite on a Quaternary basalt, sampled about 50 ft. below the ground surface (R.P.S.)

Maui-Haw-4 : roadcut, 1.2 mi. SW of Pauwela Pt., N. coast of Maui Is.; elev.~250 ft.; saprolite on a Quaternary basalt, sampled about 50 ft. below the ground surface. (R.P.S.)

Maui-Haw-5 : roadcut, 0.6 mi. E. of Hawea Pt., NW coast of Maui Is.; elev.~100 ft.; saprolite on a Quaternary basaltic agglomerate, sampled about 15 ft. below the ground surface. (R.P.S.)

Maui-Haw-6 : roadcut, 0.6 mi. E. of Hawea Pt., NW coast of Maui Is.; elev.~100 ft.; saprolitic cobble in a Quaternary basaltic agglomerate, sampled about 15 ft. below the ground surface . (R.P.S.)

Maui-Haw-7 : roadcut, 1.4 mi. E. of Hawea Pt., NW coast of Maui Is.; elev.~100 ft; clay nodule in a dark reddish-brown saprolite on a Quaternary basalt, sampled about 6 ft. below the ground surface. (R.P.S.)

Maui-Haw-8 : roadcut, 1.4 mi. E. of Hawea Pt., NW coast of Maui Is.; elev.~100 ft.; clay-rich band in a dark red-brown saprolite on a Quaternary basalt, sampled about 8 ft. below the fround surface . (R.P.S.)

Maui-Haw-9 : roadcut, 0.8 mi. E. of Lipoa Pt., NW coast of Maui Is.; elev. ~200 ft.; clay seams in a saprolite on Quaternary basalt, sampled about 25 ft. below the ground surface . (R.P.S.)

Maui-Haw-10 : roadcut, 0.8 mi. E. of Lipoa Pt., NW coast of Maui Is.; elev.~200 ft.; saprolite of a Quaternary basalt, sampled about 25 ft. below the ground surface. (R.P.S.)

Boi-Ida-4 : S. side of Idaho Rt. 21, 9.2 mi. E. of Lowman; elev.~5900 ft.; outer portion of a spheroidally weathered boulder in a Tertiary granitic rock sampled about 15 ft. below the ground surface.

Boi-Ida-5 : E. side of Idaho Rt. 21, 33.1 mi. NE of Lowman; elev.~6900 ft, clay-rich ground water alteration zone in a Tertiary granitic rock, sampled about 15 ft. below the ground surface.

Cle-Ida-1 : N. side of road between Ahsahka and Cavendish, 4 mi. E. of Ahsahka; elev. ~1250 ft.; spheroidally weathered boulder in a Mesozoic granite, sampled about 5 ft. below the ground surface.

Ida-Ida-1 : N. side of U.S. Rt. 12, 37.5 mi. W. of Montana-Idaho border; elev. ~2830 ft.; clay-rich ground water alteration zone in a Mesozoic gabbroic rock, sampled about 20 ft. below the ground surface.

Lat-Ida-1 : E. side of a dirt road 2.5 mi. S. of Helmer ; elev. ~2770 ft.; dark brown A-zone of a soil on a Miocene basalt, sampled about 1 ft. below the ground surface.

Mad-Mis-1 : N. side of Missouri Rt. 72, 0.1 mi. W. of St. Francis R., elev. ~1500 ft. red-brown moderately developed C-zone of a soil on a Precambrian granite, sampled about 1 ft. below the ground surface.

Jef-Mon-1 : N. side of U.S. Rt. 10, about 6 mi. E. of Butte at the Homesake turnoff; elev. ~ 6240 ft.; bright orange clay-rich ground-water alteration zone in a L. Tertiary granodiorite, sampled about 10 ft. below the ground surface.

L.a.C.-Mon-1 : E. side of a dirt road to Rimini, 0.7 mi. S. of U.S. Rt. 12; elev. ~ 5500 ft.; two samples: a brown clay and a gray sandy clay developed along jointing in Cretaceous andesitic volcanics, sampled about 10 ft. below the ground surface.

L.a.C.-Mon-2 : N. side of U.S. Rt. 12, 2.8 mi. E. of McDonald Pass summit; elev. ~ 5500 ft.; gray sandy clay developed along jointing in a L. Tertiary granodiorite, sampled about 20 ft. below the ground surface.

Mis-Mon-1 : N. side of U.S. Rt. 12, 3.4 mi. NE of Lolo Hot Springs; elev. ~ 4330 ft.; clay-rich ground-water alteration zone in a Mesozoic granodiorite, sampled about 8 ft. below the ground surface.

Mid-N.J.-1 : near Metuchen, New Jersey, soil developed on glacial drift. (Taylor and Epstein, 1964)

Colf-N.M.-1 : N. side of U.S. Rt. 64, 3.6 mi. W of Ute Park, elev. ~7300 ft.; brown clay from a spheroidally weathered boulder in porphyritic latite, sampled 20 ft. below the ground surface.

Monr-N.Y.-1 : Fairport, New York, sandy loom soil . (Taylor and Epstein, 1964)

Rock-N.Y.-1 : NE side of N.Y. Rt. 210, 3.0 mi. E. of Palisades Parkway; elev. ~ 1000 ft.; clay-rich ground-water alteration along jointing in a Precambrian gneiss, sampled about 6 ft. below the ground surface.

Clev-N.C.-1 : near Shelby, North Carolina; residual soil on a gneiss. (Taylor and Epstein, 1964)

Clev-N.C.-2 : near Kings Mtn., North Carolina; a loam soil. (Taylor and Epstein, 1964)

Com-Okl-1 : N. side of Oklahoma Rt. 49, 5.3 mi. W. of j'n of Rt. 49 and Oklahoma Rt. 58; elev. ~2100 ft.; two samples: (1) a fragment of disintegrated Precambrian granite samples 6 ft. below the ground surface, (2) outer weathered surface of the granite, sampled about 15 ft. below the ground surface.

Gre-Okl-1 : E. side of road in Quartz Mtn. St. Park, 0.2 mi. N. of the end of the road; elev. ~ 2000 ft.; outer portion of a spheroidally weathered boulder of Precambrian granite, sampled 2 ft. below the ground surface.

H.R.-Ore-1 : E. side of Oregon Rt. 35, 4.5 mi. S. of town of Mt. Hood; elev. ~ 1460 ft., red-brown moderately well developed B-zone of a soil on a U. Tertiary basalt, sampled 3 ft. below the ground surface.

Lan-Ore-1 : W. side of a road NE of Springfield, 2.9 mi. N. of Mabel; elev. ~ 960 ft.; red-brown well developed B-zone of a soil on Tertiary andesitic volcanics, sampled about 2 ft. below the ground surface.

Mar-Ore-1 : roadcut, SW 1/4, SW 1/4, sec. 18, T8S, R1E, NE of Sublimity; elev. ~1030 ft.; poorly developed red-brown B-zone of a soil on a Mid-Tertiary basalt, sampled 2 ft. below the ground surface.

Mul-Ore-1 : SW side of Larch Mtn. road, 6.0 mi. E. of j'n of Larch Mtn. road and Scenic Drive, elev. ~1860 ft.; two samples: (1) brown A-zone of a well developed soil on a Pliocene basalt, sampled 1 ft. below the ground surface, (2) spheroidally weathered boulder of basalt, sampled about 6 ft. below the ground surface.

Mul-Ore-2 : N. side of Larch Mtn. road, 12.9 mi. E. of j'n of Larch Mtn. road and Scenic Drive, elev. ~ 3770 ft. ; well developed brown C-zone of a soil on a U. Tertiary basalt, sampled about 8 ft. below the ground surface.

Wash-Ore-1 : SW side of Oregon Rt. 26, C. of NE 1/4, sec. 23, T2N, R4W, Forest Grove Q.; elev. ~325 ft.; weathered boulder of basalt in a Pleistocene gravel, sampled 25 ft. below the ground surface.

Wash-Ore-2 : S. side of Oregon Rt. 6, NE 1/4, SW 1/4, sec. 34, T2N, R4W, Forest Grove Q.; elev ~300 ft.; weathered boulder of basalt in a Pleistocene gravel, sampled 40 ft. below the ground surface.

Yam-Ore-1 : N. side of Carlton-Beaver road, 8 miles W. of Carlton; elev. ~850 ft.; spheroidally weathered boulder of gabbroic rock, sampled about 5 ft. below the ground surface.

Lla-Tex-4 : E. side of Texas Rt. 1431, 1.7 mi. S. of Texas Rt. 29; elev. ~1200 ft.; red-brown well developed C-zone of a soil on Precambrian granite, sampled about 3 ft. below the ground surface. (see photo #2)

Photograph #2 : IIa-Tex-4
(The numeral 2 is on a 3 x 5 in. card)

Park-Wyo-1 : N. side of Wyoming Rt. 16, 20.4 mi. E. of the Yellowstone R.; elev.~8000 ft.; spheroidally weathered boulders in granite, sampled about 20 ft. below the ground surface.

E.B.-Nica-1 : El Bluff, Nicaragua; elev.~10 ft.; bright orange intensely weathered volcanic rock. (M.N.B.)

Antarctic Soils

T.G.-Anta-1 : 77° 25' S, 161° 40' E, bulk surface soil. (R.E.C.)

R.I.-Anta-1 : 77° 25'S, 163° 45' E, bulk surface soil. (R.E.C.)

R.I.-Anta-2 : 77° 29' S, 163° 45' E, bulk surface soil. (R.E.C.)

R.I.-Anta-3 : 77° 58' S, 162° 0' E, bulk surface soil. (R.E.C.)

Ancient Kaolinite Deposits

H.S.-Ark-1 : sample no. HS-7 ; gray plastic somewhat sandy clay, Eocene Wilcox Fm., (Williams and Plummer, 1951, p.65, see map).

Pike-Ark-1 : locality no. 2 white kaolin, U. Cretaceous, Tokio Fm.; (Herald and Heyl, 1942, p. 13, see Plate I).

Pul-Ark-2 : sample no. P-1, gray sandy clay, Eocene Wilcox Fm., (Williams and Plummer, 1951, p. 71).

Sal-Ark-2 : NW1/4, SE1/4, SE1/4, sec. 9, T2S, R14W, residual Eocene weathered zone in nepheline syenite, about 1 ft. above fresh parent rock; (Bramlette, M.N., 1936, Plate IX).

Hue-Col-1 : W1/2, SW1/4, sec. 19, T26S, R64W, silty, sandy shale in the L. Cretaceous Dakota Sandstone; (Waagé, K.M., 1953, Figure 17).

Pue-Col-1 : SE1/4, SE1/4, NE1/4, sec. 22, T22S, R67W, gray concoidal fireclay in the L. Cretaceous Dakota Sandstone; (Waagé, K.M., Plate V).

Cle-Ida-1 : 4 mi. N. of Cavendish on Idaho Rt. 7; gray plastic clay containing numerous rounded quartz pebbles, Miocene; (Hosterman, J.W., 1961; Skeels, F.H., 1920).

Lat-Ida-2 : open pit mine, A.P. Green Company, 2 mi. N. of Helmer; two samples collected beneath Quaternary gravel: (1) plastic clay and (2) siliceous clay, Miocene; (Hosterman, J.W., 1961; Skeels, F.H., 1920).

Lat-Ida-3 : sample no. 29 clay containing abundant quartz and muscovite, Miocene; (Skeels, F.H., 1920, p. 42).

N.P.-Ida-1 : 5 mi. N. of Cavendish on Idaho Rt. 7; white clay containing abundant rounded quartz pebbles, Miocene; (Hosterman, J.W., 1961; Skeels, F.H., 1920).

Cal-Mis-1 : SE1/4, sec. 3, T46N, R9W (see map in ref.); flint clay, Cheltenham Fm., Pennsylvanian; (McQueen, H.S., 1943).

Fra-Mis-1 : on boundary of sec. 35 and 36, T42N, R4W, white concoidal clay, Cheltenham Fm., Pennsylvanian; (McQueen, H.S., 1943, see map).

Fra-Mis-2 : sec. 26, T42N, R4W; white concoidal clay, Cheltenham Fm., Pennsylvanian; (McQueen, H.S., 1943, see map).

Gas-Mis-1 Cl : sec. 9, T41N, R5W, hard white siliceous clay, Cheltenham Fm., Pennsylvanian; (McQueen, H.S., 1943, see map).

Cas-Mon-1 : NW1/4, SW1/4, sec. 31, T19N, R7E, 0.5 mi. SE of Armington; dark gray colored shale in a sandstone-shale sequence, Kootenai Fm., L. Cretaceous; (Fisher, C.A., 1908).

Mid-N.J.-1 : locality no. 45, near Perth-Amboy, sandy clay, Rariton Fm., L. Cretaceous, (Ries, H. et al., 1904, p. 174-177, Plate XI).

Mid-N.J.-2 : E. edge of pit, locality no. 40 near Perth-Amboy; two samples: (1) clay lens in coarse-grained, cross-bedded sandstone (2) mixed white clay and fine sand; Rariton Fm., L. Cretaceous; (Ries, H. et al., 1904, p. 178, Plate XI).

Cla-Ore-2 : locality no. 7; gray sandy clay underlying a tuffaceous sandstone, Miocene (Wilson and Treasher, 1938, p. 45-46, Figure 18).

Mari-Ore-1 : locality no. 11; white concoidal clay, Miocene; (Wilson and Treasher, 1938, p. 49-54, Figure 23).

Mari-Ore-3 : locality no. 18, tuff. in a sedimentary sequence altered to clay, Miocene; (Wilson and Treasher, 1938, p. 59-60, Figure 23).

Aik-S.C.-N11-11 : near Bath, South Carolina; pure kaolinite, U. Cretaceous; (Savin, 1967).

Che-Tex-1 : Thermo Fire Brick Company Clay Pit, 1.2 mi. SW of Henry's Chapel; gray sandy clay, Eocene Wilcox Fm.; (Stenzel and Pence, 1950, Plate I).

Che-Tex-2 : General Refractories Company Clay Pit, 1.4 mi. W. of Henry's Chapel; gray sandy clay, Eocene Wilcox Fm.; (Stenzel and Pence, 1950, Plate I).

Eas-Tex-1 : locality no. 13, gray clay of the Quinn clay, Cisco group, Pennsylvanian; (Plummer et al., 1949, Plate II).

Ste-Tex-1 : locality no. 22; gray clay of the Quinn clay, Cisco group, Pennsylvanian; (Plummer et al., 1949, Plate IV).

You-Tex-1 : locality no. 28; gray clay of the Curry clay, Cisco group, Pennsylvanian; (Plummer et al., 1949, Plate V).

Ben-Ver-1 : locality no. 6; white clay from an overgrown pit, Miocene; (Burt, 1927-8, p. 65-84, Figure 9).

Pie-Wash-1 : NE1/4, NW1/4, SE1/4, sec. 25, T17N, R4E; gray residual clay alteration of Miocene andesitic volcanics; (Glover, 1941, p. 205-14).

Pie-Wash-3 : S1/2, NW1/4, SE1/4, sec. 25, T17N, R4E; gray residual clay alteration of Miocene andesitic volcanics; (Glover, 1941, p. 205-14).

Spo-Wash-1 : SE1/4, SW1/4, sec. 14, T24N, R44E; brown sandy sedimentary clay, Miocene; (Glover, 1941, p. 244-52).

Spo-Wash-2 : SE1/4, NW1/4, sec. 23, T24N, R44E; pure white kaolinitic clay found in bulldozer diggins; Miocene; (Glover, 1941, p. 244-52).

Spo-Wash-3 : NW1/4, NW1/4, sec. 1, T23N, R44E; kaolinite pseudomorphic after feldspar in a residual granitic saprolite, Miocene; (Glover, 1941, p. 244-52).

RPFM-3, 7, 10 : W. of Boulder, Colorado, three samples from a Pre-Pennsylvanian weathering profile on Precambrian granodiorite; (Pliler and Adams, 1962).

CH-13 : Cyprus Hills, Alberta, Canada; sandy light gray clay in a shale-sandstone sequence; Paleocene; (Folinsbee, R.E., personal communication).

Ancient Illite Deposits

Coco-Ariz-5: 0.1 mi. S. of Plateau Pt., W. of Bright Angel Trail, Grand Canyon; fossil soil on Precambrian gneissic complex, Brahma Schist, overlain by the Tapeats Sandstone, sample of a spheroidal boulder about 6 ft. below the Tapeats. (Sharp, 1940)

Coco-Ariz-6 : location same as Coco-Ariz-5; alteration of a mafic dike in the Brahma Schist, about 6 ft. below the Tapeats Sandstone. (Sharp, 1940)

S.B.-Cal-15 : NW1/4, NW1/4, SW1/4, sec. 12, T5N, R14E, SW Danby Q.; 1 ft. thick fossil soil on a Precambrian granite overlain by a Precambrian quartzite.

Montmorillonites

Coco-Ariz-7 : W. side of Arizona 89, 22.8 mi. N. of the N. abutment of the Little Colorado R. Bridge; bentonite in the Chinle Fm., Triassic; (Kerr and Kulp, 1949; Longwell et al., 1923).

Fer-Mon-1 : E. side of U.S. Rt. 191, 2.9 mi. N. of Judith Gap, bentonitic shale in the Claggett Shale, U. Cretaceous; (Tourtelot, 1962). (see photo #3)

H.R.-Ore-2 : S. of Interstate 80N, 0.3 mi. E. of Wyeth; red and gray mixed clay-rich fossil soil developed on a L. Tertiary andesite; (A.G. Waters, personal communication).

Was-Ore-3 : roadcut, along the old Columbia R. road in the city of The Dalles, S. 32° E. of the north end of the bridge over the Columbia R.; glass rinds of a Miocene pillow lava weathered to clay.

Was-Ore-4 : W. side of U.S. Rt. 197, W. 1/2, SE1/4, NW1/4, sec. 14, T3S, R13E, Postage Stamp Butte Q.; glass rinds of a Miocene pillow lava weathered to clay.

Was-Ore-6 : W. side of U.S. Rt. 197, SW1/4, SW1/4, NW1/4, sec. 22, T3S, R13E, Postage Stamp Butte Q.; 1 ft. thick fossil soil between Miocene basalt flows.

Was-Ore-8 : W. side of U.S. Rt. 197, SW1/4, NE1/4, SW1/4, sec. 14, T3S, R13E, Postage Stamp Butte Q.; 3 in. fossil soil developed on a vesicular Miocene basalt overlain by a massive Miocene basalt.

Was-Ore-9 : E. side of U.S. Rt. 197, SW1/4, SE1/4, SW1/4, sec. 11, T3S, R.13E, Postage Stamp Butte Q.; two samples: (1) upper bright red 1 ft. zone and (2) lower yellow brown 2 ft. zone of a fossil soil developed on a vesicular Miocene basalt overlain by a massive Miocene basalt.

Was-Ore-10 : E. side the road 2 mi. N. of Simnasho; about 5 ft. thick bright red fossil soil developed on an Oligocene andesite overlain by an Oligocene rhyolite tuff.; (A. C. Waters, personal communication).

Nio-Wyo-1 : E. side of U.S. Rt. 85, 2.5 mi. S. of Red Bird; Kara bentonitic member of the Pierre Shale; (Gill and Cobban, 1966, Figure 2, p. A7).

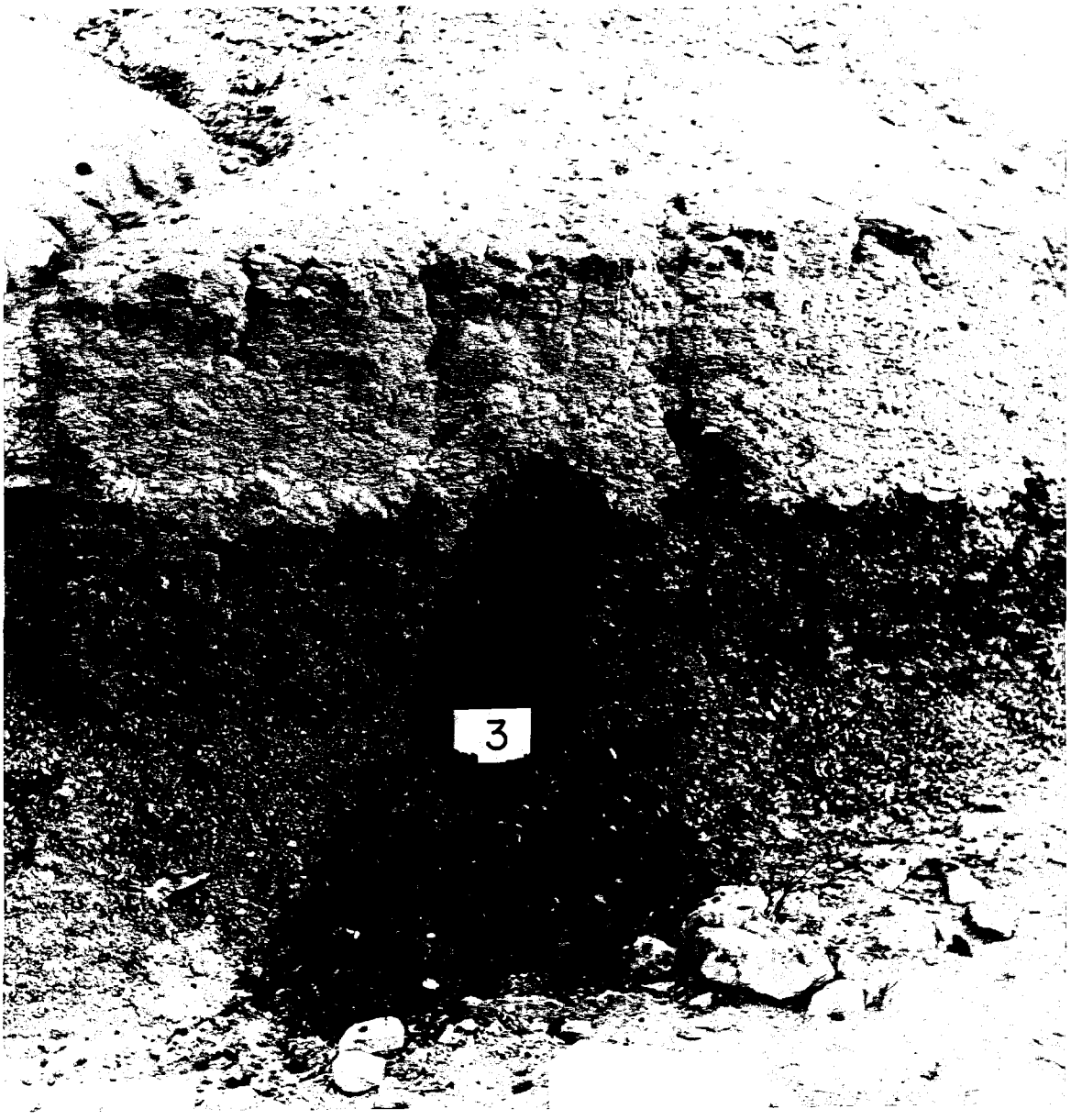

Photograph #3 : Fer-Mon-1
(The numeral 3 is on a 3 x 5 in. card)

Nio-Wyo-2 : N. side of dirt road NE1/4, NW1/4, NE1/4, sec. 26, T38N, R62W; Ardmore bentonitic member of the Pierre shale; (Gill and Cobban, 1966, Plate 1).

Wes-Wyo-1 Cl : about 3 mi. NW of Upton; bentonite taken from the Western Company bentonite plant, sample from about 5 mi. E. of the plant in the Graneras Shale, U. Cretaceous.

TW-10-116 : 22°N. latitude, Mid Atlantic Ridge, Atlantic Ocean; dredge haul, alteration of basaltic glass "probably formed at temperatures between 100°C and 300°C." (Banks and Melson, 1966, p.9).

TW-1-50-F-M and TW-1-G : E. Pacific Rise, off Mexican coast, Pacific Ocean; dredge haul, alteration of a basaltic glass by submarine weathering; (M. Bass, personal communication).

Carr II-DR-9-L-M : E. Pacific Rise, off Mexican coast, Pacific Ocean; alteration product of a basalt by submarine weathering; (M. Bass, personal communication).

68 A to 20 : near Umiat Mtn., N. slope of Alaska; bentonite Seabe Fm., U. Cretaceous; (Brosgé and Whittington, 1966).

S.Be.-1 : 500 ft. N. of El tiro Pit, Silver Bell copper deposit, about 50 mi. NW of Tucson, green clay, supergene alteration (Mid Tertiary) of an alaskite; (H.P. Taylor, personal communication).

S. Be.-3 : C. of Oxide Pit, Silver Bell copper deposit, about 50 mi. NW of Tucson; two samples : (1) a white clay and (2) a light green clay, supergene alteration (Mid Tertiary) of a quartz monzonite; (H.P. Taylor, personal communication).

SH-12 : near Edmonton, Alberta, Canada; bentonite in a shale-sandstone sequence, Paleocene; (R.E. Folinsbee, personal communication).

Shales

Inyo-Cal-5 : Waucoba Canyon, White Mtns.; Ordovician shale (Tech collection, T391, C.I.T.).

B.C.-Can-1 : Fossil Knob, Cranbrook; Eager argillite, Cambrian (Cranbrook collection, Crb T65, Rice, C.I.T.).

B.C.-Can-3 : base of Cranbrook Mtn., Siyeh Fm. Argillite, Precambrian Belt Series (Cranbrook collection, Crb 55, Rice, C.I.T.).

She-Ind-1 : near Waldron; Waldron shale, Niagaran, Silurian (stratigraphic collection no. 32, C.I.T.).

Mis-Mon-3 : N. side of U.S. Rt. 90, 1.2 mi. E. of Van Buren St. turnoff, Missoula; shiny green shale, Precambrian Belt Series (H.P.T.).

Mis-Mon-4 : W. side of U. S. Rt. 12, 1.0 mi. N. of j'n of Rt. 12 and U.S. Rt. 93: two samples: (1) green shale, Precambrian Belt Series (2) soil on shale; (H.P.T.).

Pow-Mon-7 : NNE of Jens on the Hoover Creek Rd, NE1/4, sec. 9, T10N, R11W; green shale, Flood member of the Blackleaf Fm., Cretaceous; (H.P.T.).

Liv-N.Y.-1 : near Leicester; Moscow Shale; Erian, Devonian; (stratigraphic collection no. 42, C.I.T.).

Monr-N.Y.-2 : near Rochester; Vernon Shale; Cayugan, Silurian; (Anderson, K., C.I.T.).

Ham-Ohio-1 : in Cincinnati; Southgate member, Eden Shale, U. Ordovician; (M.S.).

Glacial Lake Clays

8:3 : Spring Grove Cemetery on Mill Creek Expressway, Cincinnati, Ohio; Illinoian glacial lake clay; (M.S.).

8:4 : Spring Grove Cemetery on Mill Creek Expressway, Cincinnati,Ohio; Illinoian glacial lake clay; (M.S.).

10:4 : j'n of Henry Court and Alexandria Pike, Cold Springs, Kentucky; Pre-Illinoian glacial lake clay; (M.S.).

Perlites

Ben-Wash-1 : Prosser deposit; Eocene perlite; (Huntting, M.T., 1949,p.57).

Che-Wash-1 : Crum Canyon deposit; Eocene perlite; (Huntting, M.T., 1949, p. 55-57).

Pie-Wash-4 : Mashel River deposit; Eocene perlite; (Huntting,M.T.,1949, p. 51-52).

Pie-Wash-5 : Divide deposit; Eocene perlite; (Huntting,M.T.,1949,p.51-52).

Meteoric Waters

Iny-Cal-1 : Alabama Hills near Lone Pine; Lone Pine Creek, elev. ~ 5000 ft., June 1967 .

L.A.-Cal-4 : Malibu Lake, near Cornell, W. Santa Monica Mtns., elev. ~ 900 ft., July 17, 1967 .

Mar-Cal-1 : 2.2 mi. N. of Pt. Reyes Station on road to Pt. Reyes; 1 ft. deep stream, elev. ~10 ft., July 19, 1967 .

Mon-Cal-2 : Little Sur River; elev. ~10 ft., April 1967 .

Mon-Cal-4 : 5 mi. W. of Greenfield; Arroyo Seco River; elev. ~65 ft., July 17, 1967 .

S.L.O.-Cal-1 : 10 mi. NE of San Luis Obispo; spring; elev. ~2000 ft., April 1967.

S.C.-Cal-1 : 4 mi. N. of Santa Cruz on Rt. 9; 6 in. deep creek, elev. ~ 420 ft., July 18, 1967.

Boi-Ida-5 : 33.1 mi. E. of Lowman on Idaho Rt. 21, 6 in. deep stream, elev. ~6900 ft., July 28, 1967.

Lat-Ida-1 : 3 mi. S. of Helmer in a campground; pump water, elev. ~2500 ft., July 31, 1967 .

Jef-Mon-2 : S. side of U.S. Rt. 90 , 12 mi. E. of Butte; 2 ft. deep stream, elev. ~4630 ft., July 29, 1967 .

Mis-Mon-1 : N. side of U.S. Rt. 12, 3.4 mi. E. of Lolo Hot Springs; spring in a roadcut, elev. ~4330 ft., July 30, 1967 .

Bak-Ore-1 : Wetmore N. F. Campground, on U.S. Rt. 26, 3.5 mi. E. of Blue Mtn. Summit; tap water from the compground, elev. ~ 4340 ft. , July 27, 1967.

Gra-Ore-1 : Bull Prairie N.F. Campground, 2.4 mi. E. of Oregon Rt. 207, tap water in campground, elev. ~4000 ft., July 27, 1967 .

H.R.-Ore-2 : W. side of Oregon Rt. 35, 11 mi. S. of Mt. Hood (town); spring in a roadcut, elev. ~2500 ft., August 4, 1967.

Kla-Ore-2 : next to road to Fort Klamath, 11.9 mi. N. of Oregon Rt. 140; Cheery Creek, elev. ~4290 ft., July 21, 1967 .

Kla-Ore-4 : N. of Odell Lake on Oregon Rt. 58; spring in roadcut, elev. ~ 4990 ft., July 21, 1967.

Mul-Ore-3 : next to Larch Mtn. road, 8.5 mi. from the j'n of Larch Mtn. road and Scenic Drive; spring, in roadcut, elev. ~ 2460 ft., July 25, 1967 .

Til-Ore-1 : Castle Rock campground, on Oregon Rt. 22; pump water in campground; elev. ~325 ft., July 22, 1967 .

Was-Ore-1 : next to U.S. Rt. 26, 2.9 mi. S. of road to Clear Lake; 6 in. deep stream; elev. ~3400 ft., July 26, 1967.

Wash-Ore-1 : Park Farms Creek, Forest Grove Q.; 1 ft. deep stream, elev. ~300 ft., July 23, 1967 .

APPENDIX II

X-RAY DIFFRACTION PATTERNS OF SELECTED SAMPLES FROM THE ELBERTON, GEORGIA AND BIG SUR, CALIFORNIA WEATHERING PROFILES

The X-ray diffraction patterns of a sequence of samples from the Elberton profile (15-1 to 15-6) going from fresh quartz monzonite to a kaolinite-rich saprolite are shown below. Note the increase in kaolinite content (7Å peak, $\sim 12^{\circ} 2\theta$) and the corresponding disappearance of feldspar (3.1 to 3.3 Å peaks, $\sim 28^{\circ} 2\theta$) going from 15-1 to 15-6. Also note the alteration of biotite (10Å peak, $\sim 9^{\circ} 2\theta$) to hydrobiotite (12.4 and 25 Å, $\sim 7^{\circ}$ and 3° 2θ) in going from 15-1 to 15-6.

The X-ray diffraction patterns of two clay-rich samples, a gray clay (6Clg) and a brown clay (6Clb), from the Big Sur profile are also shown. Note the close similarity in the X-ray patterns of the two samples.

Elberton, Georgia Profile

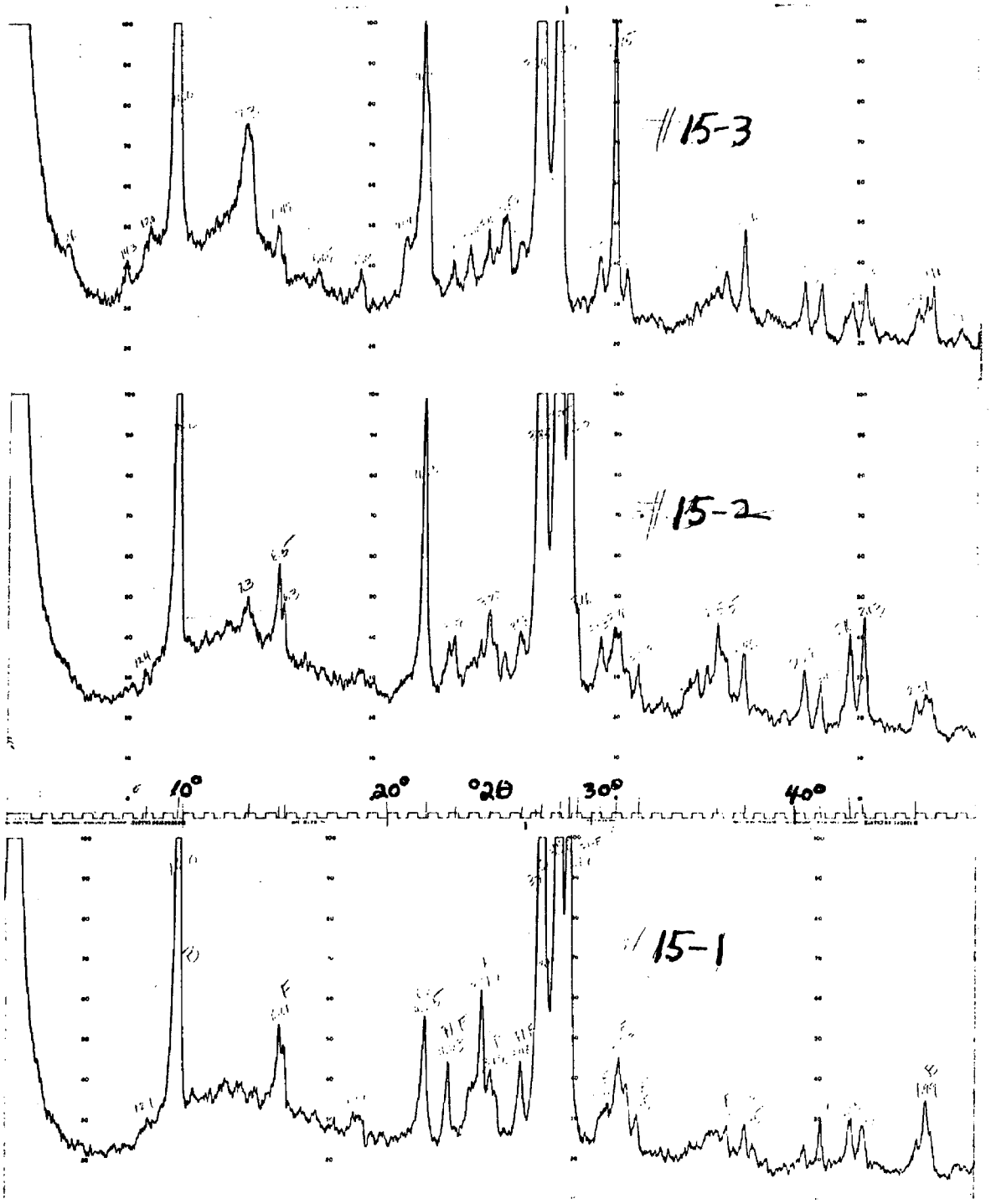

Elberton, Georgia Profile

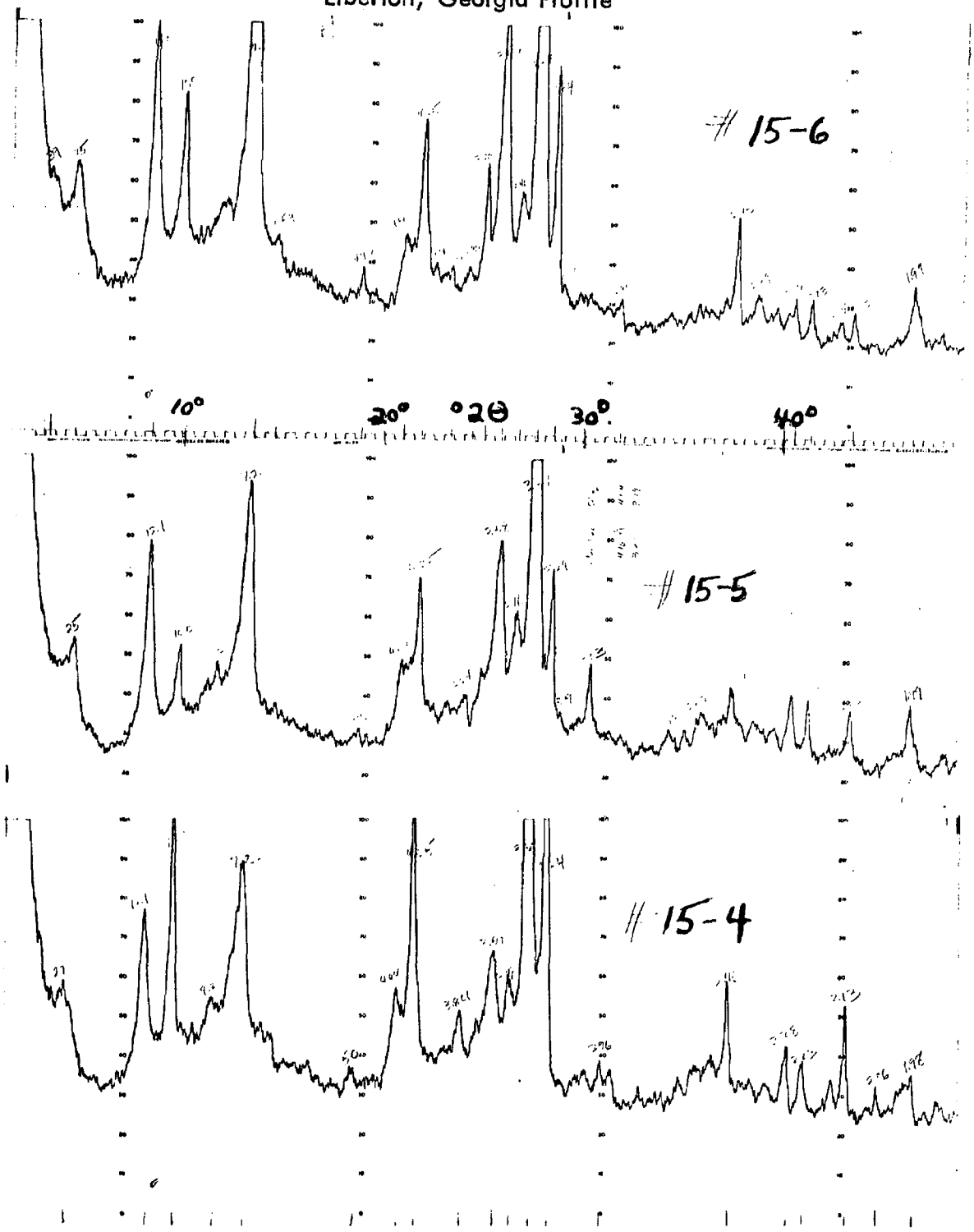

Big Sur, California Profile

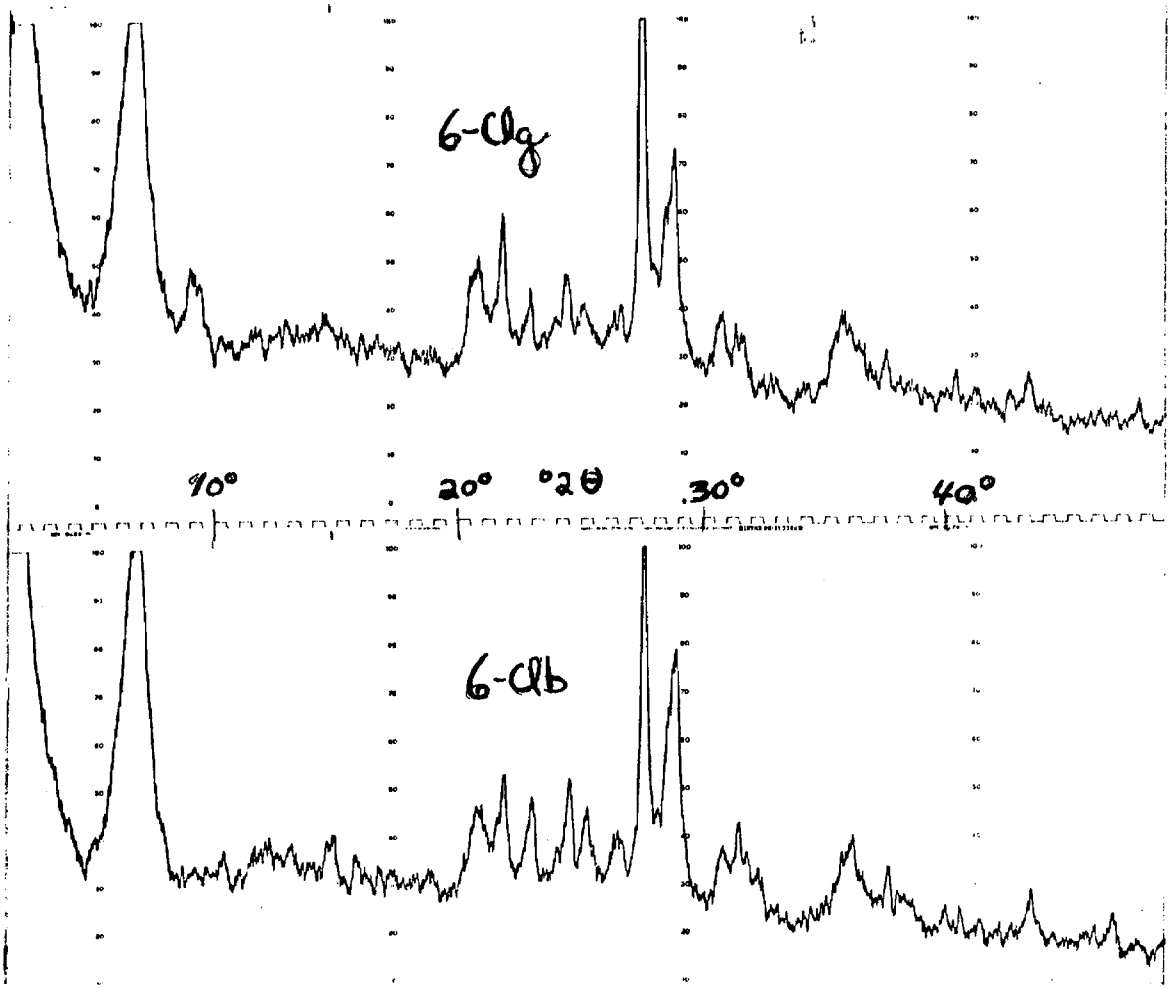

APPENDIX III

OXYGEN ISOTOPIC REPRODUCIBILITY OF THE KAOLINITE AND ROSE QUARTZ STANDARDS

During the course of this research, two working standards (a kaolinite and Rose quartz) were routinely included in each set of six samples analyzed for their δO^{18} content. The δO^{18} value of the kaolinite was taken at +21.70 and that of the Rose quartz was taken at +8.42 relative to Standard Mean Ocean Water (SMOW). The δO^{18} values of these two standards measured against the mass spectrometer reference gas are shown below along with the factor (Q_2, see Table 2-3) used to correct for background and valve leakage. They are subdivided into three groups, two kaolinite groups and a Rose quartz group. The slight differences in the average δO^{18} values between the two kaolinite groups were due to a slight change in the isotopic composition of the mass spectrometer reference gas. (The δO^{18} content of the mass spectrometer reference gas changes slightly each time a new standard reference gas is prepared.)

These raw working standard δO^{18} values and the values +21.70 and +8.42 were then used to calculate an average change of standard correction factor for each group using the formula from Table 2-3. The δO^{18} value of each sample was then corrected using the formula in Table 2-3 including the contemporaneous background and leakage correction factor and the above mentioned change of standard correction factor.

Group 1 (kaolinite)

Date	δO^{18} raw	Background and Leakage Correction Factor (Q_2)
11/21/68	-3.05	1.0326
11/21/68	-3.15	1.0326
11/21/68	-3.22	1.0326
11/21/68	-2.93	1.0326
11/21/68	-3.19	1.0326
12/10/68	-3.23	1.0583
12/13/68	-3.07	1.0488
12/19/68	-3.06	1.0452
12/23/68	-3.10	1.0393
1/8/70	-3.05	1.065
1/15/70	-2.93	1.0397
1/23/70	-2.97	1.0440
1/29/70	-3.16	1.0397
1/30/70	-3.05	1.0397
2/26/70	-3.10	1.0385
2/28/70	-3.15	1.0370
3/4/70	-3.02	1.0374
3/6/70	-3.18	1.0358
3/18/70	-3.16	1.0358
3/31/70	-3.32	1.0370
4/4/70	-3.17	1.0397

Group 1 (continued)

Date	δO^{18} raw	Background and Leakage Correction Factor (Q_2)
4/7/70	-3.33	1.0385
4/9/70	-2.65	1.0385
5/7/70	-3.12	1.0306
5/8/70	-2.99	1.0326
5/13/70	-2.98	1.0317
5/16/70	-3.13	1.0310
5/19/70	-3.04	1.0294
5/22/70	-3.28	1.0294
5/29/70	-3.12	1.0500
6/2/70	-3.17	1.0601
6/10/70	-2.80	1.0330
	Group 2 (kaolinite)	
7/7/69	-3.36	1.0266
7/23/69	-3.75	1.0314
8/1/69	-3.33	1.0282
8/3/69	-3.46	1.0282
8/7/69	-3.17	1.0206
9/10/69	-3.25	1.0238

Group 3 (Rose quartz)

Date	δO^{18} raw	Background Leakage and Correction Factor (Q_2)
10/21/69	-15.97	1.0278
10/28/69	-16.00	1.0306
10/28/69	-15.84	1.0278
11/6/69	-16.00	1.0270
11/18/69	-15.96	1.0286
11/21/69	-15.86	1.0282